THE
PHYSICAL REVIEW
A Journal of Experimental and Theoretical Physics
VOL. 46, NO. 4 AUGUST 15, 1934 SECOND SERIES

The Polarization of General X-Radiation from Thick Targets

Y. F. CHENG, *Stanford University*
(Received June 11, 1934)

The method applied in this experiment is that of 90° scattering combined with the balanced filter method. Bands of the x-ray spectrum between the *K*-absorption limits of molybdenum and columbium, of palladium and rhodium and of tungsten and tantalum, from targets of tungsten, copper and aluminum have been tested for polarization, using potentials from about 20 kilovolts to 100 kilovolts. Besides the confirmation of the previous experimental results[1] about the relation between polarization and voltage and the relation between polarization and wave-length, two other points have been demonstrated more quantitatively. First, while the maximum experimental value of polarization was not over 60 percent, the polarization at the quantum voltage of the band by extrapolation is nearly complete for all targets and all wave-length bands. Second, the polarization of x-rays of a given wave-length from targets of lower atomic number is higher than that from targets of higher atomic number, except near the quantum voltage where they approach 100 percent.

INTRODUCTION

THE experiments on x-ray polarization date back to 1896,[2] one year after the discovery of x-rays. The first systematic study was made by Barkla[3] in 1905, following which Haga,[4] Herweg,[5] Bassler,[6] Vegard[7] and Ham[8] worked on the problem. These investigations all showed definite polarization in continuous x-ray spectra. Later Kirkpatrick[9] found that the polarization increased approximately linearly with decrease of wave-length for x-rays emitted at constant voltage but even at the short wave-length limit, the polarization was still far from complete. These results partially confirmed the classical electromagnetic pulse theory.[10] From the standpoint of radiation quanta, Bubb[11] predicted partial polarization of x-rays of all wave-lengths but a greater polarization for rays of shorter wave-length. Sommerfeld[12] by the application of wave mechanics, at first obtained the general conclusion that at the short wave-length limit there should be complete polarization, but later concluded that at this limit, the polarization should not always be complete but should vary for spectra produced at different voltages.[13] According to the theory of Sugiura[14] the polarization cannot be complete, even at the quantum

[1] P. A. Ross, J. O. S. A. and R. S. I. **16**, 375 (1928). H. Kulenkampf, Phys. Zeits. **30**, 513 (1929).
[2] J. W. Gifford, Nature **54**, 172 (1896).
[3] C. G. Barkla, Phil. Trans. Roy. Soc. **A204**, 467 (1905); Proc. Roy. Soc. **A77**, 247 (1906).
[4] H. Haga, Ann. d. Physik **23**, 439 (1907).
[5] J. Herweg, Ann. d. Physik **28**, 398 (1909).
[6] E. Bassler, Ann. d. Physik **28**, 808 (1909).
[7] L. Vegard, Proc. Roy. Soc. **A83**, 379 (1910).
[8] W. R. Ham, Phys. Rev. **30**, 96 (1910).
[9] P. Kirkpatrick, Phys. Rev. **22**, 226 (1923).
[10] G. Stokes, Proc. Manchester Lit. and Phil. Soc., 1898. J. J. Thomson, Phil. Mag. **45**, 172 (1898).
[11] F. W. Bubb, Phys. Rev. **24**, 177 (1924).
[12] A. Sommerfeld, J. Frank. Inst. **208**, 571 (1929); Proc. Nat. Acad. Sci. **15**, 393 (1929).
[13] A. Sommerfeld, Ann. d. Physik **403**, 257 (1931).
[14] Y. Sugiura, Sci. Pap. Inst. Phys. and Chem. Rev., Tokyo **11**, No. 207, 251 (1929); **13**, No. 234, 23 (1930); **17**, No. 339, 89 (1931).

limit, the possible maximum polarization being about 85 percent.

Unfortunately experimental results in recent years have also shown great variation. Ross[1] found that the polarization of a fixed wave-length from a thick target increased as voltage decreased. The curve of polarization against voltage indicated complete polarization at the short wave-length limit. Kulenkampf[15] obtained a similar relation with a thin aluminum target. Wagner and Ott[16] found no indication of high polarization toward the quantum voltage of a band, the maximum polarization obtainable being below 50 percent. Also no variation of polarization with atomic number could be demonstrated. Duane[17] using a mercury vapor target and Dasanachyra[18] using thin aluminum, both obtained maximum average polarizations less than 50 percent for different wave-lengths.

The lack of good agreement either between theory and experiment or between the results of different experiments necessitates the present research which, following the preliminary experiment of Ross with several modifications, investigates the state of polarization of different spectral bands and of the radiation from different target materials. It also investigates the relation between polarization and the exciting voltage and the question of the completeness of polarization at the short wave-length limit.

Apparatus and Procedure

The general arrangement of apparatus for this research is shown in Fig. 1. A glass x-ray tube, together with its pumping system was mounted on a frame fastened to a stand which was free to rotate about a vertical axis and which could be moved in both longitudinal and transverse directions. When the frame was loosened, the tube also could be adjusted in these two directions with respect to the stand. The cathode could be adjusted horizontally and vertically without breaking the vacuum of the tube in the manner described by Webster.[19] The target

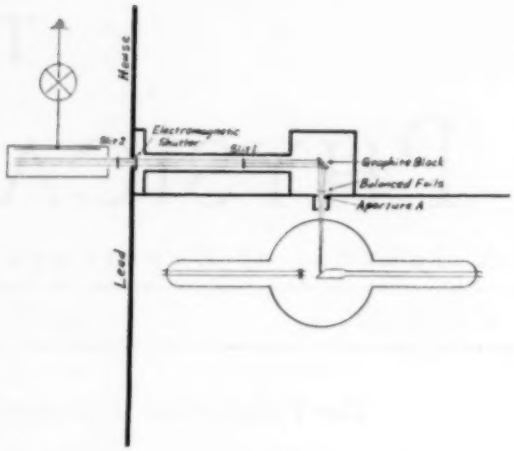

Fig. 1. General arrangement of apparatus for the study of polarization.

surface was inclined 45° to the cathode-ray stream. The focal spot of the target was set accurately on the axis of rotation with the aid of x-ray pinhole photography.

The primary radiation passed vertically through an aperture A and was scattered by an analyzing graphite block inclined at 45° to the vertical. In the case of the tungsten target the aperture A was circular, with a diameter of 0.5 cm, but in order to get sufficiently intense scattered beams from the copper and aluminum targets while preserving 90° scattering, a rectangular aperture of 0.5 cm wide and 4 cm long in a direction normal to the plane of scattering was used. The maximum deviation from 90° scattering was less than $\pm 0.5°$. A lead collimating system between the tube and the aperture A prevented x-rays from the target stem from striking the scattering block. A pair of balanced foils was mounted on a carrier above the aperture so that either foil might be slid into position by means of a pulley system controlled from outside of the lead house indicated in Fig. 1. Besides the slit window on the lead house, the two other horizontal slits shown in Fig. 1 were placed in the path of the secondary rays. As the slit aperture on the lead wall was horizontal, the electromagnetic shutter had to open and close vertically so as to insure uniformity of exposure for ionization. This shutter, equipped with suitable counterweights, was operated by impulses from a standard laboratory clock through a selector clock which automatically counted the

[15] H. Kulenkampf, Phys. Zeits. **30**, 513 (1929).
[16] E. Wagner and P. Ott, Ann. d. Physik **85**, 425 (1928).
[17] W. Duane, Proc. Nat. Acad. Sci. **15**, 805 (1929).
[18] B. Dasanachyra, Phys. Rev. **36**, 1675 (1930).
[19] D. L. Webster, W. W. Hansen and F. B. Duvenneck, Rev. Sci. Inst. **3**, 741 (1932).

TABLE I. *Polarization of Pd-Rh band from W-target.*

			$I_\perp$							$I_\parallel$							
			0°			180°				90°			270°				
kv	m.a.	sec.	Pd	Rh	diff.	Pd	Rh	diff.	Mean diff.	Pd	Rh	diff.	Pd	Rh	diff.	Mean diff.	Percent P
23.7	12	60	512.2	494.8	17.4	515.0	497.0	18.0	17.7	368.2	362.6	5.6	364.6	357.4	5.2	5.4	53.3
24.0	12	60	556.6	519.4	37.2	561.0	525.0	36.0	36.6	417.5	403.3	14.2	415.8	401.2	14.6	14.4	43.5
24.5	12	60	626.4	561.5	64.9	632.0	566.4	65.6	65.3	490.0	455.8	34.2	486.6	453.4	33.2	33.7	32.0
25.0	12	60	664.2	581.0	83.2	667.4	585.6	81.8	82.5	521.4	473.7	47.7	519.3	471.0	48.3	48.0	26.4
25.5	12	50	661.3	578.8	82.5	666.9	584.8	82.1	82.3	532.0	478.9	53.1	531.0	478.5	52.5	52.8	21.8
26.0	12	40	590.3	512.6	77.7	596.3	516.2	80.1	78.9	470.0	415.9	54.1	467.6	412.9	54.7	54.4	18.4
27.0	12	36	610.9	520.8	90.1	617.3	529.2	88.1	89.1	518.6	451.9	66.7	510.8	443.5	67.3	67.0	14.2
28.0	12	30	572.2	478.4	93.8	577.2	483.2	94.0	93.9	468.8	394.8	74.0	460.8	386.0	74.8	74.4	11.6
30.0	11	30	682.3	571.0	111.3	689.3	574.4	114.9	113.1	581.2	485.7	95.5	574.8	479.1	95.7	95.6	8.36
32.0	9	30	711.0	592.8	118.2	718.9	598.6	120.3	119.3	619.0	514.8	104.2	614.8	510.2	104.6	104.4	6.67
35.0	9	20	635.5	529.4	106.1	639.2	531.8	107.4	106.8	559.0	461.5	97.5	558.4	459.7	98.7	98.1	4.24
40.0	7	16	627.9	533.4	94.5	633.9	540.0	93.9	94.2	560.4	469.9	90.5	555.8	466.1	89.7	90.1	2.22
45.0	5	16	659.4	577.0	82.4	665.4	580.4	85.0	83.7	595.8	513.8	82.0	591.2	510.4	80.8	81.4	1.39

proper time of exposure and made the opening and closing switch contacts. In order to eliminate scattering by air as much as possible, the scatterer, the slit system and the shutter were screened by lead tubes and boxes.

Since the high voltage d.c. source has been described elsewhere,[20] it should be sufficient to say that it was a 500 cycle, kenotron rectified, full-wave high voltage outfit producing potentials up to 100 kv with a ripple of only about 4 volts at 10 m.a. The voltage was measured by the electrostatic voltmeter described by Clark.[21] It was calibrated by comparison with the voltage drop across a 6 megohm resistance.

The large ionization chamber was filled with methyl bromide at a pressure of 51 cm Hg. Ionization currents were read by means of a modified Compton electrometer at a sensitivity of 6000 scale divisions per volt. The linearity of the scale was checked by potentiometer measurements. Natural ionization was compensated for by a radioactive leak.

Polarization data were obtained by alternating the balanced foils in the path of the primary x-rays when the tube was set in a position with the cathode rays perpendicular to the scattering plane. The mean of a set of readings for each foil was computed and the difference of the two means for both foils calculated. The tube was then turned 180°. The readings were repeated and the mean of each set of readings and the difference of the two means were again calculated. The average of the two differences was then taken as the measure of the component of primary radiation of the spectrum band between the two K-absorption limits of the balanced foils with electric vector parallel to the cathode rays. Similar measurements were then made of the component of the same band with electric vector perpendicular to the cathode rays.

DATA AND CALCULATIONS

The polarization was calculated by the formula

$$P=(I_\perp-I_\parallel)/(I_\perp+I_\parallel),$$

in which $I_\perp$ is the electrometer deflection observed with the cathode rays perpendicular to the scattering plane and $I_\parallel$ is the deflection with the cathode rays parallel to the scattering plane. For illustration, values of polarization and of intensities $I_\perp$ and $I_\parallel$ for the tungsten target at various voltages and for the palladium-rhodium spectrum band are given in Table I.

In this table, each datum is the average value of at least five readings. In data of other targets, ten readings were usually taken. The 0°, 180°, etc., are some arbitrary marks on the graduated circle of the stand of the x-ray tube, indicating the position of the tube.

Due to the low intensity of the radiation from the aluminum target, the Pd-Rh and Mo-Cb spectrum bands which have low corresponding quantum voltages could not be tested. Instead the W-Ta band was used. In experiments on this band, voltages higher than 100 kv were not tried in order to avoid the danger of puncturing the glass of the tube.

Fig. 2 and Fig. 3 show the graphs of polarization against voltage. Pairs of dotted lines show

[20] D. L. Webster, Proc. Nat. Acad. Sci **6**, 269 (1920). D. L. Webster and Hennings, Phys. Rev. **21**, 301 (1923).
[21] H. Clark, Rev. Sci. Inst. **1**, 615 (1930).

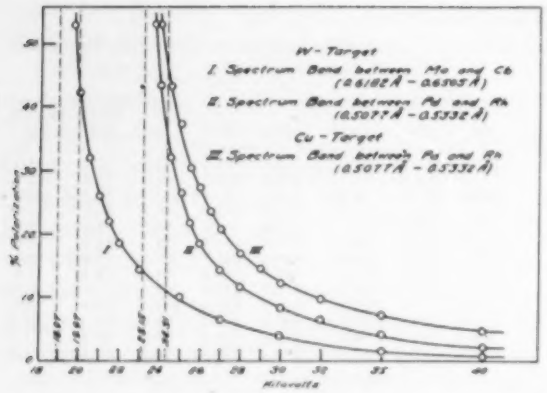

FIG. 2. Polarization of general x-radiation as a function of voltage.

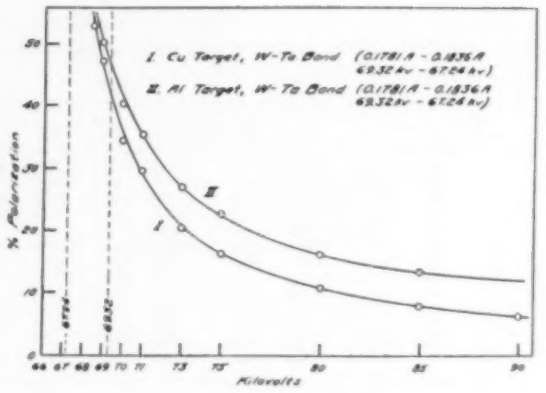
I. Cu Target, W-Ta Band (0.1781Å - 0.1836Å
69.32kv - 67.24kv)
II. Al Target, W-Ta Band (0.1781Å - 0.1836Å
69.32kv - 67.24kv)
% Polarization
Kilovolts

FIG. 3. Polarization of general x-radiation as a function of voltage.

the region of voltage corresponding to the wave-length of the two sides of each band. In Fig. 4 the graphs show the values of polarization for different targets and different spectrum bands against V/V_q, where V is the tube voltage and V_q is the quantum voltage of the band. In this way all the curves are shown on the same scale. By the quantum voltage of each band we here mean the quantum voltage of the edge of the band on the long wave-length side.

The largest experimental values of polarization are not over 60 percent. Since the actual functional form of these curves (Fig. 4) is unknown, the exact extrapolation to the quantum voltage of the band is not possible. Such extrapolation is facilitated however by the fact that the graph of $1/P$ against V' is nearly linear. The most probable representative line for this graph can be determined by the application of least square formulas[22] and the most probable value of polarization corresponding to the quantum voltage of the band in question and the probable error of the same can be computed from the value of y at $x=0$. The results of these calculations are given in Table II.

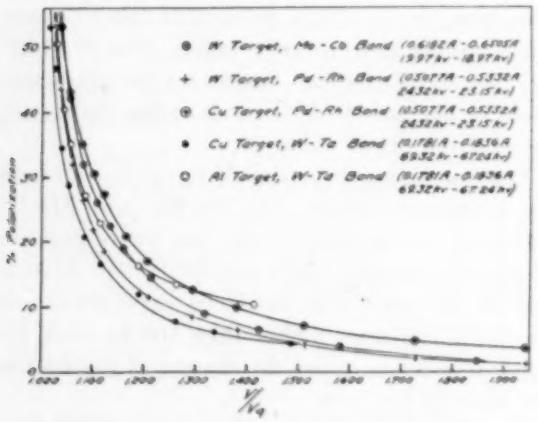

FIG. 4. Polarization of general x-radiation as a function of v/vq.

TABLE II. *Polarization at short wave-length limit by least squares extrapolation.*

Target	Spectrum band	Percent Polarization
Tungsten	Molybdenum and columbium	96.24 ± 4.76
Tungsten	Palladium and rhodium	100.95 ± 6.66
Copper	Palladium and rhodium	94.63 ± 3.41
Copper	Tungsten and tantalum	98.36 ± 3.18
Aluminum	Tungsten and tantalum	97.51 ± 2.33

If one assumes that the value of polarization at the short wave-length limit should be the same for all targets, one can calculate the weighted mean of polarization and its probable error to be 97.165 ± 0.529 percent by assigning a weight proportional to the inverse of the square of the probable error to each value of polarization shown in the above table.

Fig. 5 shows the graph of $1/P'$ against V'. The points are calculated values while straight lines are least square reductions. It is to be noted that a few points near the high voltage end (not shown in the graphs) of the tungsten and copper curves have been rejected in the calculation by least squares, because they do not fall on a straight line very closely. On the whole the

[22] R. T. Birge, Rev. Mod. Phys. **1**, 5 (1929).

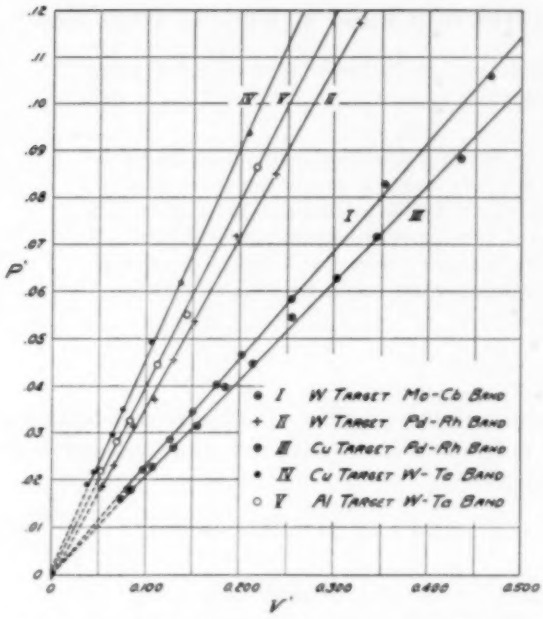

FIG. 5. Graphs for the extrapolation of polarization to the short wave-length limit. *Note:* The ordinates in this figure are $1/P'$ not P' as shown on the axis.

points in each graph lie fairly well on a straight line showing no consistent indication of curvature. One may therefore place considerable confidence in the method used and the value of polarization deduced.

DISCUSSION AND CONCLUSION

All the curves in Fig. 2 and Fig. 3 indicate clearly that polarization increases as voltage decreases and increases very rapidly as the quantum voltage of the band is approached. This agrees with both classical and recent theories and also agrees with Ross', Kulenkampf's and Dasanachyra's experimental results.

From the comparison of the curves I and II in Fig. 2 it can be seen that in the continuous spectrum of the same target (tungsten) at a constant voltage, for instance 27 kv, the polarization of the Pd-Rh band is higher than that of Mo-Cb band. That is, in any one continuous spectrum, the polarization of the band of shorter wave-length is higher than that of longer wave-length. This has been predicted by classical and recent theories and has been shown by previous experiments using the method of filtering out the longer wave-length.

In Fig. 2 curves II and III show polarization for the same Pd-Rh band from targets of tungsten and copper, respectively. It is evident that with the same voltage, polarization is always higher for copper than for tungsten. Also in Fig. 3 the two curves for W-Ta band from copper and aluminum targets indicate that with the same voltage, the polarization for aluminum is higher than that for copper. From these results, one may therefore conclude that the polarization of x-rays from elements of lower atomic number is higher than the polarization of x-rays from elements of higher atomic number. This result is in fact required by the wave-mechanical theory developed by Sommerfeld although it does not check with the experimental work of Wagner and Ott.

The result shown in Table II gives some evidence that at the short wave-length limit, the polarization of x-rays is nearly complete for all targets and all wave-length bands. This confirms the results of Ross and Kulenkampf in a more quantitative way.

In conclusion, the writer wishes to express his gratitude to Professor P. A. Ross under whose direction this work was carried out; to Professor P. Kirkpatrick for his frequent and valuable advice and to Professor D. L. Webster for his helpful suggestions.

The Interpretation of X-Ray Diffraction Patterns of a Fluid at Various Densities*

N. S. Gingrich and B. E. Warren, *George Eastman Laboratory, Massachusetts Institute of Technology*

(Received June 18, 1934)

It is shown that existing calculations for the intensity of x-rays diffracted by a fluid at various densities can be applied only over a small range of densities, and it is pointed out that this is due to the distribution of atoms about any one atom chosen for the calculation. The distribution is discussed qualitatively for gases and liquids, and a reasonable approximation to the true distribution is assumed. From this a set of intensity *vs.* angle curves are drawn for several densities. These curves are compared with Stewart's experimental curves for ether at various densities.

1. Introduction

X-RAY diffraction patterns of gases and of liquids have been studied by many investigators, but relatively little work has been done on the diffraction patterns of a fluid at various densities. For a review of gas diffraction, one should refer to the paper of Wollan,[1] and for a review of liquid diffraction, reference should be made to the article by Debye and Menke.[2] A calculation of the diffraction effects of a gas at various densities was made by Debye[3] in 1925, but the results of this calculation are applicable only to a relatively rare gas. Excellent experimental studies of the x-ray diffraction by ether at various densities have been made by Stewart[4] and Spangler,[5] and the results of these studies are interpreted qualitatively in terms of the cybotactic theory. Recently, Harvey[6] has made a brief preliminary report of work on the diffraction of x-rays by nitrogen at high pressure.

Debye's calculation showed that diffraction effects in a gas should occur simply because two atoms cannot approach each other closer than a certain minimum interatomic distance, a. Upon the assumption of no atoms at a distance less than a from any one atom, and a continuous distribution of atoms thereafter, this calculation led to the result that the intensity of x-rays diffracted by a gas should depend upon the density of the gas. The equation for the intensity of coherent x-rays scattered from a monatomic gas is

$$I = Kf^2\{1-(\Omega/V)\Phi(sa)\}, \tag{1}$$

where f is the atomic scattering factor, $s = (4\pi \sin\theta)/\lambda$, Ω/V is proportional to the ratio of the actual density to the maximum density of the gas, and

$$\Phi(sa) = \frac{3}{(sa)^2}\left\{\frac{\sin sa}{sa} - \cos sa\right\}. \tag{2}$$

A plot of the intensity of x-rays *vs.* sa at several values of Ω/V and using an arbitrary f^2, is shown in Fig. 1. Although the general manner of variation with density is in accord with experiment, the shapes of the curves for high values of Ω/V do not agree with those of available experimental curves. Moreover, the definition of Ω is such that $\Omega/V = 1$ corresponds to the case of a gas under pressure, but considerably removed from the liquid case. Thus, for very dense gases, or for liquids, this equation would lead to negative values for the intensity. The cause for these discrepancies at high densities is obviously that the assumption of having continuous distribution of matter beyond the smallest distance of approach of two atoms is not valid for a fluid at high densities.

2. Derivation of More Suitable Equation

In the present paper, an attempt is made to find an expression which will more nearly approximate the experimental curves for x-ray diffraction by a fluid at various densities. Use

* Paper presented at the Cambridge Meeting of the American Physical Society, December, 1933.

[1] E. O. Wollan, Rev. Mod. Phys. **4**, 205 (1932).

[2] P. Debye and H. Menke, Ergeb. der Techn. Röntgenkunde **II**, 1 (1931).

[3] P. Debye, J. Math. and Phys. **4**, 133 (1925).

[4] G. W. Stewart, Trans. Faraday Soc. **29**, No. 148, 982 (1933).

[5] R. D. Spangler, Phys. Rev. **45**, 756 (1934).

[6] G. G. Harvey, Phys. Rev. **45**, 848 (1934).

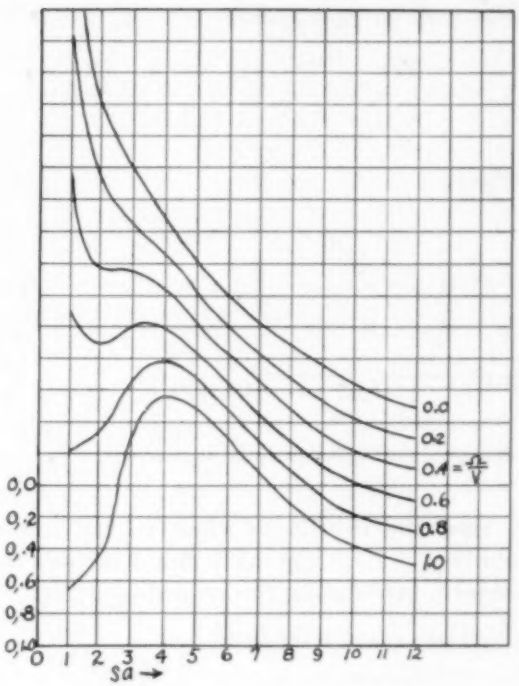

FIG. 1. Plots of Debye's equation for several values of Ω/V.

is made of the method of Zernike and Prins,[7] which has been applied successfully to certain gases, liquids and solids. Consider a monatomic substance, having spherical atoms, in which each atom is surrounded in the same way as every other atom. If x-rays are incident upon this substance, the intensity of coherent scattered x-rays as a function of angle is given by

$$I = Nf^2\left\{1+\int_0^\infty 4\pi r^2 g(r)[(\sin sr)/sr]dr\right\}, \quad (3)$$

where f is the atomic scattering factor, r is the distance measured from any one atom, and $g(r)$ is the density distribution function of atoms about any one atom. Thus, in order to calculate the intensity, I, it is necessary to know the atomic scattering factor f, and the density distribution function, $g(r)$. It can be seen that this equation will result in essentially Debye's equation, if the integration of the second term is taken with the lower limit a, and with $g(r)$ a constant. A more reliable calculation of the intensity could be made, however, if the density distribution function were known, or if a more reasonable approximation to it were made.

The general features of the distribution of atoms about any one atom in a gas or liquid can be seen from several considerations. For a gas, the density distribution can be calculated from Morse's[8] potential function, and this shows that there will be no atoms closer than a certain minimum distance and that there will be a slight concentration of atoms at about this distance, beyond which the density of atoms will rapidly become constant. For a liquid, in which the atoms are approximately close packed, the same minimum distance of approach should exist, and there should be a marked concentration of atoms at this distance, with a deficiency of atoms just beyond, after which the density distribution curve should oscillate about the average density a few times before becoming constant. Experimental support for this type of distribution may be found in the work of Debye and Menke[9] on mercury.

The calculation of the intensity of coherent scattered x-rays by a fluid can be made if the true density distribution function is known, or if a reasonable approximation to it is assumed. Fig. 2(a) shows a typical distribution curve for a gas, and Fig. 2(b) represents an assumed distribution, which leads to the equation

$$I = Nf^2\left\{1+M\frac{\sin sa}{sa}+\int_a^\infty 4\pi r^2\rho\frac{\sin sr}{sr}dr\right\}. \quad (4)$$

Integration of the last term of this equation results in $(4\pi/3)a^3\rho\Phi(sa)$ where $\Phi(sa)$ is defined by Eq. (2), and ρ is the constant average density in atoms per unit volume. The upper limit of this integral gives rise to no observable diffraction effects, as long as it is large compared to the interatomic distance, a. This can be seen from plots of $\Phi(sr)$, for this function is appreciable only for small values of sr, and if r is very large, s must be very small; that is, diffraction effects due to matter at very large r are confined to very small angles. The coefficient of this term represents the amount of matter removed from

[7] F. Zernike and J. A. Prins, Zeits. f. Physik **41**, 184 (1927).

[8] P. M. Morse, Phys. Rev. **34**, 57 (1929).

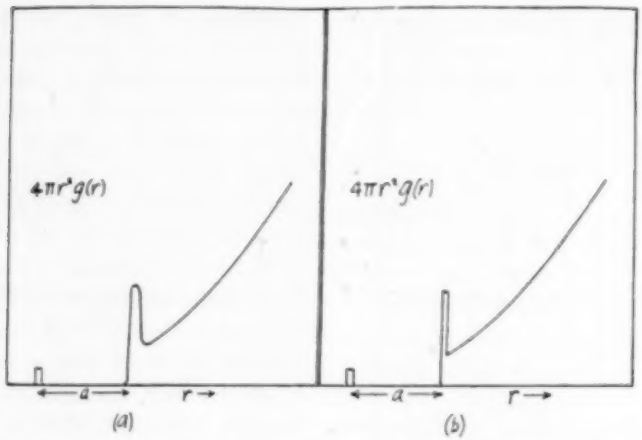

FIG. 2. Density distribution of atoms about any one in a gas, (a) as calculated, (b) as assumed.

the sphere of radius a in the continuous distribution. The coefficient of the second term, M, must equal the amount of matter removed from the sphere of radius a, less the one atom at the origin. The closest packing of spheres is the face centered cubic arrangement, and in this case, the volume per atom is $a^3/2^{\frac{1}{2}}$ so that $(4\pi a^3/3 - a^3/2^{\frac{1}{2}})\rho$ represents the amount of matter to be concentrated at a distance a. Thus, one obtains

$$I = Nf^2\left\{1+\left(\frac{4\pi}{3}a^3-\frac{a^3}{2^{\frac{1}{2}}}\right)\rho\frac{\sin sa}{sa} - \frac{4\pi}{3}2^{\frac{1}{2}}\frac{a^3}{2^{\frac{1}{2}}}\rho\Phi(sa)\right\}. \quad (5)$$

If $a^3/2^{\frac{1}{2}}$ is the volume per atom, in closest packing, then the density of close packed atoms would be $\rho_0 = 2^{\frac{1}{2}}/a^3$, the maximum density of the substance. Introducing this, and simplifying,

$$I = Nf^2\{1+(\rho/\rho_0)[4.92(\sin sa)/sa - 5.92\Phi(sa)]\}. \quad (6)$$

Curves plotted from this equation show that for values of ρ/ρ_0 less than 0.5, better qualitative agreement with experimental curves is obtained than with Debye's equation, but for higher values of ρ/ρ_0, negative intensities at small angles appear. These negative intensities are obviously due to the crude approximation of density distribution for the liquid. The density distribution for a liquid should be roughly of the type shown in Fig. 3(a), and for purposes of calculation, that shown in Fig. 3(b) has been

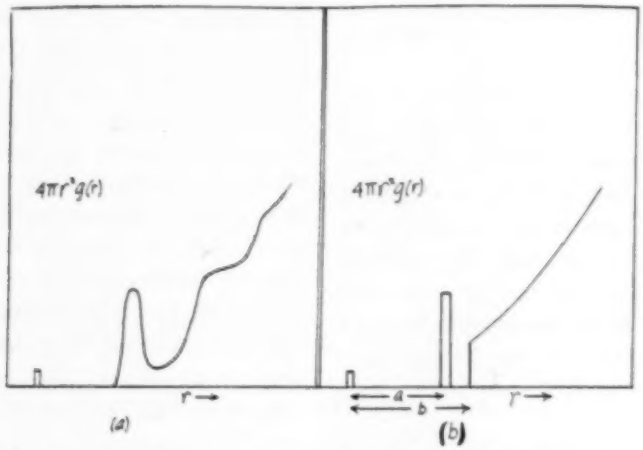

FIG. 3. Density distribution of atoms about any one atom in a liquid, (a) as it probably is and (b) as assumed.

assumed. This distribution leads to the equation

$$I = Nf^2\left\{1 + M\frac{\sin sa}{sa} + \int_b^\infty 4\pi r^2 \rho \frac{\sin sr}{sr} dr\right\}, \quad (7)$$

which becomes

$$I = Nf^2\{1 + (\rho/\rho_0)[K_1(\sin sa)/sa - K_2\Phi(sb)]\}, \quad (8)$$

where the coefficients K_1 and K_2 depend upon the ratio b/a. The ratio $b/a = 1.18$ has been found to be both reasonable and suitable, and this results in a value of $K_2 = 9.7$. However, this value of K_2 is too large, partly because of the assumption of close packing and partly because of neglect of density variations beyond the first concentration and first dip. To allow for these two effects we arbitrarily take a somewhat smaller value for K_2. K_1 is then immediately fixed by the condition that all the matter removed from the continuous distribution must equal the excess in the concentrations. The equation obtained in this way is

$$I = Nf^2\{1 + (\rho/\rho_0)[5(\sin sa)/sa - 6\Phi(1.18sa)]\}. \quad (9)$$

The maximum intensity will occur at a definite value of sa, so that the scattering angle for maximum intensity will depend upon a, the smallest distance of approach of atoms, and will depend on the density only inasmuch as the factor f^2 tends to shift the peaks for small density towards small angles.

3. Application of Equation to Experimental Results

From Eq. (9), plots of intensity *vs.* sa may be made for several values of ρ/ρ_0, and compared with experimental results. Such plots are shown in Fig. 4(b), for which plots, a value of f was used to approximate the effective f for ether. For comparison with experimental curves, one should have data on a monatomic gas for which the scattering factor is known, but no such data exist. However, experimental curves for ether at various densities have been obtained by G. W. Stewart and R. D. Spangler, and a set of their curves, which they very kindly sent us, is reproduced in Fig. 4(a). Similarities between the calculated and experimental curves can be seen. By means of certain arbitrary refinements, one can produce nearly exact fits between the curves, but it is felt that such manipulation in the case of ether is meaningless.

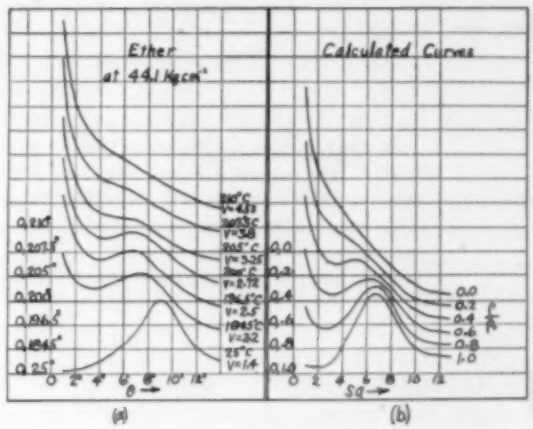

Fig. 4. Plots of intensity *vs.* θ, in the case of ether curves and *vs.* sa in the case of curves calculated from Eq. (9).

4. Summary

The interpretation, here presented, of the diffraction of x-rays by fluids at various densities is based on the ordinary theory of x-ray diffraction, but it cannot be made rigorous without a more complete knowledge of the density distribution of atoms about any one atom in gases and liquids, and the manner in which it changes in going from the gas to the liquid state. However, by introducing reasonable approximations to these distributions, it is shown that the general characteristics of diffraction curves of a fluid at various densities can be predicted.

Experiments with Arcs at Atmospheric Pressure

C. G. SUITS, *General Electric Company, Schenectady, New York*

(Received June 20, 1934)

In the equation for the static characteristic of the electric arc at atmospheric pressure, $E=A+B/I^n$, the exponent n has been interpreted by Nottingham and others as a constant independent of arc length and dependent linearly upon the boiling point of the anode material. This view is criticized from a consideration of new experimental data showing that the spread in measurements of n is necessarily very large. The conclusion that "n varies directly as the boiling point of the electrode (anode) material" is not given support by these experiments.

IN a comprehensive investigation of the steady state volt-ampere characteristics of atmospheric pressure arcs between metallic electrodes, Nottingham[1] proposed the relation,

$$E=A+B/I^n, \qquad (1)$$

between the arc voltage E and the current I, where A, B and n are constants. It was found experimentally that the exponent n was independent of arc length but not of electrode material. In particular, n depends upon the material of the anode and is numerically greater for materials like W and Pt than for Sb, Pb, Cu and Au. In the case of a 3 mm copper arc, for example, $n=0.665$, while the average value for ten arc lengths, between 1 mm and 10 mm, is given as $n=0.670$. The data suggest that there may be some fundamental dependence of this exponent n on the boiling point of the anode material, as shown for example by Fig. 1, where values given by Nottingham,[1] Anderson and Kretchmar,[2] and Myers[3] are plotted. The original data lie remarkably close to a straight line. It should be pointed out, however, that (1) in the case of Ni, Al, Cu and Zn, it was necessary to use the boiling point of an oxide to provide agreement, and (2) more recent determinations of the boiling points of W, Pt and Ag take these points well off the curve, particularly in the case of W.

If the relation of Nottingham between the boiling point and n could be confirmed and extended, it would be of practical importance to the study of arcs, in spite of the fact that it has absolutely no theoretical background. In view of the importance of this work, and the firm root it has taken in the literature on atmospheric arcs, it has seemed desirable to investigate the foundations on which this arc equation rests.

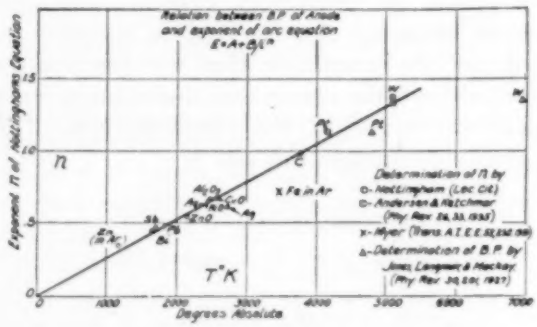

FIG. 1.

EXPERIMENTAL METHOD

For the first series of measurements the method of Nottingham was duplicated as nearly as possible. In this method the arc voltage is obtained by a voltmeter in parallel with the electrodes; the arc current (plus the v.m. current) was obtained from an ammeter in series with the arc; and the arc length was adjusted and measured by projecting an enlarged image on a suitably calibrated screen. The current limiting element in series with the arc was nominally a pure resistance. The voltage supply was in some cases a 500 volt battery, and in other cases a 1500 volt d.c. generator.

The electrodes ($\frac{1}{2}$" diameter cylinders) were turned smooth on a lathe after every reading for the high currents, but were used for several readings at the low currents where the electrode

[1] Nottingham, J. A. I. E. E. **42**, 12 (1923); Phys. Rev. **28**, 764 (1926).
[2] Anderson and Kretchmar, Phys. Rev. **26**, 33 (1925).
[3] Myers, Zeits. f. Physik **87**, 1, 2 (1933).

burning was less. Three observers, located respectively at the ammeter, voltmeter, and screen, took simultaneous readings. The time required to take a reading, after starting the arc, varied between three seconds to a minute or more.

Although the arc current is maintained at a relatively constant value, the arc voltage shows large random fluctuations so that the spread of the measurements is very great. An enormous number of readings were taken of different arc lengths, electrode diameters, electrode surfaces, electrode materials and positions. An oscillogram illustrating the case is shown as Fig. 2, which was

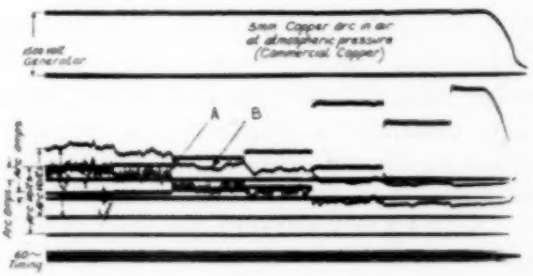

FIG. 2.

obtained by a method to be described in detail later. In this method the current through the arc was increased in steps by a commutator in such a manner that the complete volt-ampere data were obtained in a relatively short time. The arc voltage is given at (*A*), as it appeared to the standard, low sensitivity, high frequency (8000 cycle) galvanometer. The trace (*B*) is the arc voltage which one would observe on a conventional laboratory d.c. voltmeter. For this record (*B*), the time constant of the galvanometer circuit was increased, with an inductive shunt, to agree with the time constant of the mechanical system of a laboratory voltmeter. It should be noted that this oscillogram was taken after the arc had burned for some minutes, or in approximately the time required to take a reading by the voltmeter-ammeter method. It can be observed from both traces of this oscillogram that (1) changes in arc voltage are large (15–45 percent); and (2) random in character.

From a great deal of data it is concluded that the spread of the measurements, due to the random nature of the arc voltage variations, is such as to preclude the possibility of an accurate determination of n by this method.

NEW MEASUREMENTS OF n BY AN OSCILLOGRAPHIC METHOD

To eliminate the human element and to shorten the time required for readings and hence electrode heating, burning and associated errors, a completely automatic method for taking the volt-ampere data was used. The oscillograph trip mechanism is used to start a motor driven commutator which successively short-circuits portions of the current limiting resistance to increase the arc current and decrease the arc voltage in steps. Two current elements are used on the oscillograph so that both high and low current ranges are read with accuracy. The high sensitivity current element is shorted by the commutator to protect it from the heavy current. The arc length is adjusted by a thickness gauge with cold electrodes before starting the arc. The total change in arc length due to electrode expansion during the course of a run (*circa* 5 sec.) leads to a negligible error. Some errors in arc length occur if the arc travels to the edges of the electrodes and forms an outward bow. Records for which this was observed were thrown out.

For electrodes three kinds of pure copper were used, one with known analysis, together with one sample of commercial purity for comparison purposes. The electrode surfaces were lathe turned, except for a series of records taken with highly polished surfaces—to be described in a separate publication. The method of taking data is automatic and rapid so that an enormous number of records, each a complete volt-ampere characteristic, may be taken quickly and with a high order of accuracy. The arc voltage was in some instances taken with a galvanometer element employing an inductive multiplier (trace (*B*), oscillogram Fig. 2), and in some cases with a non-inductive multiplier, as noted. In the case of the copper records, where the changes in arc voltage appear to be random in character, the inductive element was used. In this case the *average value* of arc voltage throughout each current step was the recorded value.

3 mm Copper Arc

A typical record for a 3 mm copper arc is shown as Fig. 3. Data taken from 15 oscillographic records of 4 kinds of copper are summarized in Fig. 4. It can be seen from these data that (1) the spread is relatively small, and (2) there are no systematic differences which may be ascribed to the type of copper used. In particular, the vacuum melted copper gave the same performance, within the spread of the measurements, as the same copper not so treated, and all pure samples agreed with commercial copper as far as the volt-ampere characteristic was concerned. From the volt-ampere curve of Fig. 4, one might determine n graphically, as in Fig. 5. Depending upon the choice of the asymptote A, the value of n lies some place in the range $0.1 < n < 0.4$. One could state quite certainly that it is not greater than 0.5, but a determination to the first significant figure is somewhat questionable, and a value of n carried to the third decimal place, as $n = 0.665$ (3 mm Cu arc, Nottingham[1]), would appear to be decidedly unwarranted. It is important to point out that the lack of accuracy is not fundamentally due to the graphical method used in determining n, but to the nature of the phenomena being investigated. If, for example, n is calculated by fitting three experimental points to a curve, the numerical value will vary greatly with the choice of the points.

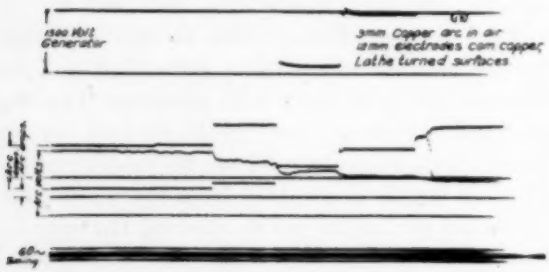

Fig. 3.

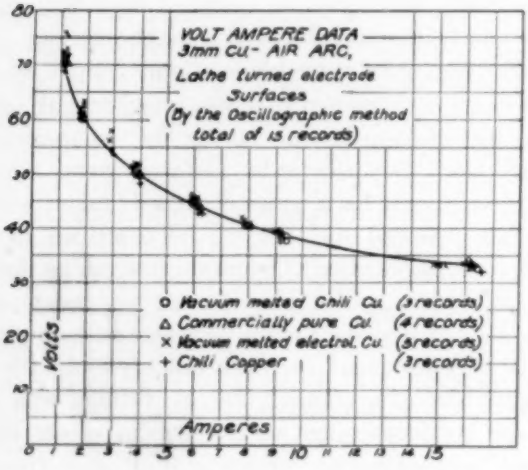
VOLT AMPERE DATA
3mm Cu- AIR ARC,
Lathe turned electrode Surfaces
(By the Oscillographic method total of 15 records)
o Vacuum melted Chili Cu (3 records)
Δ Commercially pure Cu (4 records)
× Vacuum melted electrol. Cu (3 records)
+ Chili Copper (3 records)
Volts
Amperes

Fig. 4.

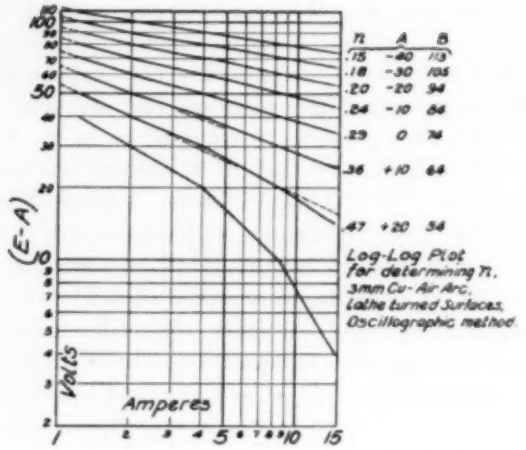

Fig. 5.

No question is raised as to the possibility of representing the experimental arc characteristic of Fig. 4 by an equation of the form of (1). The difficulty lies in the fact that n is not a sensitive constant. It is believed from these experimental data and from the considerations given that the evidence does not warrant the interpretation "the exponent n varies directly as the boiling point of the electrode (anode) material."[1]

Inverse Piezoelectric Properties of Rochelle Salt

C. Irwin Vigness, *University of Minnesota*

(Received June 20, 1934)

The relation between the change of lattice spacing of the (021) planes of Rochelle salt as a function of the change in voltage applied along the *a*-axis of the crystal has been determined by x-ray methods over the temperature range from approximately 10°C to 30°C. Measurements with a microscope of the strain set up in the crystal, due to a change in voltage applied along the *a*-axis, indicate that there is a one to one correspondence between the change of lattice constant as measured by x-rays and as determined from the measurements of strain. The piezoelectric modulus, d_{14}, as determined by the inverse piezoelectric effect is larger than the values determined from the piezoelectric effect.

THE strain corresponding to a change in electric stress along the *a*-axis of a Rochelle salt crystal has been measured.[1] There has been a question as to how this strain is distributed within the crystal, whether this displacement might take place in main between mosaic or a secondary lattice structure of the type postulated by Zwicky,[2] between any large groupings of molecules, or whether this displacement takes place chiefly in the primary lattice. A study of the change in the primary lattice constant, by means of x-rays, as a function of the change in voltage applied along the *a*-axis of the crystal together with measurements of the overall displacement of the crystal give sufficient information to answer the above question.

Rochelle salt crystals obtained from the Brush laboratories were cut into small rectangular blocks, one face being parallel to the (100) planes and another parallel to the (021). The lattice constants were taken as determined by Staub,[3] namely;

$$a=11.91\text{A};\quad b=14.32;\quad c=6.20.$$

Thus the normal to the (021) planes would make an angle of 40° 53′ with the *b*-axis, which is nearly the direction (45°) of greatest linear deformation within the crystal when the voltage is applied along the *a*-axis.

In order that a moist crystal might be dealt with, the crystals were kept in a bell jar that contained a saturated solution of Rochelle salt. When one was to be used it was taken from the bell jar, polished on a fine moist ground glass, and tin foil electrodes fastened to the crystal by means of a xylol Canada balsam solution so that the electric field would be along the *a*-axis. The crystal was then, together with a small cup of the saturated Rochelle salt solution, sealed in a controlled-temperature container, the x-rays entering and leaving this chamber through waxed paper windows. The x-ray camera consisted of an evacuated tube 103 cm in length from the slit to the plate. It was possible by an externally controlled screen within the camera to expose but half of the plate at a time. The procedure followed was to expose one-half of the plate with the voltage applied to the crystal in a given direction and to expose the other half of the plate with the voltage reversed. We would then obtain a picture (Fig. 1) with the lines on the upper and lower parts of the plate displaced slightly. This displacement is called $2\Delta s$ to correspond to the change of $2E_x$ in voltage. The time of exposure varied between 10 and 15 minutes using a 0.1 mm slit and $K\alpha_1$ and $K\alpha_2$ of copper excited by 10 m.a. at 28 kv.

Fig. 1. Displacement of the copper $K\alpha_1$ and $K\alpha_2$ lines reflected from the (042) planes of Rochelle salt due to a voltage applied along the *a*-axis.

[1] C. B. Sawyer and C. H. Tower, Phys. Rev. **35**, 269 (1930).
[2] Zwicky, Helv. Phys. Acta **3**, 466 (1930).
[3] Staub, Helv. Phys. Acta **7**, 3 (1934).

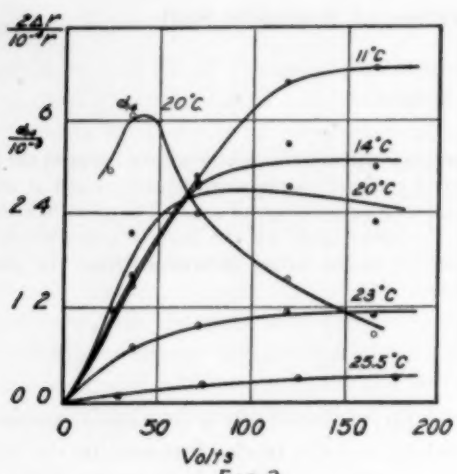

Fig. 2

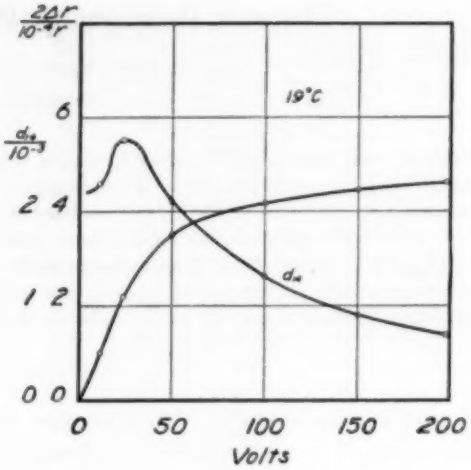

Fig. 3

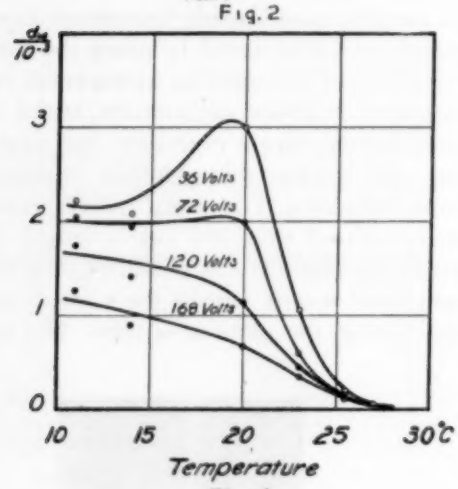

Fig. 4

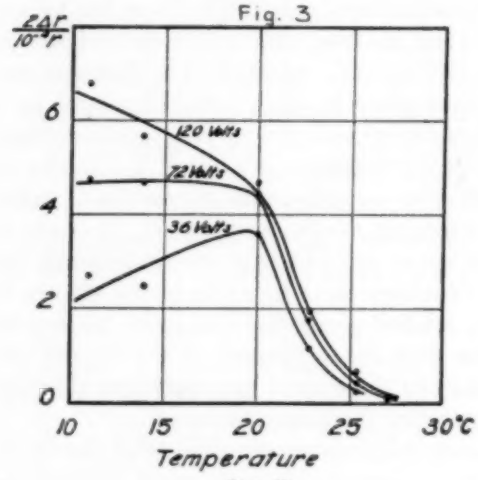

Fig. 5

FIG. 2. Relation between the lattice displacement and piezoelectric modulus as a function of voltage along the a-axis as determined from x-ray measurements.

FIG. 3. Relation between the lattice displacement and piezoelectric modulus as a function of voltage along the a-axis as determined by measurements of deformation made by means of a microscope.

FIG. 4. Piezoelectric modulus determined from x-ray measurements as a function of temperature.

FIG. 5. Lattice displacement determined from x-ray measurements as a function of temperature.

The measurement of this displacement was accomplished by aligning the negative in a comparator so that the cross hair of the comparator microscope, which is perpendicular to the screw, is parallel to the spectrum line, and so that the field of view of the microscope includes both the upper and lower lines of the negative. The displacement is measured within a few thousandths of a millimeter.

If $2\Delta r$ is the displacement of the crystal lattice in the direction of r due to a change in voltage from a positive value of E_x to an equal negative value of E_x, then it can be shown that

$$\Delta r/r = -\Delta s/2R \tan\theta,$$

where R is the distance between the camera slit and the plate and θ is the Bragg angle. The reflections were taken from the (042) planes which gave us an angle of 19° 10′.

Voigt[4] has shown that for a crystal of the

[4] Voigt, *Lehrbuch der Kristallphysik*, Chapter 8, Leipsig (1910).

symmetry of Rochelle salt the relations connecting the six strain components and electric field reduce to

$$y_z = d_{14}E_x; \quad z_x = d_{25}E_y; \quad x_y = d_{36}E_z;$$

y_z, z_x and x_y are strain components, d_{ij}, the piezoelectric moduli, and E_x, E_y, E_z the components of voltage along the respective axes. By the use of the proper equations of elasticity and with the voltage impressed along the a-axis it can be shown that the value of

$$d_{14} = -\Delta s/2RmnE_x \tan\theta,$$

m and n are the direction cosines with respect to the y and z axes of the normal to the $(0jk)$ plane considered. E_x is the voltage in e.s.u. along the a-axis of the crystal.

In Figs. 2–5 the displacements, $2\Delta r/r$, correspond to a change in the voltage from the value indicated to a negative potential of the same value. The temperature is kept constant within a few tenths of a degree throughout the time of exposure.

By comparison of Fig. 2 and Fig. 3 we see at once that the lattice displacement corresponds to the change in external dimensions of the crystal.

The results given by Sawyer and Tower[1] for the relation between strain and the peak electric field of a 60 cycle applied potential give results essentially the same as have been determined here, with the exception that a considerable voltage must be applied before the crystal shows an appreciable deformation, whereas the results given in this paper merely show a slight decrease in the slope of the strain voltage relations at the lower values of voltage. The reason for this difference is due to the sluggishness of response of the crystal at the lower voltages. The time required for the crystal to reach its maximum deformation may be of the order of several minutes for the small potentials, while for the higher values the maximum is reached so quickly that a sharp click is emitted. Frank C. Isely[5] has shown that for a given stress applied to a crystal, the crystal quickly reached an initial strain followed by a further gradual deformation lasting about fifteen seconds if the active faces of the crystal were short-circuited, and about twice that time if they were not. This might lead us to conclude that the effect is due to a conduction equalization of charges set up within the crystal by a non-uniform distribution of stress or strain. As the voltage applied became large the effect of these distributed charges would become negligible due to saturation effects.

The maximum value of d_{14} as calculated from the inverse piezoelectric effect is about forty times the maximum value, 8.1×10^{-8}, as calculated by Valasek[6] from the piezoelectric effect. The value of d_{14} is strongly a function of the moisture content of the crystal and of the stress applied, in the case of the direct effect, and of the voltage applied in case of the inverse effect. If the stress applied corresponds to a rather large value of voltage the difference in the piezoelectric modulus and the inverse piezoelectric modulus is of the order of ten times. It is quite likely that this difference is due in part to an "absorbed" charge caused by a gradual electrical polarization of the dielectric as a result of the long application of the voltage that was necessary for the x-ray measurements. The maximum strain in a crystal along the normal to the (021) planes due to an application of voltage along the a-axis, is larger by a factor of about two than the comparable strain as measured by Isely.[5] This is probably due to a difference in crystal.

It has been the privilege of the author to carry on this work under the supervision of Joseph Valasek.

[5] Frank C. Isely, Phys. Rev. **24**, 569 (1924).
[6] Valasek, Phys. Rev. **20**, 639 (1922).

The Energy Spectra of the Neutrons from the Disintegration of Fluorine, Boron and Beryllium by Alpha-Particles

T. W. Bonner* and L. M. Mott-Smith, *The Rice Institute, Houston, Texas*

(Received June 12, 1934)

By using an expansion chamber filled with hydrogen or methane at a pressure of about 15 atmospheres, range-distribution curves have been obtained of the recoil protons from Po-F, Po-B, and Po-Be neutrons. These curves revealed the presence of numerous groups of neutrons in the radiation from the three sources. In the case of Po-F five neutron groups were found. These were fitted into a disintegration scheme, made by assuming that the α-particle enters the nucleus through resonance levels and by using the energies of these levels, which are known from the disintegration of fluorine with proton emission. For Po-B eight groups were detected, but it was not possible to arrange a disintegration scheme. The maximum energy of the neutrons from Po-B was found to be 4.2 M.E.V., a value considerably higher than the previously accepted figure, 3.3 M.E.V. This value decreases the mass of the neutron calculated from the disintegration of B^{11} from 1.0067 to 1.0058. It is suggested that it is possible to explain the high value, 1.0098, obtained by Curie and Joliot from the disintegration of B^{10}, by assuming that both B^{11} and B^{10} emit neutrons. If the maximum energy of the neutrons from B^{10} were about 7.5 M.E.V. it would bring this mass into agreement. Reasons are given for believing that at least 10 times as many neutrons come from B^{11} as from B^{10} so that there may be a few as yet undetected neutrons from B^{10} extending up to this energy. About 22 groups were found in the neutron emission of Po-Be. A possible scheme of disintegration is given.

Introduction

THE early work on the energy distribution of the neutrons produced by α-particle bombardment of beryllium and boron was concerned principally with finding the maximum energy for the purpose of obtaining the mass of the neutron. Subsequent work[1, 2, 3, 4] began to reveal more exactly the nature of the energy distribution and indicated the existence of neutron groups analogous to the groups of protons which have been found in the disintegration of light elements with the ejection of a proton. In the case of fluorine previous experiments indicated the existence of neutron emission but no direct energy measurements had been made. The present experiments were undertaken to find the energy distribution of the neutrons from Po-F and to obtain further data on the neutrons from Po-Be and Po-B. Preliminary accounts have been given for fluorine[5] and for boron.[6]

Experimental Method

To obtain the energy of a neutron it is necessary to observe the energy which it gives to an atom in a collision. The energy given to a recoil atom can be found by determining its range by means of ion-counters and absorbing screens, by the Wilson cloud-chamber, or photographically in the manner used by Blau.[3] Ion-counters have the advantage of recording recoil atoms more rapidly than the other methods. As ordinarily used, however, they do not give the actual range of the particle but only the number of particles with ranges greater than a minimum determined by the stopping power of the screens. Accordingly, so-called integral range-distribution curves are ordinarily obtained by this method, and these are not as suitable for detecting groups as the true or "differential" distribution. Ion-counters also suffer from the existence of the residual counting-rate which in the presence of a strong source limits their accuracy when working in regions of low intensity. Another difficulty is that ordinarily the recoil atoms have to be obtained from a thick layer of material (usually protons from paraffin) which results in a further distortion of the energy distribution. On the other hand, with the expansion chamber, if the recoil tracks are formed in the gas, this difficulty is avoided. Also, the actual range is observed, so

* Now National Research Fellow, California Institute of Technology.

[1] I. Curie and F. Joliot, Comptes Rendus **194**, 876 (1932).
[2] J. Chadwick, Proc. Roy. Soc. **A142**, 1 (1933).
[3] M. Blau, J. d. Physique, **5** 61 (1934).
[4] J. R. Dunning, Phys. Rev. **45**, 586 (1934).
[5] T. W. Bonner and L. M. Mott-Smith, Phys. Rev. **45**, 552 (1934).
[6] L. M. Mott-Smith and T. W. Bonner, Phys. Rev. **45**, 554 (1934).

that the true range distribution can be obtained. In using an expansion chamber various recoil atoms such as H, He, N, O, A may be used. Heavy atoms (O, N, A) are not very satisfactory because their ranges are much too short for accurate measurement with any but the neutrons of highest energy. In addition, to infer the energy distribution of the neutrons from the observed energies of the recoil atoms, it is necessary to take into account that the recoil atom obtains only a portion of the energy of the neutron, and this depends on how direct a collision occurs. It is therefore desirable to use a recoil atom for which as large a fraction as possible of the collisions are nearly head-on. It appears from studies of the angular distribution of recoil protons by Kurie[7] that this condition is probably more satisfactorily met by protons than by heavier atoms. He found a pronounced maximum for protons ejected in the forward direction, and this is confirmed by some results presented below. It is not possible, however, to use recoil protons produced in the gas of an ordinary expansion chamber because their ranges are too great (up to about 150 cm for beryllium), and also because a sufficient number of recoil tracks cannot be obtained without taking an excessively large number of photographs. In order to be able to do this we have employed a special expansion chamber (filled with H_2 or CH_4) in which the pressure of the gas could be raised to about fifteen atmospheres, thereby reducing the range of the protons and also increasing the yield. In this way we could measure recoil protons having ranges up to about 90 cm in air, and increased the yield by roughly a factor of fifteen.

The expansion chamber was of a simple type using a stretched thin rubber diaphragm as the piston, such as the one recently described by Wilson,[8] and operated pneumatically. It consisted of a heavy brass casting, the inside dimensions, or working volume, being 10 cm in diameter by 3.5 cm deep. The top was closed by a thick fused quartz plate (chosen for its superior strength and transparency) through which the interior was photographed. The tracks were formed by condensation of alcohol vapor instead of water vapor. It was found to be more convenient because it requires a smaller expansion-ratio and has less tendency to fog the windows.[9]

The neutrons were produced by bombarding thick targets of Be, B, or CaF_2 with α-particles from polonium. The polonium was deposited on a small silver button and had an average activity of about 10 millicuries during the course of the experiment. The source was placed at the side of the chamber in a recess where the thickness of the side-wall was approximately 0.7 cm (see Fig. 1).

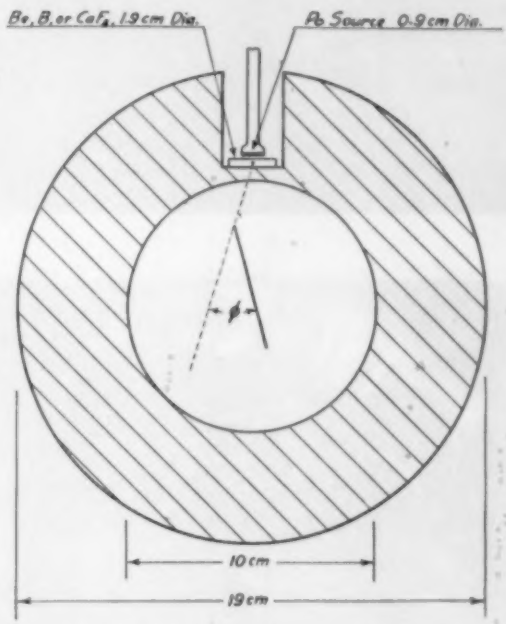

FIG. 1. Diagram of the expansion-chamber and the source of neutrons, as seen from the position of the camera.

The tracks were photographed on 35 mm motion-picture film with a camera taking stereoscopic pairs of photographs at an angle of 16°. Measurement of the lengths of the tracks was carried out by projecting the photographs with the camera lens system in the usual way. A card carrying a scale was adjusted until the two images of the track coincided and lay along the scale. The length could be read to 0.1 mm but due to possible errors in adjusting for coincidence of the images the track lengths might be in error by as much as 0.2 mm. In making the reconstruction it was necessary to take into account the displacement of the images produced by the

[7] F. N. D. Kurie, Phys. Rev. **44**, 463 (1933).
[8] C. T. R. Wilson, Proc. Roy. Soc. **A142**, 88 (1933).
[9] The details of design and operation will be submitted for publication in Rev. Sci. Inst.

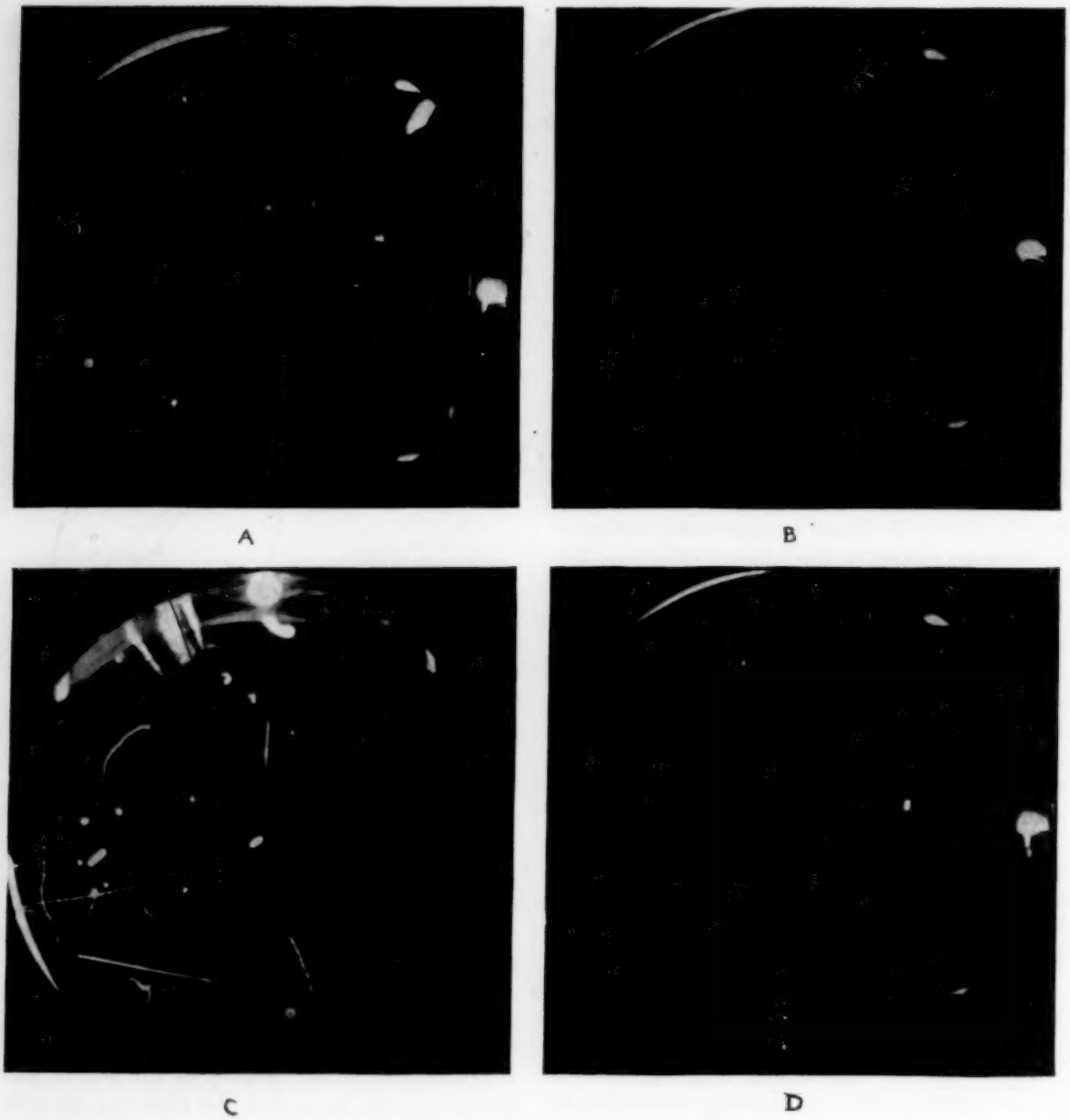

FIG. 2. Tracks of recoil-protons observed with the gas of the expansion-chamber at 12.9 atmospheres pressure. The source of neutrons is behind the center of the illuminated area in the upper left-hand portion of the photographs. (A) A recoil-proton from a fluorine neutron, produced in hydrogen. The actual length of the track was 1.65 cm, corresponding to a range of 5.28 cm in air at 76 cm and 15°C. (B) A recoil-proton from a boron neutron, produced in methane. The actual length was 2.10 cm, corresponding to a range of 22.5 cm in standard air. (C) A long recoil-proton from a beryllium neutron, in methane. The actual length was 5.33 cm, corresponding to a range of 57.0 cm in standard air. (D) A short recoil-proton from beryllium, in hydrogen. The actual length was 1.08 cm, corresponding to a range of 3.68 cm in standard air. This track is nearly in the direction of the source so that (neglecting the possibility that it was produced by a scattered neutron) the proton obtained practically the entire energy of the neutron. *Note:* (C) is incorrectly placed. It should be turned 90° in a clockwise direction.

thick quartz plate. This was done by projecting through a piece of plate glass which gave the same displacement as the quartz plate.

On the photographs were found numerous straight dense tracks which began and ended in the chamber and thus could definitely be

identified as recoil protons. Examples of such tracks are shown in Fig. 2. With methane in the chamber many recoil carbon atoms must have been produced, but the length of the longest carbon track was much shorter than the shortest proton track which was measured in methane. Thus there is no possibility that carbon atoms were mistaken for protons. Only sharp narrow tracks were included. Many were found which were rather broad because the proton was projected before completion of the expansion. These were rejected because in this case the stopping power of the gas at the time the ion-track was formed could not be determined.

Hydrogen with a pressure after expansion of about 13 atmospheres was useful for investigating neutrons having energies corresponding to recoil protons up to a range of about 18 cm in air. Methane at the same pressure allowed measurement of protons up to about 90 cm equivalent air range, but could not be used below about 7 cm because the tracks were too short (<0.6 cm) to measure with sufficient accuracy. The hydrogen was obtained from commercial cylinders. The only impurity of consequence was about one percent air which was allowed for in calculating the stopping power. The methane was also obtained from a cylinder; there were no impurities which could appreciably alter the stopping power.

Results

Fluorine

About 9000 pairs of photographs were taken with hydrogen in the chamber. On the photographs 163 protons were found which were suitable for measurement of the range. In addition, since a knowledge of the angular distribution of the recoil protons was of importance in deciding how to treat the observed data on the proton ranges, the angle of projection was measured for 101 of these protons. Only a portion of the total number was used because some of the tracks start at points in the gas too near the source to allow measurement of the angle. The results on the angular distribution are presented in the curve of Fig. 3, where the number of protons in 15° intervals is plotted against the angle (ϕ of Fig. 1) between the direction of the neutron and that of the recoil proton. Since the

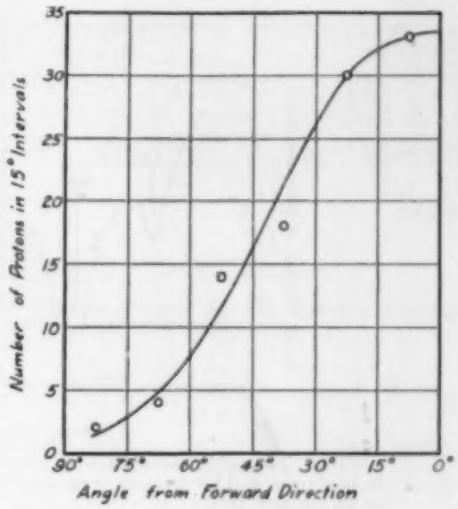

FIG. 3. The angular distribution of the recoil protons from Po-F neutrons.

lengths of the tracks used in constructing this curve were small in comparison to the dimensions of the chamber, the longest being 2.3 cm in actual length, the observed distribution should approximate the true distribution without the necessity of making geometrical corrections. It is noted that a large majority of the protons are projected in nearly the forward direction. This result agrees with Kurie[7] but not with the results of Monod-Herzen[10] or Meitner and Philipp.[11] This lack of agreement is probably due to differing geometrical conditions. It is clear, however, that with our arrangement the majority of the protons which were used for determining the neutron energies were mainly in the forward direction and thus in the majority of cases obtained nearly the entire energy of the neutron. Accordingly, in inferring the energy distribution of the neutrons from the range distribution of the recoil protons it seemed unnecessary to take the angle of projection into account. In fact if it is attempted to do this, by computing the energy of the neutron from the range of the proton and the angle, serious error may be made because of the presence of scattered neutrons. For instance, if a fast neutron were scattered into the chamber at 90° and produced a fairly long proton at nearly right angles to the direction from the source, and

[10] G. Monod-Herzen, J. d. Physique **5**, 95 (1934).
[11] L. Meitner and K. Philipp, Zeits. f. Physik **87**, 484 (1934).

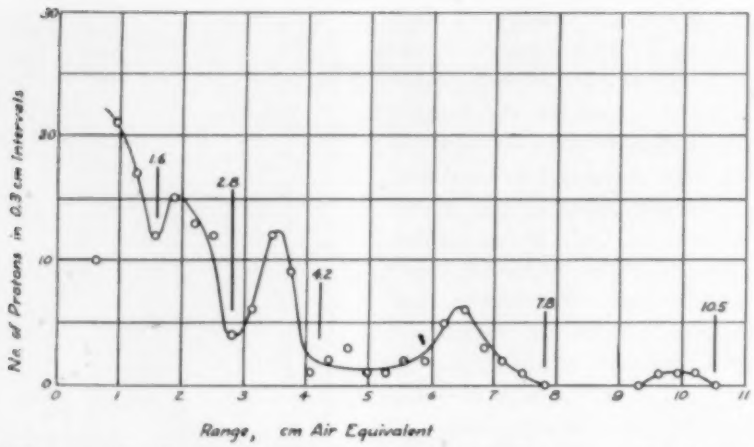

FIG. 4. The range distribution of the recoil protons from Po-F neutrons. The observed ranges in hydrogen at 12.9 atmospheres and 25°C have been converted to the equivalent ranges in air at 76 cm and 15°C.

if this were classed as a proton produced by a neutron coming directly from the source, the computation would lead to an excessively high energy for the neutron. If the angular correction is not made the presence of neutrons scattered from the brass walls of the chamber introduces no serious error because the maximum energy that a neutron can lose in a single elastic collision with a copper or zinc nucleus is only about six percent of its original energy.

The data on the range-distribution are presented in Fig. 4, where the number of protons in 0.3 cm intervals of range is plotted against the air-equivalent range (76 cm, 15°C). These experiments were carried out with hydrogen in the chamber whose pressure after expansion was 12.9 atmospheres at the temperature of the chamber, 25°C. The actual ranges extended from about one mm, the shortest track which could be identified as a proton, to 3.2 cm, the longest observed. These ranges were converted to air under standard conditions by using the differential stopping power data given by Gurney.[12] From these data a curve was obtained relating the stopping power to the range. This curve was extended beyond the ranges investigated by Gurney by assuming that his values of the differential stopping power at long ranges, 0.206, represents the limiting value which should apply to all longer ranges. It will suffice here to give the values of the stopping power from this curve at 2 cm proton-range and at 10 cm. These stopping powers are 0.237 and 0.218, respectively. In making this conversion it was necessary also to take into account the stopping power of the alcohol vapor in the chamber. The stopping power was computed from data given by Philipp.[13]

It will be noted that the range-distribution curve (Fig. 4) shows distinct maxima and minima.[14] Since the number of protons is not very large, an appreciable amount of statistical fluctuation is expected, but it is believed that the points lie too consistently on a smooth curve, particularly in the regions where the larger counts were obtained, to be able to attribute the peaks entirely to this cause. Additional evidence that the peaks represent a real property of the neutron emission was obtained by plotting separately the first and second halves of the data. It was found that substantially the same maxima and minima were present in both curves. The presence of peaks in the range distribution of the recoil protons evidently means that a large fraction of the neutrons are emitted in groups and not with a continuous distribution of energy. From curves of this type it is not possible to obtain the exact energy distribution of the neutrons of a group nor the relative intensities of the groups,[15] but it is possible to find their

[12] R. W. Gurney, Proc. Roy. Soc. **A107**, 340 (1925).

[13] K. Philipp, Zeits. f. Physik **17**, 23 (1923).

[14] This curve differs somewhat from the one previously published (reference 5). The change was caused by a more careful measurement of the proton ranges.

[15] The range distribution curves do not directly give the intensity distribution of the neutrons because the target

maximum energy, which is the maximum energy of the corresponding group of recoil protons. The curve shows five groups of protons, whose maximum energies were chosen as indicated in the figure.

To explain the presence of neutron groups it may first be noted that since the α-particles were allowed to strike a thick piece of CaF_2 they had a continuous distribution of velocity in the material. Accordingly, if groups of neutrons are observed, it must mean that α-particles having certain particular values of the velocity, or narrow ranges of velocity, are more effective in the production of neutrons than others. In the disintegration of light elements by means of an α-particle which results in the emission of a proton, similar results have been obtained and have been shown to be due to the entrance of the α-particle into the nucleus through resonance levels. The resonance levels for the entrance of an α-particle into the fluorine nucleus have been found by the studies of this type of disintegration. Chadwick and Constable[16] found three resonance levels and further that two groups of protons were produced by α-particles entering through each level. For each resonance level the group of protons having the shorter range is produced when the resulting nucleus (Ne^{22} in this case) is left in an excited state. This nucleus then returns to the normal state with the emission of a γ-ray.

It is found that a satisfactory explanation of the neutron groups can be obtained by assuming the same type of process for the disintegration with emission of a neutron. The proposed disintegration scheme is shown by the energy diagram of Fig. 5 and in Table I. The energy of the recoil protons is obtained from the range-velocity data given by Blackett.[17] This scheme was obtained in the following manner. The resonance levels were taken to be the same as

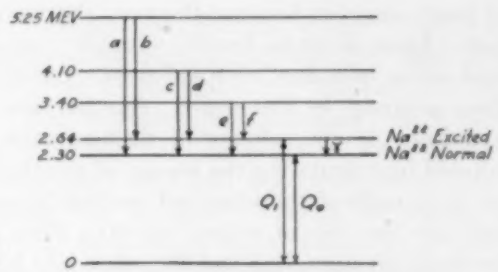

FIG. 5. Energy diagram for the fluorine disintegration scheme.

TABLE I. *Fluorine disintegration scheme.* (Energies in M.E.V.)

E_α	E_{n_0}	E_{n_1}	E_{n_0}	E_{n_1}	Energy of disintegration
	(Calc.)		(Obs.)		
5.25	(a) 2.54	(b) 2.15	(a) 2.54	(b) 2.12	$Q_0 = -2.30$ $Q_1 = -2.68$
4.1	(c) 1.43	(d) 1.09	(c) 1.45	(d) 1.09	$Q_0 = -2.28$ $Q_1 = -2.60$
3.4	(e) 0.72	(f) 0.37	(e) 0.68	(f) ——	$Q_0 = -2.34$ $Q_1 =$ ——
					Av. $Q_0 = -2.30$ Av. $Q_1 = -2.64$ Av. $E_\gamma = 0.34$

$E\alpha$ = energy of resonance level for α-particle.
E_{n_0}, E_{n_1} = maximum energies of neutron groups.
Q_0, Q_1 = energies of disintegration.
E_γ = energy of γ-ray.

those for the proton disintegration (because in both cases the α-particle enters the same nucleus). The observed neutron group of highest energy (group (a)) was attributed to the highest resonance level; and when the neutron obtains this energy it is supposed that the resulting nucleus is left in the normal state. The energies of groups (c) and (e) were then calculated by using the α-particle energies given by the energies of the resonance levels and the energy of disintegration (Q_0), obtained from group (a) and the energy of the first resonance level. Groups (b), (d) and (f) were obtained by assuming a value for (b) and calculating (d) and (f) as before. The value of (b) was chosen to give the best agreement with the experimental data. It was found that better agreement was obtained if the energy of the second resonance level was taken to be 4.1 M.E.V. instead of the value 4.0 M.E.V. given by Chadwick and Constable. An analysis of their data indicated that the value 4.1 M.E.V. is not inconsistent with it. The calculated values of the neutron groups agree reasonably well with the observed values. The group of lowest energy has

area for a collision between the neutron and the hydrogen nucleus increases rapidly with decreasing energy of the neutron, and also because a greater fraction of the longer tracks have to be rejected because they strike the walls of the chamber. The second reason is not as important for fluorine-neutrons as it is for beryllium-neutrons where many of the tracks are considerably longer.

[16] J. Chadwick and J. E. R. Constable, Proc. Roy. Soc. **A135**, 48 (1932).

[17] P. M. S. Blackett, Proc. Roy. Soc. **A135**, 132 (1932), and Blackett and Lees, Proc. Roy. Soc. **A134**, 665 (1932).

not been observed because the very short recoil tracks (2 mm in actual length) which it produces could not be measured with sufficient accuracy to detect a group in this region. Another test of consistency of the scheme of disintegration is obtained by calculating the energy of disintegration from each of the observed neutron groups. There are two sets of values, one (Q_0) when the nucleus is left unexcited and the other (Q_1) when it remains excited. The three values in each set should of course agree with each other. Reasonably good agreement was found, as shown in Table I. The energy of the γ-rays is given by the energy difference Q_0-Q_1. By using the average values of Q_0 and Q_1, this comes out 0.34 M.E.V. This predicted γ-radiation presents no difficulty since it is known that soft γ-rays are produced when fluorine is bombarded by α-particles. The γ-rays predicted by the neutron disintegration have about half the energy of those predicted by the proton disintegration, so that it is expected that a careful analysis of the γ-rays from the disintegration of fluorine by α-particles should reveal these two lines. The scheme of disintegration which is presented above was found to be the only one which is able to account for the observed groups using the three given resonance levels.[18]

The maximum energy of the neutrons from Po-F is found from the curve to be 2.5 M.E.V. This is considerably lower than the value 4.2 M.E.V. which we find for boron, and confirms Bonner's previous work[19] which indicated that the neutrons from fluorine have less energy than those from boron.

Boron

4000 pairs of photographs were taken, about half of these with hydrogen and the rest with methane, both gases being at the same pressure as before. The observed ranges were converted to air-equivalent length as before. The conversion for the hydrogen data was made in the same manner as for fluorine. For the observations in methane a range-stopping-power curve was drawn in the same way using data from Van der Merwe.[20] In order to be able to convert long-range protons it was necessary to make a rather large extrapolation from his data, but since the stopping power of methane changes only slowly with the range at long ranges it is believed that the extrapolated values cannot be in error by more than a few percent. The values adopted for methane at 76 cm and 15°C relative to air were 0.85 at 10 cm range and 0.83 at 70 cm, the intermediate values lying linearly between these. The results are presented in the curves of Fig. 6.

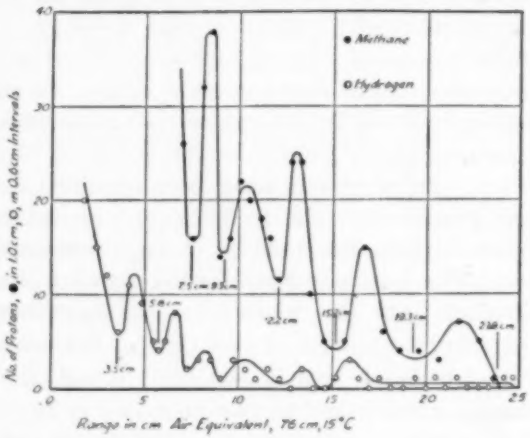

FIG. 6. The range distribution of the recoil protons from Po-B neutrons. Upper curve: recoil protons in methane. Lower curve: recoil protons in hydrogen. The observed ranges have been converted to the equivalent ranges in air.

It is seen that six groups are indicated by the methane curve, while two additional groups are shown by the hydrogen data below the 7.0 cm range where the tracks in methane become too short to measure accurately. Where the two curves overlap the hydrogen curve also gives indication of the presence of peaks which correspond approximately to those of the methane curve. As in the case of fluorine separate plots of the first and second halves of the data again gave consistent results, so that as before we believe that the maxima and minima represent the effect of neutron groups. The values of the maximum range corresponding to each group are indicated in the figure; these values and their corresponding energies are given in Table II.

TABLE II. *Boron neutron groups.*

Maximum range of recoil proton group (cm)							
23.8	19.3	15.2	12.2	9.3	7.5	5.8	3.5
Energy of neutron group (M.E.V.)							
4.16	3.65	3.17	2.75	2.35	2.05	1.77	1.29

[18] This scheme is substantially the same as one of two schemes kindly suggested to us by Dr. Wu in a private communication.

[19] T. W. Bonner, Phys. Rev. **45**, 601 (1934).

[20] C. W. Van der Merwe, Phil. Mag. **45**, 379 (1923).

In the case of boron it is not possible to fit the eight observed neutron groups into a disintegration scheme because of lack of knowledge of the resonance levels. It seems that four resonance levels would be needed. From neutron excitation curves (number of neutrons as a function of the α-particle energy) Curie and Joliot[21] have found only one level. From the present results it seems probable that others exist. For boron it is not possible to use the resonance levels found from the disintegration with emission of a proton, as was done for fluorine, because of complications caused by the existence of the two isotopes. The proton disintegration has been satisfactorily explained by the reaction $B_5^{10}+\alpha \rightarrow C_6^{13}+p$ involving the isotope B^{10}. For the neutron disintegration two reactions have been proposed. Chadwick[2] assumed $B_5^{11}+\alpha \rightarrow N_7^{14}+n$, while Curie and Joliot[22] suggest $B_5^{10}+\alpha \rightarrow N_7^{13}+n$, followed by $N_7^{13} \rightarrow C_6^{13}+e^+$. It seems possible that both the above reactions occur. B^{11} would be expected to give the greater neutron intensity. The number of α-particles captured by B^{11} should be about five times as great as the number for B^{10} since it is about five times more abundant in the isotopic mixture. In addition B^{10} may disintegrate either with emission of a proton or with a neutron so that the relative number of neutrons from B^{10} is still further reduced, perhaps by a factor of two.

An estimate of the relative numbers of neutrons from B^{10} and B^{11} can be obtained in another way. It is evident that in the neutron disintegration of B^{10} a positron must accompany each neutron, while only neutrons are given by B^{11}. Thus by comparing the relative numbers of neutrons and positrons an estimate of the relative numbers of neutrons from the two reactions can be obtained. It is possible to do this by comparing the emission of neutrons and positrons by boron with that by aluminum.

Using an ionization chamber filled with hydrogen at 20 atmospheres and using a 2 cm lead filter to absorb the γ-rays, it was found that the ratio of the ionization currents produced by boron and aluminum neutrons was 25/1. Correcting for the fact that the maximum energy of the boron neutrons is about double[23] that of the aluminum neutrons, it appears that boron gives from 10 to 20 times as many neutrons as aluminum. On the other hand Curie and Joliot[24] found that positrons are produced in roughly equal numbers by boron and aluminum. From this it appears that the large excess in the number of neutrons from boron must be due to B^{11}. Both arguments indicate an approximate factor of 10 or more between the neutron emission of B^{11} and B^{10}.

The maximum energy of the neutrons from boron as obtained from the curve of Fig. 6 is higher than that found by Chadwick[2] and by others.[21] We find the value 4.2 M.E.V. while the earlier value was 3.3 M.E.V. This difference is not surprising since the tendency has been toward detecting neutrons of higher energy as more data are accumulated. It may be pointed out that we observe a rapid decrease in the number of protons at about 3.2 M.E.V. which might have been taken as the maximum by previous observers. If both isotopes give neutrons, the neutrons having a maximum energy of 4.2 M.E.V. may be due to either B^{10} or B^{11} but since the intensity of this group seems fairly high, it is probable that they come from B^{11}. Assuming that they come from B^{11}, this higher value of the maximum energy reduces the mass of the neutron, as calculated by Chadwick from the disintegration of B^{11}, from 1.0067 ± 0.0010 to 1.0058 ± 0.0010. The new value agrees somewhat more satisfactorily with the value of the upper limit, 1.0063 ± 0.0008, which has been calculated by Bainbridge[25] from the disintegration of lithium by α-particles. For the disintegration of B^{10} the mass as calculated by Curie and Joliot[21] is considerably higher using either the old value of the neutron energy or the new. A possible explanation of this discrepancy is that there is a relatively small number of neutrons from B^{10} with a maximum energy of about 7.5 M.E.V. Since according to the argument given above the number of neutrons from B^{10} is only about 1/10 or

[21] I. Curie and F. Joliot, J. d. Physique **4**, 278 (1933).
[22] I. Curie and F. Joliot, Nature **133**, 721 (1934).

[23] The maximum energy of the neutrons from aluminum is given by Curie-Joliot as 2 M.E.V., those from boron as 3.3 M.E.V. Using our value for boron (4.2 M.E.V.) we obtain a somewhat higher ratio.
[24] I. Curie and F. Joliot, J. d. Physique **5**, 153 (1934).
[25] K. T. Bainbridge, Phys. Rev. **43**, 367 (1933).

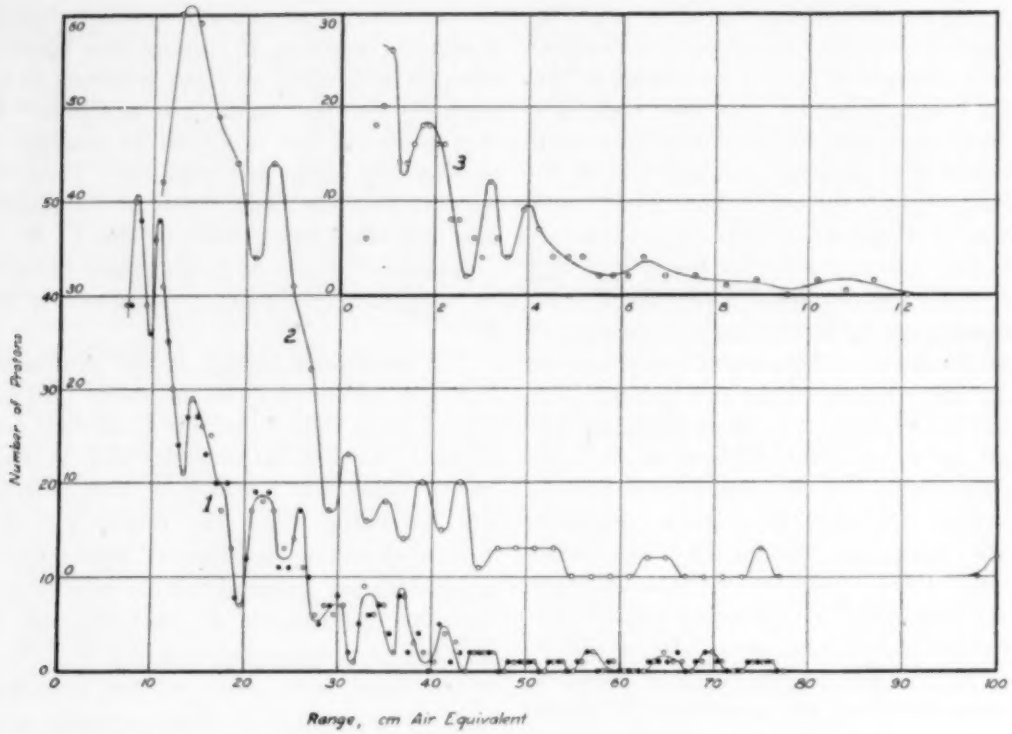

FIG. 7. The range distribution of recoil protons from Po-Be. The points on curve 1 (two sets of overlapping intervals are used) show the distribution of recoil protons in methane; curve 3 gives the data for recoil protons in hydrogen; curve 2 (shifted upward 10 divisions) is a reproduction of Blau's curve.

less of the number from B^{11}, they might have escaped detection.

Beryllium

A total of about 8000 photographs were taken, 3000 with hydrogen and 5000 with methane, the pressure being the same as before. 180 recoil protons were measured in hydrogen, 575 in methane. The observed ranges were converted to air-equivalent range in the manner described above. The results for methane are given in curve 1 of Fig. 7, those for hydrogen in curve 3 of this figure. The longest proton track which was measured corresponds to a length of 76 cm in air, though two tracks which collided with the wall of the chamber had lengths greater than 85 cm. This is approximately the maximum length of track which could be measured with our arrangement, and thus does not mean that these protons are the protons from Po-Be with the maximium energy. The maximium energy for Po-Be is probably at present best obtained by calculation from Dunning's work[4] with radon-Be. It is found to be approximately 11.7 M.E.V. corresponding roughly to a proton-range of 150 cm.

Again it is noted that the curves show maxima and minima and that for Be these seem to be very numerous. Apparently then it seems that beryllium disintegrates with the emission of a large number of neutron groups. Table III gives a list of the maximum ranges of all the groups which are indicated by the curves. Many of

TABLE III. *Beryllium neutron groups.*

Rp (cm)	*En* (M.E.V.)	*Rp* (cm)	*En* (M.E.V.)
1.3	0.58	31.8	4.87
2.7	1.07	36.0 (?)	5.26 (?)
3.5	1.31	39.7	5.57
5.4 (?)	1.68 (?)	43.5 (?)	5.85 (?)
7.5 (??)	2.06 (??)	47.3 (??)	6.13 (??)
9.75	2.42	51.5 (??)	6.42 (??)
13.5	2.94	54.5 (??)	6.64 (??)
16.5 (??)	3.32 (??)	60.0 (?)	7.06 (?)
19.5	3.65	67.3 (??)	7.49 (??)
24.3	4.20	71.5 (??)	7.76 (??)
28.0 (?)	4.56 (?)	77.5 (??)	8.10 (??)

Rp = maximum range of recoil-proton groups.
En = maximum energy of neutron groups.

these, however, are questionable, and some, particularly at the higher energies, where we were unable to obtain large counts, must be considered very questionable. These are indicated by question marks. Apparently the only other "differential" distribution curve for the neutrons from Po-Be is one recently given by Blau.[3] It has been reproduced in Fig. 7 (displaced upward ten divisions). It is seen that this curve also indicates numerous groups. For ranges between 15 and 45 cm the same groups are indicated at approximately the same maximum ranges. Between 10 and 15 cm agreement cannot be expected because the range intervals on Blau's curve are too large. Above 45 cm both curves are not reliable on account of the small number of protons but it may be noted that even in this region the three groups indicated by her curve are also indicated by ours. Blau's curve also indicates a group at 100 cm which is outside of the region we were able to investigate.

In order to account for the observed large number of groups it is evident that a large number of resonance levels are needed. In fact, Kirsch and Slonek[26] apparently have found five resonance levels in the relatively narrow range of energy which they investigated, between 3.7 and 5.3 M.E.V. The work of Rasetti,[27] Curie-Joliot,[21] Chadwick,[2] and others indicates two further resonance levels at about 2.6 and 1.5 M.E.V. However, to account for all the neutron groups we find it necessary to assume four additional levels lying between 3.7 and 1.4 M.E.V. and forming, along with Kirsch and Slonek's levels and the ones at 2.6 and 1.5 M.E.V., a series of roughly equally spaced levels. In this way, and by assuming that the resulting nucleus (C_6^{12}) can be left in two possible excited states, it has been possible to explain fairly satisfactorily the observed neutron groups as well as the γ-rays produced by this disintegration. It was necessary to assume two excited states instead of the single excited state which was adequate for fluorine in order to explain both the group at about 12 M.E.V. and the groups of very low energy extending down to about 0.6 M.E.V. This disintegration scheme is given in Table IV. The first column gives the resonance levels. The first five

TABLE IV. *Beryllium disintegration scheme.*

$E\alpha$ (M.E.V.)	En_0 (M.E.V.) calc.	obs.	En_1 (M.E.V.) calc.	obs.	En_2 (M.E.V.) calc.	obs.
5.3	11.3	11.7*	7.1	7.06	4.2	4.20
4.8	10.8	—	6.6	6.64	3.7	3.65
4.4	10.4	—	6.2	6.13	3.3	3.32
4.1	10.1	—	5.9	5.85	3.0	2.94
3.7	9.8	—	5.5	5.57	2.7	—
3.4 (?)	9.5	9.5**	5.2	5.26	2.4	2.42
3.0 (?)	9.1	—	4.9	4.87	2.1	2.06
2.6	8.7	—	4.5	4.56	1.7	1.68
2.2 (?)	8.3	8.10	4.1	4.20	1.3	1.31
1.8 (?)	7.9	7.76	3.7	3.65	1.0	1.07
1.4	7.5	7.49	3.3	3.32	0.6	0.58

$Q_0 = 6.2$ M.E.V. $E\gamma_1 = 4.1$ M.E.V.
$Q_1 = 2.1$ M.E.V. $E\gamma_2 = 6.8$ M.E.V.
$Q_2 = -0.6$ M.E.V.

* This maximum energy for the neutrons from Po-Be was calculated from Dunning's data.
** The 100 cm group found by Blau.

are those given by Kirsch and Slonek. The lowest one was taken at 1.4 instead of the rough value of 1.5 given by Chadwick because it fitted better into the scheme. The second, third and fourth columns give the values of the calculated and observed energies of the neutron groups for the cases when the resulting nucleus is left unexcited or excited to either the first or second energy-level, respectively. The scheme predicts several groups which have not been observed, but all but one of these is at long ranges which are beyond the region investigated. On the other hand, it gives fairly well all but one of the observed groups, and this group is one which is very doubtful. Two γ-ray lines are predicted, one having an energy of 4.1 M.E.V., the second, 6.8 M.E.V. The experimental data on the energy of the γ-rays from Po-Be, does in fact indicate the presence of a line at about 4.5 M.E.V. and possibly a small amount of radiation at around 7 M.E.V.[2, 28, 29] The disintegration scheme which has been given is of course rather arbitrary because of lack of exact knowledge of the resonance levels and also of the energy of the γ-rays. A confirmation of this scheme or the development of a more satisfactory one must await further experimental data.

In closing we wish to thank Dr. J. Cramer Hudson whose gift of spent radon tubes materially aided this work.

[26] G. Kirsch and W. Slonek, Naturwiss. **21**, 62 (1933).
[27] F. Rasetti, Zeits. f. Physik **78**, 165 (1932).
[28] I. Curie and F. Joliot, J. d. Physique **4**, 494 (1933).
[29] J. Chadwick, P. M. S. Blackett and G. P. S. Ochialini, Proc. Roy. Soc. **A144**, 235 (1934).

The Heat of Dissociation of CO and the Electron Affinity of O

W. Wallace Lozier,* *Palmer Physical Laboratory, Princeton University*

(Received June 16, 1934)

An apparatus previously described has been employed in a study of the dissociation produced by primary electron impact in CO and O_2. The processes studied in O_2 are $O_2^- \rightarrow O^- + O$ at 2.9 v and $O_2^- \rightarrow O^- + O^*$ at 12.0 v with an estimated accuracy of ± 0.2 v. These figures refer to the potential energy of the dissociation products, the normal molecule considered as zero. These results give two values of E_e, the electron affinity of the oxygen atom, both equal to 2.2 ± 0.2 v. The processes studied in CO are $CO^- \rightarrow C + O^-$ at 9.5 v, $CO \rightarrow C^+ + O^-$ at 20.9 v, and $CO^+ \rightarrow C^+ + O$ at 22.8 v, with an estimated accuracy of ± 0.1 v. It is concluded that $D(CO)$ may have one of two possible values, 9.6 ± 0.1 or 11.6 ± 0.1 v. These experiments are unable to decide between the two but most of the evidence from other sources points to the lower value. If $D(CO) = 9.6$ v we must admit the possibility of stable excited O^- ions. However, if $D(CO) = 11.6$ v, these experiments on CO give two values of E_e, 1.9 and 2.1 v. The processes involved in the formation of negative ions by electron impact are discussed.

Introduction

WHEN an electron suffers an impact with a gas molecule the phenomena which may be exhibited are many and varied. Especially interesting are those phenomena in which the molecule after impact manifests ionization. This paper will deal with certain aspects of ionization in diatomic gases. Numerous mass-spectrograph studies[1] have shown that the most probable type of ionization by electron impact in diatomic gases is the removal of one electron from the molecule. Next in probability is the formation of atomic ions, positively charged. In recent years a distinctly different product of ionization has been observed—namely, the negative atomic ion.[2, 3, 4, 5, 6] This product is far less abundant than the products of simple ionization and dissociation with ionization.

Another new aspect of ionization phenomena is the observation of atomic ions with large kinetic energies (several volts). Such processes were studied by Bleakney[7] in H_2 and later by the author and others[4, 8, 9, 10] in H_2, N_2 and CO. They give important information on the molecular binding in different electronic states. A description of improved apparatus and revised results in H_2 and N_2 has recently been published.[10] This paper describes similar results in O_2 and CO.

The specific relation between the maximum kinetic energy of the ions formed and the electron energy may be repeated here for future reference.[4] If a molecule is put into an unstable state by the communication of potential energy V_i, and subsequently dissociates into two parts of masses m_1 and m_2, the kinetic energy of constituent 1 is given by

$$(\text{K.E.})_1 = [m_2/(m_1+m_2)][V_i - (U_2 - U_1)], \quad (1)$$

where U_1 is the potential energy of the molecule before impact and U_2 is the potential energy of the dissociated constituents of the molecule. This relation is a linear one with the slope determined by the ratio of the masses of the dissociating partners. The quantities measured experimentally are V_i (the appearance potential) and the kinetic energy of the ions; from these we calculate $U_2 - U_1$. Two procedures are available for this determination. One is to plot the kinetic energies of the ions against V_i and extrapolate the straight line to zero kinetic energy, at which point $V_i = U_2 - U_1$. The other is to substitute the experimental quantities into Eq. (1), by using the proper mass ratio, and solve for $U_2 - U_1$. Both procedures are used in the following report.

Apparatus

Without repeating the description of the apparatus[10] we may recall that the ionization cur-

* The experimental part of this work was done while the writer was a National Research Fellow.

[1] H. D. Smyth, Rev. Mod. Phys. **3**, 347 (1931).
[2] W. W. Lozier and Walker Bleakney, Phys. Rev. **36**, 1417L (1930).
[3] A. L. Vaughan, Phys. Rev. **38**, 1687 (1931).
[4] J. T. Tate and W. W. Lozier, Phys. Rev. **39**, 254 (1932).
[5] J. T. Tate and P. T. Smith, Phys. Rev. **39**, 270 (1932).
[6] H. D. Smyth and D. W. Mueller, Phys. Rev. **43**, 116 (1933).
[7] Walker Bleakney, Phys. Rev. **35**, 1180 (1930).
[8] W. W. Lozier, Phys. Rev. **36**, 1285 (1930).
[9] W. W. Lozier, Phys. Rev. **43**, 776A (1933).
[10] W. W. Lozier, Phys. Rev. **44**, 575 (1933).

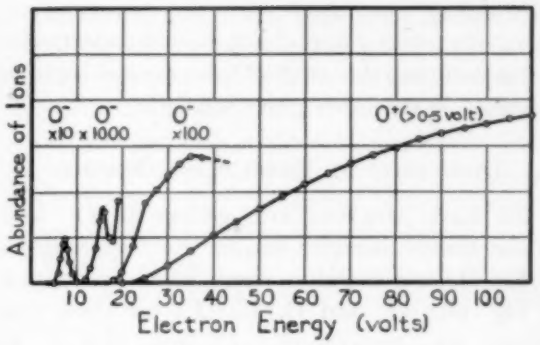

FIG. 1. Products of ionization of O_2, O_2^+ not included here.

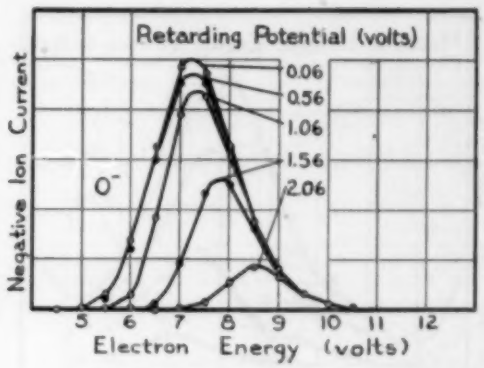

FIG. 2. O^- ionization curves in O_2 for different retarding potentials.

rent reaching a collector is measured as a function of either the energy of the bombarding electrons or the potential retarding the ions. Letters used in the detailed description of procedure below refer to Fig. 1 of reference 10.

The CO was generated by the action of formic acid on sulphuric acid and dried by liquid air. The O_2 was prepared electrolytically, and dried by P_2O_5. As before the rate of flow method was used for the admission of the gas into the tube. The gas pressure in the experimental chamber was maintained between 5×10^{-5} and 1×10^{-5} mm Hg.

RESULTS ON OXYGEN

Fig. 1 depicts, with the exception of O_2^+, the ionization products of electron bombardment of O_2 and gives a rough estimate of their relative numbers. The identification of the first and third groups (O^-) has been made by Bleakney.[11] The fourth group (O^+) has been observed in all mass-spectrograph investigations[1] of O_2. The second group of O^- ions at 15 v has not been identified or observed elsewhere but the data to be given almost certainly identify it as O^-. The first two groups of negative ions have been analyzed as regards their kinetic energy. The electron voltage scale was fixed by assuming the ionization potential[12] of O_2 as 12.5 v.

Let us consider first the group of O^- ions at 7.2 v. Fig. 2 illustrates the change with retarding potential of the O^- current *vs.* electron energy curves. These curves show no ions having energies below about one volt. Greater retarding potentials stop first the ions formed at low electron energies. The fact that the curves merge at high electron energies means that not only are high speed electrons necessary to form high speed ions but they form only high speed ions. Fig. 3 shows a plot of the kinetic energies of these ions against their appearance potentials. For kinetic energies greater than 1.3 v the curve obeys the requirements of Eq. (1), i.e., a linear relation with slope 0.5. A projection of this straight line to zero kinetic energy requires $U_2-U_1=2.9$ v.

In Fig. 4 are shown curves of the negative ions at 15 v electron energy. As mentioned above these ions have not been observed elsewhere and consequently have not been identified definitely as O^-. But the fact that they can possess kinetic energies

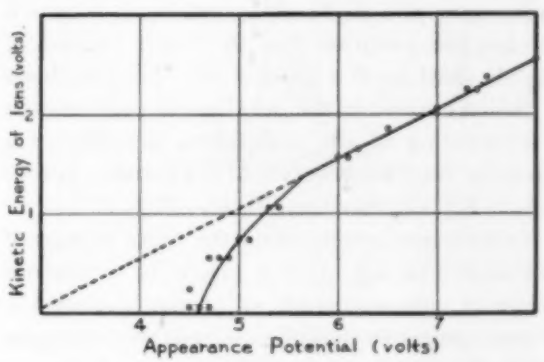

FIG. 3. A plot of the kinetic energy of the O^- ions of Fig. 2 plotted against their appearance potentials (see Eq. (1)).

[11] Dr. Walker Bleakney very kindly analyzed a sample of the O_2 used.

[12] R. S. Mulliken and D. S. Stevens, Phys. Rev. **44**, 720 (1933) have calculated the I.P. of O_2 as 12.2 ± 0.2 v and cited reasons why the experimental values should be higher. Since our experimental conditions more nearly approximate those of reference 5, we use the older value and allow a greater probable error, ±0.2 v, to these measurements.

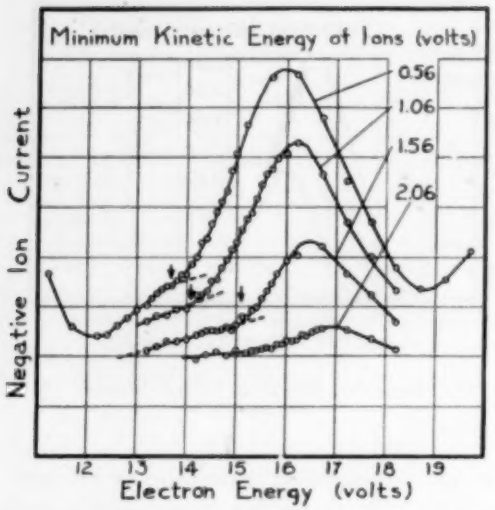

FIG. 4. O^- ionization curves in O_2 for different retarding potentials.

of as much as 2 v makes it almost necessary that the origin of this kinetic energy is a dissociation of the molecule into an atomic ion and a neutral atom. This ion being negatively charged must be O^- if it results from O_2. The possibility remains that it results from impurities. Our strongest evidence against this is that of all the other gases studied, none have negative ions at this electron energy. In lieu of any evidence to the contrary we shall designate this ion as O^- resulting from O_2.

It is difficult to obtain a test of Eq. (1) from the curves of Fig. 4. The upper curve shows traces of an unresolved peak on the low electron energy side of the main group, making impossible a precise determination of the appearance potential. The next two curves have determinable appearance potentials separated by 1 v which satisfies the condition that the linear relation of Eq. (1) must have a slope of 0.5. The smallness of the ion current in the lower curve prevents the determination of the appearance potential. On inserting the two observable appearance potentials in Eq. (1) there results $U_2-U_1=12.0$ v.

No data are presented on the other groups of ions shown in Fig. 1. For above 20 v electron energy it was impossible to obtain a condition of zero current to the collecting electrode in spite of a field arrangement suitable for keeping away all ions formed at the electron beam. This effect is probably associated with the photoelectric effect of excited gas molecules on the electrodes and is certainly due to the O_2 because of its nonexistence in the other gases studied.

Discussion of Results on Oxygen

We have observed two groups of O^- ions whose kinetic energies satisfy the requirements of Eq. (1) and therefore result from dissociation of O_2^- into O^- and O. U_2-U_1 for these two groups are, respectively, 2.9 and 12.0 v. In neither of these cases do we know the state of excitation of the dissociation products. We know that U_2-U_1 for dissociation into normal atoms, i.e., $O(^3P)+O(^3P)$ is 5.1 v. Thus from the first group of negative ions E_0, the electron affinity of the oxygen atom, is equal to $(5.1-2.9)$ v plus the excitation energy of the O and O^-.

Thus E_0 is ≥ 2.2 v. The neutral atom is probably unexcited for if it were in even the first excited state (^1D), E_0 would be ≥ 4.2 v. A plot of the square root of the ionization potential *vs.* atomic number curve for the proper series (FI, Ne II) gives E_0 as 3 to 4 volts and these curves, in all cases where the electron affinity is known, give too large a value. The O^- is very probably in a normal state for general considerations make it improbable that a negative ion will have many stable excited states. If such states exist they probably lie very near the ionization limit and this coupled with the 2.2 v binding energy mentioned above would call for a very large electron affinity, $E_0 \gg 2.2$ v.

Very little is known of the energy states of negative ions. However, the following examples support our contentions that stable excited states are scarce. The empirical data on the energy of the $1s2p\ ^1P^0$ state of two electron systems can be fitted to a power series in Z, the atomic number $aZ^2+bZ+\cdots$. On extrapolating to $Z=1$, we find this state is unstable for H^- (by about 0.3 v).

Likewise, Fermi[13] has made a rough calculation of the electron affinity of the iodine atom using the Fermi-Thomas atomic field. He finds a stable normal state but only unstable excited states of I^-.

[13] E. Fermi, Leipziger Vorträge, 109 (1928).

This scarcity of stable states of negative ions is undoubtedly due to the extremely rapid decrease of the atomic field outside the extranuclear electron cloud where the nuclear charge is very completely shielded. The above discussion[14] is no assurance of the non-existence of stable excited states; but it is probable that such states will lie near the continuum, i.e., they will not be very stable.

Proceeding to a discussion of the second group of O^- ions with $U_2 - U_1 = 12.0$ v, we point out that the lower portion of the energy level system of OI is well separated[15] with ^3P at 0.0 v, ^1D at 1.96 v, ^1S at 4.17 v, $^5S^0$ at 9.10 v and $^3S^0$ at 9.47 v. The identification of the neutral atom as any of the first three excited states is improbable because it would require the O^- ion to possess more potential energy than normal O. The next possibility is that the neutral atom is in the $^5S^0$ state which would make $E_0 = 2.2$ v plus any excitation energy of the O^- ion. For the same reasons as given above we assume the O^- is unexcited. This is exactly the same value for E_0 as we obtained before. Having made the identification of the neutral partner as $O(^5S^0)$ we can say the dissociation products $O(^1D$ and $^1S)$ would be concealed by the 7.2 v peak.

Results on Carbon Monoxide

A general idea of the types of ions and their relative abundance is shown in Fig. 5 as a function of the incident electron energy. The CO^+ curve was not determined in this work but was taken from that of Vaughan.[3] In the following discussion we shall consider in detail the different ions shown here. The absence of O^+ ions is confirmed by the work of Vaughan.

Let us consider first the group of O^- ions having their efficiency maximum at an electron energy of about 10 v. The identification of the ions was made by Vaughan[3] and they have been observed by others.[4, 5, 9] Fig. 6 shows this same current as a function of electron energy for different retarding potentials on the ions. The electron voltage scale was corrected by the observation of CO^+ ionization, which is known to appear at 14.1 v.[1, 5] Fig. 7 shows the complete curves for which Fig. 6 gives the initial portions.

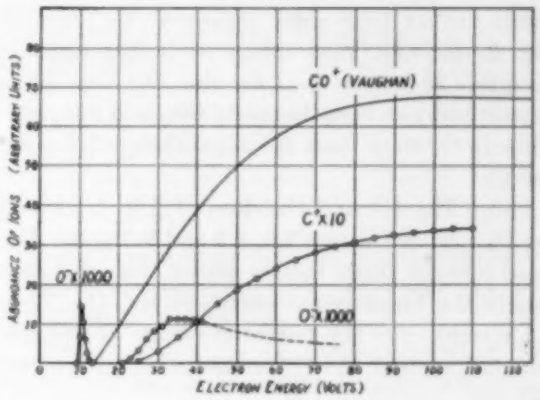

FIG. 5. Products of ionization of CO, with their relative numbers, as a function of electron energy.

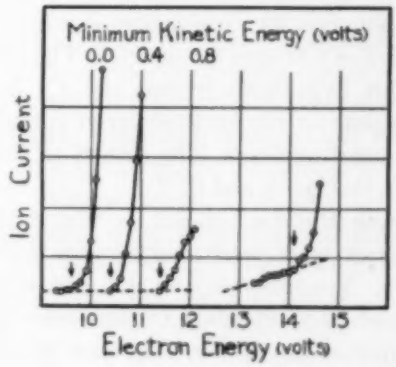

FIG. 6. Curves showing onset of O^- ionization in CO for different retarding potentials.

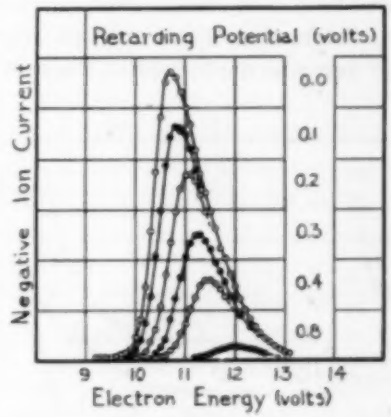

FIG. 7. Curves showing O^- ionization in CO for different retarding potentials.

[14] O. Oldenberg, Phys. Rev. **43**, 534 (1933). See especially footnote 9 there.

[15] All atomic energy values are from Bacher and Goudsmit, *Atomic Energy States*, McGraw-Hill (1932).

These curves bear some similarity to those of Fig. 2—namely, they merge at higher electron energies. However in CO, the O^- ions have kinetic energies lying between zero and one volt; while in O_2 no O^- ions have less than $\sim$1.3 volts energy.

Using Eq. (1) and the data of Fig. 6 we find for U_2-U_1 the values 9.6, 9.5 and 9.5 volts. The constancy of these figures shows that the data satisfy the linear requirements of Eq. (1). Thus 9.5 v represents the potential energy of the dissociated system $C+O^-$ measured from normal CO.

We shall next consider in detail the C^+ and O^- ionization shown in Fig. 5 occurring at about 20 v electron energy. In the earlier work it was suspected that this O^- ionization resulted from dissociation of CO into C^+ and O^-. The obvious test of this hypothesis is that the C^+ and O^- should appear at the same electron energy and occur in equal numbers. The results of this test are shown in Figs. 8 and 9.

To obtain the data shown in Fig. 8 the C^+ and O^- ions were separated by the following procedure. To observe the C^+ ionization a potential of 10 v retarding O^- ions was applied to the interval $L-M$ (see reference 10, Fig. 1) and a potential of 10.57 v retarding C^+ ions was placed on the interval $O-L$, the net effect being the collection of C^+ ions having energies greater than 0.57 v. To record the O^- current the potentials were reversed and the net potential retarding O^- ions was made 0.43 v. These energies 0.57 (C^+) and 0.43 (O^-) are in the ratio 4 to 3, the inverse ratio of the masses; so that, in accordance with the law of conservation of momentum, when all C^+ ions having energies >0.57 v are collected, all their dissociation partners (O^-) will be able to traverse a retarding potential of 0.43 v. The total minimum kinetic energy associated with the two ions is 1.0 v. Fig. 8 illustrates the behavior of C^+ and O^- current subject to the conditions described above, the lower curve shows the difference C^+-O^-. From an electron energy of 22.0 to 23.8 v the C^+ and O^- occur in equal numbers indicating that the O^- results from a splitting of the CO molecule in C^+ and O^-. At 23.8 v a new process contributes to the formation of positive ions. This process has a much greater probability than the splitting process. Fig. 9 shows the difference current C^+-O^- for higher retarding potentials subject to the same conditions as in Fig. 8. As in Fig. 8 the curves are characterized by the equality of C^+ and O^- ionization up to the indicated potentials, where the excess positive ionization occurs. The appearance potential of this ionization shifts by 1 v in successive curves. This likewise is the increment of ion kinetic energy between successive curves assuming the positive ionization is due to C^+. The equality of these increments verifies the identification of this positive ionization as C^+. Use of Eq. (1) yields U_2-U_1 as 20.9 v for the equal C^+ and O^- ionization and U_2-U_1 as 22.8 v for the excess positive ionization.

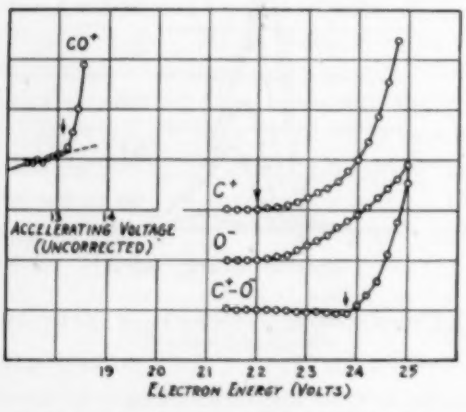

FIG. 8. Curves showing the equality of the initial portions of the C^+ and O^- ionization curves, suggesting splitting of CO into C^+ and O^-.

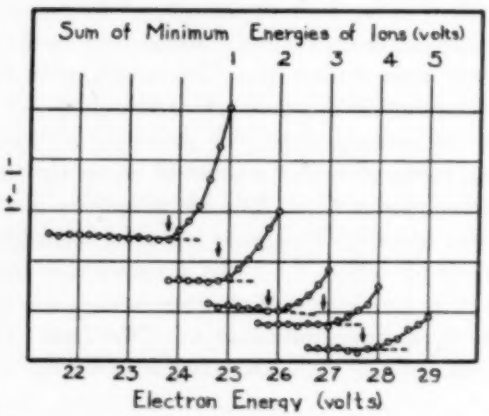

FIG. 9. Curves of difference between C^+ and O^- ionization for retarding potentials higher than in Fig. 8. The numbers at the top refer to the curves which terminate immediately below.

Independent evidence for the correctness of our identification of these latter ions comes from the work of Vaughan.[3] His mass-spectrograph studies of CO showed the appearance of the main part of the C^+ ionization at 22.5 ± 0.1 v. However, his C^+ curves[16] show current, which he attributed to imperfect resolution of H_2O^+ and C^+, persisting down to about 20.5 v electron energy. We believe this current is due to the C^+ ions associated with the O^- ions occurring at 20.9 v. The failure of Vaughan[3] to observe O^+ ionization agrees with our identification of the ionization beginning at 22.8 v as due to the dissociation of CO^+ into $C^+ + O$.

Discussion of Results on CO

To summarize our findings we may say that the potential energies of the dissociation products are as follows: $C+O^-$ at 9.5 v, $C^+ + O^-$ at 20.9 v, and $C^+ + O$ at 22.8 v. These values are believed accurate to ±0.1 v. Since our experiments can tell us nothing concerning the state of excitation of these dissociation products, we must have recourse to independent information. If we can make the proper identification we can calculate $D(CO)$ and obtain information concerning E_0, the electron affinity of the oxygen atom.

In the following it will be shown that there are two interpretations between which we cannot discriminate with certainty. The first of these is based on the assumption of normal dissociation products for the system $C^+ + O$ at 22.8 v. This requires $D(CO)$ to be 11.6 v. We note that the products $C^+ + O^-$ lie below $C^+ + O$ by 1.9 v while $C+O^-$ lie below $C+O$ by 2.1 v. These figures 1.9 and 2.1 v would then be interpreted as the affinity of O for an electron. These values are in agreement with the value 2.2 ± 0.2 v obtained from the results on O_2.

The other interpretation is based on the assumption that the dissociation products $C^+ + O$ at 22.8 v are excited. Possible identifications and the consequent values of $D(CO)$ are given below.

C^+	O	$D(CO)$
^2P	^1D	9.6 v
^2P	^1S	7.4
^4P	^3P	6.4

Of these, the last two are unreasonably low. The first is in good agreement with the hitherto accepted value of $D(CO)$. This value, 9.8 v, is obtained from the following equations:

$O \rightarrow \frac{1}{2}O_2$	-2.55 v[17]
$C \underset{gas}{\rightarrow} C_{solid}$	-6.1[18]
$C_{solid} + \frac{1}{2}O_2 \rightarrow CO$	-1.14[19]
$C_{gas} + O \rightarrow CO$	-9.8 v.[20]

The 0.2 v difference could be ascribed to errors in the thermochemical data, especially the heat of sublimation of carbon.

The interpretation of other results of this paper are more involved for $D(CO)=9.6$ v than for 11.6 v. We have observed the products $C+O^-$ at 9.5 v and $C^+ + O^-$ at 20.9 v. Using $D(CO)=9.6$ v we calculate $C^+ + O$ (both normal) to be at 20.8 v. We observe that the systems $C+O^-$ and $C^+ + O^-$ occur experimentally at just the energy we calculate for the corresponding products with uncharged O. This points to two possibilities; either the electron affinity is very small (≤ 0.1 v) or the products $C+O^-$ and $C^+ + O^-$ observed in our experiments are in each case excited, furthermore the excitation energy $\geq$ the electron affinity. The results on O_2, giving $E_0 = 2.2\pm0.2$ v, exclude the first of these alternatives. Following out the interpretation demanded by the second alternative we immediately find it impossible to assume that the C^+ or C possess this 2.2 v excitation energy. C^+ has no appropriate excited states, the lowest being at 5.2 v. C has ^1D at 1.25 v and ^1S at 2.67 v.[21] The $C+O^-$ data could be interpreted as $C(^1D)+O^-$ ($\sim$1 v excited) or as $C(^3P)+O^-$ ($\sim$2 v excited). But the $C^+ + O^-$ products necessitate $C^+(^2P)+O^-$ ($\sim$2 v excited). We may summarize the consequences of the interpretation on the basis of $D(CO)=9.6$ v by saying that they require the existence of the stable excited negative ion (O^-).

The results of the above discussion can be put briefly as follows. $D(CO)$ may have one of two possible values 11.6 or 9.6 v. The first value

[16] See Fig. 5 in reference 3.

[17] W. Jevons, *Report on Band Spectra of Diatomic Molecules*, Cambridge Press (1932).

[18] H. Kohn and M. Guckel, Zeits. f. Physik **27**, 305 (1924).

[19] Int. Crit. Tab. **5**, 181.

[20] H. Sponer, *Landolt-Börnstein*, 2nd Ergänzungsband, 2nd part, pp. 1611–20.

[21] The unknown $^5S^\circ$ term of CI need not be considered here for Backer and Goudsmit, using a new method, have calculated its energy as 4.1 v, Phys. Rev. **45**, 559A (1934).

(11.6) would yield $E_0=1.9$ and 2.1 v for our results on O^-; while the second (9.6) would require the O^- ion to have about 2 v excitation energy. If the latter value (9.6) is correct, the observation of a discrete negative ion spectrum should be possible. These experiments in themselves are unable to discriminate between $D(CO)=11.6$ and 9.6 v; however, the numerical values of the possibilities are correct and if subsequent experimental data should ever fix upper or lower limits which fall in this range we can immediately state the proper value.

There is one bit of evidence which supports the numerical correctness of our two possibilities for $D(CO)$. CO possesses an electronic level, designated the F level, discovered by Birge and Hopfield.[22] This state is characterized[17] by $\omega_e=2112$ cm^{-1} and by extremely large $\omega_e x$ (198 cm^{-1}). A linear extrapolation yields a vibration level convergence between levels 4 and 5 and a heat of dissociation of 0.57 v. Since levels are known to $v=4$, 0.57 volt should be an accurate estimate of $D(F)$.[23] Using $\nu_0=12.30$ v, the total energy of the dissociation products of the F level is 12.87 v. Possible identifications of the dissociation products and the consequent values of $D(CO)$ follow.

C	O	$D(CO)$
^1D	^3P	11.62 v
^3P	^1D	10.91
^1S	^3P	10.20
^1D	^1D	9.66

We find that both our values 9.6 and 11.6 v are possible. This merely supports the numerical correctness of our results without deciding between them. An identification of the multiplicity of the F level would help to decide this question.[24] A singlet state would require $D(CO)=9.6$ v while a triplet state would allow the other three possibilities.

We can present now the evidence which discriminates between the two possibilities for $D(CO)$. First, let us present the data for $D(CO)=9.6$ v. Coster and Brons[25] have recently observed a predissociation at 11.07 v in the upper state of the Angstrom bands of CO. This requires $D(CO)\leq 11.07$ v. However, they have further interpreted the observation as a predissociation into $C(^1D)+O(^3P)$ giving $D(CO)\leq 9.82$ v.

Secondly, Kaplan[26] has interpreted the nonappearance of more than one vibrational level for the b state of CO as a predissociation. This occurs at an energy of 10.34 v, requiring $D(CO)\leq 10.34$ v. Both of these results give upper limits for $D(CO)$ which lie below our higher possibility; then according to our work $D(CO)=9.6\pm 0.1$ v.

Probably the most important consequence of a knowledge of the correct value of $D(CO)$ is the calculation of λ_e, the heat of sublimation of carbon to atoms. This quantity has been the subject of a number of researches and discussions[27] during the past fifteen years. The vapor pressure data of Kohn and Guckel[18] have until recently been considered reliable and interpreted as giving $\lambda_e=140$ Cal. (6.1 v). Using the cycle already mentioned we calculate λ_e using the two possibilities of $D(CO)$.

$D(CO)$	λ_e
11.6 v	7.9 v (182 Cal.)
9.6 v	5.9 v (136 Cal.)

Vaughan and Kistiakowsky[28] have recently shown that the interpretation (and possibly the data) of Kohn and Guckel is inconsistent with statistical calculations and come to the conclusion that λ_e is somewhat higher than 140 Cal. In a later paper Kistiakowsky and Gershinowitz[29] showed by a number of thermochemical cycles that λ_e can scarcely be less than 150 Cal. If these considerations are reliable we can say from the above discussion that the only possible value of λ_e is 182 Cal. and therefore $D(CO)=11.6\pm 0.1$ v is the correct value. As a matter of fact Marshall and Norton[30] have recently obtained $\lambda_e=177$ Cal. in good agreement with our value 182 Cal.

[22] J. J. Hopfield and R. T. Birge, Phys. Rev. **29**, 922A (1927).

[23] I am indebted to Professor R. T. Birge for sending me the detailed information concerning this electronic state.

[24] See reference 17, p. 109.

[25] D. Coster and F. Brons, Nature **133**, 140 (1934); Physica **1**, 155 (1934); see also D. N. Read, Washington Meeting, Am. Phys. Soc., Phys. Rev. **45**, 752A (1934).

[26] J. Kaplan, Phys. Rev. **37**, 1406 (1931).

[27] For a discussion see article by A. L. Marshall in Treatise on Phys. Chem. Vol. I, p. 326, D. Van Nostrand (1931).

[28] W. E. Vaughan and G. B. Kistiakowsky, Phys. Rev. **40**, 457 (1932).

[29] G. B. Kistiakowsky and H. Gershinowitz, J. Chem. Phys. **1**, 432 (1933).

[30] A. L. Marshall and F. J. Norton, J. Am. Chem. Soc. **55**, 431 (1933).

Concerning this quantity it is pertinent to mention the observations of Smyth and Blewett.[31] In the primary ionization of CS_2 by electron impact they have observed the occurrence of C^+ ions at an electron energy of 21.5 ± 1.0 v. The interpretation advanced is that this corresponds to the formation of $C^+ + S + S$ giving the products $C+S+S$ at 10.3 ± 1.0 v. Thermochemistry plus band spectrum[32] data tell us $CS_2 + 4.5\text{ v} \rightarrow C_{\text{solid}} + S + S$. The combination of these results gives 5.8 ± 1.0 v for λ_c. When we consider that the measurements of Smyth and Blewett can give only an upper limit for the potential energy of $C^+ + S + S$; we see that in spite of the large probable error this presents good evidence for $\lambda_c = 5.9$ v and $D(CO) = 9.6$ v.

In spite of the simplicity of the interpretation of our results on the basis of $D(CO) = 11.6$ v we believe the weight of evidence favors $D(CO) = 9.6$ v as the proper interpretation of our data. In this connection we would emphasize that this requires that the negative ions in CO possess excitation energy. In spite of previous failures with other atoms, it may be possible to observe a portion of the negative ion spectrum of the oxygen atom.

At this point something can be said of the process of formation of the O^- ions represented by Figs. 2 and 7. Smyth and Mueller[6] have discussed in detail the similar H^- formation in H_2O. Though the case of H_2O is complicated by its being triatomic, they reached the conclusion that the negative ions were formed as a result of primary impact. We have determined that the O^- current of Fig. 7 is linear with electron current and pressure; these are facts which, coupled with the absence of positive ions at these electron energies, require a primary impact resulting in the attachment of the incident electron and spontaneous dissociation.

As we have already mentioned, Figs. 2 and 7 tell us that the range of electron energies over which we can obtain an O^- ion with a specified kinetic energy is very small—in fact, our data are not inconsistent with this range being just the energy distribution of electrons in the incident beam. This would mean that an electron of a given energy can produce a negative ion having only a precise kinetic energy and not a range of kinetic energies.

Consider the potential energy curve of the interaction of the dissociation products—a neutral atom and a negative atomic ion. If the potential energy of this curve, for nuclear separations of the order of those present in the normal molecule vibration, is above the potential energy of infinite separation, the distinctive features of Figs. 2 and 7 can be explained. The first step in the negative ion formation would be the excitation of the normal molecule to this unstable state of the negative molecular ion. The capture of the incident electron requires a very close equality between the kinetic energy of the incident electron and the potential energy of the unstable state; the conversion of a given electron energy means excitation to one definite point on the potential energy curve; and this gives rise to a definite ion energy.

There is this difference in the results on the negative ions in the two gases. The process in CO giving $C+O^-$ at 9.5 v produces O^- ions with kinetic energies 0 to $\sim$1 volt. This means that the potential energy curve involved is probably not strictly repulsive but possibly has a minimum; and a careful search with a mass-spectrograph might reveal CO^- ions at about 9.5 v. In O_2, however, the process giving $O+O^-$ at 2.9 v produces no O^- ions with energies lower than $\sim$1.3 v. This points to a repulsive potential curve and the non-existence of O_2^-.

Conclusions

From the O_2 data two types of dissociation have been considered and interpreted as follows

$$O_2^- \rightarrow O(^3P) + O^- \text{ (normal) at } 2.9\pm0.2 \text{ v.}$$
$$O_2^- \rightarrow O(^3S^\circ) + O^- \text{ (normal) at } 12.0\pm0.2 \text{ v.}$$

These data have permitted a determination of E_0, the electron affinity of the oxygen atom, as 2.2 ± 0.2 v.

From the CO data three types of dissociation processes have been discussed.

$$CO^- \rightarrow C + O^- \text{ at } 9.5\pm0.1.$$
$$CO \rightarrow C^+ + O^- \text{ at } 20.9\pm0.1 \text{ v.}$$
$$CO^+ \rightarrow C^+ + O \text{ at } 22.8\pm0.1 \text{ v.}$$

[31] H. D. Smyth and J. P. Blewett, Washington Meeting, Am. Phys. Soc., Phys. Rev. **45**, 752A (1934).

[32] *Landolt-Börnstein*, Vol. 2, p. 1490; 1st Ergänzungsband, p. 809; and 2nd Ergänzungsband, p. 1498. Also A. Christy and S. M. Naudé, Phys. Rev. **37**, 903 (1931).

From these data we have determined that $D(CO)$ may have one of two possible values, 9.6 or 11.6 v. The assumption of the first requires the O^- ion in both cases to have excitation energy; while the assumption of the value 11.6 v allows the calculation of E_0 as 1.9 and 2.1 v. Evidence is given which points to the lower value as the correct one.

The processes involved in the formation of the negative ions have been discussed.

The writer is deeply indebted to a number of people for their patient and helpful discussions. Particularly, he wishes to thank Professors H. D. Smyth, E. U. Condon, J. Franck and Mr. F. Seitz.

Ionization of Carbon Disulphide by Electron Impact

H. D. SMYTH AND J. P. BLEWETT, *Palmer Physical Laboratory, Princeton University, Princeton, N. J.*

(Received June 16, 1934)

The ionization of CS_2 by electron impact has been studied. It has been found that the CS_2^+, CS^+, S^+ and C^+ ions are produced at 10.4 ± 0.2, 14.7 ± 0.5, 14.0 ± 0.5 and 21.5 ± 1.0 volts, respectively. The absence of S_2^+ ions and the high appearance potential for C^+ indicate a linear molecule. By raising the filament temperature free CS and S_2 are produced and their I.P.'s determined as 10.6 ± 0.3 and 10.7 ± 0.3 volts. Heats of dissociation for various processes are deduced from the experimental data.

IN several previous papers[1,2] results have been reported on the ionization of common triatomic molecules by electron impact. Here we wish to record similar data on the ionization of carbon disulphide.

It may be well to recall briefly the method used. It is to determine by a mass-spectrograph the nature of the ions produced in the gas by electrons of known energy. The numbers of different types of ions are then studied as functions of electron energy.

The particular apparatus used on carbon disulphide was that used previously by Smyth and Stueckelberg[1] and Smyth and Mueller.[2] Considerable difficulty was experienced in investigating CS_2 on account of dissociation by the heat of the filament. This dissociation occurred in spite of the gas flow method employed to prevent it and could be overcome only by using an oxide-coated filament operated at the lowest possible temperature and removed two millimeters further from the ionization space than it had been in previous work.

Under these conditions with CS_2 that had been redistilled in vacuum, ions were observed at masses 76, 44, 32 and 12. No ion was detected at mass 64. Current *vs.* voltage curves for these ions are shown in Fig. 1. No negative ions were observed. The voltage scale was calibrated by the ionization of mercury vapor. Runs taken in mixtures of mercury and CS_2 and in the pure gases agreed in showing the ionization potential for the production of CS_2^+ the same

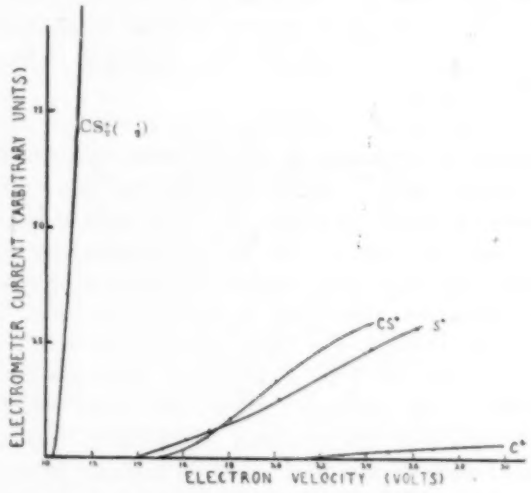

FIG. 1. Current *versus* voltage curves for various ions formed by electron impact in CS_2.

[1] Smyth and Stueckelberg, Phys. Rev. **36**, 472 & 478 (1930).
[2] Smyth and Mueller, Phys. Rev. **43**, 116 & 121 (1933).

as for mercury, i.e., 10.4 volts, within the limits of experimental error. The results on undissociated CS_2 are given in the first part of Table I.

For the calculation of the I.P.'s for the last column we have available only the I.P.'s of the C and S atoms which are 11.3 and 10.2 volts, respectively, and the heat of dissociation of CS_2 for the process $CS_2 \rightarrow C+S+S$.[3] This last may be obtained from the value of the heat of reaction $(CS_2)+3(O_2)\rightarrow(CO_2)+2(SO_2)+265.1$ kc but involves the heats of dissociation of CO and of SO_2. Taking the former to be 9.6 volts[4] and the latter to be 10.9,[5] we get 10.1 volts for the heat of dissociation of CS_2. This added to the I.P. of carbon gives the value quoted in the last column of the table for the $CS_2 \rightarrow C^+ + S + S$ ionization. It is seen to be in agreement with the experimental value.

The non-appearance of the S_2^+ ion and the appearance of the C^+ ion at a potential considerably higher than the appearance potentials of the other ions may be taken to indicate a linear structure for the CS_2 molecule, the C atom being placed in the center thus:

$$S-C-S$$

so that to obtain the C^+ ion both S atoms must be removed. This structure is also indicated by chemical evidence. From our data on the appearance potential of S^+ we are able to calculate the heat of dissociation of CS_2 into CS+S as 3.8 $\pm$0.5 volts.

By varying the experimental conditions a plentiful supply of thermally dissociated products could be made available. Overheating the filament caused the CS_2 molecule to break up into CS+S or C+S+S as was indicated by the appearance of both C^+ and S^+ at electron velocities as low as their respective atomic I.P.'s.

TABLE I. *Ionization processes in carbon disulphide.*

Ion observed	Appearance potential	Probable process	Calculated minimum energy required
CS_2^+	10.4±0.2 volts	$CS_2 \rightarrow CS_2^+$	—
S_2^+	Not observed		
CS^+	14.7±0.5	$CS_2 \rightarrow CS^+ + S$	—
S^+	14.0±0.5	$CS_2 \rightarrow CS + S^+$	—
C^+	21.5±1.0	$CS_2 \rightarrow C^+ + S + S$	21.4
	In thermally dissociated gas		
CS^+	10.6±0.3	$CS \rightarrow CS^+$	—
S_2^+	10.7±0.3	$S_2 \rightarrow S_2^+$	—

Under these conditions S_2^+ also appeared, indicating that free sulphur atoms had united in pairs to assume the usual form of sulphur vapor. It is improbable that these S_2^+ ions are formed by disruption of S_6 or S_8, the other common sulphur molecules, since neither S_6^+ nor S_8^+ appeared in our mass spectrograph analysis.

Since the I.P.'s of the two diatomic molecules CS and S_2 are not known they were measured and found to be 10.6±0.3 volts and 10.7±0.3 volts, respectively, as shown in the lower part of the table. The value for CS enables us to check our calculation of the heat of dissociation of CS_2 into CS+S. We obtain in this case a heat of dissociation of 4.1±0.5 volts which agrees within the experimental error with the result obtained above. A value for this heat of dissociation is given by Henri[6] from predissociation as $\leqq$4.4 volts which agrees within the experimental error with our mean value.

From the heats of dissociation of CS_2 obtained experimentally for the two processes $CS_2 \rightarrow C+S+S$ (10.2 volts) and $CS_2 \rightarrow CS+S$ (3.9 volts) —we obtain the heat of dissociation of CS to be 6.4±1.5 volts. Similarly, if we put the first heat of dissociation into the thermochemical data mentioned above, we can calculate the heat of dissociation of CO as 9.7 volts.

[3] Landolt-Börnstein, Vol. 2, p. 1490.
[4] Lozier, Phys. Rev. **46**, 268 (1934).
[5] Franck, Sponer and Teller, Zeits. f. physik. Chemie **B18**, 97 (1932); or Smyth and Mueller, reference 2.
[6] Debye, *Structure of Molecules* (English translation), p. 128 (Blackie, 1932).

The Pressure of Plasma Electrons and the Force on the Cathode of an Arc

LEWI TONKS, *Research Laboratory, General Electric Company, Schenectady, New York*

(Received June 13, 1934)

It is pointed out that the electrons in a plasma, and particularly in that at the cathode spot of an arc, exert a pressure nkT that has hitherto been overlooked. Numerically, the major portion of the force on the cathode spot can be accounted for in this way.

THE force on the cathode of an arc, which has been ascribed both to high temperature evaporation of the cathode material[1] and to an accommodation coefficient, α, less than unity for ions neutralized at the cathode surface,[2] must be largely due to the pressure of the plasma electrons which are reflected from the cathode sheath. This factor must also be very important in the deflecting vane experiments intended to measure accommodation coefficients,[3] although heating effect experiments for the same purpose[4] are not influenced unless electrons are actually collected by the thermal element.

A momentum change accompanies the rebounding of plasma electrons from the positive ion sheath covering a negatively charged electrode. From the simple kinetic point of view this must appear as a pressure $p=nkT$. Since the force causing the velocity reversal is the repulsion between the negative charge on the electrode and the electron, this pressure is exerted on the electrode. The essential difference between the action of the electrons and ions is that the latter acquire momentum in the electric field of the electrode and then return it to the electrode on impact, whereas the former acquire oppositely directed momentum in the same field but deliver it elsewhere—ultimately to the walls of the discharge tube.

Consider the one-dimensional case of a region extending from x_0 to x_1 in which the field E accelerates ions from x_0 toward x_1. Let the ion density be n_p and suppose that the electron density n varies with potential V and electron temperature T according to the Boltzmann law. Subscripts 0 and 1 refer to values of the variable at x_0 and x_1, respectively. Suppose, further, that no ion ever collides with any atom which may be in the space. The gain of positive ion momentum per second per unit cross section in this region is

$$M=e\int_{x_0}^{x_1} En_p dx. \tag{1}$$

Poisson's equation converts this to

$$M=(1/4\pi)\int_{x_0}^{x_1} EE'dx+e\int_{x_0}^{x_1} Endx. \tag{2}$$

By using the Boltzmann equation and integrating, we obtain

$$M=(E_1^2-E_0^2)/8\pi+(n_0-n_1)kT. \tag{3}$$

If we locate x_0 at the potential maximum in the plasma so that $E_0=0$, then M is the total momentum acquired from the field by all the ions reaching x_1. Neglecting the small initial momentum of the ions when they are formed, this is the total momentum carried by the ions to a collector C at x_1.

If, in a neutralizing impact on C, the ions have an accommodation coefficient α, additional momentum beyond M will be conveyed to C to an amount $M(1-\alpha)$.

A third contribution to the pressure is that of the electrons striking C. If all are reflected without loss of energy, this pressure will be n_1kT; if all are absorbed, it will be $\frac{1}{2}n_1kT$; and for a reflection coefficient ρ and accommodation coefficient α_e, the pressure will be

$$\tfrac{1}{2}[1+\rho(1-\alpha_e)]n_1kT. \tag{4}$$

[1] Tanberg, Phys. Rev. **35**, 1080 (1930); Kobel, Phys. Rev. **36**, 1636 (1930).

[2] K. T. Compton, Phys. Rev. **37**, 1077 (1931).

[3] Lamar, Phys. Rev. **43**, 169 (1933); Compton and Lamar, Phys. Rev. **44**, 338 (1933). The electron pressures on the two sides of the vane should balance when the vane is centered in the tube. Its displacement will make the electron pressures on its two sides unequal and will produce a net force depending on vane position such as was actually observed.

[4] Van Voorhis and Compton, Phys. Rev. **35**, 1438 (1930); **37**, 1596 (1931).

The fourth component of force is the electrostatic pressure $-E_1^2/8\pi$ due to the field at the collector surface.

The total pressure P is the sum of these four parts:

$$P = M[1+(1-\alpha)^{\frac{1}{2}}]+\tfrac{1}{2}[1+\rho(1-\alpha_e)^{\frac{1}{2}}]n_1kT - E_1^2/8\pi, \quad (5)$$

M being given by Eq. (3) with $E_0=0$.

In the simplest case where $\alpha=1$ and n_1 is negligible,

$$P = n_0kT, \quad (6)$$

so that the net pressure is purely electron kinetic. When $\alpha<1$,

$$P = M(1-\alpha)^{\frac{1}{2}}+n_0kT. \quad (7)$$

Now M can be calculated from the positive ion current density I_p to C, for

$$M = (I_p/e)m\bar{v} \cong (2m/e)^{\frac{1}{2}}I_p(V_0-V_1)^{\frac{1}{2}}. \quad (8)$$

The use of V_0 is not quite exact since the ions originate over a small range of potentials. Eqs. (7) and (8) afford a means for determining α.

When the ions make collisions with gas atoms, they strike C with momentum less than M. But the deficiency is made up by the increased gas pressure resulting from the ion-atom impacts. The pressure component $M(1-\alpha)^{\frac{1}{2}}$ will be affected, although not greatly if few collisions occur in the sheath and the potential difference between potential maximum and sheath edge is small compared to that between sheath edge and C.

A rough estimate of the kinetic electron pressure at a mercury cathode spot can be made. Since we have no exact knowledge of the gas density in the cathode glow, but the indications are that the mean free path of the ions is at least comparable with the distances they travel, formulas based on long free paths should give approximately correct results. For this case the positive ion current density is related to the electron concentration in the plasma by the equation[5]

$$I_p = s_0h_0en_0(2kT_e/m_p)^{\frac{1}{2}} \quad (9)$$

with $s_0=0.4046$, $h_0=0.8513$. Denoting the fraction of the arc current carried by electrons at the cathode by f, and the total current density there by j, we have

$$I_p = (1-f)j. \quad (10)$$

Accordingly, under the conditions applicable to Eq. (6), the kinetic pressure of the electrons gives a force per unit current of

$$n_0kT/j = (1/s_0h_0e)(km_p/2)^{\frac{1}{2}}(1-f)T^{\frac{1}{2}} \quad (11A)$$

$$= 2.74(1-f)T^{\frac{1}{2}} \text{ dynes/amp.} \quad (11B)$$

for mercury. Taking $T=5\times10^4$ in the plasma immediately outside the cathode spot and $f=0.9$, the force is found to be 61 dynes/amp. This is to be compared with the average value 40 dynes/amp. calculated from Kobel's measurements[1] on the Hg arc and 17 dynes/amp. from Tanberg's data[1] on the Cu arc.

Finally, it should be noted that the partial pressure of the electrons is present in any arc stream. It may even predominate over the gas pressure itself when the degree of dissociation exceeds a few percent because of the far higher temperature of the electrons.

[5] Tonks and Langmuir, Phys. Rev. **34**, 876 (1929), Eq. (55A) and Table IIa.

Excitation of Light by Alkali Ions*

ROBERT E. HOLZER, *Ryerson Laboratory, University of Chicago*

(Received June 16, 1934)

Light emission produced by slow alkali ions in the rare gases was observed for ion accelerating potentials below those necessary to produce ionization. It was found that light could be observed in helium, neon and argon at the lowest ion accelerating potential for the particular alkali ion that lay closest to the gas in the periodic table. A sodium ion beam in neon produced light at lower accelerating potentials than those reported for neon ions in neon.

INTRODUCTION

IN most experiments on the ionization of gases by positive ion impact, the metal parts of the apparatus are exposed to any radiation which may be produced in the ion beam. It is, therefore, of some interest to know at what velocity appreciable amounts of radiation are produced in a beam of ions passing through a gas at low pressure. Since the most complete work on the ionization of gases by slow positive ions has been done on the inert gases and alkali ions, this group of ions and gases were chosen for the present experiment.

APPARATUS

The experimental tube shown in Fig. 1 consists of an ion source, F, two collimating slits, S_1 and S_2, an observation space and a collector, C. The source was a platinum filament coated with natural ores of the alkali silicates by essentially the same process described by Bainbridge.[1] Li^+ ions were obtained from spodumene, Na^+ from jadeite, K^+ from leucite, and Cs^+ from pollucite. These sources tested in a mass-spectrograph were found to emit very small percentages of impurities, in all cases less than 4 percent. The filament was placed 3 mm from the first collimating slit. Each slit was 5 mm in diameter and the slit separation 1 cm. The observation space beyond the slits was 1.5 cm long and the collector at the end of the tube was 5 cm deep. The internal diameter of the tube, and the diameter of the collector were each 3 cm.

The metal parts of the tube were covered with a carbon deposit to cut down scattered light. Since the source gave copious emission of ions when heated to dull red, the scattered light was negligible except at the limit of visibility of the beam.

The gases used were He, Ne, and A, 98 percent pure as they were taken from their containers. They were further purified by the evaporation of K and Ca in the tube at low pressures. In the case of He and Ne a charcoal trap immersed in liquid air was kept on the tube throughout the experiment. The gas pressures were measured by a McLeod gauge connected directly to the tube.

The accelerating potential for the ions applied between the filament and first slit could be varied between 50 and 600 volts. In every case an ion beam of good intensity was obtained for accelerating potentials between 200 and 300 volts with a gas pressure as high as 2×10^{-2} mm. The current which reached the collector, of the order of 10^{-7} ampere, was measured by a galvanometer.

MEASUREMENTS

In the first case[2] tried, Li^+ in Ne, the beam was accelerated into the field free observation space with a flat plate at the mouth of the collector. A clearly visible and fairly well-defined beam extended to the plate. As a retarding field for the ions was applied in the observation space the beam fell short of the plate. Figs. 2 and 3 show two diagrams sketched from photographs of the beam made with a 4.5 lens and Ilford panchromatic plates. The exposure time was two hours.

The method was not satisfactory for determining the velocity of the ions at which excitation was first observed since it was difficult to

* Experiment done during tenure of National Research Fellowship.

[1] K. T. Bainbridge, J. Frank. Inst. **212**, 333 (1931).

[2] A. J. Dempster and R. E. Holzer, Phys. Rev. **43**, 365 (1933).

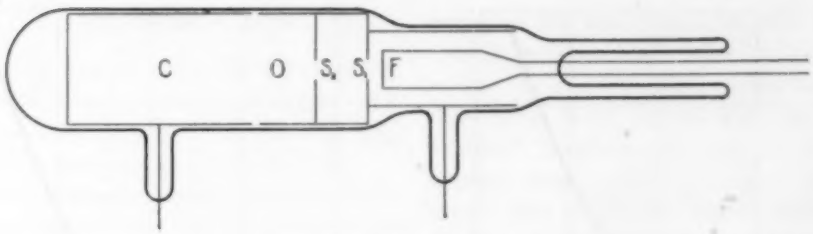

FIG. 1. Experimental tube.

observe the exact limit of the beam and since the camera was not as sensitive as the eye. It was, therefore, abandoned in favor of a direct photometric measurement of the intensity of the beam for Li^+ in Ne and all other ion and gas combinations.

The comparison source consisted of a 25 watt tungsten filament lamp in a shielded box with two apertures approximately the width of the beam at the point measured. The apertures were screened for color matching and intensity reduction. The comparison source was then calibrated against an arbitrary standard.

In making photometric measurements the observer remained in a dark room for a period of 20 minutes to sensitize his eyes to faint light. A second observer always regulated the voltages, and read the meters so that the first observer did not have to expose his eyes to light intensity stronger than that from the beam at any time. In taking the readings, one observer always watched the beam and made the photometric settings, the second recorded the accelerating potential, the current to the collector and current in the photometric lamp. Below a certain minimum of light intensity it was impossible to make a satisfactory photometric setting. To determine the least accelerating potential at which light from the beam could be detected the accelerating potential was lowered and the beam flashed off and on. The process was then repeated with increasing accelerating potential.

The curves shown in Figs. 4 and 5 give light intensity in arbitrary units as a function of the accelerating potential of the positive ions. Zero on the scale represents the least observable light intensity. Corrections were made for the decreased current at low voltage.

Several points arise in the interpretation of the results which must be checked experimentally. In the first place, it is possible that gaseous ions were produced in the accelerating field by electrons liberated from the negative plate. These gaseous ions would then be accelerated into the observation space together with the alkali ions from the filament. To determine whether gaseous ions were present in the beam in observable numbers, a bare platinum filament of the same dimensions as the coated filament was substituted for it. The dummy filament was heated to the same temperature and the gas pressure was reduced until no beam of gaseous ions was produced. The pressures used in the experiment were kept well below the point at which a beam of gaseous ions were produced in the accelerating field.

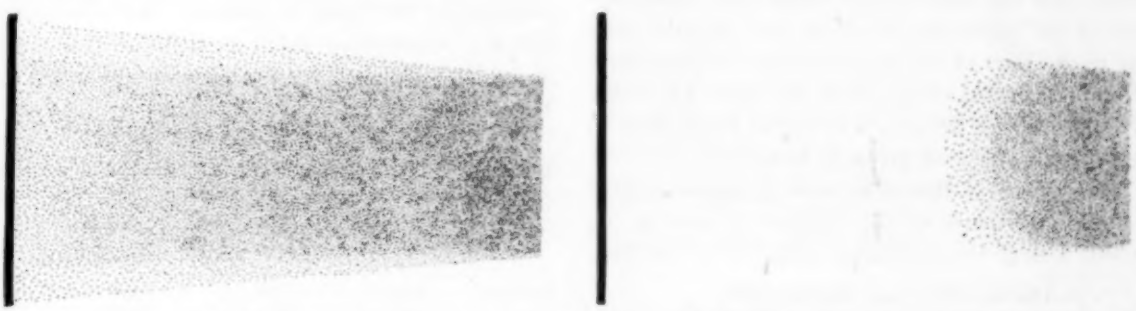

FIGS. 2 AND 3. Sketches of light beam produced by Li^+ ions in Ne. Accelerating potential 600 volts in both cases. Retarding potential zero for Fig. 2, 600 volts for Fig. 3.

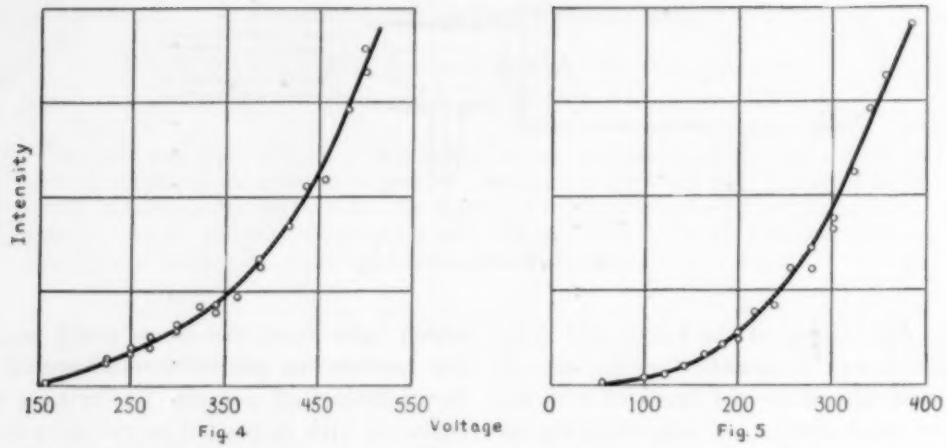

FIGS. 4 AND 5. The intensity of the light beam in arbitrary units shown as a function of the ion accelerating potential in volts. Fig. 4 for the case of Li^+ in Ne, Fig. 5 for K^+ in A.

The possibility that a part of the excitation was due to secondary electrons liberated by ion impact at the edges of the slit was also considered. The fact that the beam was deflected only slightly by a magnetic field and in the direction of a positive current indicated that the light was due to the positive ion beam. When the collector was placed in a magnetic field the current was not measurably altered indicating that few secondary electrons liberated from the walls of the collector were escaping the collector and that the current measured was essentially the ion current.

It is also possible that a certain part of the light emitted from the beam is due to excitation of the ions instead of the gas atoms. A spectroscopic examination of the light from the beam was found impractical with the particular experimental arrangement since it was calculated that the minimum exposure for satisfactory plates was some 200 hours. However, the fact that in every case the color of the beam was characteristic of the gas rather than the ion suggests that the major part of the light was due to excitation of the gas atoms rather than the ions. The color of the beam for all ions was red in neon, blue in argon and yellowish green in helium.

The current to the collector was approximately a correct measure of the number of ions in the beam. Using the available data[3, 4, 5, 6] on free paths of alkali ions in gases, it was found that for the particular pressure and lowest ion velocities used in the present experiment, 60 percent of the ions that pass S_1 should enter the collector for the case of Cs^+ in A, while 95 percent of the ions should reach the collector for Li^+ in He. The free path data used in these calculations were all obtained with collectors of small aperture. Since the angle subtended by the collector at S_1 was 110° and since for large aperture collectors the apparent free path is larger than for small aperture collectors,[6] the percentage of the ions reaching the collector is actually much higher than calculated above. The error introduced by neglecting free path calculations is no larger than that in estimating the light intensity of weak beams.

Measurements were made on the minimum accelerating potential in volts at which light from a beam of ions of 10^{-7} amperes would produce an observable amount of light at a gas pressure of 10^{-2} mm of mercury. Li^+, Na^+, K^+ and Cs^+ ions were used in each of the three gases, He, Ne and A. The results are given in Table I.

TABLE I. *Minimum potential for the excitation of light by positive ion impact.*

	Li^+	Na^+	K^+	Cs^+
He	140	152	200	280
Ne	150	128	140	192
A	60	64	60	120

[3] F. M. Durbin, Phys. Rev. **30**, 844 (1927).
[4] C. Ramsauer and O. Beeck, Ann. d. Physik **87**, 1 (1928).
[5] R. Kennard, Phys. Rev. **31**, 423 (1928).
[6] J. S. Thompson, Phys. Rev. **35**, 1196 (1930).

Conclusions

It is interesting to note that light excitation was observed in every case well below the ionization potentials reported by Beeck and Mouzon[7, 8] for the corresponding cases.

It is also interesting to note that the light beam was observed at the lowest accelerating potentials for those cases in which Beeck and Mouzon observed lowest ionization potentials. That is, for any gas the light beam was observed at the lowest ion accelerating potential for that ion which is closest to the gas in the periodic table.

The minimum accelerating potential at which Na^+ ions were able to produce a visible light beam in Ne was approximately 130 volts while Güntherschulze and Keller[9] have found that Ne atoms do not produce excitation in Ne below 300 volts. This agrees with the prediction of Weizel[10] based on the theory of ionization by impact developed by Weizel and Beeck. He states that ionization and excitation of light in the inert gases may be produced at lower energies by alkali ions than ions of the inert gases; applied to this specific case, ionization and excitation may be produced in Ne at lower energies if Na^+ is the moving particle rather than Ne^+.

In conclusion, the writer wishes to express his appreciation to Professor A. J. Dempster for his valuable criticisms of this work.

[7] O. Beeck and J. C. Mouzon, Ann. d. Physik **11**, 737 (1931).
[8] O. Beeck and J. C. Mouzon, Ann. d. Physik **11**, 858 (1931).
[9] A. Güntherschulze and F. Keller, Zeits. f. Physik **72**, 143 (1931).
[10] W. Weizel, Zeits. f. Physik **76**, 259 (1932).

Relative Multiplet Transition Probabilities from Spectroscopic Stability*

C. W. Ufford and F. M. Miller, *Allegheny College*

(Received June 11, 1934)

With the method based on the principle of spectroscopic stability, the relative transition probabilities of different multiplets in Russell-Saunders coupling have been calculated for the transitions d^3p-d^4, dp^2-pd^2, and $d^2p^2-d^3p$. A formula is given for getting the transition probabilities, in terms of the core transition probabilities, for the pair of electron configurations which are obtained by adding the same non-equivalent s electron to each core configuration.

Theory

THE method, based on the principle of spectroscopic stability, of calculating the relative transition probabilities of different multiplets in Russell-Saunders coupling has been given by Condon and one of us.[1] This method is used here to calculate the transition probabilities for the transitions d^3p-d^4, dp^2-pd^2, and $d^2p^2-d^3p$. The results of these calculations are given for d^3p-d^4 in Table I, dp^2-pd^2 in Table II, and $d^2p^2-d^3p$ in Table III, where the notation is the same as that used in the previous paper.[1]

We have also found a simple formula for getting the transition probabilities which arise when a non-equivalent s electron is added to a pair of core configurations. These transition probabilities are given in terms of those between the two core configurations. The added s electron must not be equivalent to any core electrons either in the initial or the final state. The relative transition probability in Russell-Saunders coupling is given by

$$(asN^{2S+1}L,\ a'sN'^{2S+1}L') = (2S+1)[1/(2S+2)(aN^{2S+2}L,\ a'N'^{2S+2}L') + (1/2S)(aN^{2S}L,\ a'N'^{2S}L')], \quad (1)$$

where S is the total spin angular momentum, L

* Presented at the Washington Meeting of the American Physical Society, April 27, 1934.
[1] E. U. Condon and C. W. Ufford, Phys. Rev. **44**, 740 (1933).

TABLE I. *Relative transition probabilities for the transition* d^3p-d^4.

		d^4										
		^5D	^3H	^3G	$2\,^3F$	^3D	$2\,^3P$	^1I	$2\,^1G$	^1F	$2\,^1D$	$2\,^1S$
	^5G	y	x	x	x	x,y	x,y	x,y	x	x	x,y	x,y
	^5F	2800	x,y	x	x	x	x,y	x,y	x	x	x	x,y
	$2\,^5D$	6500	x,y	x,y	x	x	x	x,y	x,y	x	x	x,y
	^5P	2700	x,y	x,y	x,y	x	x	x,y	x,y	x,y	x	x
	^5S	y	x,y	x,y	x,y	x,y	x	x,y	x,y	x,y	x,y	x
	^3I	x,y	780	y	y	y	y	x	x,y	x,y	x,y	x,y
d^3p	$2\,^3H$	x,y	5412	1188	y	y	y	x	x	x,y	x,y	x,y
	$4\,^3G$	x,y	9648	5427	4365	y	y	x,y	x	x	x,y	x,y
	$5\,^3F$	x	y	6345	6615	2160	y	x,y	x	x	x	x,y
	$6\,^3D$	x	y	y	9180	2700	4020	x,y	x,y	x	x	x,y
	$4\,^3P$	x	y	y	y	2340	3060	x,y	x,y	x,y	x	x
	$2\,^3S$	x,y	y	y	y	y	1560	x,y	x,y	x,y	x,y	x
	^1I	x,y	x	x,y	x,y	x,y	x,y	1820	y	y	y	y
	$2\,^1H$	x,y	x	x	x,y	x,y	x,y	4420	860	y	y	y
	$3\,^1G$	x,y	x	x	x	x,y	x,y	y	3465	855	y	y
	$4\,^1F$	x	x,y	x	x	x	x,y	y	4315	805	1320	y
	$4\,^1D$	x	x,y	x,y	x	x	x	y	y	1700	2100	y
	$3\,^1P$	x	x,y	x,y	x,y	x	x	y	y	y	1380	960
	^1S	x,y	x,y	x,y	x,y	x,y	x	y	y	y	y	0

and L' the initial and final values of the total orbital angular momentum, a and a' the initial and final core configurations, and N and N' are the number of multiplets of the same kind occurring in the given configuration. The N's are in general different for the multiplets of different multiplicity. In some cases either the first term or the second term on the right-hand side of Eq. (1) does not exist and so is omitted in determining the new transition probability. Thus to illustrate Eq. (1)

$$(d^3ps10\,^2D,\ d^4s\,^2F)$$
$$=2[\tfrac{1}{3}(d^3p6\,^3D,\ d^42\,^3F)+1/1(d^3p4\,^1D,\ d^4\,^1F)]$$
$$=2(\tfrac{1}{3}9180+1700)=9520, \quad (2)$$

where the values of $(d^3p6\ ^3D,\ d^42\ ^3F)$ and $(d^3p4\ ^1D,\ d^4\ ^1F)$ are taken from Table I.

Eq. (1) was obtained as follows. When a non-equivalent s electron is added to a configuration, the L values of the terms are unchanged. The values of S are increased and decreased by $\frac{1}{2}$ or the multiplicities by unity. Thus the new terms of as are the sums of the terms of a having the same L value but of multiplicity one greater and one less. Now for given values of M_L and M'_L the part, $(LM_L|\mathbf{r}|L'M'_L)$, of each matrix element[1] of

TABLE II. *Relative transition probabilities for the transition* $dp^2-d\,^2p$.

		d^2p										
		^4G	^4F	$2\,^4D$	^4P	^4S	^2H	$2\,^2G$	$3\,^2F$	$3\,^2D$	$3\,^2P$	^2S
	^4F	162	350	76	y	y	x,y	x	x	x	x,y	x,y
	^4D	y	112	200	108	y	x,y	x,y	x	x	x	x,y
dp^2	^4P	y	y	324	0	108	x,y	x,y	x,y	x	x	x
	^2G	x	x	x,y	x,y	x,y	198	162	18	y	y	y
	$2\,^2F$	x	x	x	x,y	x,y	y	648	168	87	y	y
	$3\,^2D$	x,y	x	x	x	x,y	y	y	507	300	123	y
	$2\,^2P$	x,y	x,y	x	x	x	y	y	y	153	162	27
	^2S	x,y	x,y	x,y	x	x	y	y	y	y	57	0

$e\mathbf{r}$ which depends on M_L in the LSM_LM_S scheme, and the square of which appears as a coefficient in the equation for the part of the matrix element of $e\mathbf{r}$, $|(N\,^{2S+1}L|er|N'\,^{2S+1}L')|^2$, independent of M_L, will be the same for a given pair of states of as, $a's$ as for the pair of core states of a, a' with the same values of L and L'. In the zero order scheme for given values of M_S, M_L and M'_L one group of the states of as, $a's$ will arise by adding s^+ to the core states with the same values of M_L and M'_L where M_S is less by $\frac{1}{2}$, and the other group will arise by adding s^- to the core states with the

TABLE III. *Relative transition probabilities for the transition $d^2p^2-d^2p$.*

d^2p^2 \ d^2p	^4G	^4F	$2\,^4D$	^4P	^4S	^2I	$2\,^2H$	$4\,^2G$	$5\,^2F$	$6\,^2D$	$4\,^2P$	$2\,^2S$	^1I	$2\,^1H$	$3\,^1G$	$4\,^1F$	$4\,^1D$	$3\,^1P$	^1S
^4G	6750	4050	y	y	y	xy	x	x	x	xy	xy	xy	xy	x	x	x	xy	xy	xy
^4F	4050	3150	5400	y	y	xy	xy	x	x	x	xy	xy	xy	xy	x	x	x	xy	xy
$2\,^4D$	y	5400	13500	2850	y	xy	xy	xy	x	x	x	xy	xy	xy	xy	x	x	x	xy
^4P	y	y	2850	3600	1200	xy	xy	xy	xy	x	x	x	xy	xy	xy	xy	x	x	x
^4S	y	y	y	1200	0	xy	xy	xy	xy	xy	x	x	xy	xy	xy	xy	xy	x	x
$2\,^2H$	x	xy	xy	xy	xy	10530	10098	4122	y	y	y	y	x	x	x	xy	xy	xy	xy
$3\,^2G$	x	x	xy	xy	xy	y	15642	18063	6795	y	y	y	xy	x	x	x	xy	xy	xy
$6\,^2F$	x	x	x	xy	xy	y	y	32895	20055	13830	y	y	xy	xy	x	x	x	xy	xy
$5\,^2D$	xy	x	x	x	xy	y	y	y	21030	13800	6570	y	xy	xy	xy	x	x	x	xy
$6\,^2P$	xy	xy	x	x	x	y	y	y	y	17820	8370	3780	xy	xy	xy	xy	x	x	x
^2S	xy	xy	xy	x	x	y	y	y	y	y	1800	0	xy	xy	xy	xy	xy	x	x
^1I	xy	xy	xy	xy	xy	x	x	xy	xy	xy	xy	xy	2730	390	y	y	y	y	y
^1H	x	xy	xy	xy	xy	x	x	x	xy	xy	xy	xy	3120	1716	774	y	y	y	y
$4\,^1G$	x	x	xy	xy	xy	xy	x	x	x	xy	xy	xy	y	11094	6291	3135	y	y	y
$3\,^1F$	x	x	x	xy	xy	xy	xy	x	x	x	xy	xy	y	y	5895	4375	2330	y	y
$6\,^1D$	xy	x	x	x	xy	xy	xy	xy	x	x	x	xy	y	y	y	8870	5350	3030	y
$2\,^1P$	xy	xy	x	x	x	xy	xy	xy	xy	x	x	x	y	y	y	y	2830	720	240
$3\,^1S$	xy	xy	xy	x	x	xy	xy	xy	xy	xy	x	x	y	y	y	y	y	1920	0

same values of M_L and M'_L where M_S is greater by $\frac{1}{2}$. Therefore the matrix elements of er between states arising from core states of different values of M_S will be zero since the values of m_s for the non-equivalent s electron are different. This s electron does not jump and therefore must have identical quantum numbers in the initial and final states which can differ by at most one individual set of quantum numbers.[2] Hence for given values of M_S, M_L, and M'_L, the sum of the squares of the matrix elements of er in the zero order scheme for the states of as, $a's$ is equal to the sum of the squares of the matrix elements of er in the zero order scheme for the cores with the same values of M_L and M'_L where M_S is less by $\frac{1}{2}$ plus the sum of the squares of these matrix elements where M_S is greater by $\frac{1}{2}$. Thus, since the coefficients in the linear equations for the squares of the matrix elements, $|(N\,^{2S+1}L|er|N'\,^{2S+1}L')|^2$, for the states of as, $a's$, are the same as in the two core equations; and since the constant term is the sum of the constant terms for the two core equations, the solution obtained for the states of as, $a's$ will be the sum of the two solutions obtained for the core equations with the same values of M_L and M'_L and the components of total spin angular momentum equal to $M_S+\frac{1}{2}$ and $M_S-\frac{1}{2}$. To get the relative transition probabilities, the square of the matrix element, $|(N\,^{2S+1}L|er|N'\,^{2S+1}L')|^2$, has to be multiplied by factors depending on L and S to sum over the initial and final states.[1] As L is the same for the states of as, $a's$ and the core states of a, a', the only factors which are different are the multiplicities. The multiplicities, $2S$ and $2S+2$, of the core states must be removed from the transition probabilities of the core states before they are added to give the transition probability between the states of as, $a's$. Finally the sum must be multiplied by $2S+1$, the multiplicity of the states of the configurations as and $a's$ containing the s electron.

[2] E. U. Condon, Phys. Rev. **36**, 1121 (1930).

The Band Spectrum of NaK

F. W. Loomis and M. J. Arvin, *University of Illinois*

(Received June 4, 1934)

The spectrum of the NaK molecule has been studied in absorption and in magnetic rotation throughout the visible and photographic infrared regions. By means of magnetic rotation the upper vibrational levels of the orange system have been followed nearly to dissociation, permitting accurate determinations of the energies of dissociation of four states of the molecule, that of the ground state being 0.62 ± 0.03 volt. Two new band systems, in the green and infrared, have been found and analyzed. The fourth theoretically expected system has not been found and is presumably covered by strong Na_2 and K_2 systems. The magnetic rotation spectra in the green and red have no simple relation to the absorption spectra and are probably to be interpreted as due to perturbations, like the red magnetic rotation spectrum of Na_2.

HITHERTO the only known visible band system of NaK has been the one in the neighborhood of the sodium *D*-lines.[1] There are, however, two visible systems of Na_2 and a visible and infrared system of K_2, in each case involving transitions from a $^1\Sigma$ molecular ground level which dissociates into normal sodium, or potassium, atoms to excited molecular $^1\Sigma$ and $^1\Pi$ levels both of which dissociate into one normal atom and one in the resonance (^2P) state. Theory indicates that there should be four systems of NaK bands in the visible and infrared, since, besides the ground level which dissociates into normal sodium and potassium atoms, there should be a pair of levels, $^1\Sigma$ and $^1\Pi$, dissociating into normal sodium and excited potassium and a similar pair dissociating into normal potassium and excited sodium.

In the present investigation the apparatus used by Loomis and Nusbaum[2] for the study of the absorption and magnetic rotation spectra of Li_2, Na_2 and K_2 has been used in a search for the three unknown band systems of NaK. Two of them have been found and their vibrational structure analyzed and, in addition, the previously known orange system has been extended far enough to yield an accurate value of the heat of dissociation.

The chief difficulty has been that the strong band systems of Na_2 and K_2 cover nearly the whole of the visible and infrared spectrum. It has been possible to overcome this to some extent by taking advantage of the fact that the concentrations of the three molecules are respectively proportional to the products of the concentrations of their constituent atoms and by working with sodium with just a trace of potassium in the regions of the spectrum where the potassium bands, or lines, were troublesome and *vice versa*. As a consequence, it has been necessary to select, with considerable care, for each of many rather narrow spectral regions, the appropriate concentration, temperature, exposure, spectrograph and type of photographic plate. The concentration of either constituent cannot be decreased indefinitely by the above method because the total pressure eventually becomes so high as to cause troublesome broadening of the band lines.

The spectra were studied over the range 4500–11,500A, with the use, for the longer wavelengths, of the new Eastman Q type plates.

The constants of the levels concerned in these systems are given in Table I. The infrared, orange and green systems are transitions from the ground state (G) to the excited levels A, C and D, respectively. The bands which we earlier[3] erroneously reported as constituting the fourth system have since been found to be merely the part of the infrared ($A \leftarrow G$) system which lies to the high frequency side of the potassium resonance lines. The constants T_e, ω_e, $x_e\omega_e$, $y_e\omega_e$, $z_e\omega_e$ in Table I are those in the usual expansion

$$T(v) = T_e + \omega_e(v+1/2) - x_e\omega_e(v+1/2)^2 + y_e\omega_e(v+1/2)^3 + z_e\omega_e(v+1/2)^4 \cdots \quad (1)$$

[1] Ritschl and Villars, Naturwiss. **16**, 219 (1928).

[2] Loomis and Nusbaum, Phys. Rev. **38**, 1447 (1931); **40**, 380 (1932); **39**, 89 (1932).

[3] Loomis and Arvin, Phys. Rev. **44**, 126 (1933).

TABLE I. *Constants of the various levels for NaK.*

State	T_e	ω_e	$\omega_e x_e$	$\omega_e y_e$	$\omega_e z_e$	D_e volts	Dissociation products	Type
G	0	123.29	+0.400			0.62	Na+K	$^1\Sigma^+$
D	20,090.55	82.17	+0.350	−0.00814		0.24	Na′+K	$^1\Pi$
C	16,991.37	72.60	+1.475	+0.02436	−0.000545	0.14	Na+K′	$^1\Pi$
B	Not found						Na′+K	$^1\Sigma^+$
A	12,139.65	79.852	+0.0872	−0.003887		0.74	Na+K′	$^1\Sigma^+$

TABLE II. *Frequencies of absorption bands of the green system.*

v',v''	Intensity	Obs.	Obs.−Calc.	v',v''	Intensity	Obs.	Obs.−Calc.	v',v''	Intensity	Obs.	Obs.−Calc.
0,10	0	18882.0	+0.9	2,2	3	19987.2	−0.7	8,0	1	20697.3	+0.1
0,9	1	18999.5	+3.1	4,3	3	20025.4	−0.4	12,2	1	20744.7	+3.3
0,8	3	19113.8	+1.3	3,2	1	20066.3	−1.5	9,0	1	20771.3	+0.2
0,7	5	19229.6	+0.2		1	20079.1		15,3	0	20820.6	−2.6
3,9	1	19240.4	+2.0	2,1	1	20109.2	−0.4	10,0	1	20844.0	+0.2
1,7	2	19310.8	−0.1	4,2	2	20145.3	−1.4	16,3	1	20889.7	+1.8
	1	19329.9		9,5	2	20168.3	+1.7	11,0	1	20915.7	+0.4
0,6	5	19346.1	−1.0	4,1	2	20269.7	+1.3	13,1	0	20930.0	−2.0
1,6	3	19428.8	+0.2	3,0	2	20315.6	+3.6	17,3	0	20953.3	+2.2
0,5	3	19463.7	−1.8	8,3	0	20329.1	−3.0	12,0	0	20984.4	−1.2
1,5	3	19548.7	−1.3	5,1	2	20346.2	−0.4	14,1	0	20999.0	−0.6
0,4	1	19581.3	−3.7	6,1	2	20426.2	+2.6	16,2	0	21010.3	+1.5
1,4	3	19665.4	−0.9		1	20461.5		13,0	1	21053.3	−1.2
2,4	5	19744.1	−2.8	7,1	1	20499.4	−0.3	14,0	1	21121.7	−0.4
	1	19773.5		9,2	1	20525.5	−1.4	16,1	0	21129.8	−0.7
1,3	5	19785.8	−0.6	6,0	1	20545.5	−0.6	15,0	0	21191.4	+3.1
2,3	3	19865.4	−1.6		1	20605.5		17,1	0	21191.4	−2.3
3,3	3	19947.3	+0.4	7,0	1	20623.6	+1.4	16,0	1	21253.1	+0.1
	1	19954.5		9,1	1	20648.7	+0.1	17,0	0	21313.5	−2.7
	2	19964.7		11,2	1	20670.7	−0.4				

for the vibrational energy of a diatomic molecule. D_e represents the energy of dissociation of the particular state, in volts, from the *equilibrium* energy for that state; all the others are based on the extrapolation of the C state, which is believed to be the most accurate.

Tables II, III and IV give the frequencies of all band heads measured, in the green, orange and infrared systems, respectively, with the quantum numbers assigned to them and the differences between the frequencies observed and those calculated from the differences of the terms in Eq. (1) with the constants in Table I. The intensities reported are rough visual estimates. In each system the assignments become dubious near the short wave-length end, due to overlapping.

The extrapolations of the A, C and D levels to dissociation are shown in Figs. 1, 2 and 3, respectively. The full curves represent the values calculated from Eq. (1) and the constants of Table I. The dashed curve in Fig. 2 represents what appears to be the best extrapolation of the C level, based on the magnetic rotation measurements. The energy of the products of dissociation, $(T_d)_C$, so estimated, relative to the equilibrium energy of the ground state, is 18,087 cm^{-1}. It is apparent from Fig. 2 that this figure can hardly be in error by more than 250 cm^{-1} or, say, 0.03 volt. Now the D levels have been followed as far as 21,313 cm^{-1}, and converge somewhat above this, say at 22,000±400 cm^{-1}, so the products of dissociation must be different from those of the C levels and, in fact, the excess of energy, so estimated, $(T_d)_D-(T_d)_C=3913$ ±400 cm^{-1} is about equal to the difference of

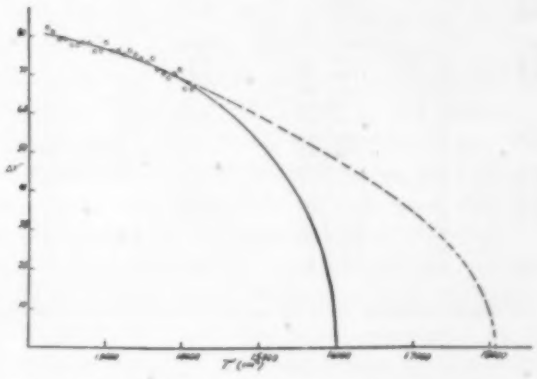

FIG. 1. Extrapolation of the A level to convergence. The full curve represents Eq. (1) and data in Table I. The dashed curve is an extrapolation consistent with that of the C level.

TABLE III. *Frequencies of the magnetic rotation spectrum of the orange system.*

v',v''	Intensity	Observed	Obs.–Calc.
18,0	0	17858.61	+0.27
	0	17838.65	
22,1	0	17833.44	+1.76
	0	17825.76	
	0	17818.14	
21,1	0	17811.10	−0.63
	0	17805.96	
16,0	0	17797.14	+2.10
	0	17793.86	
	0	17786.02	
15,0	0	17759.86	+0.06
25,2	0	17755.12	+4.09
	0	17748.18	
24,2	1	17742.14	+1.54
18,1	0	17736.06	+0.21
	0	17727.31	+0.55
14,0	0	17723.15	+0.69
	1	17719.48	
	1	17714.10	
22,2	1	17710.59	+0.59
17,1	1	17705.00	−0.41
	1	17701.24	
21,2	1	17689.46	−0.58
13,0	2	17683.57	+0.74
16,1	2	17672.78	+0.23
20,2	0	17668.89	+1.57
	1	17655.78	
12,0	3	17640.15	−0.85
19,2	1	17641.92	−0.20
15,1	1	17638.88	+1.57
25,3	1	17635.76	+5.63
	1	17626.63	
24,3	0	17618.65	−1.05
18,2	1	17612.98	−1.18
23,3	0	17607.43	+1.56
14,1	3	17601.21	+1.24
11,0	3	17597.63	+0.54
22,3	1	17589.43	+0.33
17,2	1	17585.13	+1.41
	1	17580.68	
	3	17577.61	
21,3	2	17567.68	−1.47
13,1	2	17560.22	−0.12
10,0	3	17550.90	−0.11
16,2	1	17551.18	−0.32
20,3	2	17545.78	−0.65
	0	17539.95	
	1	17553.90	
	1	17528.96	
19,3	0	17521.95	+0.72
12,1	2	17518.38	−0.13
15,2	0	17515.84	+0.22
25,4	2	17512.17	+2.13
	3	17510.37	
9,0	5	17502.71	−0.07
24,4	2	17500.32	+0.71
	0	17497.71	
18,3	0	17491.61	−1.66
23,4	1	17486.30	+0.52
	0	17483.98	
14,2	1	17477.83	−0.46
22,4	0	17470.92	+1.91
17,3	0	17465.75	+2.92
	0	17462.64	
	0	17458.01	
8,0	4	17452.45	+0.03
21,4	2	17445.60	−3.46
	0	17440.62	
13,2	1	17438.70	+0.05
16,3	0	17432.44	+2.47
10,1	1	17427.94	−0.58
20,4	0	17424.94	−1.40
	0	17413.50	
	0	17406.73	
19,4	4	17400.54	−0.60
7,0	8	17399.73	−0.13
12,2	2	17395.85	−0.97
25,5		17395.85	−5.10
	2	17388.34	
24,5	0	17380.18	−0.18
9,1	0	17380.18	−0.11
	1	17374.99	
18,4	1	17371.55	−1.63
23,5	0	17364.93	−1.56
14,3	1	17356.79	−0.60
11,2	0	17351.44	−1.47
22,5	0	17351.44	+1.72
6,0	4	17345.22	+0.15
17,4		17345.22	+2.48
	1	17335.34	
8,1	0	17329.29	−0.64
21,5		17329.29	−0.48
	1	17320.45	
13,3	1	17316.25	−1.51
10,2	3	17307.39	+0.56
	4	17297.57	
	8	17288.19	+0.19
19,5	3	17282.38	+0.53
7,1	1	17277.74	+0.37
25,6		17277.74	+5.48
15,4	1	17272.14	−2.50
	1	17266.07	
24,6	1	17260.81	−1.02
9,2		17260.81	+2.21
18,5	1	17254.99	+1.10
23,6	1	17246.97	−1.03
	1	17243.26	
14,4	2	17236.27	−1.03
11,3	8	17231.18	−0.84
22,6		17231.18	−0.05
4,0	4	17228.87	+0.24
17,5	2	17225.00	+1.55
6,1	1	17221.82	−0.76
	3	17218.30	
21,6	0	17212.20	+0.92
8,2	2	17207.65	−0.59
	1	17203.39	
	1	17201.00	
13,4	1	17196.90	−0.77
	1	17193.54	
16,5	1	17190.95	+0.36
20,6		17190.95	+2.39
	10	17181.57	
	3	17175.87	
		17170.59	+9.15
26,7			
3,0	8	17166.20	−0.60
5,1	5	17164.78	−0.73
19,6		17164.78	+1.42
25,7	3	17159.82	+5.25
7,2	3	17157.17	+1.49
	1	17151.27	
	3	17148.53	
24,7	2	17142.05	−2.09
18,6	3	17135.71	+0.31
23,7	1	17131.57	+1.26
	2	17128.82	
	3	17126.00	
	3	17120.93	
14,5	6	17118.26	+0.25
22,7	6	17113.45	−0.09
11,4	6	17109.97	−1.96
4,1	15	17105.81	−0.33
2,0	10	17102.68	+0.23
6,2		17102.68	+1.79
	4	17093.97	
	5	17092.12	
	5	17090.75	
8,3	8	17086.93	−0.43
	10	17082.28	
13,5	10	17078.78	+0.40
16,6	10	17071.83	−0.27
	15	17068.60	
10,4	*20	17065.25	−0.60
	20	17061.28	
0,1	15	16844.11	+0.85
	10	16837.42	
	10	16834.33	
	10	16829.46	
	12	16825.32	
	8	16811.20	
	8	16807.70	
5,4	6	16805.50	+2.66
3,3	8	16797.48	−4.25
1,2	8	16789.85	−1.44
	3	16782.36	
	3	16771.07	
	3	16757.81	
4,4	3	16741.79	−1.68
6,5	3	16740.36	−0.26
2,3	3	16736.55	−0.83
0,2	3	16720.79	−0.78
	3	16717.30	
	3	16714.21	
	3	16706.40	
	4	16703.22	
	1	16699.85	
	1	16694.87	
	1	16689.71	
5,5	1	16686.70	+3.15
3,4	2	16680.55	−1.09
1,3	6	16670.08	−0.32
	2	16654.60	
	1	16641.67	
	1	16629.37	
4,5	2	16623.64	−0.54
6,6	2	16623.64	+1.51
2,4	0	16617.01	−0.28
	0	16613.12	
0,3	8	16600.75	+0.07
	0	16580.08	
	0	16567.50	
5,6	0	16565.46	+0.40
3,5		16560.97	−1.38
1,4	3	16549.91	−0.40
	3	16544.74	
	1	16532.90	
	2	16528.22	
	2	16520.45	
4,6	1	16507.95	+2.26
6,7	1	16501.40	−3.04
2,5	1	16496.89	−1.11
	1	16493.29	
0,4	10	16480.27	−0.32
	1	16465.49	
	0	16458.33	
5,7	0	16449.74	+2.47
3,6	1	16443.07	−0.79
	0	16439.19	
	1	16434.89	
1,5	1	16430.41	−0.61
	0	16418.20	
	1	16405.05	
	1	16400.56	
	1	16394.19	
4,7	0	16387.81	−0.19
6,8		16387.81	+0.26
2,6	4	16379.23	−0.28
	0	16373.45	
0,5	8	16361.41	+0.11
	0	16344.63	
1,6	0	16312.40	−0.13
	0	16306.39	
	0	16293.60	
0,6	3	16243.29	+0.48

* Estimates of intensities in the vicinity of the *D*-lines are unreliable.

TABLE IV. *Frequencies of the absorption bands of the infrared system of NaK.*

v',v''	Intensity	Observed	Obs.–Calc.	v',v''	Intensity	Obs.	Obs.–Calc.	v',v''	Intensity	Observed	Obs.–Calc.
0,10	3	10931	+2.9	9,3	1	12459	−1.4		3	13335	
0,9	4	11041	−3.4	6,1	1	12472	+2.1		2	13344	
1,9	1	11126	+1.9	11,4	1	12490		16,0	3	13356	+1.5
0,8	5	11158	−2.5	8,2	2	12504	0.0		1	13364	
1,8	1	11241	+0.8	7,1	3	12546	−1.8	18,1	0	13378	−0.5
0,7	3	11274	−3.4	6,0	1	12594	+1.6		3	13384	
1,7	1	11356	−1.1	11,3	2	12614	+0.1	25,5	1	13392	+3.3
0,6	1	11391	−4.0	8,1	2	12626	+0.3		1	13398	
1,6	1	11472	−2.7		2	12631		20,2	1	13400	−0.7
0,5	1	11512	−1.5		1	12636			3	13412	
1,5	1	11594	+0.8	10,2	1	12656	−2.2	22,3	0	13421	−0.3
2,5	1	11672	−0.6	7,0	2	12670	−0.4	17,0	3	13428	+0.0
1,4	4	11714	+1.5	9,1	0	12705	+2.0	24,4	0	13441	+1.2
2,4	4	11793	+1.1	14,4	0	12721	+0.4	19,1	2	13455	+4.0
4,5	1	11830	−0.9	11,2	3	12734	−0.8		1	13462	
1,3	0	11835	+2.4	8,0	2	12749	+0.8		1	13469	
3,4	3	11873	+1.9	10,1	0	12780	+0.1	21,2	1	13474.0	+2.2
2,3	5	11912	+0.1	15,4	1	12795	−0.2	23,3	2	13490	+0.9
1,2	3	11954	+0.5	12,2	1	12810	−0.9	18,0	3	13503	+2.0
3,3	10	11990	−1.0	9,0	1	12828	+2.5	20,1	1	13525	+2.6
5,4	1	12026	−2.8	14,3	0	12840	−0.7	22,2	2	13543	+0.8
2,2	5	12034	+1.1	11,1	2	12856	+0.5		1	13548	
4,3	5	12072	+1.7	13,2	0	12887	+0.6		1	13570	
3,2	5	12113	+0.9	18,5	0	12893	−3.5	19,0	2	13577	+3.8
5,3	2	12151	+2.1	10,0	3	12903	+0.6	21,1	1	13593	−0.5
2,1	1	12155	+0.4	12,1	1	12930	−2.6	25,3	3	13626	−2.0
7,4	0	12187	+1.8	16,2	1	13112	+1.7	20,0	0	13648	+3.1
4,2	5	12192	+0.8	13,0	2	13130	−0.6	22,1	0	13665	+1.1
3,1	2	12232	−1.8	18,3	1	13136	+0.1	26,3	1	13697	+1.5
11,6	1	12257	+1.0	15,1	1	13159	+1.1	21,0	0	13718	+2.0
8,4	1	12263	0.0	17,2	2	13182	−1.8	23,1	1	13735	+1.5
5,2	1	12268	−1.8	14,0	3	13205	−0.8	25,2	1	13750	+1.0
2,0	1	12275	−2.1	16,1	1	13233	+1.0	22,0	1	13790	+3.6
7,3	0	12306	+0.7	23,5	2	13251	−0.5		1	13797	
4,1	2	12315	+2.1	18,2	1	13258	+1.2	24,1	1	13806	+3.5
6,2	2	12348	+0.2	15,0	3	13281	+0.6	16,2	0	13816	−0.4
5,1	3	12392	+0.5	17,1	2	13308	+2.5		1	13829	
10,4	0	12418	+0.8	24,5	0	13322	+1.5	25,1	0	13872	+1.3
7,2	0	12424	−2.2	19,2	1	13329	0.0				

the frequencies of the resonance doublets of sodium and potassium, 3951 cm^{-1}, so that it is natural to conclude that the C level dissociates into normal (3^2S) sodium and excited (4^2P) potassium and that the D level dissociates into normal (4^2S) potassium and excited (3^2P) sodium,[4] as stated in Table I. Assuming that the ground state of the molecule dissociates into normal atoms, as in Li_2, Na_2 and K_2, the energy of dissociation of the ground state

$$D_e''=(T_d)_G=(T_d)_C-13{,}015\ cm^{-1}$$
$$=5072\ cm^{-1}=0.62\ volt,$$

where 13,015 cm^{-1} is the average frequency of the resonance doublet of potassium. This is verified, well enough to confirm the above conclusions as to products of dissociation, by a direct extrapolation of the vibrational levels of the ground state. It will be noted that this value is, as expected, intermediate between the heats of dissociation of Na_2 and K_2 which are 0.76 and 0.51 volt, respectively. The most precise value of the energy of dissociation of the D state can then be obtained by

$$(T_d)_D=(T_d)_G+16{,}966\ cm^{-1}=22{,}038\ cm^{-1},$$

where 16,966 cm^{-1} is the average frequency of the sodium resonance doublet. It is to this point that the dashed curve in Fig. 3 is extrapolated. The extrapolation of the A levels is long and dubious but if it is assumed that the products of dissociation are normal sodium and excited potassium, as stated in Table I, the energy of dissociation $(T_d)_A$ must be the same as $(T_d)_C=18{,}087\ cm^{-1}$. The dashed curve in Fig. 1 is drawn to this point. It will be seen that this extrapolation is at least plausible. This is not true of an attempt to extrapolate this level to $(T_d)_D=22{,}038\ cm^{-1}$. Moreover this assignment accords better with the non-appearance of the fourth system. If the assignment in Table I is correct the B level may be expected to lie a little above the A level and the $B\leftarrow G$ system will be covered by the infrared systems of both Na_2

[4] Calculations by Margenau, Phys. Rev. **40**, 398 (1932), indicate that at distances of approach greater than 5 or 6A, the forces of interaction between an excited (3^2P) Na atom and a normal (4^2S) K atom are repulsive. The existence of the stable D state clearly shows that at smaller distances, at which the equations of Margenau should not be expected to hold, this repulsion is overcome by ordinary valence forces.

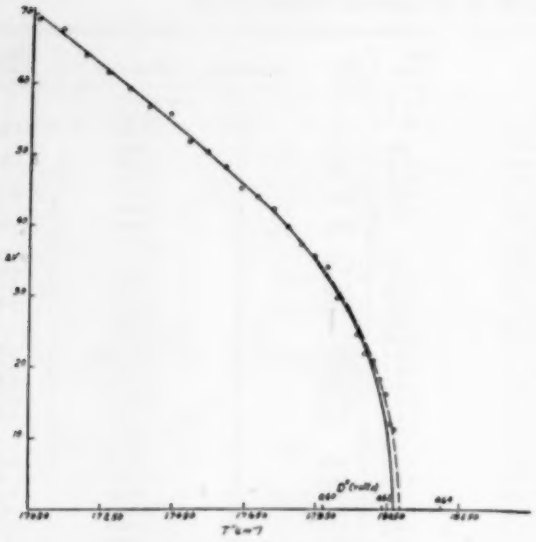

FIG. 2. Extrapolation of the C level to convergence. The full curve represents Eq. (1) and data in Table I. The dashed curve is the best extrapolation of the points.

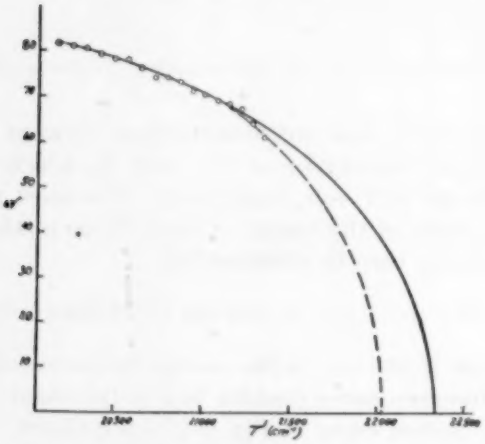

FIG. 3. Extrapolation of the D level to convergence. The full curve represents Eq. (1) and the data in Table I. The dashed curve is an extrapolation consistent with that of the C level.

and K_2 and by the $A \leftarrow G$ system of NaK. If the assignment were incorrect, the $B \leftarrow G$ system should lie on the long wave side of the $A \leftarrow G$ system and should have been observed.

With the apparatus of Loomis and Nusbaum,[2] magnetic rotation spectra have been observed in the region of each of the three absorption systems. The frequencies of the principal magnetic rotation lines of the orange system coincide approximately with those of the absorption band heads, just as do those in the $^1\Pi \leftarrow {}^1\Sigma$

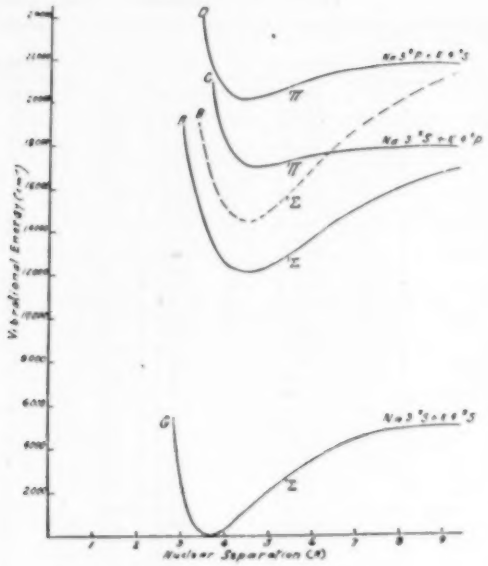

FIG. 4. Potential energy curves. That for the B state is hypothetical.

systems of lithium, sodium and potassium; and this analogy, together with the location of the origin of the system, indicates that the C state is $^1\Pi$. The measured frequencies of those magnetic rotation lines to which quantum numbers could be assigned are included in Table III, together with roughly estimated intensities. It will be observed that, as with Li_2, Na_2 and K_2, it has been possible to extend these assignments to higher values of v' than in absorption and the accuracy of the extrapolation to dissociation results chiefly from these measurements.

The magnetic rotation spectra in the regions of the green and infrared systems appear to resemble that of the red system of sodium. That is, although an interval approximately equal to the vibrational interval of the ground state is apparent on superficial inspection, nevertheless it is not possible to find any simple correspondence between the absorption and magnetic rotation spectra. An interpretation of this red magnetic rotation of sodium has been given by Fredrickson and Stannard,[5] to the effect that it is due to perturbations of the upper $^1\Sigma$ state by an unknown $^3\Pi$ state, which shares with the $^1\Sigma$ state some of its magnetic properties. Presumably this interpretation can also be applied

[5] Fredrickson and Stannard, Phys. Rev. **44**, 632 (1933).

to the infrared magnetic rotation spectrum of NaK, which also lies in the region of a $^1\Sigma \leftarrow {}^1\Sigma$ system; and also to the infrared magnetic rotation spectrum of K_2, which has been found incidentally to the work here reported. It is a little surprising, however, to have to call on the same hypothesis to account for the green magnetic rotation spectrum of NaK, since the upper level concerned in the green absorption system can, by analogy with Li_2, Na_2 and K_2, be hardly other than $^1\Pi$. It is true, however, that even in the green magnetic rotation system of Na_2 there are many lines, including all those with what Wood[6] has called the positive direction of rotation, which do not fit into the vibrational analysis, nor correspond to absorption heads. One can suppose that these are also of the perturbation type; and one can then account for the non-appearance of a regular magnetic rotation spectrum of NaK in the green system by supposing that it is masked by a perturbation type of magnetic rotation which, for some reason, is considerably stronger.

Fig. 4 is a set of potential energy curves for the levels concerned in the above spectra, together with a dashed curve indicating the existence of the hypothetical B level. The curves are calculated according to the Morse formula, by using the values of ω_e and D_e in Table I and, for want of measurements on rotational structure, taking the values of r_e from Badger's[7] recently published empirical formula in which d_{34} for NaK has been given the value 1.20 obtained by interpolating between $d_{33}(Na_2) = 1.05$A and $d_{44}(K_2) = 1.35$A.

Fig. 5 is an improved[8] Franck-Condon diagram for the three systems, in which T'' is plotted as abscissa and T' as ordinate, downwards. The

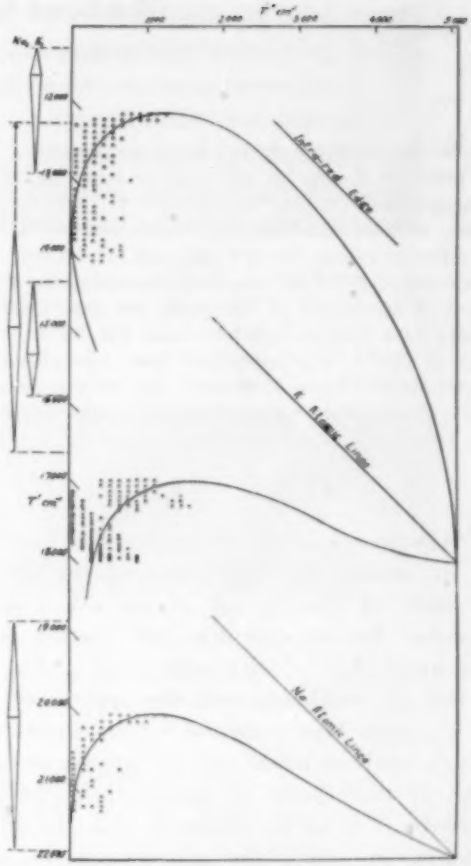

FIG. 5. Improved Franck-Condon diagram for the three systems. Overlapping systems of Na_2 and K_2 are schematically indicated in the left margin.

frequency of each band head can be found by projecting at 45° to the left and upwards on to the T' axis. The frequencies of the overlapping Na_2 and K_2 systems are schematically indicated on the margin. The curves are the theoretical loci of maximum intensity obtained in the usual way from the potential energy curves of Fig. 4. The long wave-length edge to the infrared system which, according to the theoretical curve should lie at 10,150 cm^{-1} is actually found at 9600 cm^{-1}.

[6] Wood, Proc. Am. Acad. **42**, 235 (1906); Astrophys. J. **30**, 339 (1909).
[7] Badger, J. Chem. Phys. **2**, 128 (1934).
[8] Loomis and Nusbaum, Phys. Rev. **38**, 1447 (1931).

The Band Spectrum of Caesium

F. W. Loomis and P. Kusch, *University of Illinois*

(Received June 6, 1934)

Measurements of five distinct band systems of Cs_2 have been made, in absorption with high and low dispersion, in magnetic rotation, and in fluorescence. Three of these systems, with maxima at 6250A, 7200A, and 7667A, have been reported before, but not analyzed. The fourth with a maximum at 4800A and the fifth, extending from 8950A to limit of sensitivity of the plate, are new. Quantum numbers have been assigned to some 218 bands in the system at 7667A. The upper and lower vibrational frequencies are 34.28 and 41.99 cm^{-1}, and an extrapolation yields 0.45 volt as the energy of dissociation of the ground state. This system, and the one beyond 8950A, apparently correspond to the green and red systems of sodium, respectively. The origin of the fifth system lies beyond the region of sensitivity of even the new Eastman *Q* plates. Some regularities in the other systems have been found, but no complete analysis could be made, though a fluorescence spectrum was obtained in the 6250 system which showed the lower state to be the same as in the 7667A system. This 6250A system is extraordinarily complex and appears to contain some bands degraded to the red, some to the blue and some narrow regions of absorption bounded by edges on both sides. No magnetic rotation spectrum was found.

THIS investigation was undertaken in order to extend our knowledge of the spectra and heats of dissociation of the alkali metal molecules. Rather complete information is already available[1, 2, 3] with regard to Li_2, Na_2 and K_2, but, although some of the spectra of Rb_2 and Cs_2 have been reported,[4, 5] no satisfactory analysis has been made, nor are any trustworthy values of their heats of dissociation available. Moreover it is to be expected that the heavy elements, in which the atomic spectra show strong spin-orbit interactions, will show in their band spectra an approach to a new type of coupling, at least in the neighborhood of dissociation.

Because caesium is so expensive, it is not feasible to use quite the same apparatus and methods as have been employed with Li_2, Na_2 and K_2. Fortunately, however, its vapor pressure becomes high enough to give well-developed molecular absorption spectra at temperatures so low that glass is only very slowly attacked. The work was therefore done with caesium which was prepared by heating dry caesium chloride with metallic calcium and then distilled, in several stages, *in vacuo*, into the glass absorption tube. In use, the absorption tube was heated to temperatures between 180° and 350°C by means of a coil of wire wound around its whole length and with a little closer winding near the ends to keep the windows hotter than the rest and therefore free from condensed caesium. The absorption spectra were photographed with instruments of various dispersions, including the first order of a 21 foot 30,000 line/inch concave grating in a Paschen mounting, which gave a dispersion of 1.3A/mm. This proved necessary to effect satisfactory resolution of the *vibration* structure in many regions; in no region was it adequate to resolve the rotational structure.

The spectra were also photographed when the caesium was in the presence of 40 cm of argon. The effect of argon was in all regions to cause the bands to appear at lower temperatures. No selective effect was noticed, not even a difference between diffuse bands and those with structure.

An attempt was made to find a magnetic rotation spectrum of Cs_2, to aid in the analysis. The glass absorption tube was put into the solenoid used by Loomis and Nusbaum[1] and long exposures taken in all regions of the visible and photographic infrared spectrum, without success. It cannot be concluded, however, that Cs_2 does not possess any magnetic rotation spectrum, for it may well be that there is one in the infrared, as is to be expected by analogy with Li_2, Na_2 and K_2, but that it cannot be photographed in a reasonable time with the plates available in that region.

Attempts were also made to find fluorescence spectra. Unfortunately there is a dearth of strong lines, suitable for excitation, in the regions

[1, 2, 3] Loomis and Nusbaum, Phys. Rev. **38**, 1447 (1931); **39**, 89 (1932); **40**, 380 (1932).
[4] Walter and Barratt, Proc. Roy. Soc. **A119**, 257 (1928).
[5] Rompe, Zeits. f. Physik **74**, 175 (1932).

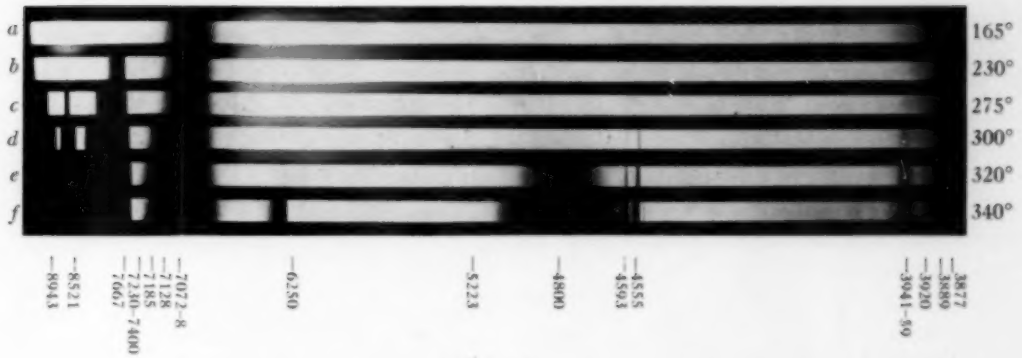

FIG. 1A.

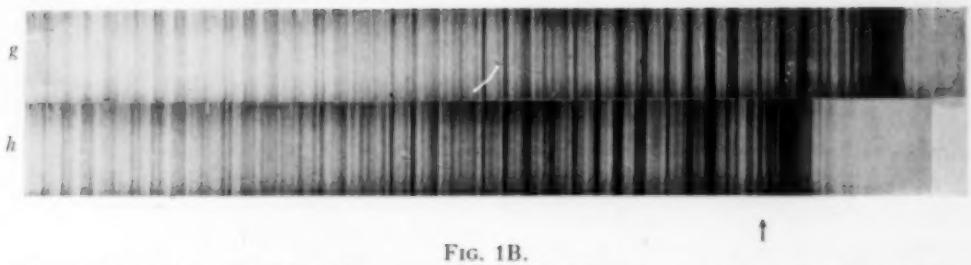

FIG. 1B.

FIG. 1. The band spectra of Cs_2. The spectrograms on the left, *a–f*, were taken on an Eastman 3P plate; those to the right on an Eastman hypersensitive panchromatic plate.

of the caesium absorption bands. Excitation by hydrogen, helium and mercury yielded no results, but a long U-shaped neon tube placed parallel to a caesium tube, and used with Wood's light-furnace[6] technique, yielded a series of fluorescence lines excited by Ne 6402A and with a spacing of 40 cm^{-1}. This demonstrated, what would not otherwise have been evident, that the absorption system at 6250A has a lower state with a vibrational interval 40 cm^{-1} and which is presumably the ground state and identical with the lower state of the 7667A system.

All the band spectra of Cs_2 which have been found in the region 3880–10,500A are shown in Fig. 1, *a–f* which was taken, for this purpose, with a Hilger E63 spectrograph at the temperatures indicated. The following distinct features are apparent:

I. At the extreme right is the 3877, 3889A, $8^2P \leftarrow 6^2S$ doublet of the principal series, in which, at high temperatures, the structure reported by Kuhn[7] and explained by him in terms of polarization molecules, becomes apparent.

II. At 3920A is a single faint sharp band, degraded to the blue, appearing at 300°C, previously reported by Kuhn.

III. A band which Kuhn has reported as a diffuse maximum with a long wave-length edge at 3961A appears at 270°C and at higher temperatures can be clearly seen on our original plates to contain four heads, degraded to short wave-lengths, at 3941, 3947, 3953 and 3959A and to be accompanied, on the long wave-length side by faint diffuse maxima at approximately 3983, 4006, 4035 and 4065A. It was not certain that these diffuse maxima belong to the caesium band systems. They may be part of a band system due to NaCs reported by Walter and Barratt[4] which lies between 3931 and 4315A, and which faintly appears on our plates.

IV. In the neighborhood of the 4555, 4593A, $7^2P \leftarrow 6^2S$ doublet of the principal series appears the structure reported by Kuhn and attributed to polarization molecules.

V. At about 300°C a band system begins to develop in the blue-green, having its maximum intensity at about 4800A. With increasing temperature this system spreads out in both directions. On the short wave-length side, it

[6] Wood, Phil. Mag. [6] **35**, 235 (1918).
[7] Kuhn, Zeits. f. Physik **76**, 782 (1932).

approaches, and perhaps finally crosses, the 4555, 4593A doublet. On the long wave-length side it terminates rather abruptly at high temperatures in an edge at 5223A, not visible in Fig. 1, which appears very similar to the infrared edge reported and explained by Loomis and Nile[5] in the red system of Na_2 and to other red edges which have since been found in corresponding systems. From these general features, which are very much like those of the $^1\Sigma \leftarrow {}^1\Sigma$ systems of Li_2, Na_2 and K_2 it appears very likely that this is a $^1\Sigma \leftarrow {}^1\Sigma$ system associated with the second doublet of the principal series of caesium. The only previous mention of this system which we have found is by Walter and Barratt[4] who call it a diffuse band with an edge, on the red end, at 5224A. We believe there can be no doubt that it actually belongs to Cs_2, since the faintness of the lines of the other alkali atoms shows that they cannot be present in important amounts, and since this band system does not coincide with any of those attributed by Walter and Barratt[4] to mixed alkali molecules. This system does not, on superficial inspection, appear in any way unusual, but we have not succeeded in making a satisfactory analysis of it. The heads near the center of the system are rather diffuse. In the region of somewhat longer wave-lengths some regularities are apparent and we have been able to assign vibrational quantum numbers to a number of bands, except for unknown additive constants in both v' and v''. The frequencies of these bands, together with those we have been unable to assign, are given in Table I. The numbers n' and n'' are, except for additive constants, equal to v' and v''. The upper vibrational interval is 31 cm^{-1} and the lower is 40 cm^{-1} which latter approximately agrees with that for the ground state of the 7667A system.

VI. At about 360° a very faint system, not previously reported, begins to appear near 5600A. It is too faint to be seen in Fig. 1, but is developed fairly well by the admixture of 40 cm of argon. As the temperature of the caesium-argon mixture is raised the system extends only slightly towards the blue but broadens considerably toward the red and eventually overlaps the system at 6250A.

[5] Loomis and Nile, Phys. Rev. **32**, 873 (1928).

TABLE I. *Band heads in the system at 4800A.*

v observed	n''	n'	v observed	n''	n'	v observed	n''	n'
21368.8			20971.2			20228.7		
21344.1			20960.2			20268.0	5	0
21315.1			20928.6			20228.2	6	0
21305.4			20827.2			20187.7	7	0
21287.6			20800.1			20164.5		
21276.9			20758.4			20148.3	8	0
21253.2			20704.5			20122.9		
21234.1			20562.3			20108.2	9	0
21221.4			20500.2	0	1	20067.8	10	0
21196.9			20491.1	1	2	20021.7		
21168.7			20461.1	1	1	19982.5		
21139.5			20450.7	2	2	19935.0		
21112.9			20420.1	2	1	19887.1		
21082.1			20410.1	3	2	19851.0		
21056.0			20389.2	2	0	19807.1		
21030.9			20379.4	3	1	19739.3		
21002.9			20339.1	4	1	19696.4		
20988.6			20308.0	4	0	19658.3		

Under low dispersion, in argon, the system appears almost completely diffuse; but in a grating photograph, taken through caesium in vacuo, it is seen to consist of a hopeless confusion of very fine and incompletely resolved lines, with no apparent heads or regularities of any kind.

VII. At about 230°C a prominent, but very complex, band system appears near 6250A. Under low dispersion it appears to terminate fairly sharply on the short wave-length side, and to degrade toward long wave-lengths. With higher temperatures it has been followed as far as 6550A. This system has been reported by Rompe.[5] It appears in Fig. 1, *g* and *h*, which are from grating photographs. The bands show no sign of rotational structure, even under the highest dispersion. They vary widely in appearance. Some degrade to the red, some to the blue; some appear as almost sharp lines and some as narrow bands with heads on both sides. Some 258 of them have been measured. We have by no means attained a complete analysis or understanding of this system, or systems, but some regularities have been uncovered.

First, the 6402A line of neon excites a fluorescence series of lines whose frequencies and frequency intervals are given in Table II. It follows that the lower state of this system has a vibrational interval of about 40 cm^{-1}, and this agrees with the ground interval of the system at

TABLE II. *Fluorescence series excited by the 6402A line of neon.*

ν observed	$\Delta\nu$ observed
Ne 15615.2	
	39.9
15575.3	
	41.6
15533.7	
	39.7
15494.0	
	38.7
15455.3	
	38.6
15416.7	

7667A. With this as a basis, the heads of 31 bands, all degraded to the blue, have been assigned to a square array. Their frequencies can be expressed by the formula

$$\nu = 16{,}045.06 + 29.38(n' + \tfrac{1}{2}) - 0.0796(n' + \tfrac{1}{2})^2 - [41.990(v'' + \tfrac{1}{2}) - 0.080051(v'' + \tfrac{1}{2})^2 - 0.000164266(v'' + \tfrac{1}{2})^3], \quad (1)$$

in which the lower vibration interval agrees with that of the 7667A system. Since the system could not be traced to the origin, n' presumably differs from the true v' by some unknown constant. The observed frequencies, the intensities, quantum numbers and the differences between the measured values and those calculated from Eq. (1) are given in Table III. It is rather surprising however that bands with these upper and lower intervals should be degraded to the blue.

Second, it is clear that there is an important set of intervals beginning with 54.0 cm^{-1} and converging toward the red at the rate of about 0.6 cm^{-1} per quantum number. This can be seen in Fig. 1, *g* and *h*, which are two prints of the same grating photograph, displaced by an amount which, at the points indicated by the arrow, corresponds to 54 cm^{-1}. It will be seen that the spectral regions which are thus brought into conjunction are almost, but not quite, entirely alike, even to the finer details.

TABLE III. *Band heads in the system at 6250A.*

ν observed	I	v''	n'	$\nu_{obs.}-\nu_{calc.}$	ν observed	I	v''	n'	$\nu_{obs.}-\nu_{calc.}$
15770.37	7	7	0	0.02	15594.25	4	15	5	0.04
15758.96	6	8	1	0.07	15587.08	4	13	2	−0.03
15747.38	3	9	2	−0.06	15583.43	4	16	6	0.10
15729.77	5	8	0	0.10	15576.17	4	14	3	−0.19
15695.78	5	11	3	−0.05	15572.57	4	17	7	0.10
15684.60	3	12	4	0.01	15561.41	4	18	8	−0.23
15678.08	4	10	1	0.04	15554.92	4	16	5	0.01
15666.86	5	11	2	−0.07	15544.37	6	17	6	0.17
15655.79	4	12	3	−0.05	15533.70	6	18	7	0.17
15644.74	4	13	4	−0.02	15522.87	6	19	8	0.01
15633.75	4	14	5	0.06	15515.88	5	17	5	0.10
15626.93	4	12	2	−0.01	15505.41	4	18	6	0.15
15622.76	4	15	6	0.13	15495.10	3	19	7	0.35
15611.75	5	16	7	0.15	15484.22	3	20	8	−0.05
15605.06	5	14	4	−0.05	15445.77	5	21	9	−0.09
15600.38	3	17	8	−0.20					

Third, there is a set of intervals, starting from about 14 cm^{-1} and converging toward the red, which has been reported by Rompe, and is quite apparent on our plates, but which we are inclined to consider as sequence intervals.

VIII. At 7072, 7075 and 7078A there are three sharp edges, degraded to the blue, which appear as a single diffuse band in Fig. 1 and were so reported by Rompe. The frequencies of their heads, with the intervals between them in parentheses, are: 14,136.79 (6.41) 14,140.38 (6.55) 14,123.83 cm^{-1}. There are also two bands which may really be diffuse, at 7128 and 7185A.

IX. In the region 7230 to 7400A there occurs at 300°C a faint system of ten sharp and accurately measurable bands, degraded to the red. Their frequencies can be expressed by the formula

$$\nu = 13{,}741.74 + 38.46n' - 49.41n'' \quad (2)$$

but since no convergence is apparent in either level, and since neither vibrational interval is the same as any other known interval, the numbers n' and n'' cannot be definitely identified with quantum numbers, nor can certain alternative arrangements, whose spacings are simple linear functions of the above, be excluded. However, the assignment according to Eq. (2) arranges the bands into a more plausible square array than any other. The system extends in both directions until it is overlapped by other structures which make it impossible to follow it further. The measured frequencies of the bands, together with the differences between the observed frequencies and those calculated from Eq. (2) are given in Table IV.

X. The strongest system of the entire spectrum, with its origin at 7667A, appears at about 170°C and with increasing temperature extends in both directions, moving rather slowly toward the blue and rapidly toward the red. The bands are sharp, and accurately measurable on the

TABLE IV. *Band heads in the system at 7200A.*

ν observed	n''	n'	$\nu_{obs.}-\nu_{calc.}$	ν observed	n''	n'	$\nu_{obs.}-\nu_{calc.}$
13818.29	0	2	−0.37	13681.37	2	1	−0.01
13780.25	0	1	0.05	13642.86	2	0	−0.06
13758.80	2	3	0.50	13593.00	3	0	−0.51
13730.81	1	1	0.02	13544.04	4	0	−0.06
13692.50	1	0	0.17	13494.90	5	0	0.21

grating plates, and are degraded to the red. It is possible to see that they have rotational structure but it is not sufficiently resolved to be measured. We have measured 343 band heads in this system and have assigned vibrational quantum numbers to 211 of them, including 7 bands for which two alternative assignments are possible. Most of the unidentified bands lie at the red end of the system where it crosses the diffuse bands (XI); a few of them lie near the blue end where there is much overlapping. Near the origin of the system all bands are assigned.

The frequencies of all assigned bands can be represented with satisfactory accuracy by the equation

$$\nu = 13{,}043.87 + 34.230(v'+\tfrac{1}{2}) - 0.077986(v'+\tfrac{1}{2})^2 - 0.000188149(v'+\tfrac{1}{2})^3 - [41.990(v''+\tfrac{1}{2}) - 0.080051(v''+\tfrac{1}{2})^2 - 0.000164266(v''+\tfrac{1}{2})^3]. \quad (3)$$

The quantum numbers, the measured frequencies, and the differences between the measured frequencies and those calculated from Eq. (3) are given in Table V. The unidentified bands are also included, and in the case of many such bands near the red end of the system their arrangement into apparent sequences is indicated, the sequences being designated by roman numerals and the ordinal numbers of the band heads by arabic ones. Unfortunately, it has not been found possible to fit these sequences, unambiguously, into the quantum number scheme.

The upper and lower vibrational terms of all assigned band heads are plotted in Fig. 2, which is an improved[1] Franck-Condon diagram for the 7667A system. It will be noted that this diagram for this system is a little unusual in that the right arm of the locus is much more extensive, and even extends to higher values of v', than the left arm. This is because the left arm curves to the right so much that the weaker bands, with high v's overlap the stronger ones and cannot be distinguished. Another contributing factor is that the transition probabilities on the left arm are much smaller than on the right arm. This has been found to be the case with the other alkali molecules, notably in Wood's fluorescence experiments with Na_2, and is to be expected theoretically since the left arm corre-

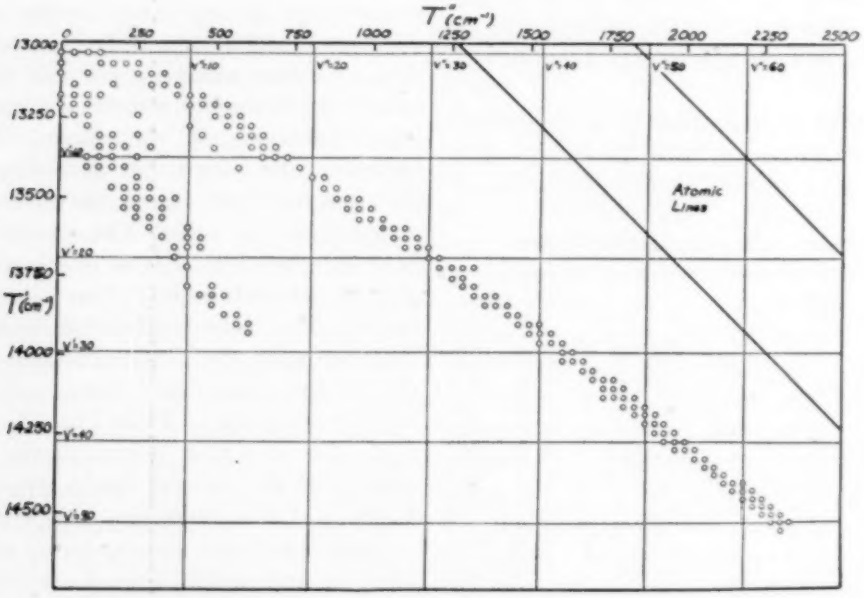

FIG. 2. Improved Franck-Condon diagram for the 7667A system of caesium.

TABLE V. *Band heads in the system at 7667A.*

ν observed	v''	v'	νobs.−νcalc.
13372.42	10	23	0.34
13362.56	11	24	0.44
13352.55	12	25	0.40
13342.30	13	26	0.14
13332.99	14	27	0.82
13328.87			
13327.55	5	15	0.27
13325.36			
13323.71	2	11	0.69
13322.58	12	24	0.46
13322.58	15	28	0.42
13321.23	9	20	0.55
13318.47	6	16	0.55
13311.07	10	21	−0.03
13308.33	7	17	−0.22
13305.02	4	13	0.36
13302.32	14	26	−0.19
13299.43	8	18	0.29
13298.80			
13298.24			
13297.70			
13297.22			
13295.86	5	14	0.39
13294.35			
13292.32	12	23	0.41
13292.32	15	27	−0.37
13291.53			
13290.81	2	10	0.29
13290.19	9	19	0.45
13288.40			
13287.15			
13286.80	6	15	0.52
13284.45			
13283.61			
13282.60	13	24	0.31
13281.98	3	11	0.47
13277.30	7	16	0.24
13263.61	5	13	0.13
13254.63	6	14	0.17
13249.15	3	10	0.14
13249.15	10	19	−0.25
13240.45	4	11	0.28
13236.66	8	16	0.28
13222.84	6	13	0.37
13221.01			
13219.13	10	18	0.84
13216.82	3	9	0.47
13213.68	7	14	0.07
13209.52	0	5	0.47
13209.52	11	19	0.29
13208.11	4	10	0.44
13205.07	8	15	0.33
13203.89			
13200.84	1	6	0.30
13199.33	5	11	0.34
13193.51			
13192.18	2	7	0.15
13190.51	6	12	0.20
13187.36	10	17	0.36
13183.91	3	8	0.39
13181.75	7	13	0.13
13180.07			
13178.31	11	18	0.19
13176.97			
13175.43	0	4	−0.13
13175.43	4	9	0.42
13173.03	8	14	0.10
13167.26	1	5	0.04
13163.26			
13161.11			
13159.02	2	6	0.15
13142.66	4	8	0.48
13133.88	1	4	0.15
13133.88	5	9	0.05
13131.70	9	14	−0.72
13125.79	2	5	0.24
13125.79	6	10	0.31
13108.17	0	2	0.07
13100.12	1	3	0.04
13091.95	2	4	−0.11
13074.14	0	1	0.01
13060.64	6	8	0.65
13053.73			
13051.79	7	9	−0.18
13050.76	3	4	0.21
13048.30			
13039.99	0	0	−0.02
13024.66	2	2	0.06
13014.88			

ν observed	v''	v'	νobs.−νcalc.
12998.29	1	0	0.11
12993.74	6	6	−0.09
12975.62	4	3	0.06
12956.52	2	0	0.01
12949.07	3	1	−0.05
12920.12			
12915.11	3	0	0.11
12907.81	4	1	0.03
12866.57	5	1	−0.03
12864.76	10	7	0.15
12863.08			
12861.46			
12859.77	6	2	0.21
12857.39	11	8	−0.05
12852.45	7	3	−0.07
12850.38	12	9	0.11
12836.36	14	11	0.41
12825.67	6	1	0.08
12818.83	7	2	0.12
12811.84	8	3	0.00
12805.08	9	4	0.10
12798.18	10	5	0.05
12777.99	8	2	−0.04
12771.23	9	3	−0.10
12764.72	10	4	0.08
12757.97	11	5	0.01
12751.34	12	6	0.06
12744.65	13	7	0.04
12738.11	14	8	0.15
12731.25	15	9	−0.06
12724.40	11	4	−0.07
12724.40	16	10	−0.27
12717.89	12	5	−0.07
12711.54	13	6	0.07
12705.18	14	7	0.22
12698.17	15	8	−0.31
12691.88	16	9	−0.13
12685.54	17	10	0.00
12677.96	13	5	−0.17
12671.80	14	6	0.00
12665.60	15	7	0.12
12659.14	16	8	−0.04
12652.95	17	9	0.07
12646.68	18	10	0.09
12640.00	19	11	−0.32
12634.03	20	12	−0.03
12627.78	21	13	−0.05
12621.56	22	14	−0.03
12614.91	23	15	−0.44
12608.83	24	16	−0.31
12595.65	21	12	0.00
12589.66	22	13	0.06
12583.41	23	14	−0.14
12577.38	24	15	−0.12
12571.28	25	16	−0.18
12565.31	26	17	−0.12
12559.51	27	18	0.10
12553.20	28	19	−0.20
12545.62	24	14	−0.07
12539.80	25	15	−0.02
12533.84	26	16	−0.12
12528.08	27	17	−0.04
12522.17	28	18	−0.12
12516.19	29	19	−0.28
12510.33	30	20	−0.34
12504.68	31	21	−0.20
12498.70	32	22	−0.40
12492.89	33	23	−0.44
12490.90	28	17	−0.10
12487.18	34	24	−0.38
12485.17	29	18	−0.19
12481.36	35	25	−0.46
12479.57	30	19	−0.16
12473.83	31	20	−0.29
12468.14	32	21	−0.38
12462.51	33	22	−0.42
12456.95	34	23	−0.40
12451.42	35	24	−0.36
12445.69	36	25	−0.54
12440.29	37	26	−0.39
12435.74			
12435.01	38	27	−0.13
12432.20	33	21	−0.15
12429.17	39	28	−0.44
12423.65	40	29	−0.44
12415.86	36	24	−0.32
12414.32			
12412.50	42	31	−0.58
12410.40	37	25	−0.44

ν observed	v''	v'	νobs.−νcalc.
12405.12	38	26	−0.36
12399.62	39	27	−0.52
12396.09	34	21	−0.28
12394.32	40	28	−0.49
12390.53	46	35	−0.68
12388.72	41	29	−0.77
12383.52	42	30	−0.66
12378.34	43	31	−0.54
12373.08	44	32	−0.52
12367.63	45	33	−0.70
12364.89	40	27	−0.39
12362.37	46	34	−0.71
12359.76	41	28	−0.45
12357.29	47	35	−0.54
12354.57	42	29	−0.52
12351.87	48	36	−0.72
12349.42	43	30	−0.56
12346.65	49	37	−0.72
12344.21	44	31	−0.68
12341.45	50	38	−0.71
12339.13	45	32	−0.68
12336.38	51	39	−0.58
12334.07	46	33	−0.68
12331.23	52	40	−0.54
12328.97	47	34	−0.73
12325.99	53	41	−0.60
12323.94	48	35	−0.72
12318.95	49	36	−0.68
12314.12	50	37	−0.50
12308.99	51	38	−0.63
12304.08	52	39	−0.55
12300.70	47	33	−0.67
12299.00	53	40	−0.65
12295.70	48	34	−0.83
12294.05	54	41	−0.63
12290.95	49	35	−0.75
12289.21	55	42	−0.51
12286.14	50	36	−0.74
12284.29	56	43	−0.48
12281.44	51	37	−0.64
12279.56	57	44	−0.28
12276.59	52	38	−0.70
12274.80	58	45	−0.11
12271.92	53	39	−0.59
12270.02	59	46	0.03
12267.17	54	40	−0.57
12265.24	60	47	0.16
12262.51	55	41	−0.48
12260.55	61	48	0.37
12257.93	56	42	−0.31
12255.80	62	49	0.51
12253.28	57	43	−0.23
12251.30	63	50	0.89
12248.64	58	44	−0.15
12246.48	64	51	0.94
12244.13	59	45	0.05
12239.54	60	46	0.16
12235.12	61	47	0.43
12230.65	62	48	0.64
12229.71	I	1	
12226.21	63	49	0.87
12225.16	I	2	
12221.92	64	50	1.24
12220.79	I	3	
12216.48	I	4	
12213.85	60	45	0.38
12213.15	II	1	
12211.96	I	5	
12209.54	61	46	0.55
12209.00	II	2	
12207.61	I	6	
12205.38	62	47	0.86
12204.69	II	3	
12204.10	III	1	
12203.31	I	7	
12201.15	63	48	1.09
12200.51	II	4	
12199.01	I	8	
12197.02	64	49	1.41
12196.26	II	5	
12195.48	III	3	
12194.71	I	9	
12192.91	65	50	1.73
12192.11	II	6	
12191.37	III	4	
12190.53	I	10	
12188.87	IV	1	
12188.02	II	7	
12187.12	III	5	

ν observed	v''	v'	νobs.−νcalc.
12186.36	I	11	
12184.85	IV	2	
12183.86	II	8	
12183.14	III	6	
12182.22	I	12	
12180.89	IV	3	
12179.87	II	9	
12179.04	III	7	
12178.11	I	13	
12176.88	IV	4	
12175.83	II	10	
12175.00	III	8	
12174.12	I	14	
12173.10	IV	5	
12170.99	III	9	
12169.98	I	15	
12169.24	IV	6	
12167.13	III	10	
12163.20	III	11	
12159.32	III	12	
12157.86	V	1	
12157.19	VI	1	
12155.46	III	13	
12154.79	V	2	
12154.04	VI	2	
12151.71	III	14	
12151.71	V	3	
12150.98	VI	3	
12148.87	V	4	
12147.93	III	15	
12147.93	VI	4	
12146.40	VII	1	
12144.20	III	16	
12142.74	VII	2	
12140.41	III	17	
12139.18	VII	3	
12136.69	III	18	
12133.04	III	19	
12129.48	III	20	
12126.00	III	21	
12124.21	VIII	1	
12122.57	III	22	
12122.03	IX	1	
12120.60	VIII	2	
12119.12	III	23	
12118.42	IX	2	
12117.02	VIII	3	
12115.77	III	24	
12114.83	IX	3	
12113.81	VIII	4	
12112.34	III	25	
12109.00	III	26	
12107.55	X	1	
12105.63	III	27	
12102.23	III	28	
12101.30	X	3	
12100.23	XI	1	
12098.87	III	29	
12098.04	X	4	
12096.73	XI	2	
12095.46	III	30	
12092.06	III	31	
12088.86	III	32	
12085.92	III	33	
12082.80	III	34	
12079.56	III	35	
12078.67	XII	1	
12077.29	XIII	1	
12075.32	XII	2	
12073.97	XIII	2	
12071.95	XII	3	
12070.59	XIII	3	
12068.54	XII	4	
12065.18	XII	5	
12062.29			
12061.78	XII	6	
12061.07			
12054.98	XIV	1	
12051.57	XIV	2	
12049.59	XV	1	
12048.30	XIV	3	
12046.61	XV	2	
12043.73	XV	3	
12042.27	XIV	5	
12040.88	XV	4	

sponds to transitions to comparatively steep parts of the upper potential energy curve. Because of the limited extent of the left arm, reliable combination differences for checking the assignments to the right arm are lacking, and it is for this reason that the assignment of sequences near the red end of the system becomes ambiguous.

In Figs. 3 and 4 the vibrational intervals, ΔT, are plotted against the vibrational terms, for the lower and upper states of this system, respectively. The circles represent the experimental values; the full curves correspond to the intervals and terms calculated from Eq. (3). It will be noted that, as is usual in such cases, the last observed points begin to drop below the curves, so that the values of T' and T'' at which these curves strike the axes can be taken as maximum values for the energies of the respective products of dissociation. That is, $T_a' < 15{,}800$ cm^{-1} and $T_a'' < 4020$ cm^{-1}. On the other hand T' and T'' have already been followed as far as 14,570 cm^{-1} and 2330 cm^{-1} and are still far from convergence. It seems fairly safe to conclude that minimum values of the energies of the respective atomic products of dissociation are given by the extrapolations along the dashed curves in Figs. 3 and 4, which yield $T_a' > 15{,}050$ cm^{-1}, $T_a'' > 3300$ cm^{-1}. Now the convergences have been followed far enough to leave no doubt that, as with the other alkalis, the products of dissociation of the ground state of the molecule are two normal (6^2S) Cs atoms and that those of the upper state are a normal atom and one in the 6^2P state; but they are not sufficient to allow one to distinguish whether the excited atomic state is $6^2P_{1/2}$ or $6^2P_{3/2}$. Hence in deducing maximum and minimum values for $T_a'' = D_e''$ from the above maximum and minimum values of T_a' one must in the first case use the high frequency component, 11,732 cm^{-1}, and in the second case the low frequency component, 11,178 cm^{-1}, of the resonance doublet of caesium. These yield

$$D_e'' < 15{,}800 - 11{,}178 = 4622 \text{ cm}^{-1},$$
$$D_e'' > 15{,}050 - 11{,}732 = 3318 \text{ cm}^{-1}.$$

Since the direct extrapolation of the ground state of the molecule yields 4020 cm$^{-1} > D_e'' > 2900$ cm^{-1} one may conclude that

$$4020 \text{ cm}^{-1} > D_e'' > 3318 \text{ cm}^{-1}$$

or

$$0.496 \text{ volt} > D_e'' > 0.410 \text{ volt},$$

and one may well take $D_e'' = 0.45$ volt as the best value and feel confident that it is not in error by more than 0.04 volt.

This value is a not unreasonable extrapolation of the heats of dissociation of the other alkalis, as can be seen from Fig. 5 in which the values of D_e'' are plotted for H_2, Li_2, Na_2, K_2 and Cs_2. The smooth curve fits all points within their limits of error. Interpolation according to the curve gives 0.47 volt as a fairly reliable value for the energy of dissociation, D_e'', of Rb_2.

Several values of D_e'' have been published, all of which are smaller than the minimum value

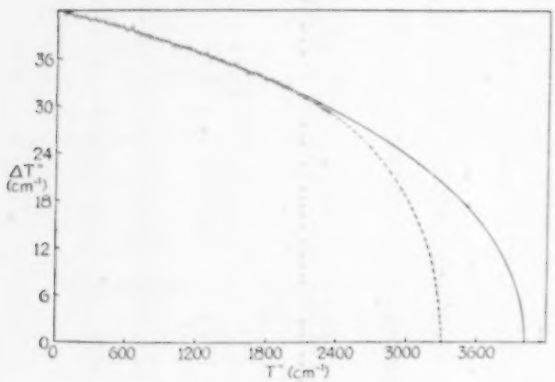

FIG. 3. $\Delta T''$ vs. T'' for 7667A system.

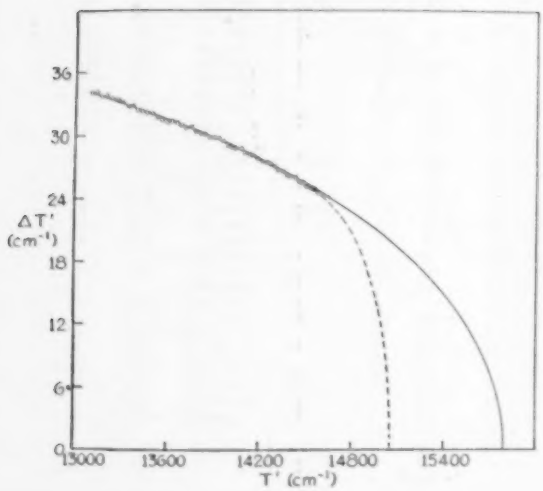

FIG. 4. $\Delta T'$ vs. T' for 7667A system.

0.41 volt, compatible with our measurements. However, the only reliable one, by Freudenberg,[9] agrees with ours within his limits of error. Our minimum value depends on the dotted extrapolation in Fig. 4 and an inspection of this curve will show that it can hardly be subject to the general suspicion that all band spectrum extrapolations are too high. It seems worth while, however, to discuss the accuracy and validity of the results of previous observers.

Minkowski and Mühlenbruch,[10] on the basis of measurements of the variation of pressure needed to annul the effect of variation of temperature on the overall intensity of the 6250A bands, concluded that 0.24 volt $> D_e'' >$ 0.04 volt. This is in conflict with our result and cannot be correct since we have already followed the vibrational levels of the ground state as far as 2330 $cm^{-1} = 0.29$ volt and are still far from convergence. Their conclusions are, however, subject to the serious error that they are based on measurements of total absorption, instead of the integral of absorption coefficients, and that the effect of increase of temperature, even when compensated by pressure variation, will be, in part, to shift the absorption from lines where it is nearly total, to higher lines where it is smaller and more nearly proportional to the absorption coefficient.

Boeckner and Mohler[11] measured the variation with temperature of the ratio between the ionization produced by atomic absorption of light of shorter wave-length than the series limit, and that produced by the assumed molecular absorption between the series lines, and concluded that $D_e'' = 0.26$ volt. Their deductions are however subject to the same source of error as Minkowski and Mühlenbruch's.

Rompe publishes values of the energy of dissociation of the ground state; but these are based on unsupported and unjustifiable interpretations as to the nature of certain bands and band systems, and need not be further considered.

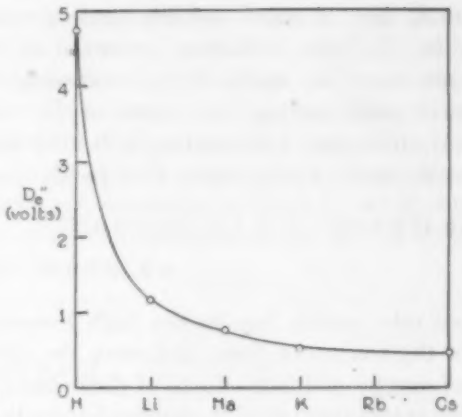

FIG. 5. Curve showing the energies of dissociation of the elements in the alkali metal group.

Freudenberg[9] concludes, on indirect evidence, that 0.55 volt $> D_e'' >$ 0.15 volt, and our value also lies between these limits but is considerably more precise. Freudenberg's value depends on his determination of the energy of activation, E, of the reaction

$$Cs'(7^2P_{3/2}) + Cs(6^2S) + E = Cs_2^+ + \text{electron}$$

as $E = 0.125 \mp 0.025$ volt, resulting from a study of the temperature dependence of photo-ionization by the 4555A, $7^2P_{3/2} \leftarrow 6^2S$ line of Cs. It also depends on his interpretation of the phenomenon observed by Boeckner and Mohler[11] that photo-ionization of caesium vapor can be caused by light not coinciding with atomic lines if its wave-length does not exceed 3800A. This effect is interpreted, both by Boeckner and Mohler and by Freudenberg, as being due to absorption of light by the neutral molecule, which is thus brought into an excited state with enough energy to auto-ionize immediately. Freudenberg concludes that J_m, the ionization potential of the caesium molecule is 3.17 ∓ 0.20 volts, corresponding to 3880A. The evidence for this interpretation, while plausible, is somewhat indirect and not absolutely conclusive. If accepted, it follows that

$$J_m = D_e'' + h\nu(4555\text{A}) + 0.125 \text{ volt} \qquad (4)$$

or $D_e'' = 3.17 - 2.71 - 0.125 = 0.33 \mp 0.2$ volt, as stated by Freudenberg. This agreement with our directly determined value of D_e'' may serve as confirmatory evidence for the above inter-

[9] Freudenberg, Zeits. f. Physik **67**, 417 (1931).
[10] Minkowski and Mühlenbruch, Zeits. f. Physik **63**, 198 (1930).
[11] Boeckner and Mohler, Bur. Standards J. Research **5**, 831 (1930).

pretation, but a more reliable and accurate value for J_m, the ionization potential of the molecule may be deduced by reversing the argument and putting our value of D_e'' into Eq. (4), retaining Freudenberg's 0.125 ∓ 0.025 volt as the heat of activation. This yields

$$J_m = (0.45 \mp 0.04) + 2.71 + (0.125 \mp 0.025)$$
$$= 3.28 \mp 0.07 \text{ volts.}$$

Since this system lies on the high frequency side of the resonance lines, and since the difference of energy of the products of dissociation of the two states concerned is approximately equal to the energy of the resonance level of the atom, it is very likely that it is a $^1\Pi \leftarrow {}^1\Sigma$ transition as the corresponding systems in Li_2, Na_2 and K_2 are known to be.

XI. At 8170, 8262, 8346 and 8733A, appear four diffuse bands, degraded to the red, the last lying between the members of the resonance doublet. These may be similar to the structure around the second and third doublets of the principal series which has been reported by Kuhn.[7] On plates of higher dispersion a finer structure can be seen, closer to the resonance lines.

XII. From between the resonance lines to at least 10,500A, the limit of effective sensitivity of Eastman Q type plates, lies a strong system of numerous bands with sharp heads, degraded to the red. It seems very probable that this corresponds to the $^1\Sigma \leftarrow {}^1\Sigma$ systems which have been found on the long wave-length side of the resonance doublets in the molecules Li_2, Na_2 and K_2. The origin of this system appears to lie beyond the region we were able to photograph, so that a complete analysis was not possible. However 44 bands have been measured and 38 have been assigned to three v' progressions. Their frequencies can be represented by the equation

$$\nu = 9596.5 + 41.66n' - 0.04642n'^2 - 34.7n'', \quad (5)$$

in which n' and n'' presumably differ by constants from the true v' and v''. The observed frequencies, the assigned n' and n'' and the differences between the measured frequencies and those calculated from Eq. (4) are given in Table VI.

TABLE VI. *Band heads in the system to the long wave-length side of the resonance doublet.*

ν observed	n''	n'	$\nu_{obs.} - \nu_{calc.}$	ν observed	n''	n'	$\nu_{obs.} - \nu_{calc.}$
10843.1				10086.8	0	12	−2.9
10838.7				10053.7	1	12	−1.3
10834.8				10047.9	0	11	−1.2
10765.6	2	29	0.1	10013.7	1	11	−0.7
10731.9	1	29	1.1	10012.5			
10688.4	1	28	−2.9	9973.2	1	10	−0.5
10652.3	1	27	−0.4	9971.8			
10612.2	1	26	−1.3	9967.3	0	9	−0.4
10574.9	1	25	0.7	9931.3	1	9	−1.7
10535.6	1	24	0.8	9926.7	0	8	−0.1
10498.0	1	23	2.6	9891.3	1	8	−0.8
10456.3	1	22	0.5	9886.3	0	7	0.5
10417.3	1	21	1.2	9851.0	1	7	−0.1
10378.1	1	20	1.7	9845.3	0	6	0.5
10338.1	1	19	1.6	9809.7	1	6	−0.4
10297.0	1	18	0.4	9768.0	1	5	−0.9
10257.2	1	17	0.6	9728.2	1	4	0.5
10216.6	1	16	0.2	9689.0	1	3	2.6
10176.3	1	15	0.1	9644.8	1	2	−0.1
10134.8	1	14	−1.1	9603.5	1	1	0.1
10127.2	0	13	−3.0	9567.5	2	1	−1.3
10094.5	1	13	−1.0	9562.4	1	0	0.6

The v' levels of this system converge very slowly, so that their extrapolation to convergence, which according to Eq. (5) occurs at 19,000 cm^{-1}, is extremely unsafe, but since such long extrapolations almost always give values which are too high, it is entirely reasonable to assume that the products of dissociation of the upper state of this system are, by analogy with similarly located bands of Li_2, Na_2 and K_2, a normal Cs atom and one in the resonance state, in which case the true convergence point would be 15,500 cm^{-1} or less.

A letter in *Nature* by Matuyama[12] has just appeared in which measurements on caesium bands are also reported. In general his measurements are less accurate and his analysis less complete than ours, and he does not get a value for the energy of dissociation. The points of agreement and disagreement are as follows: (1) His equation for the 7667A system is, as far as it goes, roughly equivalent to ours, but he assigns only 38 bands to it, while we have assigned 211 bands, which has enabled us to extrapolate to dissociation. (2) His equation for the 6250A system is somewhat like ours, but his value for ω'' of the lower state of this system differs from that of the 7667A system, while our analysis makes it accurately the same and, since it agrees also with the fluorescence interval, justifies its interpretation as the ground level. (3) He reports the lower and upper vibrational

[12] Matuyama, Nature **133**, 568 (1934).

intervals of the 7200A system as 39 and 29 cm^{-1}, based on measurements of 16 heads. We have taken them as 49.5 and 38.5 cm^{-1}, based on measurements of 10 heads, but convergence is not appreciable and it would also have been possible to assign them as Matuyama has done. This would have given equally good combination differences but the arrangement into a square array would have been abnormal. (4) We believe that the band system which he reports at 8200A is merely the red end of the 7667A system, after it has been interrupted by the diffuse bands at 8170, 8262 and 8346A. We have measured the bands in this region and reported them as unassigned sequences in Table V. (5) Matuyama also notes the existence of the new system XII.

Band Systems of BaCl

ALLAN E. PARKER, *Columbia University and Yale University*

(Received May 21, 1934)

Three band systems of BaCl have been analyzed by means of spectrograms taken in the second order of two 21 foot gratings. The green system (λ5047 to λ5322) is a $^2\Pi-{}^2\Sigma$ transition and due to the nearly equal values of ω for the two electronic states is composed of only the $\Delta v=0, \pm 1$ sequences. There are two ultraviolet systems with (0,0) bands at λ3922 and λ3692, respectively. Both are presumably $^2\Sigma-{}^2\Sigma$ transitions and have broader Franck-Condon parabolas than the green system. The isotope effect of Cl^{35} and Cl^{37} is observed but in none of the systems could any bands be definitely attributed to barium isotopes other than Ba^{138}. The dissociation products are discussed.

INTRODUCTION

THE existence of bands due to BaCl has been known for some time.[1,2] Two groups of bands were observed by King and Harnack. There is an extremely intense system in the green extending from λ5047 to λ5322. The other group is in the ultraviolet and extends from λ4005 to λ3555. This group is composed of two systems which are much weaker than the green system. Hedfeld[3] photographed the green system with a 12 foot grating, burning $BaCl_2$ in an oxy-acetylene flame, and made an assignment of certain of the bands. Schaafsma[4] also photographed these bands using an arc in a hydrogen atmosphere. He attempted unsuccessfully to assign them to a $^2\Sigma-{}^2\Sigma$ transition of BaH. The present work shows quite conclusively that this is not correct, since it is quite evident upon spectrograms taken with sufficient dispersion and intensity that what Schaafsma refers to as lines are really band heads. Furthermore the isotope effect of Cl^{35} and Cl^{37} is observed. This will be discussed in more detail later in the paper. The present analysis confirms that of Hedfeld in the main, though differing in several essentials, and it extends his analysis considerably, assigning several hundred bands instead of some thirty to forty. The analysis of the ultraviolet bands had not been previously attempted.

[1] A. S. King, Astrophys. J. **21**, 236 (1905).
[2] A. Harnack, Dissertation, Leipzig (1911).
[3] K. Hedfeld, Zeits. f. Physik **68**, 610 (1931).
[4] A. Schaafsma, Dissertation, Groningen (1932).

EXPERIMENTAL DETAILS

To excite the bands a method quite similar to that of Schaafsma was used. An arc was formed in a bulb between a water-cooled nickel anode and a copper cathode in the form of a cup, the cup containing $BaCl_2$. The bulb was filled with hydrogen to a pressure of 5–10 cm of mercury. The bands were obtained with approximately the same intensity if nitrogen was used instead of hydrogen, showing that the bands were undoubtedly not BaH. Also these bands were not obtained from an arc between barium electrodes in a hydrogen atmosphere. All spectrograms measured were taken with hydrogen in the bulb as they were much "cleaner."

Spectrograms of the various BaCl bands were obtained in the second order of the 21 foot

grating at Yale which is in a stigmatic mounting, giving a dispersion of 2.5A/mm in this order, and in the second order of the 21 foot grating at Columbia which is in an astigmatic mounting, giving a dispersion of 1.3A/mm in this order. With the first grating, exposures were of the order of fifteen minutes for the green bands and one hour for the ultraviolet bands, the arc drawing 4 amperes on a 220 volt circuit. It might be remarked here that the reduction in exposure times makes the stigmatic mounting for a grating extremely welcome for the photography of weak bands, more than making up in general for the halving of the dispersion. The green system was photographed on Eastman Panchromatic and Eastman D-C Ortho plates. Eastman 33 and 40 plates were used to photograph the ultraviolet systems. An iron arc comparison spectrum was placed on each plate. Some of the plates were measured on the comparator at Yale University and others on the comparator of New York University, and I wish to thank Professor E. O. Salant for the opportunity of using the latter.

The Green Band System

The various alkaline-earth halides all have strong band systems in the green. These are attributed to $^2\Pi - {}^2\Sigma$ transitions and the present analysis of the green BaCl bands is in agreement

Table I. *Vibrational assignments of the head-forming branches of the* $^2\Pi - {}^2\Sigma$ Ba^{138} Cl^{35} *bands.*

	$v'-v''=+1$				$v'-v''=0$				$v'-v''=-1$			
v''	R_2	Q_2	R_1	Q_1	R_2	Q_2	R_1	Q_1	R_2	Q_2	R_1	Q_1
0	19,746.2	19,736.7	19,352.7	19,344.4	19,468.2	19,452.4	19,074.6	19,063.8				
1	(51.1)	39.6			73.2	57.0	76.4	65.8	19,195.3		18,795.9	18,786.1
2	54.4	42.7			78.0	61.6	77.9	67.4	201.4	19,177.3	99.6	89.3
3	57.5	45.9			83.0	66.5	79.7	69.1	07.5	83.4	804.6	92.8
4	60.6	49.1			87.0	71.3	81.7	71.0	13.9	89.8	07.1	95.9
5	64.1	52.2			92.9	76.1	83.5	72.7	20.1	96.3	10.5	99.6
6	67.6	55.6			98.1	80.7	85.4	74.6	26.6	202.7	14.2	802.9
7	70.0	58.9			503.4	85.8	87.4	76.4	33.0	09.0	17.7	06.2
8	74.3	62.2			08.8	90.5	89.3	77.9	39.4	15.6	21.6	09.8
9	77.9	65.6			13.9	95.3	91.5	79.7	45.8	22.2	25.1	13.3
10	80.3	69.0			19.3	500.5	93.6	82.5	52.2	28.7	28.7	16.7
11	83.1	72.5			24.7	05.4	95.6	84.5	58.9	35.4	32.5	20.5
12	86.7	75.9			30.3	10.5	97.8	86.5	65.5	42.0	36.5	24.0
13	90.2	78.7			36.2	15.5	100.1	88.5	72.3	48.7	40.2	27.7
14	94.1	81.4			41.6	20.7	02.3	90.7	79.1	55.6	44.1	31.4
15	97.8	85.2			47.4	25.8	04.5		86.4	62.5	48.0	35.2
16	801.5	88.7				31.0	06.8		93.1	69.4	52.1	38.8
17	03.8	92.3	60.7			36.2	09.2		305.8	76.6	56.1	42.6
18		96.3	61.7			41.6	11.7			83.7	60.2	46.4
19		99.9	62.6			46.8	14.2			91.8	64.4	50.2
20		802.2	63.7			52.0	17.0			99.1	68.9	54.0
21		05.0	64.6	60.1		57.5				305.8	72.9	58.0
22			65.7	61.1		62.9				12.7	76.5	61.9
23				62.1		68.2				19.3	80.2	65.8
24				63.1		73.7				26.4	85.2	69.8
25				64.2		79.1				32.5	88.7	73.8
26				65.2		84.6					92.7	77.7
27				66.2		89.9					96.0	81.8
28						96.5					901.6	85.9
29						602.0						90.3
30						07.7						94.5
31						13.4						97.8
32						19.3						902.3
33						25.4						06.5
34						31.4						11.0
35												15.1
36												19.4
37												23.8
38												28.1
39												33.0
40												36.9
41												41.4
42												46.0
43												50.5
44												55.0
45												59.5
46												64.1
47												69.5
48												74.5

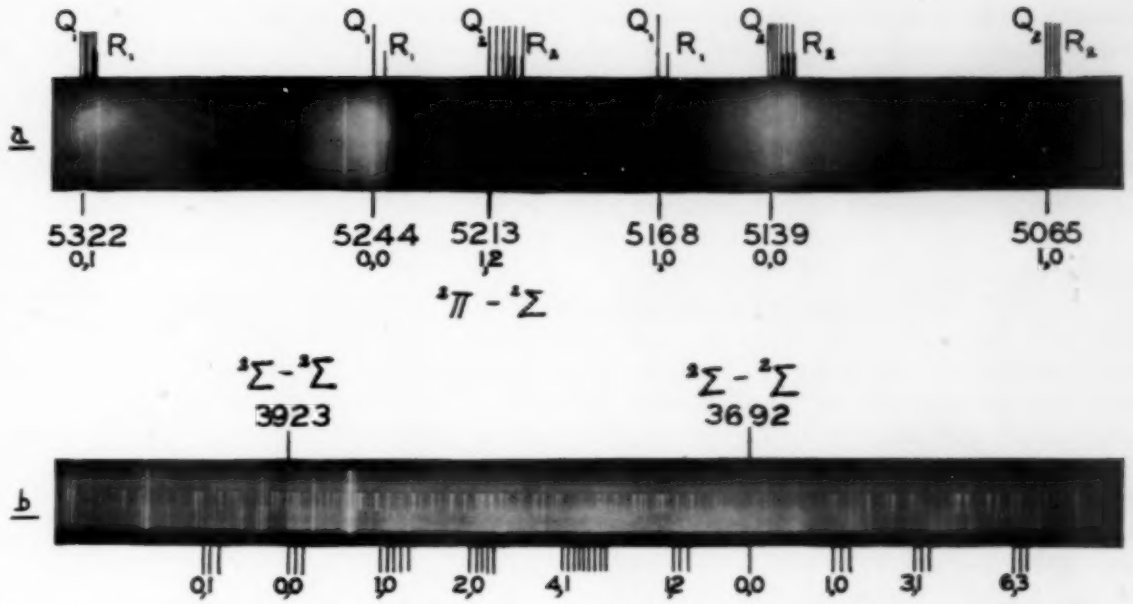

FIG. 1. Spectrograms of BaCl bands. The v values of the first head in each sequence are given. (a) $^2\Pi - {}^2\Sigma$ bands. The R and Q heads are marked. To be noted is the increased diffuseness of the heads of high v value. (b) Both $^2\Sigma - {}^2\Sigma$ transitions with the P heads marked.

with this assignment of electronic states. The bands degrade to the red until one reaches high values of v. Hence one may expect to find four strong head-forming branches, R_2, Q_2, R_1 and Q_1. The $^1R_{21}$ branch is also a head-forming branch and as the $^2\Pi$ state is close to case a, it should be a strong branch. However, no heads attributable to this branch were observed though all the observed heads were assigned with the exception of eight extremely weak ones whose real existence is doubted. The general appearance of the bands is shown in Fig. 1a. Six groups of bands are observed. The heads of the R_2 and Q_2 branches lie near each other as do those of the R_1 and Q_1 branches. The coupling constant of the upper state is quite large and hence for each of the three sequences observed there are two groups, one due to transitions originating on the T_1 levels and the other due to transitions originating on the T_2 levels. The assignments of the bands are given in Table I for the Ba^{138} Cl^{35} molecule. To be noted is the decreased spacing in the respective branches as one goes from the $v'-v''=+1$, to the $v'-v''=0$, to the $v'-v''=-1$ sequence. As a result of this the various heads of the R_1 and Q_1 branches in the $v'-v''=-1$ sequence were not observed completely to the (1,0) band. Those that were observed with high v values were assigned in Table I on the basis of their combination differences and as there are but few of these to use for the assignment, there may be

TABLE II. *$G(v)-G(v+1)$ values for the states giving rise to the green BaCl bands. $\Delta v=v'-v''$.*

	$^2\Pi$				$^2\Sigma$			
	Q_2		Q_1		Q_2		Q_1	
Δv	0, +1	−1, 0	0, +1	−1, 0	0, −1	+1, 0	0, −1	+1, 0
v								
0	284.3		280.6	279.7		279.7	277.7	278.6
1	282.6	284.3		278.1	279.7	278.0	276.5	
2	281.1	283.1		276.3	278.2	276.2	274.6	
3	279.4	281.5		275.1	276.7	274.6	273.2	
4	278.1	279.8		273.1	275.0	273.0	271.4	
5	276.1	278.0		271.7	273.4	271.5	269.8	
6	274.9	276.8		270.2	271.7	269.8	268.4	
7	273.1	274.9		268.1	270.2	268.4	266.6	
8	271.7	273.3		266.4	268.3	266.7	264.6	
9	270.1	271.8		265.8	266.8	265.1	263.0	
10	268.5	270.0		264.0	265.1	263.6	262.0	
11	267.1	268.5		262.5	263.4	262.0	260.5	
12	265.4	266.8		260.8	261.8	260.4	258.8	
13	263.2	265.1		259.3	259.9	258.0	257.1	
14	260.7	263.3			258.2	255.6	255.5	
15	259.4	261.6			256.4	254.2		
16	257.7	259.6			254.4	252.5		
17	256.1	257.9			252.5	250.7		
18	254.7	255.0			249.8	249.5		
19	253.1	252.9			247.7	247.9		
20	250.2	251.7			246.2	244.7		
21	247.5	250.2			244.8	242.1		
22		248.9			243.6			
23		247.3			241.8			
24		246.6			241.2			

an error of one or two in the values of v given to these heads.

The following equations have been derived from the Q_1 and Q_2 heads, respectively:

$$\nu = 19{,}062.9 + [280.2(v'+\tfrac{1}{2}) - 0.79(v'+\tfrac{1}{2})^2] - [278.4(v''+\tfrac{1}{2}) - 0.80(v''+\tfrac{1}{2})^2],$$

$$\nu = 19{,}450.1 + [285.0(v'+\tfrac{1}{2}) - 0.79(v'+\tfrac{1}{2})^2] - [280.5(v''+\tfrac{1}{2}) - 0.80(v''+\tfrac{1}{2})^2].$$

The $G(v)-G(v+1)$ values from which these are derived are given in Table II. The $G(v)-G(v+1)$ values for the differences of the $v'-v''=+1$ and the $v'-v''=0$ sequences were selected as being the more accurate, since the heads are formed at lower J values in the $v'-v''=+1$ sequence than in the $v'-v''=-1$ sequence. This variation in J_{head} accounts for the discrepancy between the $G(v)$ values obtained from the $\Delta v=0$, $+1$ and from the $\Delta v=0$, -1 sequences. The possibility that the $^2\Pi$ state is an inverted state as is the case for a comparable state of BeF should also be noted.

A point of interest is that the R_2 and Q_2 heads for the bands of high v value in the $v'-v''=1$ sequence are not sharp. The bands are in fact headless. This is to be expected for the reason that the B_e values of the upper and lower states must be nearly equal as they are in the ratio of the ω values, which we know are nearly the same. If there is a slight difference in the α, then the B value of the upper state may become larger than the B value of the lower state causing the direction of degradation of the bands to reverse. During the transition the bands will appear headless before degrading to the violet. This phenomenon has been observed in several other instances such as the violet CN bands, the N_2^+ bands and the BeH bands.

The continua to the red of the (0,0), (1,0) and (0,1) bands are readily ascribable to the unresolved P branches.

In Table III are listed the bands due to Ba^{138} Cl^{37} which are in the calculated position relative to the Ba^{138} Cl^{35} bands listed in Table I.

The ρ value of Ba^{138} Cl^{35} as against Ba^{136} Cl^{35} is 1.0015. Hence we see that observation of the Ba^{138} *vs.* Ba^{136} isotope effect is not to be hoped for in dealing with the $\Delta v=0$, ± 1 sequences

TABLE III. $^2\Pi-{}^2\Sigma$ *bands due to* Ba^{138} Cl^{37}.

$v'-v''$	R_2 0	Q_2 0	R_1 −1	Q_1 −1
v''				
0	19,467.3			
1	72.1			
2	76.9			
3	81.7			
4	86.7	19,470.5		
5	91.6	75.4		
6	96.6	80.1		
7	501.8	84.5		
8	06.7	89.6		
9	11.9	94.4		
10	17.1	99.2		
11	22.4	503.4		
12	27.6	08.8		
13	33.1	13.9		
14	39.2	19.3		
15	44.2	23.8		
16	49.5	29.0		
17	54.8	34.1		
18	60.1	39.2		18,853.0
19	65.3	44.2		
20	70.6	49.5	18,876.5	
21	75.9	53.2		
22		58.7		67.3
23	88.8	64.6		71.2
24	94.8	69.4		75.4
25	600.2	74.7		80.3
26	06.5			
27	12.8	87.4		88.6
28		93.1		92.6
29	24.2	98.1		96.0
30		603.7		900.1
31		09.3		03.7
32		14.8		07.7
33		20.8		11.8
34		26.6		
35		32.4		
36		39.1		20.9

TABLE IV. *Vibrational assignments of the P heads of the longer wave-length* $^2\Sigma-{}^2\Sigma$ *system.*

$v'-v''$	−2	−1	0	+1	+2	+3	+4
v''							
0			25,484.2	25,787.7	26,088.8		
1		25,205.7	509.3	810.8	109.1	26,407.1	
2		32.4	34.7	33.4	30.0	25.5	
3	24,957.2	58.8		56.1	50.6	43.9	
4				78.0	70.8	62.0	26,752.9
5					90.6	80.1	
6					209.9	97.5	83.4
7					29.1	514.5	
8						31.2	812.7
9						47.6	27.2
10						63.4	41.1
11						78.7	54.5
12						94.0	67.6
13						608.3	80.5
14							93.0

TABLE V. *Vibrational assignments of the P heads of the shorter wave-length* $^2\Sigma-{}^2\Sigma$ *system.*

$v'-v''$	−1	0	+1	+2	+3
v''					
0		27,080.9	27,391.2		
1	26,802.7	113.5	422.0	27,728.7	
2	36.5		52.8	58.1	
3	70.2		84.2	87.4	28,091.8
4	904.4			817.6	118.5
5					46.8

TABLE VI. $G(v)-G(v+1)$ *values for the longer wave-length* $^2\Sigma-{}^2\Sigma$ *system.* $\Delta v=v'-v''$.

	$G'(v)-G'(v+1)$						
Δv	−2, −1	−1, +0	0, +1	+1, +2	+2, +3	+3, +4	Ave.
v							
0		303.6	303.5				303.6
1	301.6	302.3	301.5	301.1			301.6
2			298.7	298.3	298.0		298.3
3				296.6	295.5		296.1
4				294.5	293.3		293.9
5				292.8	291.2		292.0
6					289.5	290.9	290.2
7					287.6		287.6
8					285.4	285.9	285.7
9							
10						281.5	281.5
11						279.6	279.6
12						277.7	277.7
13						275.8	275.8
14						273.6	273.6
15						272.2	272.2
16						270.4	270.4

$G''(v)-G''(v+1)$

Δv	−2, −1	−1, 0	0, +1	+1, +2	+2, +3	+3, +4	Ave.
v							
0		278.5	278.4	278.0			278.3
1		276.9	276.1	275.7	277.1		276.5
2	275.2	275.9		273.9	274.9		275.0
3				272.6	273.1		272.9
4					271.6	272.8	272.2
5					270.2		270.2
6					268.4	268.9	268.7
7							
8						265.1	265.1
9						263.8	263.8
10						262.4	262.4
11						260.5	260.5
12						259.3	259.3
13						257.9	257.9

except at very high v values where the intensity has diminished to such an extent as to make the rarer isotope of barium virtually impossible to photograph. Hence the bands which Hedfeld assigned to $Ba^{138}Cl^{37}$ must be assigned otherwise. The other isotopes of barium will have somewhat larger values of ρ but their abundance is much lower.

THE ULTRAVIOLET BAND SYSTEMS

The BaCl bands in the ultraviolet comprise two systems both of which are believed to be $^2\Sigma-{}^2\Sigma$ transitions. Fig. 1b shows the two systems. From the combination differences (compare Tables II, VI and VII), we see that these two systems and the green system must have a common lower state which is presumably the ground state of the BaCl molecule. Since the bands are single headed, we are led to the conclusion that we have here two $^2\Sigma-{}^2\Sigma$ transitions with inappreciable spin-doubling in the electronic states as is the case for the $^2\Sigma-{}^2\Sigma$ N_2^+ bands. Since the bands degrade to the violet, the heads are formed by the P_1 and P_2 branches which are observed as a single head.

The possibility that the two systems are really the P_1 and P_2 heads of a single system must be considered. But the close agreement in ω values for the lower state and the large spin-doubling that must be assumed, were this the case, are difficulties which seem to bar this proposal.

Tables IV and V give the vibrational assignments of the bands of $Ba^{138}Cl^{35}$ belonging to these two transitions. The Franck-Condon parabola for each of these systems is much broader than that of the green system, as is seen from the observed transitions. This is quite in agreement with the larger variance in the ω values. The $G(v)-G(v+1)$ values are given in Tables VI

TABLE VII. $G(v)-G(v+1)$ *values for the shorter wave-length* $^2\Sigma-{}^2\Sigma$ *system.* $\Delta v=v'-v''$.

Δv	$G'(v)-G'(v+1)$					$G''(v)-G''(v+1)$				
v	−1, 0	0, +1	+1, +2	+2, +3	Ave.	−1, 0	0, +1	+1, +2	+2, +3	Ave.
0	310.8	310.3			310.6	278.2	277.7			278.0
1		308.5			308.5	277.0		275.9		276.5
2			306.7		306.7			273.9		273.9
3			305.3		305.3				274.2	274.2
4			303.2		303.2					
5				304.4	304.3					
6				300.9	300.9					

and VII. From these the following equations are deduced for the heads of the two systems:

$$\nu = 25{,}496.9 + [304.6(v'+\tfrac{1}{2}) - 1.04(v'+\tfrac{1}{2})^2] - [279.1(v''+\tfrac{1}{2}) - 0.78(v''+\tfrac{1}{2})^2],$$

$$\nu = 27{,}097.3 + [311.5(v'+\tfrac{1}{2}) - 0.93(v'+\tfrac{1}{2})^2] - [278.8(v''+\tfrac{1}{2}) - 0.75(v''+\tfrac{1}{2})^2].$$

As remarked before, these bands are much weaker than the green system and hence the constants are not as accurately known as those for the $^2\Pi - {}^2\Sigma$ transition.

A number of bands were observed which are assigned to $Ba^{138}\,Cl^{35}$. As a result of the inherent weakness of the bands none of the rarer isotopes of barium were observed. However, due to the broader Franck-Condon parabolas, the possibility of finding these isotopes in these bands is quite a feasible one, which is not the case for the green bands.

A considerable amount of rotational structure is observed in the ultraviolet bands. The separations of the lines are quite small, of the order of 1 cm^{-1}. Three groups of some thirty lines each can be extrapolated to the (0,0), (1,1) and (0,1) band heads of the shorter wave-length system. They are therefore undoubtedly members of the P branches with very high J values. The simple energy relationship of $^1\Sigma$ states which may be applied here due to the negligible spin-doubling is

$$F(K) = BK(K+1) + DK^2(K+1)^2.$$

Neglecting terms higher than K^2, we obtain for a P line

$$\nu = \nu_e + \nu_v - (B'+B'')K + (B'-B''+D'-D'')K^2.$$

The coefficient of K^2 can be determined for the several series and it is found to be of the order of 0.002 cm^{-1}. This indicates that the B values are practically identical. Furthermore since we can determine the difference in the B values for the (0,0), (1,1) and (0,1) bands we can determine the values of $\alpha' B_0'$ and $\alpha'' B_0''$, which are found to be very approximately the same for the two states. Hence it is seen that the heads of the bands must occur at very high values of J and that there is little likelihood of a change of direction of degradation of these bands. Insufficient data are available to determine the values of B' and B''. In the series converging on the (0,0) band, there are two points which are noticeable due to a shift of the branch by approximately 1 cm^{-1}. The lines increase regularly in their separations, before and after these points, with increasing K but with separations at these points nearly 1 cm^{-1} larger than would be normally expected. This is probably due to a perturbation, a great number of which must be expected due to the large number of electronic states which are possible for the BaCl molecule as determined from the dissociation products.

Dissociation Products

To facilitate a discussion of the products of dissociation, the values of ω, $x\omega$, $\nu_{0,0}$ and D are listed in Table VIII. Fig. 2 shows the potential energy curves for the various states as determined from a Morse potential energy function. The empirical relation, $\omega r_e^3 = 3000$, has been used to estimate r_e. Therefore the value of r_e is in error to some extent but the relative values of r_e are probably very approximately correct. The

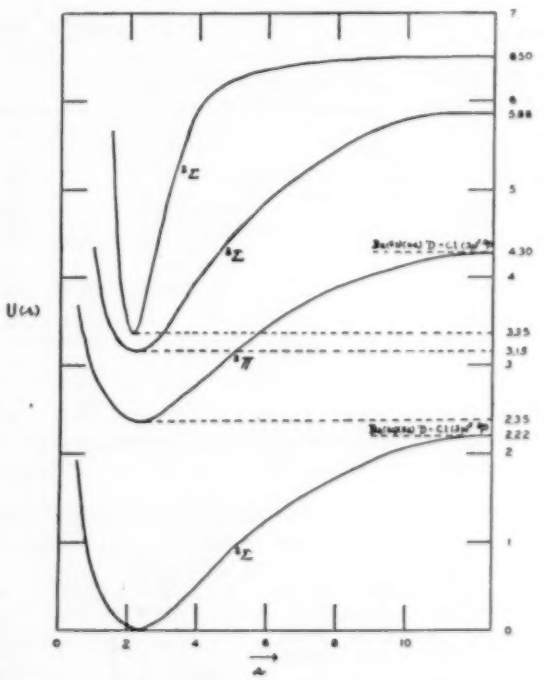

Fig. 2. Potential energy curves of the various states of BaCl plotted by means of a Morse potential energy function. r is expressed in Angstroms and the energy in electron-volts. Plausible disintegration products are shown for the two lower states.

TABLE VIII. *Constants of the BaCl states in cm^{-1} with the exception that $\nu_{0,0}+D'-D''$ is also expressed in volts and r_e is expressed in Angstroms.* $\nu_{0,0}+D'-D''$ is the energy difference between the disintegration products of the excited states and those of the ground state. The values of ω_h and $x_h\omega_h$ determined from the various transitions to the ground state are listed in the order of the upper states. The values of r_e have been computed from the empirical relationship $\omega_e r_e^3 = 3000$.

	$\nu_{0,0}$	ω_h	$x_h\omega_h$	r_e	D	$\nu_{0,0}+D'-D''$	
$^2\Sigma$	27,097.3	311.5	0.93	2.1	25,500	34,600	4.27
$^2\Sigma$	25,496.9	304.6	1.04	2.1	22,300	29,800	3.68
$^2\Pi$	19,450.1	285.0	0.79	2.2	15,800	16,800	2.08
	19,062.9	280.2	0.79	2.2			
		278.8	0.75	2.2			
$^2\Sigma$		279.1	0.78	2.2			
		280.5	0.80	2.2	18,000		
		278.4	0.80	2.2			

difference in the excitation of the dissociation products arising from two electronic states is $\nu_{0,0}+D'-D''$.

There are several possible solutions to the question of the dissociation products of the various electronic states. The $^2\Sigma$ state common to all three band systems is undoubtedly the ground state of the BaCl molecule. The difference in excitation of the $^2\Pi$ and the ground $^2\Sigma$ state is 2.08 volts as determined from the values of ω and $x\omega$. There are several possible combinations of states of the barium atom which will account for this. They involve the ground $(6s)^2\,{}^1S$ or the $(6s)(5d)\,{}^1D$ or ^3D states as the state of the barium atom resulting from disintegration of the ground $^2\Sigma$ state. The first of these does not seem to be as likely as either of the other two for two reasons though it cannot be completely ruled out. In fact the separation of the $(6s)(5d)\,{}^1D$ and $(6s)(6d)\,{}^1D$ states is 2.08 volts in exact agreement with the value obtained from the $^2\Pi$ and $^2\Sigma$ states.

In the case of BaH[5, 6] it seems fairly certain that the ground $^2\Sigma$ state does not dissociate into a barium atom in the ground $(6s)^2\,{}^1S$ state. A comparable situation exists for CaH. Lessheim and Samuel[7] and others have discussed the fact that the dissociation products of the ground state of a diatomic molecule need not be two atoms in their ground states, particularly if one of them has an $(ns)^2\,{}^1S$ state for its ground state. Hence it seems rather probable that the ground state of BaCl dissociates into either the $(6s)(5d)\,{}^1D$ or ^3D state.

The values of D' obtained from the ultraviolet bands are too inaccurate to permit of reaching any conclusion as to the dissociation products of their respective upper $^2\Sigma$ states.

The author wishes to thank Professor G. B. Pegram for the kind extension of the facilities of the Physics Laboratory of Columbia University and Professor H. C. Urey for the use of the equipment of his laboratory. Professor W. W. Watson's excellent advice and the opportunity of using the Physics Laboratory of Yale University are also gratefully acknowledged.

[5] W. R. Fredrickson and W. W. Watson, Phys. Rev. **39**, 753 (1932).
[6] W. W. Watson, Phys. Rev. **43**, 9 (1933).
[7] H. Lessheim and R. Samuel, Zeits. f. Physik **84**, 637 (1933).

Absorption Spectra of the Samarium Ion in Solids. IV. Absorption of $Sm(C_2H_5SO_4)_3 \cdot 9H_2O$ and Partial Energy Level Diagrams for the Sm^{+++} Ion as It Exists in Hydrated Crystalline Samarium Ethylsulfate, Samarium Iodide and Samarium Perchlorate

FRANK H. SPEDDING AND RICHARD S. BEAR,[1] *Chemical Laboratory, University of California*

(Received April 23, 1934)

The absorption spectrum of hexagonal $Sm(C_2H_5SO_4)_3 \cdot 9H_2O$ has been investigated in the temperature range 20° to 295°K. It is found to be simpler than that of the monoclinic $SmCl_3 \cdot 6H_2O$ previously reported. This is in agreement with theoretical conclusions that the greater symmetry of the hexagonal lattice should give rise to crystalline fields which would cause the energy levels of Sm^{+++} ion to be split apart less and to be in some cases more degenerate than would the more unsymmetrical monoclinic lattice. The ethylsulfate lines seem to be related chiefly to three lower levels, the basic one and two which are located higher on the energy scale by 55 and 65 cm^{-1}, respectively. Complete figures are given for the ethylsulfate absorption in the visible region. In addition results for the iodide and perchlorate of samarium are summarized. The lower levels found to be most important in these salts are situated at 0, 90, 107 cm^{-1} for the iodide; and 0, 104, 160 cm^{-1} for the perchlorate.

IN previous papers of this series[2] the absorption spectra of both single crystals and crystalline conglomerates of monoclinic $SmCl_3 \cdot 6H_2O$ and hexagonal $Sm(BrO_3)_3 \cdot 9H_2O$ were described. From the temperature behavior of the line intensities and from constant energy differences occurring throughout the spectrum it was possible to show the existence of certain low-lying levels of the Sm^{+++} ion in these solids, and energy level diagrams were constructed accordingly. This paper deals with a similar investigation of the absorption by hexagonal $Sm(C_2H_5SO_4)_3 \cdot 9H_2O$.

This second hexagonal salt is included in the series since the first one (the bromate) at low temperatures exhibited a phenomenon which somewhat complicated its spectrum. Though this complication could be partly eliminated in the interpretation of the spectrum, its underlying cause could not be determined definitely. It would seem desirable to have knowledge concerning a salt whose symmetry is great and whose spectrum does not have this complexity. The investigation of Spedding and Nutting[3] on the absorption of gadolinium compounds has indicated the choice of the ethylsulfate for such a purpose, and this is borne out by the facts now to be reported.

The spectra of two other salts were also found to indicate a greater symmetry of the fields about the samarium ion than in the chloride, but less than in the bromate and ethylsulfate cases. These are the iodide and perchlorate, whose absorption will be briefly described in the following.

Since in general the spectra of the three salts to be described at present resemble those of the chloride and bromate, we refer the reader to the former papers[2] for a general description of the appearance of the lines and bands, their behavior with temperature change, etc. In this report we shall treat only the points wherein the new spectra differ from the others. Just now we are content to confine ourselves to a descriptive discussion but intend at a later date, after reports on the interesting sulfate and bromide spectra appear, to make more thorough comparisons and deductions. In the meantime the data will be available to other investigators.

EXPERIMENTAL

$Sm(C_2H_5SO_4)_3 \cdot 9H_2O$ was prepared by mixing equivalent amounts of $Sm_2(SO_4)_3$ and $Ba(C_2H_5SO_4)_2$ in solution, centrifuging off the $BaSO_4$ precipitated, and recrystallizing the $Sm(C_2H_5SO_4)_3 \cdot 9H_2O$ crystals from the resulting solution by slow evaporation caused by a stream of dry air impinging on the surface. These operations were all carried out at room temperature and care was taken to avoid the presence

[1] Now National Research Fellow in Chemistry at Princeton University.

[2] Spedding and Bear, Phys. Rev. **41**, 58, 76 (1932); **44**, 287 (1933).

[3] Spedding and Nutting, J. Am. Chem. Soc. **55**, 496 (1933).

of free acid, both precautions being necessary to avoid decomposition of the samarium ethylsulfate. The compound was obtained as fairly large crystals which were hexagonal prisms similar to those observed with the corresponding gadolinium salt, described elsewhere by Spedding and Nutting[3] and also by Benedicks.[4] The samarium crystals have been described by Jaeger.[5]

In other respects the experimental procedure was similar to that described previously. Both single-crystal and conglomerate spectra were photographed at 20°, 78° and 169°K and the conglomerate at room temperature. As with the bromate, the two types of spectrum were quite similar, being less different than in the chloride. The conglomerate spectrum, as usual, contained a few more lines and emphasized faint ones. The value of the single-crystal spectrum is simply the verification that the conglomerate spectrum is the correct one and not that of different crystal forms or decomposition products.

Results

As with other salts, the general presence and location of the multiplets are those typical of the samarium ion. More specifically the ethylsulfate groups of lines are situated toward longer wave-lengths than the corresponding chloride ones, though remaining on the violet side of the bromate positions.

The temperature shift in positions of multiplets is slight in the ethylsulfate, less than in any of the other salts. In this case the high-temperature multiplets seem to shift slightly to the violet as the temperature is decreased, a behavior opposite to most, though there is not a marked difference. The red-most low temperature lines still shift to long wave-lengths. On the other hand the high temperature lines show a particularly noticeable shift to longer wave-lengths as the temperature is lowered. The result of the two factors is a very apparent widening of the groups of lines at low temperatures, as well as a shift to longer wave-lengths. This widening seems to be caused chiefly by an increase in the difference in energy between the basic level and the slightly excited lower levels from which the high temperature transitions originate.

Table I gives the positions of the lines and bands measured with estimated intensities. As in previous studies relative positions of two types of lines designated by H and L, according to whether they increase in intensity at high or low temperatures, respectively, can be used to determine low-lying energy levels. From the data obtained it is possible to state with certainty only that two levels exist apart from the basic one. These are separated from the normal state by about 55 and 65 cm^{-1}. Other low-lying levels may exist, possibly somewhere between 90 and 130 cm^{-1}, but these cannot be proved conclusively.

Fig. 1 shows a diagram indicating in a limited spectral region the possible explanation of the lines found therein. This illustration explains most of the important high temperature lines in the regions included, which are the simplest portions of the spectrum, offering possibilities for the most certain interpretation. The two lines that are most noticeably absent from the diagram are the intense high temperature lines at 20,365 and 23,898. The former is close to a correct distance from the nearest low temperature line and is possibly related to an "invisible" low temperature line. The second might be evidence for a level at about 95 cm^{-1} above the basic one if it were not for its rather too large intensity at 20°K and the slow increase in intensity at higher temperatures. Other similarly placed lines offer the same difficulty and probably also are satellites of non-appearing low temperature lines.[6] Perhaps the best evidence for higher levels is located at about 26,500, but here, as in other similar cases, the structure

[4] Benedicks, Zeits. f. anorg. Chemie **22**, 413 (1900).
[5] Jaeger, Proc. Amsterdam Acad. Sci. **16**, 1095 (1914).

[6] This difficulty is not limited to the ethylsulfate lines. An attempt was made to explain anomalous lines in such cases by the use of several levels very close to the basic one, which is the level ordinarily supposed to develop the strong low temperature lines. If selection rules favor a transition from another very close level other than the normal one, then certain constant discrepancies in the separations between the strong low temperature lines and their high temperature satellites should be noticed. Obviously other explanations are possible. Though lower temperatures (for sharpness) and instruments of higher resolving power will be necessary to decide the matter, it is quite possible that such levels, caused by crystal splitting of the $^6H_{5/2}$ level of the samarium ion, are actually present in all of the salts studied.

TABLE I. *Conglomerate absorption lines and bands of* $Sm(C_2H_5SO_4)_3 \cdot 9H_2O$ *in the visible regions of the spectrum.*

Frequencies are given at four temperatures, *R.T.* 298°, *E.T.* 169°, *N.T.* 78°, and *H.T.* 20° K. Columns of intensity and character are completely filled for *H.T.*, and only occasionally occupied for *N.T.* In all other regions at 78° relatively the same intensities as at 20° may be assumed. The "Type" column indicates by *H* and *L* the lines or bands that show their strongest intensities at high or low temperatures, respectively. *HL* signifies that probably both types overlap, and a question mark is placed beside doubtful assignments. Character of line is indicated by the following letters: *vd*, *d*, *nd*, *s*, *vs* are degrees of increasing sharpness, and *b* denotes a broad line or band. Sharp edges are noted by *se*, and a number in quotation marks signifies a probable but not clearly resolved multiplicity. Primed frequencies and wave-lengths are band edges, but all other values, including those marked *c*, are centers of intensity. Intensities are estimated on a scale of ten, with very faint or doubtful lines given as 0.

R.T. (cm^{-1})	E.T. (cm^{-1})	Type	N.T. (cm^{-1})	Int.	H.T. (cm^{-1})	Int.
—	17254	L	17248	—	17248	3s
—	—	H?	17364	—	17354	1d
—	17404	H?	17390	—	17383	2d
—	—	L?	17453	—		
—	17787′	H	17786.8	6nd	17785.0	3vs
—	17799′	H	17796.0	5nd	17795.6	3s
17850′	17845′	L	17849.5	9nd	17850.2	10vs
—	17859′	H	17854	3d	—	—
17873′	17879′	H	17880	3d	17880″	0
17893′	17893′	H	17888	3d	17890′	
—	—	L	—	—	17898.6	1s
—	17901′	L	—	—	17905.3	10s
—	—	L	17907	9d	17908.3	10s
—	17911′	L	—	—	17910.8	8s
17916′	—	L	—	—	17915.8	1s
—	—	L	—	—	17921	2d "2"
—	—	L	—	—	17930	1d
—	—	L	—	—	17937	2d
—	17941′	L	17943	4d	17943.9	3s
—	—	L	—	—	17948	1nd
—	17953′	L	17950	4d	17952.6	5s
—	—	H?	17968′	1d	17970	1d
—	—	—	17977′	—	17979	1d
—	—	L	—	—	17986	0
—	—	L	—	—	17994	0
—	—	L	—	—	18004	0
—	—	L	—	—	18010	1d
—	—	L	—	—	18025	0
—	—	L	—	—	18032	1d
18820′	18818′	H	18816.0	7nd	18814.2	1s
18841′	18832′	H	18825.0	8nd	18824.7	2nd
—	18872	L	18876.9	9s	18878.1	10s
—	—	?	19015	0vs	Faintly evident	
—	—	?	19020	0vs	Faintly evident	
—	—	L	19126.5	2s	19125.3	2vs
—	—	L	Faintly evident		19150	0
—	19186	L	19185.2	4s	19185.0	4vs
—	19958′	H	19957.0	8nd	19954.1	3vs
19967′	19968′	H	19965	1d	19964	0
—	—	H	19971	4d	19971.6	3vs
—	19978′	H	19977.1	8nd	19974.5	3vs
—	19985′	H	19986.0	2nd	19985.3	1vs
19994′	—	—	—	—	19994′	0
—	—	—	—	—	20011′	—
20017′	20017′	L	20019.4	8nd	20019.4	9s
—	20024′	L	20024.5	7nd	20026.0	9s
20034′	20039′	L	—	—	20039.9c	1vs
—	—	H	20041′	—	—	—
—	—	—	20050′	1d	—	0
—	20058′	H	20059′	—	—	—
—	—	—	20066′	1d	20075′	—
20083′	20084′	L	—		20082.3	1s
—	—	L	—		20087.6	1s
—	—	L	20093c	3d	20093.8	5nd
20098′	20102′	L	20101c	6d	20097.4	8nd
—	—	L	20117	1d	20117	2d
—	—	L	—	—	20127	1d
—	—	L	20144	1d	20145	2d
—	—	L	—	—	20156′	0
—	—	L	—	—	20185c	1d
20367′	20365′	H	20365.4	9nd	20363.2	3s
20379′	20376′	H	20370	3d	—	—
20409′	20409′	H	20411.9	8nd	20410.6	3s
—	20420′	—	—	—	—	—
—	20428′	L	20432.4	8nd	20432.8	8s
20436′	20438′	—	—	—	—	—
—	20458′	H	20463	3d	20462	2d
—	20476′	L	20474	2d	20475.7	3s
—	20498′	L	20515	7d	20517	8d
—	20525′	L	20526	3d	20526	3d
—	—	L	20550′	—	20560	2d
—	—	L	20569′	—	20571.3	2nd
—	—	L	20586	—	20584.2	2nd

R.T. (cm^{-1})	E.T. (cm^{-1})	Type	N.T. (cm^{-1})	Int.	H.T. (cm^{-1})	Int.
20593′	—	—	20599′	—	—	—
—	20607′	L	20608′	—	20603.3c	6nd
—	—	—	20613′	—	—	—
—	20623′	L	20623′	—	20620c	8d
20631′	—	L	20640′	—	20634.9	3nd
—	—	L	—	—	20650c	2nd
—	20658′	L	20661′	—	20656c	2nd
—	20674′	H	20672′	8d	20669.0	4nd
—	—	L	—	—	20679	2nd
—	20688	L	20690′	—	20688	1nd
20698′	—	L	20701′	—	20698	1d
—	20709′	L	20716′		20720.3	5nd
—	20724′	L	20727′		20724.6c	9nd
20740′	—	L	—		20735.0c	4nd
—	—	L	—		20747.4	3nd
20771′	20764′	L	20759′		20761′	9db
—	20792′	—	20796′		20796′	—
20807′	—	L	20809′		20810′	6db
—	—	—	20822′		20824′	—
—	20834′	L	20836′		20835′	8db
20850′	20848′	—	20848′		20849′	—
—	—	L	20858′		20855′	7db
—	—	—	20866′		20867′	—
—	20886′	L	20876′		20880	4d
—	—	—	20885′		—	—
—	—	—	20893′		—	—
—	—	L	20905′		20902	4d
—	—	H	20930′		20926	1nd
—	20940′	H	—	8db	20938	1nd
20948′	20956′	H	20951′		20949	5d
20970′	—	L	20972		20968	3d
—	—	—	—		20975′	—
—	20991′	L	—		20990′	8db
20995′	—	—	20996′		20997′	—
21020′	21013′	L	21013′		21011′	8db
—	21039′	L	21031′		21045′	8db
—	—	—	—		21060′	—
21054′	21058′	L	21063′		21066′	8db
21078′	21073′	—	21078′		21081′	—
—	21097′	L	21095′		21100c	5d
—	21121′	L	21116′		—	—
—	—	—	21138′		21137′	2
—	21160′	—	21162′		21163′	—
—	21179′	L	21177′		21173′	5d
—	—	—	21265′		—	—
—	—	L	21283′		21274	1d
—	—	L	21327′		21329′	0
—	—	—	21342′		21349′	—
—	—	L	21363′		21361′	0
—	—	—	21378′		21383′	—
—	—	H	21415′	1d	—	—
—	—	—	21429′	—	—	—
—	21456′	—	21452′		—	—
21468′	21477′	H	21466′	8db	21460	5d
21493′	21492′	—	21487′		—	—
21511′	21506′	H	21501′	8db	21497	5d
—	21522	H	21511′		21515′	
—	21534	H	21533′	8db	21526′	5d
—	21539′	—	—		—	—
21550′	—	L	21552		21551	7d
—	21561′	H	21562	7d	—	—
21569′	—	L	21570′		21569′	9db "2"
21591′	21589′	—	21588′		21585′	—
21626′	21626′	—	21621′		21623′	—
—	—	L	21629′		—	8db
21646′	21640′	—	21641′		21643′	—
		?	21673		Faintly evident	
		L	21697		21697	1d
		L	21718′		21723′	0
			21728′		21735′	
	21748′	L	21746′		21747′	1d
	21767′	?	21758′		21759′	
			21789		Faintly evident	

TABLE I.—*Continued.*

R.T. (cm^{-1})	E.T. (cm^{-1})	Type	N.T. (cm^{-1})	N.T. Int.	H.T. (cm^{-1})	H.T. Int.
		L	21812		21805′	0
					21820′	
	21829′					
	21841′	L	21845		21846	1d
		L			21865	0
		L	21892′		21895′	1d
			21906′		21910′	
		L	21947′		21957′	0
			21967′		21972′	
	22051′	H	22049.1	3s		
	22063′	H	22059.2	2s		
22105′		H	22100.6	3nd		
22128′	22111	L	22110.9		22111.5	9vs
		L			22162.7	2vs
22158′	22164	L	22165.7		22166.7	10vs
22174′						
		L			22345	0
		L			22382	0
	22438′	H	22441	5d	22441	0
	22450′	L	22466	1d	22464.4	2s
		H?	22479	0		
		H	22495c	3d	22495	1s
22510′	22506′	H	22505.1	8nd	22501.4	4s
	22516′	H	22517.7	7nd	22517.8	3nd
	22531′	L	22534.5		22536.2	10s
22552′	22550′	L	22547.5		22548.7	10se
	22567	L	22573.8		22573.2	10se
		L			22593c	0
		L	22614′		22603c	0
		L	22632		22633	1d
		L			22645	0
		L	22666		22662	1d
	22679′	H	22681	3d	22682	0
	22695′	H	22692	2d	22690	0
	22714′	L	22713′		22717.3c	7nd
	22729′	L	22727′		22725.5c	7nd
	22747′	L	22755		22755.9	7s
	22771′		22771		22774	1d
		L			22806	1d
	22826′	L	22827′		22819	1d
		L	22837′		22831	2d
	22845′	L	22845		22844	3d
		L	22869		22862	1d
		L			22893′	
	22908′	H?	22923	2d	22922′	1vd
	22923′	L	22943c	1d	22943.6	2s
		?	22954c	1d	Obscured by	
	22972′	H?	22964	2d	plate edges.	
	22983′					
	23026	L?	23027	6d		
		L?	23047	2d		
		H	23288′	00		
			23306′			
		H	23310	Ovs		
		L	23361.2		23361.3	3vs
23712′		H				
23735						
23761′		H				
23786						
	23808′		23807′			
	23823′	H	23820′	2d	23811	0
		H	23844	2d	23843	0nd
	23859′	H	23857	1d		
	23862′	H	23866	2d		
23871′		H	23873	2d		
23891′	23901	H	23896	5d	23897.5	4vs
	23926′		23923′		23926.9	9s
23937′	23935	H	23933′	10d "2"		
	23944	H	23939.3	9nd	23937.5	6s
23960′	23950′					
		H	23963.8	8s	23962.5	3s
	23969	H	23972.4	6s	23973.0	3s
		H	23984.7	2nd		
		L			23992.3	1nd
		H	24005	1d	24009	0
		H	24012	1d		
24021′	24017′		24020′		24021′	
		L			24022.8	10s
	24025	L	24029′		24027.6	10nd
	24039	L	24037′		24035.2	10nd
					24042′	
24048′	24047′	L	24050′		24051′	10d
		L	24066		24066.3	6s
	24073′	L			24073.6	1nd
		L			24085.0c	5nd
		L	24088		24089.8c	6nd
24100′		L	24101		24101.8	4nd
		L	24111		24113.2c	5nd
		L	24120		24120.0c	5nd

R.T. (cm^{-1})	E.T. (cm^{-1})	Type	N.T. (cm^{-1})	N.T. Int.	H.T. (cm^{-1})	H.T. Int.
		L			24137.0c	1nd
	24157′	L	24145		24147.7c	4nd
	24172c	L	24170		24165.8′	6se "2"
					24175.0′	
		L			24182	0s
		L			24186.3	2nd
	24196′	H	24197	4d	24202	1d
	24214′	L	24213		24215.2c	5nd
		L			24223.0c	3nd
	24241′	L	24232′		24238	1d
		L			24250.2	2nd
	24261′	L	24261c		24263	6d "?"
		L			24276	1nd
	24290′	L			24287	1nd
		L			24300	2nd
	24304′	L	24305		24309.7	6nd
		L	24331		24332.1	2nd
					24350′	
		L	24360		24358′	3db
					24370′	
		L			24378	1d
		L			24389	1d
	24462	H	24463c	3d		
	24492′	H	24492.8	10nd	24492.8	4s
					24497.8	2s
	24501	H	24501	10d	24502.5	6s
24505′					24507.5	9s
	24515	H	24512	10d	24514.0	2s
24526′	24523′		24519′			
		H	24528.1	9s	24526.6	2s
	24533	H	24537.3	9nd	24537.6	2nd
24542′	24541′	L	24545.0c		24544.8c	10nd
	24552′	L	24550.1c		24549.8c	10nd
24559′	24560	L	24562.1		24562.0	10s
	24570	L	24571.9		24572.7	10s
	24583′	H	24589	3d		
	24596′					
	24603′	L	24602′			
			24614′		24610	1d
	24625′	L	24624′		24623	1d
	24634′		24636′			
	24654′	L			24655′	2d "2"
	24667′		24664′		24668′	
	24684′	L			24682	3d
		L	24692′		24689	3d
	24704′	L			24697	0
	24730′	L	24722		24723.1	4nd
	24744′	H	24738	5d	24739	4d
		L			24751	1d
	24760′	H	24763	2d	24771	2d
	24781′	H	24785	4d	24784	1d
	24803′	H	24798	4d	24797	2d
	24809′		24811′			
24815′		H	24816	10d	24814.8	2nd
		H	24831	10d	24828	8d
24841′		L	24842′		24842.4	10nd
24856		L			24852.4	10nd
		L			24862.7	10nd
		L			24872′	
					24874	10d
24894′	24898′		24905′		24905′	9
24920′	24916′		24923′		24921′	
24946′	24930′	L	24944′		24941′	10db
		L			24952.7	2nd
	24965′	L			24963.6	2nd
	24980′	L	24973c		24975.6	6nd
		L			24987c	3d
24994′		L			24995c	3d
	25002′	L			25006.2	3nd
25020′	25018′	L	25011		25015.0	8nd
	25030′	L	25024		25026.1	3nd
	25040′	L			25037.5c	3nd
		L	25042		25045.6	6nd
	25061′	L	25057		25059.7	4nd
25083′			25071		25078′	2
	25091′	L	25094		25093c	9d
25103′	25103′	L			25098.8c	9nd
25112′	25118′		25124		25118′	
	25128′	L				9b
25138′	25137′				25133′	
		L			25141.9	1nd
		L			25153.7	1nd
		L			25166.0	4s
25172′	25177′	L	25175c		25176.9	4s
		L	25186		25183.7′	9se
25192′	25194′				25195.0′	
		L	25199c		25202	6d
	25223′	L	25229′		25221	1vd

TABLE I.—*Continued.*

R.T. (cm^{-1})	E.T. (cm^{-1})	Type	N.T. (cm^{-1})	N.T. Int.	H.T. (cm^{-1})	H.T. Int.
	25235′	L	25238′		25241.1c	4nd
		L	25244′		25249.6	5nd
	25253′	L	25258′		25257.6c	5nd
		L	25266		25268	1d
		L	25281		25282.4	7vs
		L			25292.8	0s
		L	25303′		25305	1d
		L	25321′		25315	1d
		L	25335′		25343	1d
		L	25356′		25359	1d
		L			25377	1d
		L			25388	0d
		L	25406		25407.9	3nd
		L	25418		25419.2	3nd
		L			25438	1d
		L	25451′		25456′	1d
			25466′		25470′	
	25501	H	25496	4d	25493	2d
25526′	25524	H	25516.5	8nd	25515.5	3nd
		L			25529	1d
					25540′	
25542′	25545′		25545c		25547′	
25554′		L	25556		25561′	9b
25569′	25563′		25567c		25566′	
		L	25584		25579	2d
25592′	25587′	L	25596	"2"	25589.9′	9se
25612′	25603′				25602.9′	
	25620	L	25620.2		25621.3	9s
25651′	25654	H	25646.0	5nd	25644	1d
	25666	H	25659.7c	3nd	25656	0
28671′		H	25669.4c	2nd	25669′	2b
		L			25681′	
	25698	H	25693.1	6nd	25691	2d
25704′		H	25701.3	2nd		
	25724	L	25723		25723.7	9s
25757′	25751	L	25752		25752.7	9s
		L			25775	1d
	25795	L	25795		25795	1vd
	25825	L	25825		25825	1vd
		L			25854	1d
		L	25861′		25868	1d
		L	25885′		25884	1d
		L	25920′		25924′	1db "2"
			25946′		25952′	
		L	25987		25980′	1db
					25997′	
		L	26023		26027	1d
	26323	H	26318.1	3nd		
		H	26474	1d		
26505′	26493′	H	26495c	1d		
26550′	26536′	H	26530c	2db	26525′	0
					26538′	
		H	26554	3d		
		L			26565.8	1nd
	26575′	H	26576.3	9nd	26575.4	3nd
		HL	26585.9c	10nd	26583.8	2s
	26598	H	26597.3c	10nd	26596.6	9nd
26604′		H	26610	10d	26609.0	7s
"2"	26615	H	26617	10d	26619.0	8s
26640′	26633c	L	26631		26629.7	10s
26662	26653	L	26650		26648.5c	10nd
		L			26654.4c	10nd
		L			26664.1	2s
26670′	26675	L	26673		26673.8	10se "2"
		L			26684	1d
26698′	26694	H	26692	9d	26691.9	3nd
	26718	L	26716.9c		26718.3	10s
		L	26723.8c		26725.5	7s
26735′		L	26735.8c		26737.4	8s
	26746	L	26746.3c		26747	9d
26770′	26759′	L	26770c		26772	6d
	26777′	L	26782′		26782	2d
	26795′	L			26794	1d
		L	26802c		26803c	5d
	26815′		26815′		26812′	"2"
		L	26826′		26827c	5d
		L			26832c	5d
26844′	26839′	L	26842c		26842.0	5nd
	26855′	L	26854		26854	6d
26873′	26875	L	26873		26875	3d
26900	26900	L	26897		26897c	7d
					26911′	"2"
	26915′	L	26921		26922	5d
		L			26934	0
26943′	26951′	L	26944		26946	6d
		L			26963	0
		L	26983		26983	2d
	26997′	L	27008		27009	3d
	27017′					
		L	27073		27075	1vd
		L	27158′		27166	1d
			27178′			

R.T. (cm^{-1})	E.T. (cm^{-1})	Type	N.T. (cm^{-1})	N.T. Int.	H.T. (cm^{-1})	H.T. Int.
		L			27197	0
		L			27225	
		H	27237	2d		0
		L			27253	0
		H	27267c	7d		
	27274′				27275.2c	4nd
27280′		H	27278c	10d	27279.7c	5nd
27300′	27290′	L			27295	1vd
	27310	H	27305.7	3nd		
	27331	L	27328.8		27329.5	9nd
		L			27334.4	3nd
		L			27348.3	2nd
27350′	27354′	L	27358.7c		27360.1	8s
27370′	27376′	L	27380′		27374	2d
		L	27406′		27407	1d
	27423′	L	27429′		27432	2d
			27440′			
	27472′	H?	27467′		27486c	8d
27480′	27485′	H?		10db "2"	27487c	10d
	27494′	H?				
	27511′		27508′			
27523′		?			27514	3d
	27530′	HL	27526′		27534c	10d
27543′	27542′	HL		10db	27544c	10d
	27547′					
27575′	27568′	H	27561′		27555	3d
	27584′	L?	27584′		27595c	10d "2"
27605	27610′	L?	27614′		27608c	10d
	27627′	L?	27629′		27636c	10d
27643	27657′	L?			27647c	10d
27685′		L	27685′		27672	5d
		L	27702		27702	4d
	27714′	L	27721		27721	6d
	27741′	L			27749	0
	27767′	L	27762		27766	1d
		L	27785		27785.7	5nd
27795′	27802′					
27825′	27822′	L	27812		27813	6d
27858′	27853′	L	27860′		27868c	5d
27883′	27886′	L	27877c		27879c	6d
	27901	L	27908		27911.5	5nd
		L	27939		27930′	2db
					27949′	
		L			28006	0
		L			28033	0
		H	28097c	2d		
28119	28109	H	28104c	3d	28103	1d
		L			28127	0
28158′	28160	L	28157		28156.4c	10vs
28180′					28160.8c	7vs
		H	28176	0		
			28188′			
28200′	28197′	H	28199	4d	28196	0
28226′	28214′	H	28210c	4d	28209	0
		?	28223.4		28224.9	1vs
		?	28230.1		28231.5	1vs
					28256c	2d
28261	28263	L	28263		28264c	9d
		L	28296		28298	3vd
		L	28330		28330	3d
		H	28590.7	1nd		
		H	28601.7	1nd		
		H	28622c	1d		
		H	28630c	1d		
		H	28643.3	4s		
28650′	28651	?	28654.4		28654.7	8vs
28672′	28677	?	28674.4		28675.0	10vs
		?	28685.6		28685.4	4vs
28800′	28803	H	28794	9d	28792.0	2nd
		?	visible		28803.1	1nd
		L	28818.2		28818.7	9nd
28830′		?			28832.2	1nd
	28848′	?	28842′		28843.5	1nd
	Too	L?	Too		28857.0	8s
	faint		faint		28882	2vd
					28901.7	7s
28933′					28928′	b
					28947′	
28973′					28963	d
Too					29003	d
faint					29019	d
					29058.3	nd
					29080	d "2"
					29100.0	nd
					29172	d
					29192	d
					29250	d
					29274	d
					29334	d
					29352	d
					29525	d
					29554.6	nd
					29582.6	nd

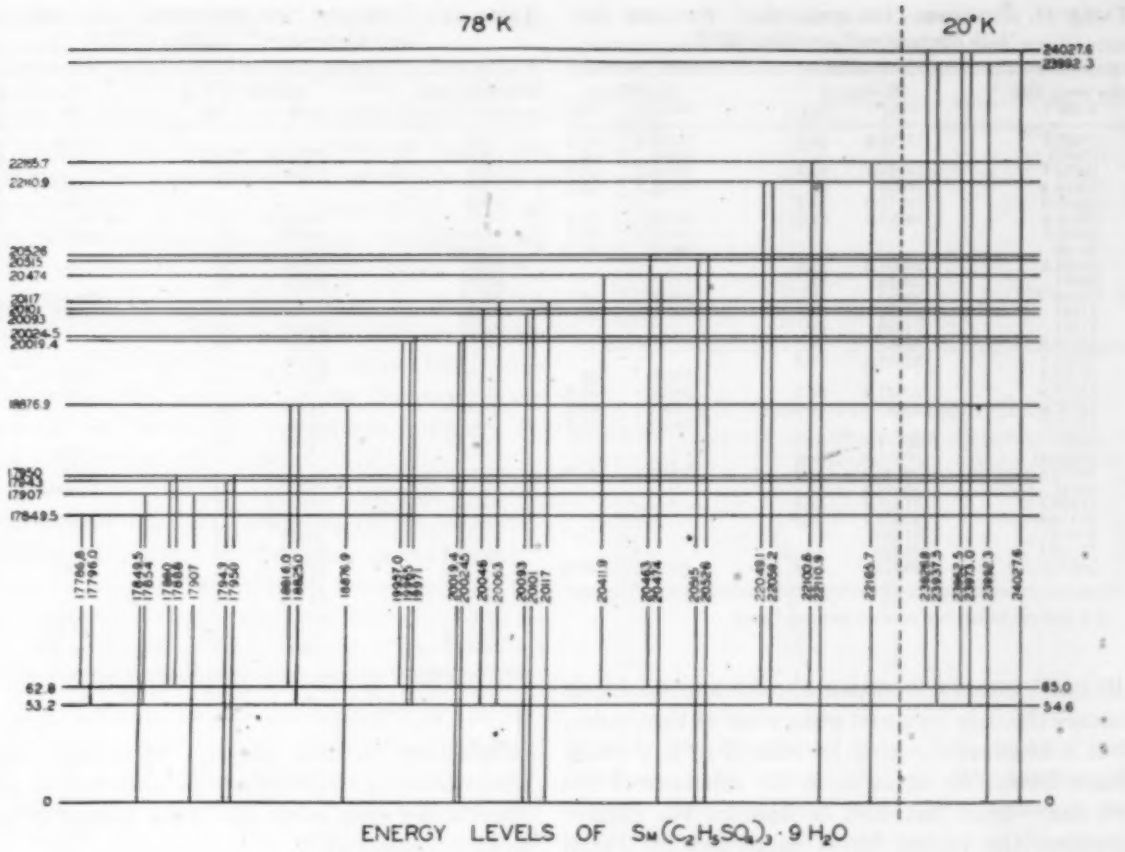

FIG. 1.

thereabout is so complex as to make it difficult to determine with which low temperature line a given satellite must be placed. Consequently, definite values for these higher levels cannot be assigned. Two very hazy bands between 23,700 and 23,800, making their first appearance at room temperature, may indicate levels over 250 cm^{-1} from the normal state, but one has to be careful in accepting too readily faint bands obtained only at high temperatures, since then there is a tendency for decomposition to occur upon absorption of the intense light beam. These particular bands, however, are not directly in positions occupied by intense sulfate bands, which would be the most probable results of decomposition. No other ethylsulfate bands offer supporting evidence for these relatively high lower levels.

Tables II and III give the evidence concerning the two levels at 55 and 65 cm^{-1}. Nearly all the lines agree within what we consider to be the accuracy in each case. The averages of the best values at the two temperatures indicate the separations 54.6 and 65.0 at 20°K and 53.2 and 62.8 at 78°. The mean position of the two excited levels is accordingly 59:8 at 20° and 58.8 at 78°. It can be estimated that the corresponding mean positions at the other temperatures are about 56 at 169° and 52 at room temperature.

Comparison with the measurements of Freed and Harwell[7] on the absorption of samarium ethylsulfate in the limited region of the violet where that is possible shows considerable discrepancies. Aside from a shift toward longer wave-lengths in their values which is several times our possible error, we are inclined to attribute most of the differences to a lack of sufficient dispersion and resolving power in the instruments available to the other authors. We were unable to locate a level at 12 cm^{-1}. The

[7] Freed and Harwell, Proc. Amsterdam Acad. Sci. 35, 979 (1932).

TABLE II. *Prominent "low temperature" lines and their "high temperature" satellites (20°K).*

Low temp. line ν cm^{-1}	Satellite A ν cm^{-1}	$\Delta\nu_A$	Satellite B ν cm^{-1}	$\Delta\nu_B$
17850.2	17795.6	54.6	17785.0	65.2
(17949)			17885	64
18878.1	18824.7	53.4	18814.2	63.9
20019.4	19964	55	19954.1	65.3
20026.0	19971.6	54.4		
20039.9	19985.3	54.6	19974.5	65.4
20475.7			20410.6	65.1
20526			20462	64
20724.6	20669.0	55.6		
20983	20926	57		
21004	20949	55	20938	66
21551	21497	54		
21577	21520	57		
22548.7	22495	54		
22573.2	22517.8	55.4		
22755.9			22690	66
23992.3	23937.5	54.8	23926.9	65.4
24027.6	23973.0	54.6	23962.5	65.1
24572.7			24507.5	65.2
26629.7	26575.4	54.3		
(26651.4)	26596.6	54.8		
26673.8	26619.0	54.8	26609.0	64.8
26747	26691.9	55		
27329.5	27275.2	54.3		
27334.4	27279.7	54.7		
27534	27480	54		
28156.4	28103	53		
28857.0	28803.1	53.9	28792.0	65.0

( ) indicates center of two strong lines.

TABLE III. *Prominent "low temperature" lines and their "high temperature" satellites (78°K).*

Low temp. line ν cm^{-1}	Satellite A ν cm^{-1}	$\Delta\nu_A$	Satellite B ν cm^{-1}	$\Delta\nu_B$
17453			17390	63
17849.5	17796.0	53.5	17786.8	62.7
17907	17854	53		
17943			17880	63
17950			17888	62
18876.9	18825.0	51.9	18816.0	60.9
20019.4	19965	54	19957.0	62.4
20024.5	19971	54		
20101	20046	55		
20117	20063	54		
20474			20411.9	62
20526			20463	63
20722	20667	55		
21552	21594	58		
21579	21522	57		
22110.9	22059.2	51.7	22049.1	61.8
22165.7			22100.6	65.1
22534.5	22479	56		
22547.5	22495	53		
22573.8	22517.7	56.1		
22755			22692	63
24261			24197	64
25723	25669.4	54	25659.7	63
26631	26576.3	55		
26650	26597.3	53	26685.9	64
26673	26617	56		
26746.3	26692	54		
27328.8	27278	51	27267	62
27358.7	27305.7	53.0		
28157	28104	53		
28263	28210	53	28199	64
28654.4	28601.7	52.7	28590.7	63.7
28674.4	28622	52		

10 cm^{-1} interval between the 55 and 65 levels causes the only frequent separation of that order, but it obviously cannot be related to any really basic levels. We agree upon the existence of the 60 cm^{-1} level but find it double. We cannot confirm the higher levels suggested by Freed and Harwell, though it is not possible to deny them positively. The fact that they have found a level at about 160 cm^{-1} and that we have discovered the most important low excited level of samarium sulfate to be at such a separation might indicate that their crystal had partly decomposed. In several of our plates decomposition to the sulfate is indicated very clearly by the appearance of some of the stronger sulfate lines. However, we were careful in obtaining the photographs upon which this report is based to use only fresh and undecomposed material each time. None of the strongest sulfate lines were observed after such precautions.

As noted before, the ethylsulfate produces the best example studied so far of the "hexagonal" type of spectrum, first introduced by the bromate. The bromate, however, had a particularly peculiar behavior at low temperatures, and because of that and other factors tending to increase the complexity, the expected greater simplicity of spectrum was not quite so marked as might have been desired. The ethylsulfate is more satisfactory in this respect. In many places components of doublets can be observed to have approached each other and small groups of lines to have coalesced.

THE PERCHLORATE AND IODIDE SPECTRA

At this point mention may be made of two other salts which at first glance seem to have the spectrum of the hexagonal type. Their most important low-lying levels are closer together than are those of the "monoclinic" spectra as exemplified by that of the chloride.

These two new salts are the perchlorate and iodide, each prepared by dissolving the oxide in the proper acid and crystallizing the salt from the resulting solution. The perchlorate forms what appears to be a glass-like solid but under closer examination seems to be an interlocking network of fine crystals. The water of crystallization is unknown, and indeed its great tendency to take up water from the air would make it difficult to determine any definite composition. The iodide crystals are known to contain nine molecules of water per molecule of salt and under microscopic examination appear to be hexagonal, though again the hygroscopic nature

of the compound makes prolonged and thorough examination difficult.

We have not attempted to make a complete study of these salts, but examination of photographs of the spectra absorbed at 78°K has disclosed the most important levels. In such a study relative position and intensity, as well as appropriate separation, of pairs of neighboring lines are used to determine the levels. In the perchlorate many satellites occur at about 104 cm^{-1} from stronger lines, while with the iodide a separation of 90 cm^{-1} is most frequently observed. Other levels at 160 for the perchlorate and 107 for the iodide are indicated. Tables IV and V give the best evidence.

The positions of the multiplets are interesting. The iodide lines are displaced to longer wavelengths than the corresponding chloride multiplets, as are also lines of other hexagonal spectra to a greater extent. The perchlorate positions are about those of the chloride. This last fact along with absence of noticeably greater simplicity of spectrum and the existence of the 160 cm^{-1} level would indicate that the perchlorate has not a hexagonal spectrum but an intermediate type with definite leanings in the monoclinic direction. The iodide, too, shows an intermediate character, but its spectrum is more nearly the hexagonal type. The terms "hexagonal" and "monoclinic" in this connection signify simply greater and less symmetry, respectively, about the samarium ion in the crystal environment.

TABLE IV. *Samarium perchlorate satellites (78°K).*

Low temp. line ν cm^{-1}	Satellite A ν cm^{-1}	$\Delta\nu_A$	Satellite B ν cm^{-1}	$\Delta\nu_B$
18037	17933	104		
18925	18821	104	18784	161
18945	18842	103		
20011	19908	103	19851	160
20088	19983	105		
20138	20036	102		
20168	20063	105		
20449	20345	104		
20488	20384	104		
20519	20415	104		
20705	20600	105		
22166	22061	105	22002	164
22207	22103	104		
22241	22136	105		

TABLE V. *Samarium iodide satellites (78°K).*

Low temp. line ν cm^{-1}	Satellite A ν cm^{-1}	$\Delta\nu_A$	Satellite B ν cm^{-1}	$\Delta\nu_B$
17799	17709	90		
17859	17769	90	17752	107
18893			18787	106
19964	19874	90	19857	107
20001	19910	91	19892	109
20562	20471	91		
21572	21482	90		
21606	21516	90		
22197	22107	90		
22414	22323	91		
23950	23859	91		

LETTERS TO THE EDITOR

Prompt publication of brief reports of important discoveries in physics may be secured by addressing them to this department. Closing dates for this department are, for the first issue of the month, the twentieth of the preceding month; for the second issue, the fifth of the month. The Board of Editors does not hold itself responsible for the opinions expressed by the correspondents.

The Pressure Broadening in the Gamma-Bands of Nitric Oxide

The γ-bands of nitric oxide are known to show strong pressure broadening either under the increase of the nitric oxide pressure itself or that of foreign gases. So far as the writer is aware the effect was discovered by Lambrey[1] who observed that the apparent absorption increased approximately as the square (the value of the exponent found by Lambrey was 1.81) of the pressure of NO. Naudé[2] made a careful study of this effect which was described in the paper in which he reported the discovery of the nitrogen isotope N^{15}. He showed that it was a pressure broadening of the individual lines of the γ-bands, and published a picture of the effect. It is very pronounced even under low dispersion; we have had to take account of it in this laboratory for some time in absorption spectra work on the nitrogen oxides.

Such a very pronounced pressure broadening leads one to suspect that some process other than mere collision is leading to the rapid shortening of the lifetime of the excited state as the number of molecular collisions increases. In the halogen molecules iodine and bromine[3] such an effect has already been observed. It has been shown, moreover, that this is in all probability due to a predissociation of the halogen molecule caused by collisions inducing predissociation normally forbidden by selection rules[4] from the excited $^3\Pi$ state of the halogen molecule which gives rise to the band absorption in the visible, into the continuous energies beyond dissociation of the lower lying triplet level. Optical transitions to this latter in absorption are very weak. They were studied by W. C. Brown.[5]

It therefore seems natural to inquire whether a similar effect in nitric oxide can account for this strong pressure broadening.[6] The recent work which has led to a lowering of the heat of dissociation of nitrogen has, of course, necessitated also a lowering of the heat of dissociation of nitric oxide. In a recent Letter to the Editor, Professor Mulliken[7] has concluded that we may probably now accept as rounded values 7.3 volts for N_2 and 5.25 volts for NO. References will be found there to the several pieces of work bearing upon this. But the upper electronic level of the γ-bands lies at 5.45 volts, thus above the energy of dissociation of the NO molecule. The rotational states of the vibrational levels built on this electronic level could, therefore, quite reasonably be broadened by collision, if there existed in NO a third level, dissociating into normal atoms, into which the induced predissociation might occur. Professor Mulliken has called my attention to the predicted low-lying $^4\Pi$ level[8] in NO, dissociating into normal atoms. Predissociation from the states of the $^2\Sigma$ level of the γ-bands into this level would be possible, were it not for selection rules[4] prohibiting it. Both multiplicity and angular momentum change in this case and these changes are normally forbidden. But as in the iodine and bromine molecules, collisions could effect a weakening of the selection rules and thereby cause a pressure broadening of the γ-bands. It seems probable that this is the explanation of this example of remarkably strong pressure broadening.

It is interesting that no such effect was found by Lambrey[1] in the β-bands of NO. The approximate position of the $^4\Pi$ level as predicted by Professor Mulliken in the figure on page 51 of reference 8 will be seen to be such as to permit transitions in conformity with the Franck-Condon principle into it from the $^2\Sigma$ level of the γ-bands, but not from the $^2\Pi$ level of the β-bands.

OLIVER R. WULF

Bureau of Chemistry and Soils,
Washington, D. C.,
July 10, 1934.

[1] Lambrey, Comptes Rendus **189**, 574 (1929); **190**, 261, 670 (1930); Annales de physique **14**, 95 (1930).
[2] Naudé, Phys. Rev. **36**, 333 (1930).
[3] Loomis and Fuller, Phys. Rev. **39**, 180 (1932); Turner, Phys. Rev. **41**, 627 (1932); Kondratjew and Polak, Zeits. f. Physik **76**, 386 (1932).
[4] Kronig, Zeits. f. Physik **62**, 300 (1930).
[5] Brown, Phys. Rev. **38**, 1179 (1931); **38**, 1187 (1931).
[6] Kondratjew and Polak, Phys. Zeits. d. Sow. **4**, 764 (1933), suggested an explanation of this effect based on an "inner predissociation" of the molecule at a time when the heat of dissociation of NO still seemed to be appreciably higher than the upper electronic level of the γ-bands.
[7] Mulliken, Phys. Rev. **46**, 144 (1934).
[8] Mulliken, Rev. Mod. Phys. **4**, 1 (1932).

Curved Quartz Crystal X-Ray Spectrograph

About a year ago we constructed in this laboratory a curved crystal focussing x-ray spectrograph of the transmission type described by Cauchois.[1] The instrument was originally designed for use with mica but we have been unable to obtain samples of mica sufficiently flat to give spectra of the desired sharpness. At the time of the original construction DuMond suggested that quartz would probably serve well as a crystal for this type of an instrument because of its elastic properties and small grating constant. The suggestion was repeated by Carlsson[2] who, however, makes no mention of having attempted to use quartz in this way.

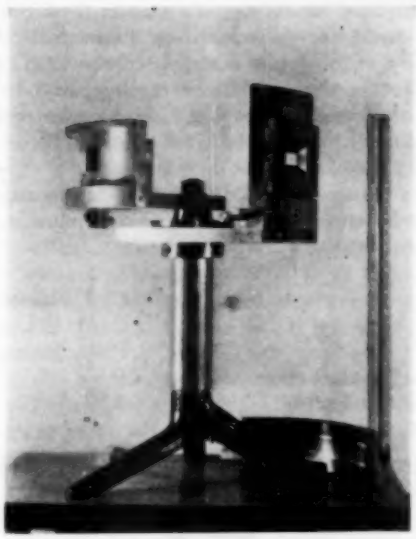

FIG. 1.

Very recently we have cut a slab of quartz parallel to the optic axis, ground it to a thickness of 0.21 mm and given it a radius of curvature of approximately 20 cm. Before bending, the quartz slab was plane and parallel to within 0.01 mm. The curvature was impressed upon this thin sheet of quartz by imprisoning it between two heavy metallic lamina machined to the required radius. The x-rays pass through an aperture (2 cm × 1 cm) cut in this crystal holder.

In addition to the crystal holder the spectrograph (Fig. 1) consists of a film holder and graduated circle which turn on the same vertical axis as the crystal holder. The film holder also consists of two heavy metallic lamina machined to one-half the radius of curvature of the crystal holder in accordance with the focussing condition outlined by Cauchois.[3] The circle is graduated in half degrees and with the help of verniers the positions of the crystal and film holders can be read to one minute of arc.

With molybdenum radiation excited under 40 kv and 15 m.a., a fluorescent spectrum of zirconium (Fig. 2) was obtained in two and a half hours. The secondary radiator was large enough to illuminate the entire crystal aperture for the first and second orders of ZrK. The first order $K\alpha$ doublet is visibly resolved.

The crystal planes which are effective in the reflection of the x-rays are those perpendicular to the optic axis. For these planes the second order reflection is stronger than the first because of the alternate spacing of oxygen and silicon atoms. Thus the effective grating constant, already small, is further reduced. The reflecting planes are approximately perpendicular to the surface of the crystal lamina and hence converge to a point near the center of curvature of the crystal.

The quartz crystal shows promise of being far superior to mica for this purpose. The luminosity of the instrument claimed by Cauchois for mica seems to be retained. In addition because of the good crystalline quality of quartz the spectra are sharp and clear which was not the case with the mica we used. Furthermore, because of the small grating constant of quartz the dispersion and resolution of the spectrograph have been greatly enhanced.

JESSE W. M. DUMOND
BERNARD B. WATSON

Norman Bridge Laboratory of Physics,
California Institute of Technology,
July 25, 1934.

[1] Y. Cauchois, J. de phys. et le rad. **4**, 61 (1933).
[2] E. Carlsson, Zeits. f. Physik **84**, 806 (1933).
[3] Y. Cauchois, J. de phys. et le rad. **4**, 320 (1932).

The Magnetic Moment of Caesium Determined from the Hyperfine Structure of the $6p\,^2P_{\frac{1}{2}}$ State

The hyperfine structure of the line λ8761.35 ($6d\,^2D_{3/2} - 6p\,^2P_{1/2}$) in the arc spectrum of caesium has been investigated with a Fabry-Perot interferometer. This line shows two components which arise from the $P_{1/2}$ state, the splitting of the $D_{3/2}$ state being too small to observe. The separation obtained, corrected for mutual influence of the components is 0.035 ± 0.001 cm^{-1}. On allowing a ratio of 0.0278 between the interval factors of the $D_{3/2}$ and the $P_{1/2}$ states the separation of the $P_{1/2}$ state becomes 0.037 ± 0.001 cm^{-1}. By using this separation and applying Goudsmit's formulas a g value of 0.70 is obtained for caesium.

L. P. GRANATH
R. K. STRANATHAN

New York University,
University Heights,
August 1, 1934.

FIG. 2.

Alpha-Particles from Lithium Ions Striking Hydrogen Compounds

We have bombarded hydrogen compounds with 240,000 volt Li ions and have observed a small but apparently significant number of α-particles resulting from the disintegration of Li (probably Li^7).

The source of high potential was a Holtz electrostatic machine with 14 motor-driven 32-inch plates. The Li ions were emitted from a platinum strip coated with spodumene and heated by means of batteries contained in an insulated metal box at the high potential end of a three stage cascade type accelerator in a horizontal 4-inch glass tube. The tube was evacuated by an oil diffusion pump (speed 30 liters per second) backed by a Cenco hypervac pump. Operating pressures were of the order of 10^{-4} mm Hg.

Three targets (copper coated with NH_4Cl, copper coated with $Al(OH)_3$ and bare copper) were mounted on a ground joint so that any one could be brought into the beam of Li ions. The targets were inclined to the beam at an angle of 45° and directly above the target was a mica window of 2.6 cm stopping power. Immediately above the window was mounted a linear point counter which was connected by means of a linear amplifier to an impulse counter. The point counter was operated at such a potential below the breakdown potential that only α-particles were counted.

With the electrostatic machine operating at full speed (approximately at 240,000 volts), the temperature of the platinum strip was adjusted so that the focal spot of the Li ions (as observed by the fluorescence of a quartz plate) was about 1 cm in diameter. Under these conditions, the current carried by Li ions striking the target was approximately 5 microamperes and counts were recorded as follows:

(1) With the NH_4Cl target, a total of 20 counts in 4 periods of 10 minutes each, i.e., 0.5 per minute.

(2) With the $Al(OH)_3$ target, a total of 13 counts in 3 periods of 10 minutes each, i.e., 0.4 per minute.

(3) Between each 10-minute period was a period of 10 minutes during which counts were taken with an absorber of approximately 15 cm stopping power between the point counter and the mica window. A total of 1 count was observed in 4 such periods, indicating that only α-particles were registered in (1) and (2).

(4) With the bare copper target, a total of 2 counts was recorded in 2 periods of 10 minutes each. This was attributed to radioactive contamination around or below the mica window, for with the high potential cut off, 8 counts were recorded in 100 minutes, i.e., 0.1 per minute, approximately, in both cases.

The net count is therefore 0.4 per minute with the NH_4Cl target and 0.3 per minute with the $Al(OH)_3$ target. These coatings were thick in comparison with Li^+ ranges. The effective solid angle was approximately 1/150 so that the total numbers of α-particles produced per minute per microampere when 240,000 volt Li ions strike NH_4Cl and $Al(OH)_3$ are approximately 12 and 9, respectively.

The small yield of α-particles indicates that 240,000 electron-volts must be only slightly above the threshold energy required for disintegration under these conditions. The threshold energy required to disintegrate Li under bombardment by protons is about 32,000 e.v.[1] If for disintegration the relative velocity of the two particles is critical, then we might expect Li to be disintegrated on bombarding hydrogen, if the Li ions had a minimum energy of about 225,000 e.v.

Due to the small yield of α-particles, no measurements have yet been made on their range which must, however, have been between 4 cm and 19 cm.

J. Zeleny
C. J. Brasefield
C. D. Bock
E. C. Pollard

Sloane Physics Laboratory,
Yale University,
August 1, 1934.

[1] M. L. E. Oliphant and Lord Rutherford, Proc. Roy. Soc. **A141**, 267 (1933).

Vibration-Rotation Bands of Hydrogen Fluoride

With a twenty-one foot, 15,000 line, concave grating spectrograph, fifteen and eleven lines, respectively, of the (3←0) and (4←0) vibration-rotation bands of HF gas have been photographed at 8790A and 6744A.

The following rotational constants in wave numbers in vacuum have been calculated and are expressed in the notation suggested by Mulliken[1] in his Eqs. (2c) through (4c). $B_e=20.917$ cm^{-1}; $\alpha_e=0.749$ cm^{-1}; $D_e=-0.00215$ cm^{-1}; $\beta_e=0.000285$ cm^{-1}. The values for the first two of these constants can be compared and are in good agreement with calculations from Czerny's[2] equation for the measurements by Imes[3] on the (1←0) band.

The vibrational constants determined from the (3←0) and (4←0) bands are $\omega_e=4123.12$ cm^{-1} and $\omega_e x_e=83.04$ cm^{-1}, but with these values, the difference between the observed and the calculated positions of the (1←0) band center is 5.5 cm^{-1}. To calculate both the fundamental and the two overtone band centers it is apparently necessary to use an $\omega_e y_e$ term, in which case $\omega_e=4141.305$ cm^{-1}, $\omega_e x_e=90.866$ cm^{-1}, and $\omega_e y_e=0.921$ cm^{-1}. Either of these values of $\omega_e x_e$ differs markedly from that which previously has been calculated with the use of observations made on the unresolved (2←0) band by Schaefer and Thomas.[4]

Longer absorption cells are no being used in an attempt to measure still higher harmonics and the work will be presented later in greater detail.

E. O. Salant
D. E. Kirkpatrick

Department of Physics,
Washington Square College,
New York University,
August 3, 1934.

[1] R. S. Mulliken, Phys. Rev. **36**, 611 (1930).
[2] M. Czerny, Zeits. f. Physik **45**, 476 (1927).
[3] E. S. Imes, Astrophys. J. **50**, 251 (1919).
[4] C. Schaefer and M. Thomas, Zeits. f. Physik **12**, 330 (1923).

Mass Ratios of Isotopes from Band Spectra

According to the simple theory of the isotope effect in diatomic band spectra the ratio B_e^i/B_e of the moments of inertia of the two molecules should equal ρ^2, the ratio of their reduced masses. It has recently been pointed out by Kronig,[1] however, that for many molecular electronic states the quantum mechanics treatment of the vibrating and rotating molecule leads to the conclusion that the equilibrium distance between the two nuclei will be slightly smaller for that molecule involving the heavier isotope. I have determined these rotational band constants for both states involved in the B band system of the molecules CaH and CaD, for which, according to mass-spectrograph findings, ρ^2 should be 0.51276. For the normal $^2\Sigma$ state which exhibits but very small interaction with other states, the ratio of the B_e constants is 0.51337. This difference is of about the same amount as that found by Holst and Hulthén[2] for the normal $^1\Sigma$ state of AlH and AlD, and is of the order of magnitude to be expected from Kronig's theory.

That the ordinary rotational energy term formula applied to the excited $^2\Sigma$ state of these B bands does not yield the correct B_v values is shown by the fact that the B_e^i/B_e ratio so obtained is 0.50788. One always obtains from the band spectrum analysis B^* values,[3] differing from the true B_v values by terms arising from the interaction with certain other states of the molecule. These correction terms are proportional to B^2 and can be evaluated only if the interaction is solely with one other known state. The interaction for this $B^2\Sigma$ state of CaH being largely with the near-lying $A^2\Pi$ state, the correction to B_0^* is about -0.067, while for CaD the correction is but -0.017. With the inclusion of these corrections the B_e^i/B_e ratio becomes 0.51365, approximately agreeing with that for the normal state.

These perturbing interactions between the various energy states of a molecule are always present and are difficult to evaluate with precision. Although seldom as large as in the present example, their effect on the B constants should be investigated in obtaining accurate mass ratios from band spectrum analysis. Other details of the several spectra of calcium deutride will be submitted for publication in this journal in the near future.

WILLIAM W. WATSON

Sloane Physics Laboratory,
Yale University,
August 1, 1934.

[1] R. deL. Kronig, Physica **1**, 617 (1934).
[2] W. Holst and E. Hulthén, Nature **133**, 496 (1934).
[3] Cf. R. S. Mulliken and A. Christy, Phys. Rev. **38**, 87 (1931).

Nuclear Stability and Isotope Shift

In a recent paper Gamow[1] advances an explanation for the anomalously large values of α-particle energies of Ra C′, Ac C′, Th C′ as compared with those of U, Th, Rn, etc. He plots the known nuclear species as points in a diagram of n_1/n_2 against n_1+n_2 where n_1 = number of neutrons, n_2 = number of protons. In this diagram he locates a wavy curve representing the location of the energy minimum for n_1+n_2 = const. This curve is considered as being the bottom of a trough on the energy surface.

It is of interest that Gamow's diagram fits in with the observed isotope shifts of Hg and Pb, if it is supposed that the nuclear radius on which the isotope shift depends[2-5] increases with the total number of nuclear particles and decreases with nuclear stability. On account of the dependence on n_1+n_2 the shift of heavy nuclei should vary regularly with the atomic weight and should produce equal spacings between adjacent even isotopes and the same equal spacings between adjacent odd isotopes. The effect of stability is to produce irregularities in these spacings which are apparently in approximate agreement with experiment. Thus consider the even isotopes $Pb^{204, 206, 208}$. The addition of two neutrons which changes Pb^{206} into Pb^{208} brings one closer to the curve of minimum energy. The nuclear stability is thereby increased and the increase in volume due to the addition of two neutrons is partly compensated. On the other hand Pb^{208} and Pb^{210} are located approximately symmetrically on the two slopes of the trough and the effect of the increase in n_1 remains by itself. We expect therefore $|W(206)-W(204)| < |W(208)-W(206)|$. According to Schuler and Jones[6] this is the case experimentally, the ratio of the two displacements being $\sim 46/52$. Among the isotopes of Hg the work of Schuler and Keyston brings out that the levels of Hg^{199} are closer to the levels of Hg^{198} than the levels of Hg^{201} are to those of Hg^{200}, the ratio of the shifts being 9/57 from Hg I λ2536, 24/31 from Hg I λ6072, 15/28 from Hg I λ6716. This fits into the picture because the formation of Hg^{199} from Hg^{198} involves an increase in stability and a consequent partial compensation of the increase in volume; the formation of Hg^{201} from Hg^{200}, on the other hand, leaves the stability unchanged or else decreases it. For the even isotopes of Hg the data on the relative order of $W(204)-W(202)$, $W(202)-W(200)$, $W(200)-W(198)$ are not self-consistent. The optical level for which large shifts have been observed[7] is $5d^9\,6s^2\,^2D_{5/2}$ of Hg II. The order of the shifts is here the theoretically expected one.

The essential point in the above explanation is not the precise shape of Gamow's trough but the fact that addition of neutrons takes one into the region of β instability. The staggering of the odd isotopes with respect to the even ones is apparently too large to be explained by the above considerations.

G. BREIT

Department of Physics,
New York University,
University Heights,
August 1, 1934.

[1] G. Gamow, Zeits. f. Physik **89**, 592 (1934).
[2] J. H. Bartlett, Nature **128**, 408 (1931).
[3] G. Racah, Nature **129**, 723 (1932).
[4] Jenny E. Rosenthal and G. Breit, Phys. Rev. **41**, 459 (1932).
[5] G. Breit, Phys. Rev. **42**, 348 (1932). According to this discussion the the direction and magnitude of observed shifts in different optical levels can be reconciled with a change in nuclear volume.
[6] H. Schuler and E. G. Jones, Zeits. f. Physik **75**, 563 (1932).
[7] H. Schuler and H. Westmeyer, Zeits. f. Physik **82**, 685 (1933).

The Spin and Magnetic Moment of the Potassium K^{39} Nucleus

We have measured the spin and magnetic moment of the potassium K^{39} nucleus by the deflection of a beam of neutral K atoms in a weak magnetic field. To attain sufficient resolution with the weak magnetic fields in question (from 5 to 210 gauss) the beam was made 142 cm long with a measured width of 0.1 mm at the receiving end. The inhomogeneous magnetic field was obtained from two parallel wires carrying currents in opposite directions[1] and was 61.5 cm long. The deflection pattern was very clearly resolved leading to entirely unambiguous results.

The spin of K^{39} as measured is 3/2 in units $h/2\pi$. The hyperfine structure separation of the $^2S_{\frac{1}{2}}$ normal state as calculated from the deflection pattern in the magnetic field is 0.0147 cm^{-1} in agreement with the value of 0.015 which Jackson and Kuhn[2] found independently from hyperfine structure measurements on the resonance lines. This leads to a nuclear magnetic moment calculated according to Goudsmit's[3] formula as extended by Fermi and Segre[4] of 0.38 in units of the nuclear magneton $\mu_0/1838$. Full details will be communicated to this journal.

SIDNEY MILLMAN
MARVIN FOX
I. I. RABI

Columbia University,
July 28, 1934.

[1] Rabi, Kellogg and Zacharias, Phys. Rev. **46**, 157 (1934).
[2] Jackson and Kuhn, Nature **134**, 25 (1934).
[3] Goudsmit, Phys. Rev. **43**, 636 (1933).
[4] Fermi and Segre, Zeits. f. Physik **82**, 729 (1933).

Proceedings of the American Physical Society

MINUTES OF THE BERKELEY MEETING, JUNE 18–23, 1934

THE 192nd regular meeting of the American Physical Society was held in Room 210, Le Conte Hall, University of California, Berkeley, over the period from Tuesday, June 19 to Saturday, June 23, 1934, in affiliation with Section B of the American Association for the Advancement of Science.

The program consisted of a symposium on spectroscopy in astrophysics in conjunction with the Astronomical Society of the Pacific, on Tuesday; a symposium on nuclear structure on Wednesday; and a symposium on fundamental physical constants on Thursday. This was followed on Friday and on Saturday morning by the regular program of ten-minute contributed papers. The program of the symposia and the ten-minute contributed papers are given on the following pages.

The meetings were exceptionally well attended, the maximum attendance being at the symposium on nuclear structure with an audience of close to 350. The meetings were presided over by Vice-President R. W. Wood of the American Physical Society, and some fifteen members from east of the Rockies were in attendance. The Physical Society met informally at luncheon on Tuesday, Wednesday, Thursday and Friday, the attendance of the luncheons varying between forty and sixty-five members. On Wednesday evening there was an informal dinner of the American Physical Society at which Vice-President Wood gave an informal talk which might have been entitled *The Physicist as a Detective.*

A short business meeting was held following the end of the sessions on Saturday, in which it was voted to hold the December meeting on the Pacific coast on Friday and Saturday, December 21 and 22, 1934, at the University of California at Los Angeles.

PROGRAM

Joint meeting with the Astronomical Society of the Pacific

Symposium on Spectroscopy in Astrophysics. Two sessions

1. TUESDAY, JUNE 19TH AT 10 A.M., ROOM 210 LE CONTE HALL

Paper I. Unidentified Interstellar Lines. DR. PAUL W. MERRIL, *Mount Wilson Solar Observatory*

II. Diffraction Gratings and Their Applications to Astronomical Problems. PROFESSOR R. W. WOOD, *Johns Hopkins University, Vice-President of American Physical Society*

2. TUESDAY, JUNE 19TH AT 2 P.M., ROOM 210 LE CONTE HALL

III. Light of the Night Sky. PROFESSOR JOSEPH KAPLAN, *University of California at Los Angeles*

IV. Spectroscopic Evidence of Galactic Absorption. DR. R. J. TRUMPLER, *Lick Observatory, Mount Hamilton, California*

V. Forbidden Lines in Astronomical Sources. PROFESSOR I. S. BOWEN, *California Institute of Technology*

Symposium on Nuclear Structure. Two sessions

1. WEDNESDAY, JUNE 20TH AT 9:30 A.M., ROOM 210 LE CONTE HALL

Paper I. The Production of High Voltage and its Application to Nuclear Research. PROFESSOR R. J. VAN DE GRAAF, *Massachusetts Institute of Technology*

II. Disintegration Experiments Using Protons and Deutons at 1200 Kilovolts. DR. MERLE A. TUVE, *Department of Terrestrial Magnetism, Carnegie Institution*

III. Recent Nuclear Investigations at the University of California. PROFESSOR E. O. LAWRENCE, *University of California*

2. WEDNESDAY, JUNE 20TH AT 2 P.M., ROOM 210 LE CONTE HALL

IV. The Emission of Neutrons and Gamma-Rays from Various Elements. PROFESSOR C. C. LAURITSEN, *California Institute of Technology*

V. Disintegrations with Positron Ejection. PROFESSOR CARL D. ANDERSON, *California Institute of Technology*

VI. The Nature of Cosmic Rays. DR. THOMAS H. JOHNSON, *Barthold Research Foundation*

Discussion of the theoretical aspects was led by Professor Felix Bloch.

Symposium on Fundamental Physical Constants. Two sessions

1. THURSDAY, JUNE 21 AT 10:00 A.M., ROOM 210, LE CONTE HALL

Paper I. The Value of the Electronic Charge. PROFESSOR R. A. MILLIKAN, *California Institute of Technology.*

II. Measurement of the Compton Shift. PROFESSOR P. A. ROSS, *Stanford University.*

III. Continuous X-Ray Spectra and the Value of $h/e^{4/3}$. DR. PAUL KIRKPATRICK, *Stanford University.*

IIIa. A Correction to the Theory of the Compton Shift.

IV. A Measurement of the Compton Shift and the Determination of the Constant h/me. DR. J. W. M. DUMOND, *California Institute of Technology.*

2. THURSDAY, JUNE 21 AT 2:00 P.M., ROOM 210 LE CONTE HALL

V. Spectroscopic Determinations of Atomic Constants. PROFESSOR W. V. HOUSTON, *California Institute of Technology*

Va. The Fine Structure of $H\alpha$ and the Determination of e/em and of the Fine Structure Constant. PROFESSOR C. D. SHANE, *University of California.*

VI. The Present Status of the Values of e, h and e/m. PROFESSOR R. T. BIRGE, *University of California*

ABSTRACTS

1. Ionization by Positive Alkali Ions in Noble Gases Using a Balanced Space-Charge Method. ROBERT N. VARNEY. *University of California.*—In recent years a number of investigations of the ionizing potentials produced by alkali ions moving in the inert gases have revealed the fact that using methods which detect the *electrons* liberated on impact, the ionization sets in at sharply defined potentials in the neighborhood of 100 volts for alkali ions whose electronic configuration is that of the inert gas. In view of the fact that by measuring the electrons liberated, sources of possible error are introduced, it seemed desirable to study these potentials using another method. To this end the balanced space charge method developed by Lawrence and Edlefsen for photoelectric studies was applied to the positive ions. Ions of potassium and sodium of varying velocity were shot into one chamber of the balanced space charge in argon and neon at pressures around 5×10^{-3} mm. The presence of positive ions of zero velocity is evidenced by a change in balance in the bridge and the nature of the arrangement makes the method exceedingly sensitive to the presence of low speed ions. Overlooking the initial disturbances created by the entrance of the very slow positive ions into the space charge chamber, virtually no change was observed above 40 volts up to 84 volts for K^+ ions in argon and 130 volts for Na^+ ions in neon. For K^+ ions in neon and Na^+ ions in argon, no de-

flection was observed below 225 volts. At the critical voltages in neon and argon, the current rose sharply and initially in an almost linear fashion. The values of these potentials are about 12 percent lower than the values obtained for ionization by Beeck. Inasmuch as any errors might lower the value of the potentials recorded some two or three volts, these results are notably different from those obtained by Beeck. In view of the fact that inelastic impacts were being detected in this case, while Beeck observed the liberation of electrons, these results need not be considered irreconcilable.

2. Further Studies on the Motion of Photoelectrons in a Gas. AUSTIN M. CRAVATH. *University of California.*—The problem and method of solution were outlined at the Stanford meeting (Phys. Rev. **45**, 138 (1934)). For fields so weak that the terminal energy does not appreciably exceed 1.5 kT, the thermal equilibrium value, the fraction of saturation of the photoelectric current is $i/i_0 = 1.88\,Eel/(1.5\,kT)$ = (energy gained in 1.88, mean free path)/(mean thermal energy). Neither the energy of photoelectric emission, $V_e e$, nor the average fraction of the average energy lost per collision, f, enters. For moderate fields, i.e., terminal energy $\gg 1.5\,kT$ but $i/i_0 \ll 1$, $i/i_0 = 2.75 f^{\frac{1}{2}}((Eel)/(V_e e))^{\frac{1}{2}}$ approximately. The differential equations have been solved for a few cases of finite anode distance. These solutions show the limits of applicability of the previous solutions for infinite anode distance on the one hand, and of the Hertz solution for no energy loss on the other. Moreover, the extent to which electrons diffuse against the field, and hence the error in considering merely the average motion, are elucidated.

3. Organic Liquids Suitable for Cloud Expansion Work. DONALD H. LOUGHRIDGE AND HAROLD C. TRUEBLOOD. *University of Washington.*—In an attempt to obtain a suitable liquid for use in the presence of gases highly soluble in water, a study of twenty-eight organic liquids has been carried out with reference to their minimum expansion ratio for condensation on alpha-particle tracks. The apparatus in use allowed a maximum expansion ratio of 1.30 and of the total number of liquids studied eleven were found to yield good results (several of these gave much sharper tracks than were obtained in water vapor) with ratios between 1.14 and 1.25. Four more gave a heavy general fog formation with expansion ratios between 1.008 and 1.20, but no ion condensation could be obtained. The remaining thirteen gave no general fog up to the maximum ratio obtainable, and no tracks could be seen. It is possible that in this latter group there are some which will allow ion condensation if a larger expansion ratio be used. All the liquids studied were chosen for their low surface tensions and a correlation with J. J. Thompson's theory was attempted, but the latter seems clearly to be unable to predict the experimental facts. Work is being continued on apparatus which will allow larger ratios.

4. The Energy of Detachment of Electrons from Negative Ions in Oxygen. LEONARD B. LOEB. *University of California.*—The *energy* of attachment of electrons to O_2 molecules to form negative ions has up to the present eluded evaluation. Cravath in 1929 and recently Bradbury (Phys. Rev. **44**, 883 (1933), have measured the probability of this attachment process. In the course of their experiments they observed what they believed to be a *detachment* of electrons from negative oxygen ions at about 0.6 volt energy. Using a high frequency arc of 10^8 cycles between Pt electrodes in O_2 as an ion source, the writer has investigated this process in detail. The mixture of electrons and ions from the arc passes through an electron filter consisting of a grid of fine copper wires 0.2 mm diameter spaced 2 mm apart between alternate wires of which an alternating potential of 3×10^8 cycles is established. This removes electrons and some few ions. The remaining ions then pass between the meshes of a similar grid of wires (3 mm in diameter 3 mm apart (ion smasher)) with an alternating potential of 3×10^8 cycles. By increasing this potential the last of the electrons begin to be removed and the current to the collector decreases to a minimum. Thereafter it *increases* slightly and then rapidly falls to zero. The increase ("hump effect" of Cravath) is explained as due to a sudden attachment of the residual electrons, which in the high field of the ion smasher suffer the inelastic impacts observed by Bradbury to lead to a fivefold increase of the electron attachment at 1.6 volts energy. Thus these electrons escape capture as the ions which they form are not captured. At about 400 volts per cm, peak value, at 2.69 mm pressure in the strong part of the field, the negative ions begin to break up to give electrons which are removed. Assuming that in these high fields the negative ions have free paths of molecular magnitudes, the ionizing energy for negative ions appears, as a preliminary result, to be 1.1 volts.

5. Some Improvements in the Technique of Kerr Cells. H. J. WHITE. *University of California.*—The quickness of cut-off of the electro-optical shutter tends to be destroyed by the presence of impurities in the liquid used in the Kerr cells. This is due to the polarization field set up in the cell by the ions of the impurities and hence the conductivity is a good indicator of a cell's usefulness. Experiments show that the conductivity of the liquid, nitrobenzene in the present experiments, should be at least as low as 10^{-11} mhos per cm³. For use in the study of spark breakdown nitrobenzene has been purified by fractional distillation and freezing so that its conductivity is as low as 3×10^{-12} mhos per cm³, which is to be compared with the lowest previously published value of 7×10^{-11} mhos per cm³. The sealing of the windows onto a Kerr cell presents difficulty because nitrobenzene dissolves most waxes and cements. A search for a satisfactory substance has resulted in the use of ceresin wax which is practically insoluble in nitrobenzene. The corrosion of the plates of the cells is prevented by gold plating them. Cells constructed in this way have proved very satisfactory for studying the early stages of spark breakdown.

6. Changes in the Energy Distribution of Thermionically Emitted Electrons Produced by High Electrical Fields. R. K. DAHLSTROM AND JOS. E. HENDERSON. *University of Washington.*—Changes produced by high electrical fields

in the energy distribution of thermionically emitted electrons have been measured utilizing a method previously used by us for the measurement of the energy distribution of field current electrons. Although the apparatus is cylindrical, the distribution with zero applied field appears to be approximately Maxwellian in form. As the field is applied to the emitter, two major changes occur in the distribution. First, the curve as a whole shifts in the direction to be expected if the field does work on the whole body of emitted electrons. Second, a group of electrons of low energy appears which apparently would not have escaped had it not been for the applied field. The emitter was of tungsten having a composite surface such that the lack of saturation with increasing anode voltage was much pronounced.

7. Thermionic Pentode Controlled Constant-Voltage Rectifiers. ROBLEY D. EVANS. *National Research Fellow, University of California.*—Replacement of batteries by rectifiers for the reliable operation of ionization chambers, electrometers, tube- and point-counters, Pliotron amplifiers, etc., demands an efficient voltage-control unit to remove fluctuations in output caused by variations in the a.c. mains. The ingenious thermionic tetrode control circuits described by Street and Johnson omit consideration of the important fact that the cathode of the voltage controlling tube is usually heated from the same a.c. mains which supply the high voltage to the rectifier unit. It can be shown both theoretically and experimentally that cathode-heater voltage fluctuations materially affect the high voltage d.c. output from such units. A balanced circuit is described which employs a single thermionic pentode to eliminate these variations as well as variations in the high voltage input. The circuit employs one 45 v dry battery in the control grid, where the absence of a current drain permits long life and a constant voltage characteristic. Under average laboratory conditions the observed output voltage fluctuations from the a.c. operated rectifier and pentode voltage control unit are about 1 part in 5000. The type '47 tube has been found better qualified than the '57, '58, '59 or '77 for this control service.

8. The Production of High Velocity Lithium Ions. R. L. THORNTON AND B. B. KINSEY (*Introduced by E. O. Lawrence*). *University of California.*—A source has been developed capable of yielding an intense and stable beam of Li ions. The method used, which was first described by Kingdon, consists in directing a stream of Li atoms from a furnace (400–500°C) on a tungsten filament at a temperature of about 1100°C. By using a filament 1 inch wide by 2 inches long, a positive ion emission from the filament of 4 mA has been obtained. With suitable electrostatic focussing, a beam of over 1 mA of Li ions has been obtained through a tube $\frac{1}{8}$ inch in diameter at a distance of about 12 inches from the filament. The maintenance of an oxygen layer on the filament by means of an adjustable oxygen leak has been found essential for the satisfactory operation of the source. The ions thus produced are accelerated in a linear multiple accelerator of the type devised by Sloan and Lawrence. Using a ten stage accelerator, a current of 1.5 μA has been obtained at 500,000 volts. It is expected that higher voltages, of the order of one million, will be reached in the near future. It is proposed to use this apparatus for the investigation of possible nuclear disintegrations under Li bombardment, for the study of the range-energy relation, etc.

9. An Amplifier and Recording Apparatus for Alpha-Particles, High Speed Protons and Neutrons. M. C. HENDERSON. *University of California.*—Improvements have been made in the Wynn-Williams type of amplifier that make it possible to record the most rapid protons, even though ions are collected from only 4 mm of track. The number of stages of amplification has been reduced to four and only commercial radio tubes are used: a 57 in the first stage and a 77, 39 and 77 in the remaining three. The variable amplification factor of the 39 is utilized to control the overall amplification. The voltage pulse produced in the output by a slow proton is 15 times as large as the R.M S fluctuation in the background noise. By placing the ionization chamber in a magnetic field it has proved possible to count some of the recoil electrons produced by gamma-rays. A "scale of eight" thyratron counter and cathode-ray oscillograph of the high luminosity type are used for recording and observing the particles. The oscillograph makes it possible to follow the performance of the amplifier at all times, and spurious effects are easily detected and allowed for. In addition, any radioactivity involving the emission of alpha-particles, protons, or neutrons with a half-life down to 0.005 sec. could be readily measured.

10. The Loss in Energy in the Disintegration of Nitrogen by Neutrons. FRANZ N. D. KURIE. *National Research Fellow, University of California.*—Thirty-four disintegration forks have been photographed in a Wilson cloud chamber placed close to the Lawrence and Livingston apparatus in which a beryllium target was being bombarded by 3 MV deutons. The cloud chamber contained nitrogen and oxygen saturated with ethyl alcohol vapor. Most of the forks were due to the break-up of nitrogen, but some were certainly due to oxygen. However, they were computed on the assumption that they were all nitrogen disintegrations. If E_n, E_α and E_β are the kinetic energies of the incident neutron, the light fragment ($_2He^4$) and the heavy fragment ($_5B^{11}$), respectively, eight examples show a gain in energy corresponding to $E_\alpha+E_\beta>E_n$. If E_n is plotted against $\Delta(=E_n-E_\alpha-E_\beta)$ a definite relation is exposed. The results of other experimenters support this relation. If we assume $\Delta(E_n)$ is a simple function then $\Delta(0)$ should be a constant and $=B^{11}+He^4-N^{14}-n^1=-1.5$ MV. This point falls on the experimental curve and seems to preclude the possibility of a mass of the neutron differing from Chadwick's by more than 2 MV. Possible explanations of this relation are being sought and will be discussed.

11. The Transmutation of Fluorine by Proton Bombardment and the Mass of Fluorine 19. E. O. LAWRENCE, M. C. HENDERSON AND M. S. LIVINGSTON. *University of California.*—Protons having energies between 0.675 and 1.63 million electron-volts have been used to bombard a target of calcium fluoride and the range and number of

alpha-particles emitted in the resulting transmutation have been measured. The range of the alpha-particles depends on the energy of the proton in the expected manner and lies between 6.0 and 7.5 cm. Particles of shorter range, observed both by us and by other workers, probably resulted from the presence of boron in the target. With the energy of these alpha-particles of longer range, the mass of the fluorine atom is calculated to be 19.0031, a value in agreement with the chemical data and with other transmutation work but not with Aston's value. Professor Oppenheimer has calculated, along the lines of the Gamow theory, the manner in which the probability of transmutation should vary with the energy of the bombarding proton. The measurements agree well with the theoretical prediction.

12. Radioactivity Induced by Neutron Bombardment. M. S. LIVINGSTON, M. C. HENDERSON AND E. O. LAWRENCE. *University of California.*—Using a beam of neutrons from a Be target bombarded by 1 microampere of 2.6 MV deutons we have investigated the type of induced radioactivity recently discovered by Fermi. The magnitude of

TABLE I.

Element	Half-life (sec.)	Approximate range of disintegration particles (cm Al)	Nuclear cross section for activation cm^2 ($\times 10^{25}$)
Ag { two groups }	26±4	0.28	1.9
	154±10	0.1	4.2
Al	570±30	0.1	0.5
Cu	420±60	0.15	0.3
F	10±.5	—	3.5

the initial activity in several elements is surprisingly large: for example a thousand beta-particles per min. were observed from 1 sq. cm of a silver surface. Some of the results are given in Table I. Magnetic deflection experiments established that both groups of disintegration particles in Ag as well as those from Al consist of electrons. Some evidence of two groups in Cu was obtained and the half-life given is possibly a mean value.

13. The Emission of Secondary Electrons from Various Metal Targets. LEO H. LINFORD. *University of California.*—Using the Lawrence and Sloan apparatus for the multiple acceleration of ions, the secondary electron emission has been studied for various metal surfaces bombarded by mercury ions with energies up to 1,300,000 volts. The total emissions from nickel, molybdenum, aluminum, copper, tungsten, tin, mercury, silver, gold and carbon fall in the range 8 to 35 electrons per ion depending upon the condition of the metal surface. The secondary emission does not depend markedly on the target metal nor on the energy of the bombarding ions above 300,000 volts. The energies of secondary electrons are in the range 0 to 15 volts. The radiation produced by the impacting ions apparently causes photoelectric currents from the chamber surrounding the target as great as the current of high speed ions.

14. Energy-Loss and the Production of Secondaries by Cosmic-Ray Electrons. CARL D. ANDERSON AND SETH H. NEDDERMEYER. *California Institute of Technology.*—Measurements of the energies of secondary electrons produced in plates of lead and carbon by cosmic-ray electrons (the word electron is used in referring collectively to both positrons and negative electrons, or negatrons) have shown that the distribution in energy of secondary negatrons is, within experimental uncertainty, in agreement with the distribution calculated from the theoretical cross section given by Carlson and Oppenheimer. Three cases have been observed of pair formation by electrons in lead, and no such cases in carbon. Measurements on electrons traversing a lead plate have shown large fluctuations in specific energy-loss and have given in some cases values of the order of 100×10^6 e.v./cm, which is much too high to interpret on the basis of normal energy-loss, *viz.*, the loss by primary ionization and by the production of secondary negatrons by close encounters with extra-nuclear electrons. This effect seems best explained by the production in an encounter with a lead nucleus of one or more photons, which carry off the excess energy. The magnitude of the effect indicates that such radiative processes may account for an appreciable fraction of the energy-loss in lead by fast electrons.

15. Absorption Measurements of Hard Gamma-Rays from Fluorine Bombarded by Protons. EDWIN MCMILLAN. *University of California.*—By using a lead-shielded ionization chamber, the gamma-rays from various targets bombarded by 1.1 million volt protons and 2.2 million volt deutons have been investigated. Absorbers could be interposed between target and chamber; the measured absorption coefficients were found to be about 6 percent low, by calibration with filtered radium gamma-radiation. With proton bombardment boron, beryllium, lithium and fluorine give strong gamma-rays, in increasing order of intensity. Absorption measurements of the fluorine radiation show it to be homogeneous. There is no evidence indicating neutrons. The yield is about 30 quanta per long-range alpha-particle. The absorption coefficients per electron ($\times10^{25}$) are: Pb, 1.75; Sn, 1.3; Cu, 1.07; Al, 0.8. Plotted against atomic number, these indicate a linear rise from the Klein-Nishina value for 5.5 million volts at $Z=0$ to a value 2.5 times this at lead. The extra absorption in lead is 1.05×10^{-25} per electron; that calculated by Oppenheimer on the basis of pair production is 1.10×10^{-25} at 5.5 million volts. The linear dependence on Z is that expected for pair-production absorption. With deuton bombardment fluorine, carbon, boron, lithium and beryllium give very strong ionization. There is evidence that part of this is due to neutrons.

16. Hyperfine Structure in the Arc Spectrum of Lanthanum. O. E. ANDERSON. *University of California.*—The hyperfine-structure analysis previously reported for the arc spectrum of lanthanum has been extended to

include a number of new lines; and the values of overall splittings of the hyperfine energy levels have been modified. The absolute splitting in several levels has now been determined by measurements on etalon patterns in which the off-diagonal components are observed. Of particular interest in the measurements are the overall separations of the hyperfine terms arising from $5d^26s\,{}^4F_{3/2,\ 5/2,\ 7/2,\ 9/2}$. Both the hyperfine and fine structures follow the Landé interval rule. It is found that the Goudsmit-Bacher equations, taking into account the interaction of the single s electron with the nucleus, are not sufficient to account for the observed splittings. However, by considering that part of the interaction is due to the $5d$ electrons, better agreement between the observed and calculated values is obtained. The hyperfine structure overall widths for the four members of ${}^4F_{3/2,\ 5/2,\ 7/2,\ 9/2}$ are -0.20, 0.18, 0.40 and 0.54 cm^{-1}, respectively. A liquid-air cooled Schüler tube and Fabry-Perot etalons were used in the investigation.

17. Anomalous Behavior of Diffraction Gratings Coated by Evaporation. JOHN STRONG. *California Institute of Technology.*—Diffraction gratings coated by evaporation with Mg, Ag or Al generally develop bright and dark bands in their continuous spectra of the order of 50A width. The number of these bands which appear decreases for the above coats in the order named. Au, Cu, Sn, Bi and Sb coats fail to develop such bands. Many bands are double, a dark band lying in juxtaposition to a bright band. All bands disappear for polarized light with the electric vector parallel to the ruling. From R. W. Wood's study (Phil. Mag. **4**, 396 (1902)) of these phenomena as exhibited by a bare speculum grating Rayleigh (Phil. Mag. **14**, 60 (1907)) suggested the following formula to explain the dependence of the wave-lengths of the bands on angle of incidence of the light $\lambda = \epsilon(1 \pm \sin i)/C$. Here C represented a passing off order and was integral. The author's measurements made with coated gratings justify this formula if C is not required to be integral. A speculum grating coated with silver and measured at 8 angles of incidence varying from 40° to 75° showed 78 bands. 61 of these were classified in three groups characterized by values of C which varied between the following limits: 5.83 to 5.86, 6.69 to 6.85 and 7.58 to 7.74. An experiment in which i and r were interchanged generally showed that if one had a bright band before the interchange one obtained a dark band after the interchange and *vice versa*—the wave-lengths of the bands being the same in both cases.

18. The Use of Schmidt Cameras in Plane Grating Spectrographs. THEODORE DUNHAM, JR. *Mount Wilson Observatory.*—A correcting plate at the center of curvature of a spherical mirror, as used by Schmidt for telescopes, has been found useful for spectrograph cameras. Such a camera, of 780 mm focus and 110 mm aperture, has been constructed with the plateholder outside the incident beam so as not to obstruct light. 3000A of the first order can be photographed at once in excellent definition. With a collimating mirror the spectrograph will be nearly achromatic and any region may be photographed by merely rotating the grating. The correcting plate curve is approximately a fourth degree paraboloid, $y = x^4/4(n-1)R^3$, combined with a sphere, as used by Schmidt. It should ideally be divided between front and back of the plate in a 3 : 1 ratio. The negative slope at the edge should equal the maximum positive slope. Chromatic difficulties are less than those of obtaining a field in monochromatic light, so that quartz or fluorite is not necessary except in the ultraviolet. A camera of 60 mm focus and 105 mm aperture ($f/0.57$) is under construction. A faster camera could be made if the correcting plate were built up of several rings spaced at different distances from the mirror. The field has a curvature whose radius equals the focus, but may be flattened in some cases by a plano-convex lens near the photographic plate.

19. The Spectra of O_4 and Other Polyatomic Polarization Molecules. WOLFGANG FINKELNBURG. *California Institute of Technology.*—The absorption spectrum of compressed, liquid and the blue solid oxygen shows a number of continuous bands which do not appear in the spectrum of gaseous oxygen at low pressure. These spectra are attributed to an O_4-molecule formed from two O_2 molecules by binding forces of the second order (polarization binding). By using the results for diatomic polarization molecules like Hg_2 the observed spectra can be explained as transitions from the small potential minimum of the ground level (dissociation energy about 0.008 volt) to excited O_4-states with dissociation energies of some hundredths of a volt. The electronic levels correspond closely to O_2 electronic levels, combinations of which with the ground state are forbidden in the undisturbed O_2. It is shown that the ultraviolet O_4-bands are independent of a similar band sequence found by Herzberg in the O_2-spectrum, and that the triplet structure of these bands has to be explained as structure due to the O_2-O_2 vibrations. The existence of similar polyatomic polarization molecules of the types A_2-A_2, A_2-B_2 and A_2-B is theoretically expected. The study of their spectra will bring an experimental proof for the explanation of the O_4-spectra.

20. New Second-Positive Bands in Nitrogen. JOSEPH KAPLAN. *University of California at Los Angeles.*

TABLE I.

Observed	4747	4737	4732	4453	4440	4435	4190
Calculated			(8,14) 4719		(8,13) 4441		(8,12) 4189
4180	4174	3180	3164	3027	3010	2886	2863
		(9,7) 3171	(7,6) 3150	(9,6) 3025	(7,5) 3002	(9,5) 2888	(7,4) 2866

The second-positive group of nitrogen, as normally observed, does not include bands originating on levels higher than $v' = 4$. In the nitrogen tube, in which many new features of the nitrogen band spectrum have been observed, the new bands listed in Table I have been found. These bands degrade to the red, and in one of the bands

in which the rotational structure was clearly developed the lines show the characteristic alternating intensities of nitrogen bands. Although the previously observed second-positive bands degrade to the violet, due to the abnormally rapid convergence of the vibrational levels of the $C^3\pi$ state, one would expect bands originating on high vibrational levels to degrade to the red. In Table I the observed wave-lengths of the band-heads are compared with the same values calculated by Vegard. When one considers that it is not possible to predict accurately the positions of these heads the agreement is surprisingly good in some cases. These bands are therefore tentatively identified as "tail-bands" in analogy with similar bands in CN and N_2^+. A more exact and detailed investigation of these bands is proposed.

21. Photographic Photometry of Iron Multiplets in Electric Furnace Spectra. ROBERT B. KING. *National Research Fellow, Mt. Wilson Observatory.*—Spectra of elements excited by the electric vacuum furnace have the property that the atoms are in thermal equilibrium. With the furnace as the source, intensity measurements are being made of lines within multiplets and of the relative intensities of multiplets in the spectrum of iron. Relative intensities of lines within a multiplet are measured at the temperature most suitable for the appearance of the multiplet and the relative intensities of multiplets are measured at several temperatures ranging from 1800°C to 2600°C. Intensities are calibrated by a lamp and step raster at the horizontal focus of the 15 ft. concave grating spectrograph, and plates are standardized by black-body radiation from a carbon plug inserted in the furnace and heated to the same temperature as that used for the iron spectrum. Calibrating exposure times are equal to those for the iron spectrum and three standard time exposures of different intensities are used for standardizing. Percentage reversals are derived from microphotometer tracings of narrow slit spectra and the corrections applied to intensities derived from very wide slit spectra. The behavior of important multiplets of different excitation potentials will be discussed.

22. Intensities in the 3400 Band of Phosphorous Hydride. PHILIP NOLAN AND F. A. JENKINS. *University of California.*—Line intensities in the rotational structure of the $^3\Pi$, $^3\Sigma$ band of PH have been measured by photographic photometry. The source was a discharge in hydrogen flowing at a pressure of 1 to 3 mm through a capillary of 2 mm diameter, phosphorous vapor being introduced into the stream just before the capillary. Plates taken in the second and third orders of the 21-foot grating were calibrated in a 3-meter quartz spectrograph by means of a step-slit. All lines of appreciable intensity in the 0,0 band, comprising 22 of the possible 27 branches, have been measured on 3 different plates. By summing the intensities from each upper level and dividing by the statistical weight, $2J'+1$, the excitation function, R, is found to correspond closely to a Boltzmann distribution at an effective temperature between 650 and 700°K, the temperature increasing for higher pressure or current density. By using this excitation function, the intensity factors, i, in the various branches are evaluated. For small quantum numbers these are found to agree with the qualitative predictions of Mulliken, for $^3\Pi$ (case a)$\rightarrow{}^3\Sigma$. At high quantum numbers, the satellite branches decrease in intensity, showing the tendency of the $^3\Pi$ state toward case b. Theoretical equations for the i factors have not yet been derived for this case.

23. Isotopic Abundance Ratios of C, N, A, Ne and He. ALFRED L. VAUGHAN, JOHN H. WILLIAMS AND JOHN T. TATE. *University of Minnesota.*—From the relative intensities of the peaks of mass-spectrograph curves as a measure of isotopic abundance ratios, numerous curves with CO, N_2, A, Ne and He gave the following abundance ratios with the indicated average deviations.

C^{13}/C^{12}	N^{14}/N^{15}	A^{40}/A^{36}	Ne^{20}/Ne^{21}
91.6 a.d. 2.2	265 a.d. 8	304 a.d. 12	337 a.d. 20

Ne^{20}/Ne^{22}	He^4/He^3
9.25 a.d. 0.08	<35,000

These are compared with the abundance ratios predicted by chemical atomic weight measurements using conversion factors based upon the oxygen isotopic abundance ratios of Mecke and Childs and of Smythe. There is no indication of any preference in the magnitude of the conversion factor that would yield better agreement between the predicted and observed ratios.

24. The Nuclear Mechanical Moment of Cobalt. KENNETH R. MORE. *University of California.*—The nuclear mechanical moment of cobalt ($Z=27$, $M=59$) has been reported by Grace (Phys. Rev. **43**, 762 (1933)) to be probably $(7/2)h/2\pi$. This value was based on a study of partially resolved hyperfine structure of the lines λ3454, $3d^84s\ {}^4F_{9/2}-3d^84p\ {}^4G_{11/2}$, λ3466, $3d^74s^2\ {}^4F_{9/2}-3d^74s4p\ {}^4G_{11/2}$ and λ3909, $3d^74s^2\ {}^4F_{9/2}-3d^74s4p\ {}^6G_{11/2}$. A value of $(5/2)h/2\pi$ was set as the lower limit for the mechanical moment while a value of $(9/2)h/2\pi$ was considered to be possible. The hyperfine structure of several lines in the visible portion of the Co I spectrum has been examined in an attempt to determine the nuclear moment more definitely. The lines λ4191, $3d^74s^2\ {}^4F_{9/2}-3d^74s4p\ {}^6F_{9/2}$, λ4234, $3d^74s^2\ {}^4F_{9/2}-3d^74s4p\ {}^6F_{11/2}$ and λ6450, $3d^74s^2\ {}^2G_{7/2}-3d^74s4p\ {}^2G_{7/2}$ all show a flag type pattern degrading toward the red. The presence of this type of pattern indicates that the upper levels have wider hyperfine splittings than the lower levels. Photometer curves of the hyperfine-structure pattern of λ4234 show definitely that there are more than six components and probably not more than eight components. The ratios of the hyperfine-structure intervals of the lines examined agree with the ratios given by the Landé interval rule for a nuclear moment of $(7/2)h/2\pi$.

25. The Nuclear Mechanical Moment of Columbium. STANLEY S. BALLARD. *University of California.*—In a preliminary report (N. S. Grace and S. S. Ballard, Phys. Rev. **44**, 128 (1933)) a value $I\geq(7/2)\cdot(h/2\pi)$ was reported for

the spin of the columbium nucleus. More detailed work has been done on the hyperfine structure of this element. Attention has been centered on a group of lines lying between λ4050 and λ4220, since these are the only classified lines in the visible region. These lines are transitions from $^6F^0$ and $^6P^0$ terms to a lower ^6D term, the configurations involved being, respectively, $4d^45p$ and $4d^45s$. Interpretation of hyperfine patterns is difficult since the splittings of the upper levels are too large to be neglected even in comparison to the very large splittings (as great as 1 cm^{-1}) due to the penetrating s-electron of the lower state. The relative intensities of the hyperfine components of λλ4117, 4137 and 4168 have been measured on plates carrying intensity calibration produced by a slit of varying aperture. These measurements favor a value $I=9/2$ for columbium, although values of 7/2 and 11/2 are not definitely excluded. Interval measurements are being carried on, and should fix the value of the spin unambiguously.

26. Investigations of the Polarization and the Spectrum of the Sky Light During the Total Solar Eclipses of August 31, 1932, at Gray, Me., and February 14, 1934, at Losap Islands, in the South Seas. WILLI M. COHN. *Berkeley, California.*—The polarization of a point in the sky was observed at a distance of 8 degrees from the sun at mid-totality. These measurements were carried out by means of polarimeters mounted rigidly. Curves were obtained during the eclipse days and two comparison days each. Both eclipses were observed under clear skies. Whereas the polarization of the 8 degree points shows smooth curves during the comparison days, a considerable increase of the polarization was observed during totality. The plane of polarization changed for all days according to the position of the sun. During totality, however, the plane of polarization was rotated by several degrees from the strictly radial polarization observed otherwise. In 1934, the spectrum of the sky light of the same 8° point was investigated by means of a Hilger grating spectrograph, dispersion 49.4A/mm. Spectra were taken on two backed Agfa Superpan plates before, during, and after the eclipse. Comparison spectra were obtained on two other days. A preliminary measurement of the spectra by means of a recording Zeiss microphotometer reveals that the sky spectrum shortly before totality shows a new maximum extending photographically from 6150 to 5910A. A further maximum seems to appear in the region from λ4700 to λ4610. The spectrum during totality is too faint for accurate measurement, but the new maximum around 6000A appears also faintly in the spectrum taken shortly after totality. These phenomena may be explained only partly by the Tyndall-Rayleigh or a similar law. An explanation is presented based on the assumption that the light of the sky contains two components: Scattered light of the sun, and self-luminescence excited by electron impact of gases in the atmosphere, such as shown in recent experiments of the author (Zeits. f. Physik **75**, 544 (1932)).

27. Improved Technique for Determination of Radon and Radium in Liquids. ROBLEY D. EVANS. *National Research Fellow, University of California.*—Important modifications in the author's method for the removal of radon from liquids (Rev. Sci. Inst. **4**, 216 (1933)), by the use of sample flasks and reflux condensers employing dry ground joints to prevent loss of radon by sorption on small rubber, wax or grease surfaces, are described. The technique is applied to measurements of the radon and radium content of water specimens collected by the Scripps Institution of Oceanography from the Pacific Ocean 13 nautical miles off shore from Point Lomas, California. The radium content is about 3×10^{-17} g Ra per cm^3 of water at the surface, increasing to about 3×10^{-15} g Ra per cm^3 at a depth of 1300 meters. At this depth (bottom) there is also present in the water some 22×10^{-16} curie Rn per cm^3 which represents emanation from the bottom mud, whose radium content of 3.2×10^{-12} g Ra per g is about three times the average content of terrestrial rocks. These data are interpreted as indicating the continuous precipitation of radium in the sea, and support the observations of high radium content in deep sea clays as found by Joly, Pettersson and Piggot. The numerical results here given are preliminary, and indicate the practicability of a general survey of the radioactivity of part of the Pacific Ocean which is now being carried on jointly with the Scripps Institution of Oceanography.

28. Growing and Testing Large Single Crystals of Ice. WILLIAM LEWIS. *University of California at Los Angeles.* (*Introduced by J. M. Adams.*)—Single crystals of ice, of dimensions of the order of 10 cm, have been grown from seed crystals taken from commercial blocks (Barnes, Proc. Roy. Soc. **A125**, 670 (1929)). A method of testing both the seed and the growth has been developed on the basis of the orientation of artificially produced cavities of simple form. Photographic records of these tests have been made.

29. An Ultramicrometer. C. L. UTTERBACK AND HENRY WIRTH. *University of Washington.*—A circuit has been designed which will permit the measurement of changes in pressure of the order of 10^{-3} dyne per square centimeter. The particular feature of the circuit is that a heterodyne frequency is produced between two oscillators which employ tubes of marked Dynatron characteristics. This frequency is amplified and made audible by means of either head phones or a loudspeaker. A beat frequency is produced between the heterodyne frequency and that of an electrically driven fork. The circuit is found to be quite stable with very little change in frequency with change in potential. With a distance of about 0.05 cm between the plates of a condenser, one of which is a liquid surface, a change in the beat note between the fork frequency and the heterodyne frequency of one beat per second is equivalent to a change of $7\cdot10^{-3}$ dyne per square centimeter. Changes in pressure of approximately one-tenth of this amount have been measured.

30. A Variable Frequency Generator for Furnishing Odd Harmonics of 60 Cycle Current of Pure Sinusoidal Form. DAVID L. SOLTAU, DONALD H. LOUGHRIDGE AND LINDSAY M. APPLEGATE. *University of Washington.*—This paper describes the control circuit for synchronizing and filtering

the output of a commercial type motor-generator set by which alternating currents of 180, 300, 420 and 540 cycles are produced and maintained. The synchronizing current is a wave of the proper frequency selected by a resonating circuit from among the harmonics produced in a bank of delta-connected transformers, operating at about 175 percent overload. This wave form is applied to the generator side of the motor-generator set in such a manner as to synchronize the speed of rotation of the generator, thus causing a constant frequency output of the desired number of cycles, which is filtered to produce a practically pure sinusoidal wave form.

31. Crystal Structure of Nickelous Acetate Tetrahydrate. ROBERT B. HULL. (*Introduced by Arthur E. Ruark.*) *University of Pittsburgh.*—Rammelsberg reported the axial ratios $a:b:c=0.7216:1:0.4143$ and the axial angle $\beta=93°\ 25'$ for monoclinic prisms of $Ni(CH_3COO)_2\cdot 4H_2O$. These values have been verified goniometrically. The habit of our crystals was essentially the same as that reported by Rammelsberg. Angle β was verified by Laue photographs. The density is $1.714\pm.001$ g/cm³ at 20°C, and from rotation photographs obtained with a camera of 8.58 cm radius the lattice spacings are $a_0=8.49\pm0.03$A, $b_0=11.77\pm0.05$A and $c_0=4.87\pm0.03$A. The unit cell contains two molecules. The possible space groups are C_s^3, C_2^2, C_{2h}^2, C_{2h}^4 and C_{2h}^5. The external symmetry of the crystals strongly indicates that they belong to the monoclinic prismatic class. If this evidence is trusted, the possible space groups are C_{2h}^3, C_{2h}^4 and C_{2h}^5. The absence of 100 and 010 reflections in odd orders and the presence of 001 reflections in all orders indicates that the nickel atoms probably occupy positions 0, 0, 0 and $a_0/2$, $b_0/2$, 0.

32. On the Development of the Intermolecular and Intramolecular Chains in Oxidation of *n*-Hexan. W. M. ZAIKOWSKY. *California Institute of Technology.*—The data obtained by the gas analysis of the oxidized air-*n*-hexan mixture are discussed in an attempt to establish the relation between the character of the persistence of the oxidation of the same hexan molecule (intramolecular chain) following the interaction with the first molecule of O_2 (or other intermolecular chain carrier) and the fundamental restrictions imposed on the energy transfers by the principle of the conservation of momentum and the loss of energy by the spontaneous radiation. The conclusion is reached that the development of the intramolecular chain is controlled rather by the related physical factors than by the oxidation temperatures of the intermediate chemical compounds.

33. Electronic Functions for a Metallic Crystal. W. V. HOUSTON AND C. B. CRAWLEY. *California Institute of Technology.*—Variation methods have been fruitful in obtaining good approximations for the characteristic functions of atoms with many electrons. A similar method can be applied to crystals. It can be shown that the functions first introduced by Bloch are good approximations to the exact solution, even when the electronic interaction is included, if the proper atomic functions are used in them. These atomic functions can be determined by the variation method. This method has been applied to lithium. The atomic functions were taken as simple $2s$ functions of Slater's type with a single parameter. They were made orthogonal to the $1s$ function by the inclusion of a suitable amount of the $1s$. The best value of the parameter was determined to get the lowest value of the energy. The results show fair agreement with the lattice constant, the lattice energy, and the compressibility.

34. A General Interpretation of Cosmic-Ray Effects. ROBERT A. MILLIKAN. *California Institute of Technology.*—Cosmic-ray researches have apparently established:—(1) That practically all cosmic-ray ionization is due to the passage of electrons (+ and −) rather than protons, alpha-rays or heavier nuclei, through the atmosphere. (2) That more than 70 percent of this ionization, probably 80 or 90 percent, is due to secondary electron-rays produced within the atmosphere by incoming photons and electrons (+ and −). (3) That there is no evidence that anywhere on the earth more than 2 or 3 percent of the ionization found at sea level is due directly to incoming electrons; their number is therefore very small. They are responsible, however, for the latitude effect, the longitude effect and the east-west effect. (4) That photons in general interact only with electrons (+ or −) whether in the nucleus or out of it. A photon colliding with a nucleus detaches one or many free electrons (+ and −) from it but not protons. (5) That the earth's magnetic field separates the low energy incoming secondary electrons formed outside our atmosphere from the high energy, letting the former in near the poles but only the latter near the equator. These latter are predominantly positive since they necessarily come from the nuclei of atoms and these have an excess of *positive* electrons. (6) That the greater part of the ionization of our atmosphere is due to photons of energy of the order of 200 (±70) million electron-volts.

35. Electrons and Positrons. C. H. DIX. *Rice Institute.*—It is shown that there is an essential ambiguity in the Dirac "hole" theory. Either (1) one may have a large finite number of energy levels so that *almost all* the negative levels may be filled and one must regard Dirac's equations as approximate since they give an infinitude of energy levels; *or* (2) one may regard the Dirac equations as exact and reinterpret the negative energy levels. We adopt the second alternative. Instead of a point electron at (x_1, x_2, x_3) we consider a composite electron formed of two point particles "located" at $(x_1+iy_1, x_2+iy_2, x_3+iy_3)$, $(x_1-iy_1, x_2-iy_2, x_3-iy_3)$. All electrons are assumed to be formed of two parts in this manner. The interaction energy of two electrons at relative rest is formed of the four Coulomb energies of the interactions of the four parts. This energy is $V_{1,2}=e^2/4[1/r+1/\bar{r}+1/r_1+1/\bar{r}_1]$ where r, $\bar{r}$ are conjugate. $V_{1,2}$ has an infinite value when the real and imaginary parts of r or r_1 are both zero. Such points of infinite energy lie on mutually perpendicular rings—two singular rings for each electron. $V_{1,2}$ is a double valued function in the sense that if the real coordinates of a "test electron" are carried over a closed path enlacing both singular rings of the electron, producing the field, $V_{1,2}$ changes its algebraic sign at the end of

its path. This is interpreted as the production of a positron. If a closed path of the "test charge" enlaces only one singular ring the terminal mutual energy is very nearly zero. This latter process is interpreted as the formation of "neutrinos." The model of the electron proposed has the following properties: (1) it behaves as a classical electron should in classical fields; (2) it may be used as a basis for the derivation of the Dirac equations; (3) it furnishes a simple, direct picture of the processes involved in the formation of positrons, neutrinos, and the Gray and Tarrant radiation. The author wishes especially to point out the experiments of Skobeltzyn in which a high energy β-particle produced a positron-electron pair.

36. The Passage of Charged Particles through the Magnetic Field and the Atmosphere of the Earth. R. M. LANGER. *California Institute of Technology.*—Convenient and reasonable approximations make it possible to handle analytically the problem of the effect of the earth's magnetic field on charged particles which ionize uniformly along their path. The important parameter is the range in air of a particle of given energy, charge and mass. Given the ionization-altitude curve at some sufficiently northerly latitude an expression can be found in terms of this parameter for the ionization at any altitude in any latitude. If the primary radiation consists of a mixture of two or more types of particles the results are much less useful except in altitude ranges in which one type predominates strongly. The recent experimental results of Millikan and Neher or of Compton and Stephenson in the upper atmosphere are hard to interpret with plausible values of the fundamental energy-range parameter for electrons or protons. Moreover, it does not seem possible to interpret the results as due to a mixture of protons and electrons of various energies. The inclusion of heavier ions or of photons may resolve the difficulty, but the uncertainty of the constants to be associated with these forms of radiation makes it impossible to deal with them satisfactorily in the manner of the present theory.

37. The Production of High Voltage X-Rays for Medical Uses. M. STANLEY LIVINGSTON AND MILTON A. CHAFFEE. *University of California.*—Under the stimulus of Dr. Stone of the Medical School and Professor Lawrence of the Physics Department, and through the interest of Mr. W. H. Crocker of San Francisco a high voltage x-ray machine of the Sloan type has been installed and is now in use for medical treatments. A resonance transformer in the form of a water-cooled coil is mounted in a steel vacuum tank. The x-ray filament is placed opposite a tungsten target on the end of the coil. Radiofrequency power is applied through demountable power-oscillator tubes in a "push-pull" circuit. Lead shielding around the tank and on the walls of the room insures protection for the patients and operators. Four x-ray portals are adjustable for any desired treatment apertures. Lead absorption curves compared with those of Coolidge show peak voltages of 800,000 volts. With about 10 milliamperes emission, intensities as measured in an air ionization chamber of 50, 30 and 20 roentgens per minute are obtainable with lead filtration of 1, 2 and 3 mm, respectively, at 70 cm from the target.

38. Disintegration with the Emission of Protons Induced by Neutrons. FRANZ N. D. KURIE. *National Research Fellow, University of California.*—A type of disintegration caused by neutrons, in which a proton (or some other particle of charge about unity) is emitted instead of the usual alpha-particle, has been photographed several times in the Wilson chamber. The neutrons were generated by bombarding beryllium with 3 MV deutons in the large cyclotron. Sufficient intensity was obtained that 3–5 nuclear recoil tracks of lengths greater than several mm together with roughly a dozen with lengths around 1–2 mm were photographed on each expansion. A disintegration of the type discovered by Feather was observed on about every tenth exposure. The new type of disintegration is characterized by a short heavy spur joined to a thin proton track. In all cases the proton has a range greater than the confines of the chamber. Unfortunately measurements on the usual type of disintegration forks indicate that the neutrons are so badly scattered before they reach the chamber that no quantitative information can be got at present concerning these forks. The chamber contained oxygen predominantly but there was some nitrogen present so that we may imagine either of two reactions occurring: ${}_7N^{14}+{}_0n^1={}_6C^{14}+{}_1H^1$ or ${}_8O^{16}+{}_0n^1={}_7N^{16}+{}_1H^1$. A reaction of this type has been postulated by Fermi to explain the chemical processes necessary to entrain the β-ray activity induced in many elements by neutrons.

39. A Study of the Initial Stages of Spark Breakdown in Gases. H. J. WHITE. *University of California.*—The electro-optical shutter is used to study spark breakdown in nitrogen, hydrogen, oxygen, helium, argon and carbon dioxide at atmospheric pressure and for gap lengths up to 1 cm. Photographs of single sparks in early stages have been obtained for several of these gases, some of the exposures being as short as 5×10^{-9} sec. Four distinct types of breakdown, as characterized by the appearance and growth of the luminous streamers, are recognizable in these gases. The velocities of the cathode streamers in hydrogen and nitrogen have been measured and are found to be about 10^7 cm per sec., which is the order of magnitude of the calculated velocities of electrons in these gases under breakdown conditions. The experiments indicate that the major portion of the current passing during breakdown is carried by electrons, and that these, for the most part, come from the cathode rather than from ionization in the gas. The shortness of the spark lag and breakdown times of sparks show that the phenomenon is essentially due to the motion of electrons, and that the space charges which cause breakdown result from the large difference in the mobility velocities of electrons and positive ions.

40. Continuous Electron Radiation in Flames and Arcs. WOLFGANG FINKELNBURG. *California Institute of Technology.*—In some recent publications we have shown that continuous spectra observed in condensed discharges at

high electron density are due to continuous electron radiation, i.e., radiation of electrons in the field of ions formed in the discharge. In the same way we expect continuous electron radiation in gases, ionized due to high temperature, i.e., in flames and arcs. The few observations published on that subject seem to confirm our expectation. The faint continuous background in the spectrum of the Bunsen flame becomes considerably stronger by introduction of the easily ionizable alkali atoms, the intensity increasing with decreasing ionization potential of the alkali. The same applies for the hydrogen-oxygen flame, all continuous spectra being stronger due to the higher temperature. Though there are in some flames also continuous spectra due to reactions, there exists always a continuous background, the intensity of which increases with increasing temperature and pressure and with decreasing ionization potential of the gas. These properties of the continuous spectrum as well as its independence of lines and bands are exactly what we expect for electron radiation. The same applies for the continuous background in arcs, which in the confined arc at high electron density becomes a strong continuous spectrum.

41. New Members of the Lyman-Birge-Hopfield System. JOSEPH KAPLAN AND LEO D. LEVANAS. *University of California at Los Angeles.*—New members of the Lyman-Birge-Hopfield system of N_2 have been photographed and identified as the bands (5,15), (6,16), (7,17), (8,18), (9,19), (10,20), (11,21), (8,17), (9,18), (10,19), (11,20), (9,20), (10,21) and (11,22). The wave-length measurements, while exact enough to identify these bands, are to be redetermined at higher dispersion, and hence they are not listed here. The band (11,22) is at 2425A, and between this and 2800 there are more bands that are probably members of this system. It was impossible with a Hilger E31 to resolve them sufficiently for identification. Their photography on a higher dispersion should yield data for vibrational levels above $v''=22$. Even with the low dispersion used in this work it was possible to notice a sudden drop in intensity and an increase in diffuseness for the bands originating above $v'=8$ in the $v'-v''=9$ sequence. This suggests predissociation, and since the energy of $v'=8$ is 10.06 volts, it must correspond to dissociation into ^4S and ^2D. This yields a maximum value of 7.7 volts for $D(N_2)$, a value lower than the 7.9 volt value of Lozier and in good agreement with the 7.4 volt value suggested by the recent discovery of the system $A^3\Sigma \rightarrow X'\Sigma$.

42. Interpolation Equation for Photo-Densitometer Charts of X-Ray Diffraction Patterns. WALTER SOLLER. *University of Arizona.*—This paper shows that a simple interpolation equation can be applied to charts produced from diffraction patterns by a photo-densitometer in which a photoelectric cell and a galvanometer are used, and the intensities obtained are of an accuracy comparable with those obtained by ionization chamber methods. The equation was first derived theoretically. Then a graphical method was developed by which the equation could be rapidly applied to the chart. A number of diffraction patterns of NaCl was taken. From these, photo-densitometer charts were made, and the intensities of the first fourteen lines determined by the graphical application of the interpolation equation. These intensities were compared with the calculated intensities from Bearden's theoretical equation.

It was found that these intensities agreed as well with the theoretical values as those determined by ionization chamber methods. These results indicated that this method of obtaining intensities increased the accuracy of ordinary diffraction pattern data, so that they now could be used for structure factor and atomic arrangement determinations, thereby allowing the advantages of applicability to all substances, correct intensities, and simple technique inherent in the powder method to be realized.

43. The Establishment of a Precision High Frequency Standard Capable of Delivering Considerable Power. FRANK G. DUNNINGTON. *California Institute of Technology.*—In the precision determination of e/m being made by a new deflection method (Phys. Rev. **43**, 404 (1933)) a source of high frequency in the region of 3 to 6×10^7 cycles (5 to 10 meters) is necessary. The requirements include: power up to at least 500 watts, peak voltage known to about ½ percent, good frequency stability and frequency known to at least 1 part in 10^6. The means of accomplishing these objectives will be outlined including the obtaining of the government standard of frequency through the use of a broadcast carrier wave as a connecting link between the government standard and the laboratory. Tests indicate that over periods as long as an hour the frequency drift averages about 1 part in 10^7 per minute.

44. The Existence of a Sharp Temperature Threshold for Catalytic Decomposition of Molecules on a Hot Platinum Surface, and the Nature of This Decomposition. OTTO BEECK. *Shell Development Company.*—By using true molecular beams of various hydrocarbons such as ethane, ethylene, etc., projected onto a platinum strip filament 4 mm² area of known and controllable temperature, the decompositions were studied instantaneously by pressure variations in a chamber large compared to the filament as indicated by a Pirani gauge. In the case of ethane, C_2H_6, decomposition set in at about 800°, gradually rose in amount as strip temperature increased yielding dehydrogenation of *all* impinging molecules at 1200°C, in the form of ethylene, C_2H_4 and H_2. This *appears* to represent a reaction proceeding according to Arrhenius' equation with a heat of activation. Ethylene, C_2H_4, shows *no* decomposition below about 830°C but within 20° (i.e., at 850°) *every molecule impinging on the surface is dehydrogenated* yielding C_2H_2 and H_2. In this case both H_2 and C_2H_2 fly off the surface after dissociation with no lingering. Below 1200° the H_2 gas produced by decomposition would be sufficient to produce an equilibrium layer partially covering the surface. In C_2H_4 about one percent of the C_2H_4 molecules incident go to remove this layer giving C_2H_2 and leaving a clean Pt surface to dehydrogenate the C_2H_4. In the case of C_2H_6 the H_2 is not removed and the partial H_2 covering reduces the efficiency of the surface. As the temperature increases up to 1200° the covering is progres-

sively removed from the surface and dissociation of impacting molecules is more complete. Control experiments with outgassing and using O_2 confirm these interpretations.

45. Terminal Energy Distribution of Electrons Driven through a Gas by an Electric Field. A. M. CRAVATH. *University of California.*—Didlaukis (Zeits. f. Physik **82**, 709 (1933)) found that the energy distribution was less than 1/20 as wide as Maxwell's unless the free path increased rapidly with speed. Didlaukis' term $D+E$ should have contained the *mean square* of the component of velocity in the direction of the field instead of the *square of the mean* component. With this correction a number of distributions have been calculated. Let $W\,dE$ = fraction of electrons having energy E in dE, and fE = energy lost in a collision. If $f=0$ when $E<E_r$, and $f=1$ when $E>E_r$, $W=2.25E_r^{-3/2}E^{1/2}\ln(E_r/E)$ and $\overline{E}$, the average energy, is $(9/25)E_r$. If $|f|\ll 1$ for all collisions (not merely for the average) and $\overline{E}\gg$average energy of molecules, $W=a\,E^{1/2}\exp(-3X^{-2}e^{-2}\int q^2(1-P)fE\,dE)$, a = a constant, X = field, q = collisions per cm, P = average cosine of angle of scattering, all for electrons of energy E. If $q^2(1-P)f=q_0^2f_0E^h$, $q_0^2f_0$ being constant, $W=aE^{1/2}\exp(-3q_0^2f_0E^{2h+2}(2h+2)^{-1}X^{-2}e^{-2})$. Unless $h>-1$ there is no terminal state. If mean free path is proportional to velocity, and P and f are constant, $h=-\frac{1}{2}$ and the distribution is Maxwellian. If mean free path, P, and f are all constant, $h=0$ and $W=1.038\overline{E}^{-3/2}E^{1/2}\exp(-0.547(E/\overline{E})^2)$, $\overline{E}=0.604Xeq^{-1}(1-P)^{-1/2}f^{-1/2}$. For elastic spheres $P=0$, $f=2m/M$, and the above becomes Druyvesteyn's distribution (Physica **10**, 61 (1930)).

AUTHOR INDEX TO ABSTRACTS OF THE BERKELEY MEETING

Anderson, Carl D. and Seth H. Neddermeyer—No. 14
Anderson, O. E.—No. 16
Applegate, Lindsay M.—see Soltau

Ballard, Stanley S.—No. 25
Beeck, Otto—No. 44

Chaffee, Milton A.—see Livingston
Cohn, Willi M.—No. 26
Cravath, Austin M.—Nos. 2, 45
Crawley, C. B.—see Houston

Dahlstrom, R. K. and Jos. E. Henderson—No. 6
Dix, C. H.—No. 35
Dunham, Theodore, Jr.—No. 18
Dunnington, Frank G.—No. 43

Evans, Robley D.—Nos. 7, 27

Finkelnburg, Wolfgang—Nos. 19, 40

Henderson, Jos. E.—see Dahlstrom
Henderson, M. C.—No. 9
—— see Lawrence
—— see Livingston
Houston, W. V. and C. B. Crawley—No. 33
Hull, Robert B.—No. 31

Jenkins, F. A.—see Nolan

Kaplan, Joseph—No. 20
—— **and Leo D. Levanas**—No. 41
King, Robert B.—No. 21
Kinsey, B. B.—see Thornton
Kurie, Franz N. D.—Nos. 10, 38

Langer, R. M.—No. 36
Lawrence, E. O.—see Livingston
——, **M. C. Henderson and M. S. Livingston**—No. 11
Levanas, Leo D.—see Kaplan
Lewis, William—No. 28
Linford, Leo H.—No. 13
Livingston, M. Stanley—see Lawrence
—— **and Milton A. Chaffee**—No. 37
—— **M. C. Henderson and E. O. Lawrence**—No. 12
Loeb, Leonard B.—No. 4
Loughridge, Donald H.—see Soltau
—— **and Harold C. Trueblood**—No. 3

McMillan, Edwin—No. 15
Millikan, Robert A.—No. 34
More, Kenneth R.—No. 24

Neddermeyer, Seth H.—see Anderson
Nolan, Philip and F. A. Jenkins—No. 22

Soller, Walter—No. 42
Soltau, David L., Donald H. Loughridge and Lindsay M. Applegate—No. 30
Strong, John—No. 17

Tate, John T.—see Vaughan
Thornton, R. L. and B. B. Kinsey—No. 8
Trueblood, Harold C.—see Loughridge

Utterback, C. L. and Henry Wirth—No. 29

Varney, Robert N.—No. 1
Vaughan, Alfred L., John H. Williams and John T. Tate—No. 23

White, H. J.—Nos. 5, 39
Williams, John H.—see Vaughan
Wirth, Henry—see Utterback

Zaikowsky, W. M.—No. 32

Proceedings of the American Physical Society

MINUTES OF THE ANN ARBOR MEETING, JUNE 28–30, 1934

THE 193rd regular meeting of the American Physical Society was held at Ann Arbor, Michigan by invitation of the Physics Department of the University of Michigan on Thursday, Friday and Saturday, June 28, 29 and 30, 1934. The headquarters for the meeting were in the Mosher-Jordan Dormitory. The presiding officers were Professor Arthur H. Compton, President of the Society, and Professors Robert S. Mulliken and N. H. Williams. The attendance at the sessions was about two hundred and fifty.

The meetings on the first day were held in Dearborn, Michigan. The morning was occupied by a visit through the Greenfield Village Museums. After luncheon at the Dearborn Inn there was a lecture by C. E. Johansson of the Ford Motor Company on *Precision Gauges*. After the lecture the members of the Society were taken to the Ford plant at River Rouge for a trip through the plant.

The scientific sessions on Friday and Saturday were held in Hutchins Hall at the University of Michigan. These lecture rooms were extraordinary both in the beauty of their appointments and in the fact that they were air-conditioned. The Friday morning program consisted of three parallel sessions of contributed papers. Friday afternoon there was a lecture by Professor George Gamow of the Polytechnical Institute, Leningrad, Russia, on *The General Nuclear Problem*. Saturday morning there was a symposium on *Nuclear Moment*. The invited papers were as follows: *Theory of the Effect of a Nuclear Moment on the State of the Atom* by G. Breit of New York University; *Measurement of Nuclear Spin and Statistics by Means of Band Spectra* by Robert S. Mulliken of the University of Chicago; *Survey of Experimental Hyperfine Structure Material. Values of Nuclear Magnetic Moments and a Discussion of Their Origin* by Robert F. Bacher of the University of Michigan; *Measurement of Nuclear Spin and Moments by Method of Molecular Beams* by I. I. Rabi of Columbia University; *Measurement of Nuclear Moments and Spin Through the Polarization of Resonance Radiation* by Alexander Ellett of the State University of Iowa.

On Friday evening one hundred and forty-three attended the Society dinner in the dining room at the Michigan League. After the dinner the Michigan Repertory Players presented the play *A Hundred Years Old* in the Lydia Mendelssohn Theatre which is also in the Michigan League Building.

Saturday afternoon was devoted to a picnic at one of the nearby lakes.

At the close of the last session the Society voted unanimously to extend its thanks to the local committee and to the University of Michigan for the splendid arrangements they had made for the comfort of all in attendance.

Meeting of the Council. At its meeting on Friday, June 29, 1934, the Council transferred one candidate from membership to fellowship and elected twenty-two candidates to membership. *Transferred from Membership to Fellowship:* Lloyd P. Smith. *Elected to Membership:* Sister M. Ambrosia, Harold F. Bennett, Robert M. Bowie, James J. Brady, Stephen A. Buckingham, William W. Buechner, Victor H. Fraenckel, Joseph Giarratana, Caryl P. Haskins, Rudolf C. Hergenrother, Tosihiko Kubo, David S. Muzzey, Jr., L. S. Palmer, H. Parodi, Sidney K. Shear, Shunji Shirai, E. Francis Steates, William E. Stephens, Frank A. Valente, H. K. Ward, Archie J. Weith and Herbert E. White.

The regular scientific program consisted of

forty-five papers, of which numbers 27 and 45 were read by title. Paper number 33 was withdrawn from the program and from the Proceedings at the request of the author. The abstracts of the contributed papers are given in the following pages. An *Author Index* will be found at the end.

W. L. SEVERINGHAUS, *Secretary*

ABSTRACTS

1. A Coincidence Test of the Corpuscular Hypothesis of Cosmic Rays. D. S. HSIUNG, *University of Chicago. (Introduced by A. H. Compton.)*—Three Geiger-Müller counters were arranged vertically so that double coincidences were recorded by counters 1 and 2 and triple coincidences by counters 1, 2 and 3 simultaneously. The third counter was permanently shielded by a lead cylinder of 2.5 cm thickness, which is sufficient to absorb the secondaries produced in the absorber. Counts were made under three conditions:

	Double($hr.^{-1}$)	Triple($hr.^{-1}$)
(*A*) Without lead	202.44±1.84	42.43±0.83
(*B*) With 20 cm of lead between counters 1 and 2	124.48±1.43	30.50±0.50
(*C*) With 20 cm of lead above counter 1	142.17±1.08	32.55±0.52

The data can be interpreted by assuming that the coincidences are due chiefly to penetrating ionizing particles, some of which are stopped by the lead (for which *B* should equal *C*), with the addition of a few coincidences in case *C* due to secondaries. It does not appear possible to account for these coincidences in terms of corpuscles excited by photons unless the photons either are completely absorbed by the atmosphere before reaching the apparatus, or are accompanied throughout their path by ionizing particles, which would practically mean treating the photons as ionizing particles.

2. Is the Neutron an Elementary Particle? ALFRED LANDÉ, *Ohio State University.*—The sum of the masses proton+electron = 1.0072+0.00055 = 1.00778 is larger than the neutron mass 1.0068 of Chadwick and Ladenburg, but smaller than the neutron mass 1.010 of Curie-Joliot. If the latter value is correct, it would be difficult to think of a neutron as a stable compound of a proton and an electron. However the interpretation of magnetic moments of higher nuclei containing an odd number of neutrons shows that the neutron has a magnetic moment of about −0.6 nuclear magnetons. The existence of a magnetic moment without a resultant charge seems to indicate that this charge zero is composed of a negative and a positive part. The negative sign of the magnetic moment means then, that the negative charge is bound to a lighter share and the positive charge to a heavier share of the mass of the neutron.

3. Magnetic Dipole Radiation and the Atmospheric Absorption Bands of Oxygen. J. H. VAN VLECK, *University of Wisconsin.*—On the basis of configuration theory, it is much more reasonable that the upper state of the $^3\Sigma_g^- - {}^1\Sigma$ atmospheric absorption bands be $^1\Sigma_g^+$ than $^1\Sigma_u^-$. With such an assignment, these bands are usually ascribed to quadrupole radiation, as $g-g$ transitions are forbidden in ordinary electric dipole radiation. The quadrupole formulas of Rubinowicz, however, yield an incorrect rotational intensity structure, as they predict transitions by two units in J, etc. On the other hand, Schlapp's intensity calculations (Phys. Rev. **39**, 806 (1932)) agreed with experiment, but assumed dipole transitions, and so apparently presupposed a $^1\Sigma_u^-$ upper state. A solution of this dilemma is obtained by interpreting the atmospheric bands as magnetic dipole radiation, of the general type treated by Brinkmann, Stevenson and Condon. The upper state is then $^1\Sigma_g^+$, and still the relative intensities are those calculated by Schlapp. The Rubinowicz quadrupole radiation would also be present, but its comparative faintness explains why double transitions in J have escaped observation. The observed absolute intensities are much greater than to be expected for Rubinowicz quadrupoles, much less than for ordinary dipoles, but of about the right order for magnetic dipoles. Details will be given in a paper to be submitted to the *Astrophysical Journal*.

4. The Four Vector Problem and Intensities in Platinum-Like Spectra. A. T. GOBLE, *University of Wisconsin.*—In a previous paper (Phys. Rev. **42**, 909 (Abstract 33) (1932)) the theories of Johnson and of Shortley (ibid. **38**, 1628 (1931); **40**, 185 (1932)) were applied to the $5d^96p$ configuration of Pb V and Bi VI. The calculations are inclusive of spin-orbit interaction, which is not small compared to the electrostatic. With a few modifications in the method of computation, the same work has been applied to the classification of all the isoelectronic sequence Pt I, Au II, Hg III, Tl IV, Pb V, and Bi VI. The agreement between theory and experiment is satisfactory in all cases except Pt I where the $5d^96s6p$ configuration perturbs the one studied. The Houston problem was also solved for the $5d^96s$ configuration for each of the elements. These results make it possible to compute the transformation matrices to go from the jj system of representation to the actual one. Thus one can compute the transition probabilities for $5d^96s-5d^96p$ in intermediate coupling. From these one can predict the relative intensities of the spectral lines. The results are in as good agreement with experiment as one can expect considering the method of excitation used and the method of estimating the observed intensities.

5. Spectral Multiplets Arising from Configurations of the Type $d^k msns$ and $d^k ms$. ($k=1\cdots9$.) ROBERT A. MERRILL, *University of Wisconsin.*—The application of Dirac's vector model to complex spectra has been considered by J. H. Van Vleck (Phys. Rev. **45**, 405 (1934)). By means

of this model and Johnson's formulae for the four vector problem (Phys. Rev. 38, 1628 (1931)) the energy values of configurations of the type $d^k msns$ may be calculated if the d^k multiplets conform to Russell-Saunders coupling. The spin-orbit energy is *not* assumed small compared to the electrostatic energy coupling d^k to ms and ns. The following multiplets have been considered: Cu I, $3d^9(^2D)4s5s$; Yt I, $4d(^2D)5s6s$; Ni I, $3d^8(^3F)4s5s$; Zr I, $4d^2(^3F)5s6s$; Co I, $3d^7(^4F)4s5s$; Fe I, $3d^6(^5D)4s5s$; Ti I, $3d^3(^4F)4s6s$. The agreement with experiment is better with the four vector problem (L_d, S_d, s_m, s_n) than with the three vector problem (L_d, S_{d+m}, s_n) both of which have been applied. The Landé interval constant is chosen whenever possible from the ion (d^k configuration) and the exchange integrals are determined from experimental data. Consistent values are obtained for these integrals as they turn out to vary but slightly among adjacent ions. Configurations with an s electron added to an ion with Russell-Saunders coupling (other than Houston's singlet-triplet case) have also been examined as a three vector problem. Some examples treated are: Ti II, $3d^3(^2F)5s$; Fe I, $3d^7(^4F)5s$; Co I, $3d^8(^3F)4s$, $3d^8(^3F)5s$; Co II, $3d^7(^4F)5s$; Ni II, $3d^8(^3F)5s$.

6. Energy Levels for a Potential Function Having Symmetrical Double Minima and Applications to the NH_3 and ND_3 Molecules. MILLARD F. MANNING, *Massachusetts Institute of Technology*.—Exact solutions for the Schrödinger equation can be found when the potential energy is given by the expression

$$V=\frac{1}{k\rho^2}\left[-C\,\mathrm{sech}^2\frac{r}{2\rho}+D\,\mathrm{sech}^4\frac{r}{2\rho}+\mu^2\,\mathrm{sech}^6\frac{r}{2\rho}\right],$$

where $k=8\pi^2m/h^2$, r is the coordinate, and C, D, ρ and μ are arbitrary constants. For certain ranges of the constants the eight lowest energy levels have been found by numerical solution of continued fractions. Values of the constants have been found which give reasonable agreement with the experimental data for NH_3 and ND_3.

7. The Energies of Some Hydrocarbon Molecules. ROBERT SERBER, *University of Wisconsin*.—The energies of a number of hydrocarbon molecules have been calculated by the Heitler-London-Pauling-Slater method with two objects in view, first, to see if simple electron pair bonding leads to the correct heats of formation, and second, to determine what significance can be attached to the empirical additivity rule for bond energies. In calculating the energies it is not necessary to know the individual carbon-carbon exchange integrals, other than C_{rrrr}, since fortunately these integrals appear in the same linear combination in all the molecules considered except acetylene. For acetylene we have used values of the exchange integrals kindly supplied the writer by Dr. W. G. Penney. Simple electron bonding has been used for $\sigma-\sigma$ bonds and for single $\pi-\pi$ bonds. However, for the multiple $\pi-\pi$ bonds in acetylene and benzene it has been found necessary to employ more accurate methods. The $C-C$ gross bonding energy has been fixed from the observed energy of ethane, and C_{rrrr}, which then determines the energy of the $C=C$ bond, has been chosen to fit the observed energy difference between ethane and ethylene. In this way we find the suspiciously large value $C_{rrrr}=3.26$ v. The calculated energies are given in the following table.

		Obs.	*Calc.*
Ethane	C_2H_6	29.6 v	29.6 v
Propane	C_3H_8	41.9	41.9
Butane	C_4H_{10}	54.1	54.0
Ethylene	C_2H_4	23.8	23.8
Propylene	C_3H_6	36.1	36.0
Acetylene	C_2H_2	17.3	17.6
Benzene	C_6H_6	58.2	58.5

The validity of an exact additivity rule for bond energies seems to be purely fortuitous.

8. Zeeman Effect of the Spectra of Arsenic. W. M. BARROWS AND J. B. GREEN, *Ohio State University*.—The spectra of arsenic have been studied in magnetic fields of about 36,000 gauss. The classifications of As I, As II and As III by Meggers, Rao and Lang, respectively, have been found to be in general agreement with the observed Zeeman effects. g-values have been calculated for As I and As II, with the results of Slater, of Houston, of Johnson and of Inglis for the electrostatic and spin-orbit coupling energy and although, in some cases, the configurations are not far from LS coupling, the g-values thus found are in very satisfactory agreement with the observations.

9. The Paschen-Back Effect. II. *jj*-coupling. J. B. GREEN AND R. A. LORING, *Ohio State University*.—The $6s\,6d$ configuration of Hg I is very close to jj-coupling, the $^3D_1$ and $^1D_2$ terms being separated by only 3 cm^{-1}, and affords an excellent test of Houston's results for this type of interaction. Four pairs of lines, λλ5790, 3663, 3131, 2967, were studied, with fields of about 36,000 gauss, and down to about 10,000 gauss. Houston's calculations have been extended to include Paschen-Back effect in addition to the simple Zeeman effect, both for position and intensity of the components. The experiment is in excellent agreement with the calculated values and furnishes some very interesting patterns which would be difficult to interpret without the aid of the theory. For example, λ5789 $^1P_1-{}^3D_1$ appears as only one side of a Zeeman pattern with an ordinarily "forbidden" component comparable in intensity to the "permitted" lines.

10. $^3S_1$ and $^3D_{3,2,1}$ Terms in Mercury. I. WALERSTEIN, *Purdue University*.—Wave-length measurements of the higher terms in the triplet sharp and diffuse series of the mercury arc spectrum were made in order to determine whether these terms follow exactly a Ritz equation. This question was raised by Shenstone and Russel (Phys. Rev. 39, 416 (1932)) in their study of perturbed series. A beam of excited mercury vapor which was allowed to diffuse from a mercury arc into a high vacuum chamber was photographed and the $2^3P_2-m^3S_1$ series was measured to $m=20$. Copper introduced into the mercury gave a sufficient number of lines in the beam of mercury vapor to make accurate measurements of the wave-lengths possible. (Iron used in a similar manner gave a fully developed spectrum in the mercury arc, but was completely absent in the vapor beam.) The terms obtained from the $2^3P_{2,1,0}-m^3S_1$ lines for the $^3S_1$ levels were found

to obey correctly a Ritz formula. Similarly the $^3D_2$ terms were developed to $m=26$ and found to follow a similar law. The $^3D_2$ terms were also measured to $m=23$, and the $^3D_1$ terms to $m=19$.

11. Action Cross Section in Collisions of the Second Kind. O. S. DUFFENDACK AND J. H. MANLEY, *University of Michigan.*—The relative intensities of a group of lines in the spectrum of Mg II as excited by a low voltage arc in a mixture of magnesium vapor and neon have been measured at various pressures of neon. Marked effect due to collisions of the second kind between magnesium atoms and neon ions or metastable atoms is found. The ratio of intensities at 2.0 and at 0.017 mm neon was taken as a measure of the enhancement or the relative collision section for the excitation of a level by these resonant effects. In cases of close resonance the results indicate a cross section of some 600 (six hundred) times that for electronic excitation but a finite section for exact resonance. Dependence of cross section on series as well as energy-discrepancy is shown by an excitation preference of terms in the order *f–s–d*, at a given energy discrepancy.

12. Ionization Potentials in the Isoelectronic Sequence A I to Mn VIII. P. GERALD KRUGER AND S. G. WEISSBERG, *University of Illinois.*—The only two lines which connect the $3p^54_s$ terms and the $3p^6\,{}^1S_0$ term of ions like Ti V, V VI, Cr VII and Mn VIII are $3p^54_s\,{}^1P_1$, $^3P_1$ to $3p^6\,{}^1S_0$. Lines corresponding to these radiations have been observed with a twenty-one foot grazing incidence vacuum spectrograph for all of the above ions. This permits a calculation of the term value of the $^1S_0$ terms and the ionization potentials. Table I gives these values with the first and second differences between the ionization potentials.

TABLE I.

Ion	$3p^6\,{}^1S_0$ in cm^{-1}	Ionization potential in volts	First difference	Second difference
A I	127,104	15.679		
			16.0	
K II	256,637	31.66		3.3
			19.3	
Ca III	413,127	50.96		4.0
			23.3	
Sc IV	(602,000)	(74.3)		4.0
			27.3	
Ti V	824,000	101.6		3.8
			31.1	
V VI	1,076,000	132.7		3.8
			34.9	
Cr VII	1,359,000	167.6		3.8
			38.7	
Mn VIII	1,672,000	206.3		

13. Fluorescence and Photodecomposition in Solutions of Chlorophyll *a*. V. M. ALBERS AND H. V. KNORR, *Kettering Foundation, Antioch College.*—The fluorescence spectrum of chlorophyll *a* in solution in anhydrous acetone, benzene and methanol has been photographed by a method previously described (H. V. Knorr and V. M. Albers, Phys. Rev. **43**, 379 (1933)). The solutions were exposed continuously to the radiation from four, 150 watt, Pyrex mercury arcs. The spectrograms were obtained by making a five minute exposure during each fifteen minute interval. Densitometer curves obtained from the spectrograms indicate that the fluorescence bands are not simple broad bands but are complex. The apparent shift previously observed in the positions of the bands can be attributed to a change in relative intensities of the individual bands and to the appearance of new fluorescence bands due to new compounds formed photochemically.

14. Fluorescence and Photodecomposition in Solutions of Chlorophyll *b*. H. V. KNORR AND V. M. ALBERS, *Kettering Foundation, Antioch College.*—The fluorescence spectrum of chlorophyll *b* in solution in anhydrous acetone, benzene and methanol has been photographed by a method previously described (H. V. Knorr and V. M. Albers, Phys. Rev. **43**, 379 (1933)). The solutions of chlorophyll *b* were treated in the same manner as those of chlorophyll *a* described in the preceding abstract. The densitometer curves made from these spectrograms show more pronounced maxima than those for chlorophyll *a* and as photodecomposition proceeds these individual maxima remain at very nearly the same wave-length while their relative intensities vary considerably. Results with chlorophyll *b* indicate more definitely, than those with chlorophyll *a*, that the apparent shift in the position of the fluorescence band is due to variation in relative intensities of the individual band components.

15. Optical Constants and the Conduction Electrons of Beryllium and Silicon. H. M. O'BRYAN, *Massachusetts Institute of Technology.*—The optical constants of beryllium as measured by the phase shift of reflected light show an abrupt increase in the strength of absorption ($n^2K\nu$) at 5000A (2.5 volts) which coincides with the minimum of reflection found by Coblentz and Stair. The increasing reflecting power and constant value of the strength of absorption toward the infrared indicates the presence of empty levels very little above those filled with conduction electrons, to which transitions are possible through collisions with the lattice. Both the optical constants and the soft x-ray emission give much greater transition probabilities for electrons more than 2.5 volts below the surface of the Fermi-Dirac distribution of conduction electrons. Silicon and germanium show a more gradual increase in the strength of absorption from 1.5μ where both are almost transparent. The strength of absorption computed from the measurements of Pfesdorf on silicon shows a decrease at 5 volts making the width of the absorption band less than four volts, while the minimum width expected from soft x-ray emission is about 7 volts. This band has a total strength of one half electron per atom and silicon has two M_{II} electrons per atom.

16. Infrared Absorption Bands of Heavy Water Vapor. W. W. SLEATOR AND E. F. BARKER, *University of Michigan.*—The infrared spectrum of water vapor in which both hydrogen atoms have been replaced by deuterium has been examined under high dispersion. As in the case of ordinary water vapor, two fundamental bands are observed, corresponding to ν_1 and ν_2, the former but not the latter

having a zero branch. The band associated with the symmetrical vibration ν_1 is probably weak, and has not been identified. The positions of the observed band centers are approximately

	ν_2	ν_3
heavy water:	1179 (8.48μ)	2784 (3.59μ)
ordinary water:	1596 (6.26μ)	3742 (2.67μ)

The wave number differences between the first line in the positive branch and the first line in the negative branch of ν_2 are 22.7 for the heavy molecule and 30.3 for the lighter one. Differences in relative intensities of the lines indicate the change in statistics when deutons replace protons in the molecule. An exact correspondence between lines in the bands ν_3 for the two varieties of water is difficult to establish, but the envelopes observed when the resolution is not too high are very similar in appearance. The maxima of the positive and negative branches are separated by about 115 cm^{-1} for the heavy molecule and 200 cm^{-1} for ordinary water.

17. Curved-Crystal X-Ray Spectrograph and Demountable Secondary-Radiation Tube for Analytical Work. RICHARD L. DOAN, *University of Chicago.*—A spectrograph has been built utilizing the focussing property of a curved crystal (mica or gypsum) first proposed by Guoy in 1916 and recently applied successfully by Cauchois. The crystal is bent to a radius of curvature of 50 cm and is clamped tangentially to a circle of 25 cm radius along which the line radiation is focussed after transmission through the crystal. The instrument can be evacuated for the longer wave-lengths. A dispersion of 10 X.U. per mm can easily be obtained and resolution is high since the lines are sharply focussed. As a generating source of both primary and secondary radiation for use in connection with the above spectrograph a demountable single-end tube of a general type developed by Dershem is employed. The fluorescing element is the surface of a slotted cap fitting over the filament and paralleling the target surface at a distance of a few millimeters. The arrangement is such that the primary and secondary radiation come out opposite sides of the tube through windows covered with beryllium foil. For compactness the filament lead is sealed close to the filament and brought out through a water path for cooling.

18. A Proposed High Resolving Power X-Ray Grating Spectrometer. ELMER DERSHEM, *University of Chicago.*—Grating measurements of x-ray spectra at present lack the desired precision principally due to the following causes. The beam is collimated for plane gratings by slits. This limits the number of useful rulings. Also the very high theoretical resolving power for inside orders cannot be utilized due to increased angular width of the diffracted beam caused by lack of parallelism of the incident rays. Concave gratings are imperfect at small glancing angles of incidence and also the diffracted rays are nearly parallel to the photographic plate. It appears possible to achieve a very greatly increased resolving power by using a section of a parabolic glass or speculum metal mirror. This section to be so chosen that x-rays diverging from a slit fall upon the mirror at a small glancing angle and are reflected in parallel rays to a plane grating. The diffracted beam is then brought to a focus by a second parabolic mirror. Calculations from data concerning the reflecting powers of various mirrors indicate that the theoretical resolving power should be 100 to 10,000 times that attainable with a plane grating used with collimating slits. Construction of such an instrument is being planned.

19. A Simple Method for Demonstrating and Measuring Approximately the Index of Refraction of X-Rays. H. C. HOYT AND GEO. A. LINDSAY, *University of Michigan.*—A spectrum line may be formed by reflection at the surface of a crystal even if that surface is not parallel to the atomic planes concerned in the reflection. If the faces are good very close to the line of their intersection, then, with a slit that is not too narrow, the same line may be reflected simultaneously from the two faces of a stationary crystal, by turning it so that for the proper reflecting angle the rays must fall at the intersection. If the wave-length of the line is such that the reflected beam from the beveled face emerges from that face at nearly grazing incidence then that portion will be refracted much more than the portion of the line reflected from the other face, and the two parts of the line are plainly separated. A very simple calculation gives the index of refraction from the width included between the two portions of the line. In this way (δ/λ^2) for a cerussite crystal has been found to agree fairly well with the calculated value.

20. Factors Causing Deviations in X-Ray Ionization Measurements. ROY C. SPENCER, *University of Nebraska.*—The following pertains to new equipment recently installed. (1) *Fluctuations in voltage.* Reduced by using a synchronous motor generator. (2) *Slow changes in filament current of the x-ray tube.* Filament operated from storage batteries floated across the field supply of the generator. (3) *α-Particles*—Reduced by methods described by Bearden. (4) *Statistical fluctuations in the number of quanta received.* Statistical theory shows that for N quanta the standard deviation is $N^{\frac{1}{2}}$. If, as in the photoelectric effect, one quantum produces one electron, then $QP^2 = 1.59 \times 10^{-38}$ where Q is the charge in coulombs and P is its standard deviation in percent. For x-ray ionization in air (assuming Kulenkampff's value of 35 volts per ion pair between 0.56 and 2A) one quantum of 1A wave-length will produce 352 pairs of ions. The corresponding equation becomes $\lambda QP^2 = 5.6 \times 10^{-33}$ where λ is the wave-length in A. The sensitivity of the FP-54 circuit must, therefore, be reduced for use with x-rays. Weak currents may be best studied by allowing the system to charge up for a long time, the sensitivity being reduced by adding capacity and decreasing the galvanometer sensitivity.

21. X-Ray Investigation of Lattice Recovery of Metals After Cold-Working. J. E. WILSON AND L. THOMASSEN, *Department of Chemical Engineering, University of Michigan.*—Copper, nickel, iron and a number of alloys have been studied to find the time-temperature relationship of

x-ray line sharpening on annealing. The line broadness of nickel was investigated as a function of annealing time at a constant temperature. After an initial drop, the broadness is constant for a certain time, then decreases to its original value. For constant annealing time, individual metals vary widely both in temperature of initial line sharpening and in temperature range of the complete recovery process. For completion of the second stage of line sharpening, an expression $T=K_1/(\log t+K_2)$ is found, where T is annealing temperature in °abs., t is annealing time in seconds, and K_1 and K_2 are characteristic constants of the metal. Results have been correlated with hardness measurements and available data on electric and magnetic recovery from cold work. These stages of recovery and recrystallization have been interpreted on basis of reformation of undisturbed outer electron shells and differences in rates of diffusion of atoms.

22. Magnetic Susceptibilities of Powdered Crystals. R. B. JANES, *University of Wisconsin. (Introduced by C. E. Mendenhall.)*—The magnetic susceptibility of a number of powdered salts has been measured by the Gouy method over the temperature range 20 to −192°C. The work done falls into two divisions. The first is the measurement of the susceptibility of several palladium salts. All of these are diamagnetic, thus diverging from the theory which holds for the iron group. The second part of the work correlates the magnetic susceptibility and the color of salts of the iron group. From their constitution most of these salts should have the same sort of crystalline fields as assumed by Van Vleck for the hydrates of these metals, and which in the case of the hydrates leads to good agreement between theory and experiment. In the work done, when the color of the salt investigated is nearly the same as that of the hydrates the susceptibility is also nearly the same. This is not true if the color is different. Many salts were also investigated which had the color of the hydrates at the higher temperatures but different colors at lower temperatures. The susceptibility at the higher temperatures was in this case also like the hydrates but it was different at the lower temperatures.

23. The Crystal Structure of Lithium Sulphate Monohydrate. G. E. ZIEGLER, *University of Chicago.*—The crystal structure of $Li_2SO_4\cdot H_2O$ was investigated because the atomic numbers are favorable for determining the rôle of H_2O in the structure. The oxygen of the H_2O was found located at one corner of a tetrahedron of oxygen surrounding one of the lithium atoms. Since x-ray data can give no information regarding hydrogen, the hydrogen is located by a consideration of the structure surrounding the oxygen of the H_2O. The position selected as being most probable resulted in an angle of 108° for H−O−H. $Li_2SO_4\cdot H_2O$ is monoclinic with a unit cell $a=5.43$A, $b=4.84$A, $c=8.14$A, and contains 2 molecules. The space group assigned, C_2^3 contains only twofold general positions, x, y, z; $\bar{x}, y+\frac{1}{2}, \bar{z}$, which necessitated the determination of the following 23 parameters. $\beta=107°\ 35'$:

	x	y	z	x	y	z
S	75°	0°	−76°	1.13A	0.00A	−1.72A
O_1	55	−50	−30	0.83	−0.67	−0.68
O_2	180	−10	−69	2.71	−0.13	−1.56
O_3	28	−28	−143	0.42	−0.37	−3.23
O_4	58	110	−71	0.87	1.47	−1.60
O_5	205	170	−139	3.09	2.28	−3.14
Li_1	−25	195	−139	−0.38	2.61	−3.14
Li_2	60	172	+1	0.90	2.31	+0.02

Sulphur and the two lithium atoms are each surrounded by tetrahedra of oxygen with the following average distances: S to O=1.49A, O to O in SO_4 tetrahedron =2.43, Li to O=1.99, O to O in Li tetrahedra=3.20. The shortest O to O distance between oxygens of different SO_4 groups is 2.85. The LiO_4 tetrahedra share corners but not edges or faces.

24. Spectroscopic Study of Restriking Phenomena in the a.c. Copper Arc. W. S. HUXFORD AND OLAV MASENG, *Northwestern University.*—The spectrum at various phases of an alternating-current copper arc in air has been investigated with particular reference to restriking phenomena. Currents from 17 to 27 amperes were supplied by a 15 kva 550 volt transformer. The arc circuit contained an air core coil with a maximum inductance of 0.06 of a henry. Light from the arc was passed through a narrow slit in a disk driven by a synchronous motor which limited the exposures to approximately one degree of cycle. No marked changes in relative line intensities were noted except near and during the "current zero" phase of the arc. The spectrograms show positive and negative bands of nitrogen appearing at the surface of the incoming cathode. These bands persist over a period of the cycle which coincides precisely with that of the "glow" state as revealed by current-potential plots. The period during which the glow discharge persisted at one of the electrodes could be varied, and with an arc 3 cm long periods up to 30° of cycle were obtained. The results indicate that the enveloping gas plays an important part in the restriking of a metal arc.

25. The Initiation of Discharges in Ion Free Gases. J. W. FLOWERS AND J. W. BEAMS, *University of Virginia.*—A study has been made of the breakdown of highly overvolted spark gaps (see Street and Beams, Phys. Rev. **38**, 416 (1931)). The gas surrounding the spark gap was carefully dried and filtered. Ions in the gap were removed by auxiliary electrical fields. The potential across the gap in each case was applied for the order of magnitude of 10^{-6} sec. With spherical brass electrodes fields of roughly 5×10^5 volts per cm were required to start the discharge in hydrogen, nitrogen, helium or air. With a wire (tungsten or platinum) and a cylinder (steel) for electrodes the field at the wire necessary to produce breakdown was independent of pressure over the range from 35 cm to 76 cm of Hg. Also it only varied by a few percent with nitrogen, hydrogen or helium in the gap. The field necessary to produce breakdown with the wire electrode negative (about 5×10^5 volts per cm for platinum) was roughly 20 percent less than with the wire positive. Results similar to the above were obtained with point and plane electrodes. It is believed that in cases where the wire or point was negative the discharge was initiated by electrons arising from field emission from the cathode. The fall of potential, during

breakdown, across these effectively ion free gaps was found to be much more rapid than for gaps in ordinary room air.

26. Observations on the Velocity of Sound in Arcs. C. G. SUITS, *Research Laboratory, General Electric Company, Schenectady, New York.*—A method has been developed for measuring the velocity of transmission of a single sound pressure front through arcs at atmospheric pressure. The sound is generated by a spark from a tungsten wire to an adjacent copper electrode. The sound receiver within the other copper electrode consists of a high voltage d.c. spark, the voltage of which changes during the passage of a sound wave. The time interval between the generation of the sound wave at one end of the arc and reception at the other end is observed on the cathode-ray oscillograph. The arc is stabilized in a glass tube by means of a corkscrew air stream so that straight, cylindrical discharges, varying between 2 and 12 cm in length, can be used. By plotting arc length and time interval, the velocity V is obtained from the slope, free from end corrections. A preliminary value for a 6.3 ampere copper arc in air at atmospheric pressure is $V=1.3\times10^5$ cm/sec. From this the arc temperature is calculated to be 4300°A. Corrections due to dissociation decrease this value by a small amount.

27. Energy Distribution in the Spectrum of Some Incandescent Lamps. W. E. FORSYTHE AND B. T. BARNES, *Incandescent Lamp Department, General Electric Company, Cleveland, Ohio.*—The intensity for standard temperature and efficiency of the radiation in the spectrum of a number of tungsten lamps has been measured for a range of wavelengths from about 3000A to 27,000A. The values obtained by direct measurements were checked in the visible spectrum by comparison with the relative values obtained from color match data of the same tungsten lamps. Values thus obtained agreed to within a percent or two throughout the visible spectrum.

28. Thermionic Electron Emission from Tungsten. W. B. NOTTINGHAM, *Massachusetts Institute of Technology.*—The electron current from an equipotential surface at 1857°K has been observed as a function of the potential v from -3.5 to 750 volts. Over the range -3.5 to -1.5 the Maxwellian curve is an exact representation of the data while between -1.5 and -0.6 volt the observed current falls below the theoretical curve. The current at -0.6 volt (zero field) is about 50 percent below that expected. The extrapolated Schottky mirror image curve obtained from the high field data falls very close to the extrapolated Maxwellian curve. Energy distribution curves taken at nine temperatures between 1218°K and 1857°K, when plotted as a function of v/T, are all exactly alike. This indicates that the effective integrated transmission coefficient at zero field is independent of the temperature and is therefore probably controlled by mechanical imperfections of the wire such as die marks, crystal irregularities, etc. If the contact potential between the filament and the collector followed the equation $V=V_0+\alpha 8.62\times10^{-5}\ T$ (where αk = temperature coefficient in ergs per degree and V_0 = contact potential at 0°K), then by plotting the observed relative positions of zero applied potential as a function of $1/T$ for the superimposed set of observed curves, the values of V_0 and α could be obtained from the slope and the intercept, respectively. This assumes that we know the contact potential at a single temperature. Observed results seem to follow two lines instead of one. This interpretation gives $\alpha=-1.1$ for 1857° to 1625° and $\alpha=-1.6$ for 1508° to 1218°K. If the best single line through all points is chosen $\alpha=0.68$.

29. The Energy Distribution of Photoelectrons from Sodium and the Photoelectric Determination of h/e. L. A. DUBRIDGE AND A. G. HILL, *Washington University, St. Louis, Mo.*—The recently developed theory of the energy distribution of photoelectrons (DuBridge, Phys. Rev. **43**, 727 (1933)) shows that the Einstein equation connecting the *maximum* energy of emission V_m with the frequency should hold accurately only at 0°K. At higher temperatures there is a temperature tail which may be extrapolated to yield an *apparent* maximum energy V_a. It is a matter of good fortune that it turns out that V_a is also a linear function of the frequency with the slope h/e, approximately. There is however no exact theoretical basis for this relation. The new theory gives a method of determining a V_m which should accurately fit Einstein's equation. The present experiments extend Roehr's previous confirmation of the theory to a sodium surface over a wave-length range from 2400 to 5460A. Plotting V_m against ν gives a value of h/e about 2 percent greater than that obtained by plotting V_a against ν. This raises the question of a possible systematic error in previous photoelectric determinations of h/e. More precise experiments are necessary and are being planned to investigate this question.

30. The Photoelectric Emission from Thoriated Tungsten. R. E. SMITH AND L. A. DUBRIDGE, *Washington University, St. Louis, Mo.*—A complete set of photocurrent *vs.* frequency curves was obtained for a 12 mil thoriated tungsten filament in various stages of activation. In this preliminary work, photoelectric measurements were restricted to single temperature (900°K) and to a single accelerating field (100 v on the collector). Gas-free conditions were maintained throughout. It was found: (1) At any stage of activation the photocurrents vary with frequency according to Fowler's equation, out to frequencies as much as 1.3 volts from the threshold. Fowler's theory thus applies to composite surfaces as well as clean. (2) Beyond 1.3 volts from the threshold the points fall below the Fowler curve, as expected. (3) At each stage of activation the photoelectric work function at 900°K (by Fowler's method) agrees with the thermionic work function, for an average temperature of 1400°K, within the limits of error. The values range from 2.6 to 4.52 v in agreement with previous thermionic work. (4) At higher activation there is a tendency for ϕ_p to be less than ϕ_t by an amount just about equal to the possible error (0.05

volt). This may be a real temperature effect. (5) The value of the constant B in Fowler's equation is the same for all surface conditions.

31. Temperature Variation of the Second Virial Coefficient for Helium. NEILL G. WHITELAW, *University of Wisconsin.*—The temperature dependence of the second virial coefficient for helium may be obtained quite accurately from the recent measurements of Roebuck and Osterberg (Phys. Rev. **43**, 60 (1933); **45**, 332 (1934)) on the Joule-Thomson effect for that gas. If the equation of state be written $PV/RT=A+B/V+\cdots$, one easily derives the relation $(d/dT)(B/T)=\mu C_p/T^2$, where μ is the Joule-Thomson coefficient. The quantity $B/T-B_0/T_0=K$, was found by graphical integration over the range of temperature, −190 to 300°C, for which Roebuck and Osterberg measured μ. Excellent agreement with the recent pressure volume determinations of B by Keesom and Van Santen (Comm. No. 227b, Leyden) is obtained for the limited range 0–100°C, which their measurements cover. If the constant of integration is determined so as to agree with Keesom and Van Santen at 0°C, we obtain $B_{100}=0.4813\times10^{-3}$, while they find $B_{100}=0.4814\times10^{-3}$.

32. The Joule-Thomson Effect in Nitrogen Argon and in Mixtures of Nitrogen and Helium. J. R. ROEBUCK AND H. OSTERBERG, *University of Wisconsin.*—Continuing the work on the Joule-Thomson effect in gases already reported (Phys. Rev. **45**, 332 (1934)), the isenthalpic curves for nitrogen and for argon have been measured over the range 1 to 200 atm., and −160° to +300°C. The general character of the families of curves is very similar to that for air. The upper and lower branches of the inversion curve of the Joule-Thomson coefficient fall within these temperature limits for nitrogen but for argon the upper branch is entirely above 300°C. The data for both gases are now the process of smoothing and will be used to calculate some of the properties, as well as to calculate the Kelvin temperature of the ice point. Measurements have also been made on four mixtures of helium and nitrogen over a more limited range of temperature. The shift in character of the family of isenthalpic curves with change in composition from nitrogen toward helium is very similar to the shift in character of one pure gas with rise in temperature. Experimental work will proceed next with helium-argon mixtures, and with pure carbon dioxide.

33. Precision Determinations of the Variation of the Dielectric Constant of Benzene with Temperature. JOHN A. MORROW, *University of Florida.* (*Introduced by A. A. Bless.*)

34. The Variation of the Dielectric Constant of a Viscous Dielectric with Temperature and with Frequency. A. A. BLESS, *University of Florida.*—The dielectric constant of tung oil was measured as a function of temperature for a number of frequencies. The constant increases at first with decreasing temperature and then decreases after passing through a maximum. The Debye theory accounts qualitatively very well for this behavior, however, the quantitative agreement is not very good. The application of the theory of polar molecules to the region of maximum value of the dielectric constant gives for the product of the frequency and the relaxation time $(k+a/T+b/T^2)^{\frac{1}{2}}$ where k, a and b, are measurable constants of the substance and T is the temperature. Comparison with experiment shows that this relation is only approximately true. Experiments also indicate the existence of rotation of these large molecules in the solid state, and show therefore that the relaxation time of the molecules is not proportional to the viscosity of the substance, except perhaps for very small values of the latter.

35. Effect of X-Rays on the Dielectric Constant of Various Liquids. J. FRED PAYNE, JR., *University of Florida.* (*Introduced by A. A. Bless.*)—A beam of x-rays from a Coolidge water-cooled tube, run at 15 milliamperes and 60,000 volts, was directed on a test cell connected to a heterodyne circuit for observing changes in capacity. The apparatus was completely shielded from thermal and electrostatic disturbances, and was piezoelectrically controlled. Changes in dielectric constants as slight as 0.001 of 1 percent could be measured, and variations of much smaller magnitudes could be detected by ear from changes in the beat note between a 1000 cycle electrically-driven tuning fork and the audio note generated by the oscillators and amplified by a resistance coupled amplifier. The following liquids were tested: benzene, nitrobenzene, ether, methyl alcohol, tung oil, and transformer oil. None of these liquids showed any perceptible changes in the dielectric constant due to x-rays. The absence of the effect indicates that the rate of recombination is very high and that the life of the ions formed by x-rays is less than 0.01 sec. at room temperature. Experiments are now in progress to determine the life of ions at lower temperatures.

36. The General Nuclear Problem. GEORGE GAMOW, *Polytechnic Institute, Leningrad, Russia.*

37. Theory of the Effect of a Nuclear Moment on the State of the Atom. G. BREIT, *New York University.*

38. Measurement of Nuclear Spin and Statistics by Means of Band Spectra. ROBERT S. MULLIKEN, *University of Chicago.*

39. Survey of Experimental Hyperfine Structure Material. Values of Nuclear Magnetic Moments and a Discussion of Their Origin. ROBERT F. BACHER, *University of Michigan.*

40. Measurement of Nuclear Spin and Moments by Method of Molecular Beams. I. I. RABI, *Columbia University.*

41. Measurement of Nuclear Moments and Spin Through the Polarization of Resonance Radiation. ALEXANDER ELLETT, *State University of Iowa.*

42. Application of the Forsythe-Watson Temperature Scale for Tungsten. W. B. NOTTINGHAM, *Massachusetts Institute of Technology.*—Forsythe and Watson (J. Opt. Soc. Am. **24**, 114 (1934)) have published new values of resistivity R and total radiation W characteristic of pure tungsten wire as a function of the temperature. The "derived functions" of Langmuir-Jones, namely $VA^{1/3}/l = X$ and $A/d^{3/2} = Y$, are more useful for the determination of the temperature in well evacuated tubes than the specific functions R and W. (R=resistivity in micro-ohm cm; W=total radiation watts per cm^2; V=potential drop over uniform filament in volts; A=current in amp.; l=length in cm; d=diameter in cm.) Tables and curves showing dependence of X_0 and Y_0 on temperature have been computed directly from R and W which apply for surroundings at 0°K from the relations $X_0=(4\pi)^{1/3}W^{2/3}R^{1/3}$ and $Y_0=\pi W^{3/2}/2R^{1/2}$. In order to determine the temperature from observed values of V, A, l and d the following correction formulae are useful:

$$X_0 = X\left(1+\frac{2}{3}\frac{W_1}{W_2}+\frac{2}{3}\frac{d}{c}-\frac{2}{3}\frac{\Delta d}{d}\right),$$

$$Y_0 = Y\left(1+\frac{1}{2}\frac{W_1}{W_2}+\frac{1}{2}\frac{d}{c}+\frac{\Delta d}{d}\right).$$

W_1/W_2=ratio of the W's for room temperature and filament temperature, respectively. In case the filament is surrounded by a collector of diameter c which has approximately the same total emissivity as tungsten over the temperature range 300°K to 600°K, the third term should be used. (Omit if the collector forms part of the outside wall.) On account of die grooves found on most filaments the true outside diameter as determined by an interferometer gauge is larger than that obtained from the weight or the resistance. The difference in these diameters is Δd. Although the Forsythe-Watson values of R and W differ appreciably from those of Langmuir and Jones, temperatures calculated from the two scales agree remarkably well over the range 900°K to 2200°K and show about the same degree of self-consistency which is not quite perfect.

43. A Simplified Interval Sorter for Spectral Analysis. C. B. ELLIS, *University of Michigan.* (*Introduced by Ralph A. Sawyer.*)—A very simple device has been constructed—in two days' time at no expense, from materials found in the laboratory—for obtaining the differences in a group of spectral lines. It will find all the differences over a range of 500 cm^{-1} to an accuracy of ± 0.5 cm^{-1}, with a speed of about 100 lines an hour. Small holes representing the lines are punched along a paper tape, the scale being 1 cm^{-1}/mm. Rollers to carry photographic paper 20 in. wide were fitted into a box having a slit in the top beneath which the paper passes. The tape is laid along the slit and successive exposures made with each hole in turn at the bottom edge of the paper. The resulting photograph has columns of dots, each dot representing a subtraction from the line at the bottom of its column. A number of dots lying in a horizontal row indicates a recurring difference in the spectrum.

44. On the Photographic Infrared Vibration-Rotation Spectrum of Mono-Deutero Acetylene. C. A. BRADLEY AND ANDREW MCKELLAR, *National Research Fellows, Massachusetts Institute of Technology.*—The absorption spectrum of "heavy" acetylene has been investigated using absorbing columns at atmospheric pressure up to twenty feet in length, in the region 6000–11,000A A 21-foot concave grating was used. The gas was made from water containing more than 95 percent D_2O and is therefore considered to be made up mainly of C_2D_2. One band was found; its origin is at 10,302A. It has the same simple structure as the known acetylene bands, namely, a single R and a single P branch. Although it occurs at a wavelength where a C_2D_2 band might be expected, it is thought to be due to the C_2HD molecule. From term differences we obtain $B_0=1.0097$ and $B=0.9951$ giving $I_0=27.39\times10^{-40}$ g cm^2 and $I=27.80\times10^{-40}$ g cm^2 for the moments of inertia in the normal and excited states, respectively. From these data and similar data on C_2H_2 we calculate the internuclear distances in the acetylene molecule to be $r_{cc}=1.24\times10^{-8}$ cm and $r_{CH}=r_{CD}=0.94\times10^{-8}$ cm. This result, based on the seemingly legitimate assumption that the internuclear distances are the same for the two acetylenes, is quite consistent with the value $r_{cc}=1.22\pm0.08$ cm obtained by Wierl from electron diffraction studies in acetylene.

45. The Behavior of Photovoltaic Cells Under X-Radiation. M. F. GRIFFITH AND P. E. BOUCHER, *Colorado College.* (*Introduced by W. L. Severinghaus.*)—Although considerable work has been done on photovoltaic cells radiated with ultraviolet, visible and infrared light, yet very little data have been reported concerning the effect of x-rays on either the dry or liquid photovoltaic cells. Several liquid photovoltaic cells, a dry "Visitron" selenium cell, and a cuprous oxide rectifier type cell have been radiated with x-rays. A General Electric 3-RB Coolidge tube with impressed peak voltages of 40 to 100 kilovolts supplied the x-radiation. It was necessary to carefully shield all instruments in order to eliminate electrostatic effects. The photo-cell current and e.m.f. were measured by means of a sensitive galvanometer and a simple potentiometer circuit. With the x-ray tube carrying 8 milliamperes at 100 kvp, the selenium cell gave photo-currents of the order of 1 microampere at 2.5 millivolts. There was no appreciable lag and only a slight amount of fatigue under a constant exposure of 6 minutes. A barrier type photovoltaic cell was constructed by using washers obtained from a cuprous oxide rectifier. Photo-currents of the order of 0.1 microampere were obtained when radiated with the x-ray tube carrying 8 milliamperes at 100 kvp. The time lag in response to x-rays was inappreciable for both cells, a result which does not agree with that of Paul R. Gleason (Phys. Rev. **44**, 330 (1933)). Comparable current values were obtained by radiating a liquid photovoltaic cell using cuprous oxide electrodes in a 0.34 normal aqueous solution of NaCl, except that due to time lag, maximum current was obtained after an exposure of 6 minutes. The return to normal dark current required several minutes.

AUTHOR INDEX TO ABSTRACTS OF THE ANN ARBOR MEETING

Albers, V. M.—see Knorr
—— **and H. V. Knorr**—No. 13

Bacher, Robert F.—No. 39
Barker, E. F.—see Sleator
Barnes, B. T.—see Forsythe
Barrows, W. M. and J. B. Green—No. 8
Beams, J. W.—see Flowers
Bless, A. A.—No. 34
Boucher, P. E.—see Griffith
Bradley, C. A. and Andrew McKellar—No. 44
Breit, G.—No. 37

Dershem, Elmer—No. 18
Doan, Richard L.—No. 17
DuBridge, L. A.—see Smith
—— **and A. G. Hill**—No. 29
Duffendack, O. S. and J. H. Manley—No. 11

Ellett, Alexander—No. 41
Ellis, C. B.—No. 43

Flowers, J. W. and J. W. Beams—No. 25
Forsythe, W. E. and B. T. Barnes—No. 27

Gamow, George—No. 36
Goble, A. T.—No. 4
Green, J. B.—see Barrows
—— **and R. A. Loring**—No. 9
Griffith, M. F. and P. E. Boucher—No. 45

Hill, A. G.—see DuBridge
Hoyt, H. C. and Geo. A. Lindsay—No. 19
Hsiung, D. S.—No. 1
Huxford, W. S. and Olav Maseng—No. 24

Janes, R. B.—No. 22

Knorr, H. V.—see Albers
—— **and V. M. Albers**—No. 14

Kruger, P. Gerald and S. G. Weissberg—No. 12

Landé, Alfred—No. 2
Lindsay, Geo. A.—see Hoyt
Loring, R. A.—see Green

Manley, J. H.—see Duffendack
Manning, Millard F.—No. 6
Maseng, Olav—see Huxford
McKellar, Andrew—see Bradley
Merrill, Robert A.—No. 5
Morrow, John A.—No. 33
Mulliken, Robert S.—No. 38

Nottingham, W. B.—Nos. 28, 42

O'Bryan, H. M.—No. 15
Osterberg, H.—see Roebuck

Payne, J. Fred, Jr.—No. 35

Rabi, I. I.—No. 40
Roebuck, J. R. and H. Osterberg—No. 32

Serber, Robert—No. 7
Sleator, W. W. and E. F. Barker—No. 16
Smith, R. E. and L. A. DuBridge—No. 30
Spencer, Roy C.—No. 20
Suits, C. G.—No. 26

Thomassen, L.—see Wilson

Van Vleck, J. H.—No. 3

Walerstein, I.—No. 10
Weissberg, S. G.—see Kruger
Whitelaw, Neill G.—No. 31
Wilson, J. E. and L. Thomassen—No. 21

Ziegler, G. E.—No. 23